



**WAVE ENERGY RESOURCE AND ECONOMIC ASSESSMENT
FOR THE STATE OF HAWAII**

FINAL REPORT
June 1992

Prepared by:

SEASUN Power Systems
124 East Rosemont Avenue
Alexandria, Virginia 22301

Principle Investigator:

George Hagerman

Prepared for:

State of Hawaii
Department of Business, Economic Development, and Tourism
Energy Division
335 Merchant Street, Room 110
Honolulu, Hawaii 96813

Project Manager:

David Rezachek

PREFACE

The first reported patent for a wave energy device was filed in Paris in 1799, by the Girards, father and son. A translation by A.E. Hidden of the Queens University of Belfast indicates that they envisioned a "ship of the line" attached to shore by a gigantic lever, which would drive pumps or machinery. Twenty years earlier, however, a similar ship would carry back to England reports of a much older and more direct use of wave energy. The probable origins of surfing, which has since spread throughout the world, are described in *The Surfer's Almanac*, by Gary Fairmont R. Filosa II (New York: E.P. Dutton, 1977):

Traveling a distance of almost 2,400 nautical miles from the South Pacific to the approximate geographic center of the North Pacific, two groups of settlers from Polynesia founded Hawaii. The first group in A.D. 400 came from the Marquesas; the second, ten centuries later, came from Tahiti, Bora Bora, and Moorea. The Marquesans brought to their new Hawaiian home their ancient sport of *paipio* - riding a wave on a small, rounded board while lying prone, the sport today called bellyboarding or kneeboarding. The Tahitians also brought their favorite aquatic pastime to Hawaii. They rode the incoming waves while standing in a *wa'a* ("canoe"), an activity they called *paka*. When did it happen that a young Marquesan using a *paipio* board to surf prone, watched a newcomer from Tahiti surfing erect in his canoe and decided to stand upon his *paipio*, discovering that if he had enough speed, he could do so? That moment was the birthdate of surfboarding.

In their vast oceanic journeys, the Polynesians who settled Hawaii were able to "read the waves", keeping course by day and on overcast nights by maintaining the alignment of their canoes with carefully selected swells, known to reliably come from distinct directions. Furthermore, by observing patterns of wave refraction, reflection, and diffraction, they were able to detect islands at a range of 20 to 40 nautical miles. The wave-reading techniques used for making landfall in Polynesia are described by David Lewis in his book, *We, the Navigators* (Honolulu: The University Press of Hawaii, 1972), and indicate a finely tuned sensitivity to the complex patterns of sea and swell.

This remarkable heritage augers well for Hawaii's use of wave power to generate electricity, produce fresh water, and circulate seawater in aquaculture ponds. *Ke nalu nei ka moana* *.

George Hagerman
Alexandria, Virginia

* "The ocean is full of waves", quoted from *The Surfer's Almanac*.

ACKNOWLEDGEMENTS

This study was sponsored by the Energy Division, Department of Business, Economic Development, and Tourism (DBED), State of Hawaii, via Purchase Order 4674004 from the Research Corporation of the University of Hawaii. It is the first complete assessment of wave power as a potential energy source for the State and grew out of discussions with John Tantlinger, following the DBED-sponsored International Renewable Energy Conference held in Honolulu on 18-24 September 1988.

While SEASUN Power Systems exercised due care and thoroughness in preparing this report, it makes no warranty as to its accuracy or completeness, and assumes no liability for the consequences of its use. In an emerging technology such as ocean wave energy conversion, changing circumstances may cause some of the material in this report to become obsolete relatively soon after its publication.

A report of this nature can be only as good as the information on which it is based. Therefore, careful attention has been paid to accurately documenting the references used in its preparation. In addition, the author gratefully acknowledges the following individuals for their assistance.

David Castel, of the Scripps Institution of Oceanography in La Jolla, California, provided digitized wave spectra from the two Hawaii sites monitored by the Coastal Data Information Program. Brian Ishii, of Edward K. Noda & Associates in Honolulu, furnished a listing of wave parameters measured by their gage moored off Upolu Point, on the Big Island.

The technology survey would not be nearly as informative or up-to-date without the cooperation of many individuals who are now working on the various wave energy devices reviewed in depth for this report. They are: Even Mehlum, of Norwave, A.S.; Andreas Tommerbakke of Kvaerner Brug A/S; Tomiji Watabe of the Muroran Institute of Technology; Doug Hicks of CHPT, Inc.; Lennart Claeson, of Technocean AB; Norman Bellamy of Coventry Polytechnic; and Tom Shaw of Shawater, Ltd. I am particularly grateful to Lennart Claeson and Bengt-Olof Sjöström, both of Technocean AB, who furnished a great deal of performance data on the Swedish heaving buoy system, which was the basis for the economic assessment presented in this report.

The completeness of this report owes much to Project Manager David Rezachek. Thanks to his patience and encouragement, it was possible to go through the time-consuming process of developing a spectral formula to represent the multi-component sea states that commonly occur in Hawaii, and to undertake a refraction and shoaling analysis, which made it possible to map the islands' wave energy resource.

EXECUTIVE SUMMARY

Hawaii's wave energy resource is large. In theory, recovering only 5-10% of the wave energy available in outer shelf waters off the northern coastlines of Kauai, Maui, and Hawaii could meet the total annual electricity demand of those islands. Less than one half of one percent of Molokai's wave energy resource could meet the electricity needs of that island. Except for Oahu, where electricity demand is comparable to two-thirds of the available resource, wave energy can be withdrawn at very low levels and still make a substantial contribution to island energy supply. In practice, however, Hawaii's wave energy development potential will be limited by the following considerations:

- Environmental constraints based on potential negative impacts and local public concerns, particularly with regard to visual appearance
- Utility constraints based on time variability of the wave resource and the limited capacity of onshore transmission lines
- Financial constraints based on the limited number of economically feasible sites for land- or caisson-based systems and risks associated with uncertainties in cost and performance projections for offshore systems

Without additional research, it is not possible to quantify the impact of these factors, but based on the findings of this report, a few general comments are made below. Recommendations for further work are outlined at the end of this summary.

ENVIRONMENTAL CONSTRAINTS

Wave power plants can be based on land, on caissons in relatively shallow water (5-15 m depth), or in deeper, offshore waters. Land- and caisson-based systems have achieved the greatest development progress to date and may be the first to find commercial application in Hawaii. Land-based systems, however, involve significant shoreline modification and attendant environmental impacts, which may severely limit their deployment. Likewise, wave energy breakwaters are likely to be acceptable only at existing ports, or where construction of a new small-craft harbor has already been approved.

Despite their less-advanced development status, offshore systems have much wider deployment potential, since they don't involve shoreline modification or breakwater construction. Floating devices have been developed that use air or seawater working fluids, eliminating the risk of chemical pollution. High-pressure seawater is particularly attractive as a working fluid, since it can produce both electricity and fresh water.

Offshore wave power plants can be spaced sufficiently far apart that wave energy passing between the plants will diffract into the calmer waters immediately behind the plants. The environmental impact at the coast would be a broad, diffuse lowering of wave energy levels. A 5-10% withdrawal of wave energy offshore would correspond roughly to a 3-5% reduction in wave heights at the coast.

Although offshore floating systems show considerable promise, their potential visual impact will be a significant public concern. To an observer standing near sea level, individual devices within the plant would tend to be obscured by wave action. When viewed from a high elevation, however, they would be more conspicuous and could represent an unacceptable visual intrusion on the offshore seascape.

UTILITY CONSTRAINTS

The first paragraph of this summary compares the total annual electricity demand on each island with the total amount of wave energy incident on the island's northern coastlines. Such a comparison of yearly totals does not consider seasonal or hourly variations in wave power and how well they are correlated with variations in demand. Although waves are consistently more energetic than wind or solar resources, supplemental generating plant or battery storage will be required at times when wave energy levels are low and demand is high. This requirement could significantly limit the amount of wave power that can be connected to a given island utility grid.

In this regard, it should be noted that the most promising coasts for wave energy development in Hawaii are those that face northeast and are partly sheltered from north Pacific swell by adjacent coastal features or neighboring islands to the northwest. They are thus fully exposed to persistent trade wind waves, yet protected from extreme winter swell associated with storms in the northwest Pacific Ocean. The output from a wave power plant along such coasts will be more consistent from day to day and from season to season than it would be along a west- or northwest-facing coast.

An accurate assessment of wave energy economics must include any reinforcement of onshore utility grids that would be necessary for transmitting wave power to load centers that are far removed from the best wave resources. Depending on the cost of such grid reinforcement, this could severely limit the amount of wave energy development that would be economically competitive with other island energy sources.

FINANCIAL CONSTRAINTS

It was beyond the resources available for this study to identify environmentally acceptable sites and develop energy cost projections for land- or caisson-based wave power plants. Based on developers' designs for locations outside Hawaii, however, it appears that commercial deployment of these systems will be limited not only by environmental concerns, but also by site-specific economic feasibility. At sites where existing shoreline topography minimizes the required amount of excavation and concrete placement, Tapered Channel power plants and land-based oscillating water column systems might be able to realize energy costs less than 10 ¢/kWh. Breakwater-based wave power plants, however, will be economically feasible only if fabrication of the concrete caissons can be financed for some other purpose, such as harbor improvement, shore protection, or perimeter construction for a very large floating platform.

To assess the economic feasibility of offshore wave power plants, levelized revenue requirements were estimated for a Swedish heaving buoy system, hypothetically located offshore Makapuu Point, Oahu. The projected cost of energy is 8.6 ¢/kWh for a 30 MWe plant, and 9.9 ¢/kWh for a 10 MWe plant. These projections, however, are sensitive to several cost and performance uncertainties.

For example, there is a large amount of scatter in the absorption efficiency data, and this uncertainty alone governs the economic feasibility of the 30 MWe reference design at Makapuu Point; the upper and lower bounds of the efficiency data are associated with energy costs ranging from 7.3 to 16.2 ¢/kWh. Other project development risks having a significant impact on the cost of energy are uncertainties in buoy fabrication cost, operating and maintenance costs, and plant availability. Although these uncertainties individually have a much lower impact than the uncertainty in absorption efficiency, the combined risk is equally great. Other offshore technologies have similar cost and performance uncertainties, and commercial financing is not likely to be available for offshore wave power projects without construction and operation of a small demonstration plant.

Compared to land- or caisson-based wave energy devices, local site conditions have much less impact on the economic feasibility of offshore systems. For a device such as the Swedish heaving buoy, however, whose absorption efficiency is strongly dependent on incident wave period, economic feasibility may depend on the degree to which a particular outer shelf location is dominated by long-period north Pacific swell or short-period trade wind waves.

RECOMMENDATIONS

Site-specific, technology-specific evaluations are required to determine the limits that environmental and utility constraints will place on wave power development in Hawaii. Construction and operation of a demonstration plant would reduce uncertainties in cost and performance projections, making it easier for developers to obtain financing for commercial projects. In the last section of this report, a four-phase program is outlined, leading to construction of a fully operational demonstration project in the year 2000. Each phase of the program would depend on the success of the previous phase before being initiated and would involve an increased share of private-sector funding by commercial developers.

Phase I would quantify wave energy's development potential on each of the five major Hawaiian islands having good northern coastal exposure - Kauai, Oahu, Molokai, Maui, and Hawaii. The utility and environmental constraints described above would be used to establish the number and size of potential projects that realistically can be developed on a given island, for six different wave energy conversion technologies. Feasibility-level designs and associated cost/performance projections would then be prepared for each developable project.

A resource supply curve would be prepared for each technology on each island with developable projects, characterizing the technology's energy cost/contribution, and providing an objective basis for determining whether the technology should be carried forward in the program and which potential project sites should be carried forward with it. Using this approach, the number of candidate technologies and sites would be narrowed down in Phase II, and again in Phase III. At the same time, however, there would be increased resource monitoring at the candidate sites, and refinement of the candidate designs.

Phase IV would involve detailed design and construction of one or two demonstration plants. While state funding would support continued resource monitoring activities at the project site, private financing, based on revenues anticipated from the sale of electricity and/or fresh water, would support the actual design and construction of the plant(s).

TABLE OF CONTENTS

Section	Page
1 INTRODUCTION	1-1
PREVIOUS STUDIES	1-1
SCOPE OF THIS STUDY	1-2
2 RESOURCE ASSESSMENT	2-1
SOURCES OF WAVE DATA	2-1
WAVE CHARACTERISTICS IN HAWAII	2-5
RESOURCE ASSESSMENT PROCEDURE	2-19
RESOURCE ASSESSMENT RESULTS	2-29
3 WAVE ENERGY CONVERSION PROCESSES	3-1
TAPERED CHANNEL	3-4
FIXED OSCILLATING WATER COLUMN	3-6
PIVOTING FLAP	3-15
HEAVING BUOY	3-18
FLEXIBLE BAG	3-23
SUBMERGED BUOYANT CYLINDER	3-27
4 ECONOMIC ASSESSMENT	4-1
LAND- AND CAISSON-BASED SYSTEMS	4-1
OFFSHORE HEAVING BUOY SYSTEM	4-6
5 CONCLUSIONS AND RECOMMENDATIONS	5-1
OVERALL ASSESSMENT	5-1
UNRESOLVED ISSUES	5-1
RECOMMENDATIONS	5-4
6 REFERENCES	6-1

LIST OF FIGURES

Figure	Page
2-1 Wave hindcast grid points and measurement sites in Hawaii	2-3
2-2 Significant wave heights at CDIP measurement sites, May 1987	2-7
2-3 Wave spectra at CDIP measurement sites, May 1987	2-8
2-4 Significant wave heights at CDIP measurement sites, August 1987	2-10
2-5 Wave spectra at CDIP measurement sites, August 1987	2-11
2-6 Significant wave heights at CDIP measurement sites, October 1987	2-12
2-7 Wave spectra at CDIP measurement sites, October 1987	2-13
2-8 Significant wave heights at CDIP measurement sites, January 1988	2-14
2-9 Wave spectra at CDIP measurement sites, January 1988	2-15
2-10 Seasonal variability of significant wave height	2-17
2-11 Fit of three-component spectra to measured spectra	2-22
2-12 Comparison of Bretschneider and three-component spectra	2-23
2-13 Accuracy of wave power estimates based on three-component spectra	2-24
2-14 Deep water directional distribution of dominant spectral components	2-25
2-15 Deep water directional distribution of wave energy	2-26
2-16 Wave power distribution along the north coast of Kauai	2-30
2-17 Wave power distribution along the northwest coast of Oahu	2-32
2-18 Wave power distribution along the northeast coast of Oahu	2-33
2-19 Wave power distribution along the north coast of Molokai	2-34
2-20 Wave power distribution along the north coast of Maui	2-35
2-21 Wave power distribution along the north-northeast coast of Hawaii	2-36
2-22 Wave power distribution along the east-northeast coast of Hawaii	2-37
2-23 Annual wave energy resource compared with annual electricity demand	2-39
3-1 Wave energy conversion processes	3-2
3-2 Tapered Channel concept and 350 kWe demonstration plant at Toftestallen	3-5
3-3 Use of non-return valves in a single-acting OWC system	3-7
3-4 Wells turbine concept and monoplane rotor design	3-9
3-5 Land-based OWC, 40 kWe test plant at Sanzei	3-10
3-6 Caisson-based, multi-resonant OWC design developed for Tongatapu	3-12
3-7 Breakwater-based OWC, 60 kWe demonstration plant at Sakata Port	3-13
3-8 Single-acting OWC system - 1.5 MWe design developed for Kashima Port	3-14
3-9 Pendulor System - concept and 1.5 MWe design developed for Muroran Port	3-16
3-10 Pendulor System - hydraulic rectifier schematic and performance	3-17

LIST OF FIGURES (continued)

Figure		Page
3-11	DELBUOY heaving buoy system for fresh water production	3-19
3-12	Swedish heaving buoy system - hose pump concept	3-21
3-13	Swedish heaving buoy system - reference design	3-22
3-14	SEA Clam - concept and straight spine configuration	3-24
3-15	SEA Clam - circular spine configuration	3-26
3-16	Bristol cylinder - absorber and pump/mooring arrangement	3-28
3-17	Bristol cylinder - platform and turbine/generator arrangement	3-29
4-1	Absorption efficiency of heaving buoy/hose pump modules in random waves	4-9
4-2	Energy cost sensitivity analysis of 30 MWe reference design at Makapuu Point	4-11

LIST OF TABLES

Table		Page
2-1	Monthly Availability of Measured Wave Data in Hawaii	2-4
2-2	Annual Average Wave Statistics at Outer Shelf Measurement Sites	2-18
2-3	Annual Average Joint Probability Distribution at Makapuu Point	2-20
2-4	North-Facing Coastal Segments for Refraction and Shoaling Analysis	2-28
4-1	Cost and Performance of Tapered Channel Power Plants Outside Hawaii	4-2
4-2	Cost and Performance of Caisson-Based Wave Power Plants Outside Hawaii	4-3
4-3	Cost and Performance of Offshore Heaving Buoy Reference Design at Makapuu Point	4-8

LIST OF APPENDICES

Appendix	Page
A WAVE ENERGY RESOURCE PRIMER	A-1
B DEEP-WATER DIRECTIONAL WAVE STATISTICS AND SPECTRA	B-1
C BATHYMETRIC CHARTS AND DATA AVAILABILITY	C-1
D ENERGY COSTING METHOD AND FINANCIAL PARAMETERS	D-1
E LISTING OF WAVE ENERGY TECHNOLOGY DEVELOPERS	E-1

Section 1
INTRODUCTION

This report provides an assessment of Hawaii's wave energy resource and the economics associated with its development. The findings of this study should be of interest to island utilities and state planners, as well as members of the academic community and private industry who are concerned with energy in general, and ocean resource development in particular.

PREVIOUS STUDIES

Although there has been quite a bit of research on ocean thermal energy conversion (OTEC) in Hawaii, very little work has been done on wave energy. The author is aware of only three studies that have been published prior to this one.

In 1978, Venezian estimated the large-scale wave energy resource in Hawaii, based on shipboard wave observations that had been compiled by the U.S. Naval Weather Service Command [1]*. More recently, Bretschneider and Ertekin extended Venezian's work, applying four different calculation methods to the same data base [2].

These two assessments cover broad areas of several degrees latitude and longitude, which makes it impossible to determine how the wave energy resource varies from island to island or how it varies along a particular island coastline. Furthermore, the compilation of ship-observed data on which these studies are based [3] covers a time span of only eight years. Measured wave data, which contain much more information than shipboard observations, are already available for seven years off Makapuu Point, Oahu, and eight years near Nihoa, in the northwestern Hawaiian Islands. Therefore, these two studies are of limited value; however, the calculation methods developed by Bretschneider and Ertekin [2] have good potential for future use as a means of determining the long-term representativeness of short-term measured or hindcast wave data (see Section 2).

In 1986, Edward K. Noda and Associates, Inc. conducted a site-specific, device-specific wave energy study for Hawaiian Electric Company, Inc. Shallow-water wave statistics were developed for three locations on Oahu: Kaena Point, Kahuku Point, and Laie Point. These were then used to estimate the annual average electrical output of a heaving-float-in-caisson device known as the Neptune System [4]. Incident wave power was not estimated, however, and no other islands were included in the study.

* Numbers in brackets are reference citations, listed in Section 6.

SCOPE OF THIS STUDY

The wave energy resource assessment is developed in Section 2, which begins with an overview of wave data sources in Hawaii. Example wave records from four measurement sites are then used to illustrate the effects of coastline orientation and sheltering on island wave climates. The islands of Kauai, Oahu, Maui, Molokai, and Hawaii are divided into a total of twenty-four coastal segments, each having a different orientation and a different degree of sheltering by adjacent coastal features or neighboring islands. Annual average incident wave power is estimated at five water depths for each coastal segment, using a spectral refraction and shoaling analysis. The total wave energy resource base for each island is then compared with the island's total annual electricity demand.

It is recommended that readers not familiar with ocean wave properties read the primer in Appendix A of this report before going on to Section 2. Even coastal and ocean engineers may find this of interest, since it is written from the particular perspective of viewing waves as an energy source.

Section 3 surveys six wave energy technologies that have near-term potential application in Hawaii:

- Land-based Tapered Channel
- Land- or caisson-based oscillating water column
- Caisson-based pivoting flap
- Offshore heaving buoy
- Offshore flexible bag
- Offshore submerged buoyant cylinder

A brief description of the working principle behind each device is given, together with an overview of its development history and present status.

Section 4 provides cost and performance projections for four of the above wave energy devices. Environmental concerns and the existence of economically feasible site conditions will probably limit the deployment of land- and caisson-based devices to a few specific locations. Identifying these sites and developing shallow-water wave statistics for them was beyond the resources available for this study. Therefore, projections for land- and caisson-based systems are based on designs developed for locations outside Hawaii. As an example of an offshore device, cost and performance projections are made for a Swedish heaving buoy system, deployed in outer shelf waters off Makapuu Point, Oahu.

Finally, Section 5 presents an overall assessment of Hawaii's wave energy resource and identifies areas requiring further investigation. Recommendations are made for a four-phase development program leading to the construction of one or two small demonstration projects in the year 2000.

Section 2
RESOURCE ASSESSMENT

This section presents an overview of wave data sources in Hawaii, and uses example wave records from four measurement sites to illustrate the effects of coastline orientation and sheltering on island wave climates. Annual, seasonal, and day-to-day variability of the wave energy resource in Hawaii is also characterized. The procedure for assessing the average annual resource base is then described, and the geographic distribution of the resource is mapped for five different water depths along twenty-four coastal segments covering the northern shorelines of Kauai, Oahu, Molokai, Maui, and Hawaii. Finally, the total incident wave energy incident on each island is compared with the island's total electricity demand.

SOURCES OF WAVE DATA

Visual Shipboard Observations

Through its Cooperative Ship and Nearshore Observations programs, the U.S. National Weather Service routinely collects marine weather reports from ships in transit. These are made at synoptic times (0000, 0600, 1200, and 1800 Greenwich Mean Time), usually by radio. Wave observations are reported as the visually estimated height and period of both sea and swell. Prior to July 1963, these parameters were reported for only the higher of the two types of waves.

Ship reports are archived at the National Climatic Data Center in Asheville, North Carolina. For a nominal fee, statistical summaries may be requested for any rectangular region of latitude and longitude (to the nearest tenth of a degree), and for any time period.

Accurate visual estimates of wave height and period from the deck or bridge of a moving ship are difficult, even for an experienced observer. One-to-one comparisons with buoy measurements indicate visual errors of up to 1 meter in wave height and 2 seconds in wave period [5]. Averaged over a sufficient number of observations, individual errors tend to cancel one another. In order to obtain a sufficiently large number of observations, however, fairly large regions must be sampled, which makes it impossible to determine how wave power varies according to coastal orientation and sheltering by neighboring islands. This is particularly true of windward island coasts, where the density of shipping traffic is generally lower but the need for data greater, since windward coasts have the best wave energy resources.

Although ship-observed data may not yield highly accurate wave power estimates, the errors are likely to be the same from one year's statistics to the next. This makes them useful for determining the degree to which short-term measured or hindcast data are representative of the long-term regional wave climate. Calculation methods developed at the University of Hawaii [2] should prove useful for this analysis.

Numerical Hindcasts

Wave hindcast models are computer programs that numerically generate and propagate wave energy based on input wind data. Wave hindcasting is used to predict wave conditions that would have occurred for a given set of past weather conditions. The same model, however, can be used to predict future wave conditions, based on weather forecasts.

Sophisticated wave hindcast models have been developed by both the U.S. Navy and the U.S. Army Corps of Engineers. The Navy's model is routinely operated as a forecast tool to support fleet operations, but is not readily available in archived form. On the other hand, the Army's model was developed to provide an archived data base for the design of shore protection structures and is thus more accessible and useful for wave energy resource assessment.

A statistical summary of this hindcast, which covers the 20-year period from 1956 through 1975, has been published [6] for seven deep water stations in Hawaii (Figure 2-1). The Corps model does not consider the sheltering effect of the islands, nor does it account for swell arriving from the southern hemisphere. Furthermore, the stations are spaced approximately 220 km apart, making it impossible to resolve wave energy gradients along an island coastline or even from one island to the next.

One valuable feature of the Corps of Engineers hindcast, however, is that directional statistics were prepared for sixteen compass points at each station. Hindcast data from Stations 30 through 33 were used in this study to determine the deep-water directional distribution of waves in open deep water north of the islands, as described later in this section.

Wave Measurements

Three organizations have operated, or operate, wave gages in Hawaii: Scripps Institution of Oceanography, Edward K. Noda and Associates, and the U.S. National Oceanic and Atmospheric Administration. Long-term records (twelve months or more) have been collected at eight wave measurement sites, charted in Figure 2-1. The availability of archived data from these sites is summarized in Table 2-2. The following text describes each of the three data collection programs and the locations where measurements have been made in Hawaii.

Since 1975, Scripps Institution of Oceanography has operated the Coastal Data Information Program (CDIP), to rapidly disseminate data on winds, waves, and currents in the coastal zone [7]. Offshore wave conditions are measured by Waverider buoys, while submerged pressure gages are used in nearshore waters (5-15 m water depth). Wave spectra are computed from 17-minute time series, which are logged once every 6 hours (except in 1989, when data at Makapuu Point were logged every 3 hours).

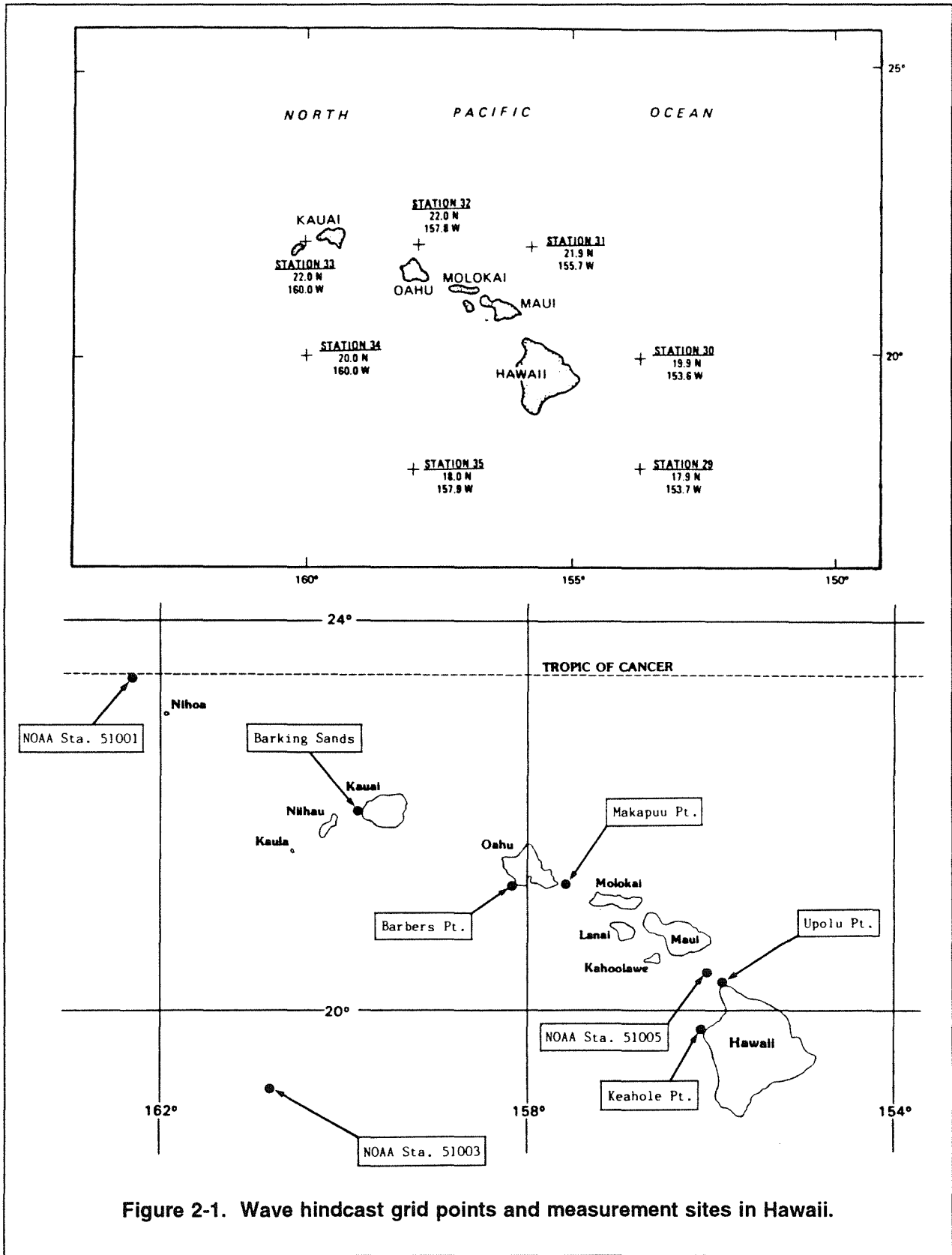


Figure 2-1. Wave hindcast grid points and measurement sites in Hawaii.

Table 2-1
Monthly Availability of Measured Wave Data in Hawaii, 1981-1990

Year:	1981	1982	1983	1984	1985
Barking Sands			*****	*****	
Makapuu Pt.	*****	*****	*****	*****	*****
Upolu Pt.				*****	*****
Keahole Pt.				*****	
NOAA Sta. 51001	*****	*****	**	*****	*****
NOAA Sta. 51003				*****	
NOAA Sta. 51005					*
Year:	1986	1987	1988	1989	1990
Barking Sands		*****		*****	*****
Makapuu Pt.	*****	*****	*****	*****	*****
Barbers Pt. Buoy	*	*****	*****	*****	
Barbers Pt. Array	*****	*****	*****	*****	*****
Upolu Pt.	*****				
NOAA Sta. 51001	***	*****	*****	*****	*****
NOAA Sta. 51003	*****	*****	*****	*****	*****
NOAA Sta. 51005	*****	*****	*****		

Asterisk indicates at least two weeks of data available for month.

Although most CDIP measurement sites are along the California coast, four gages are located in Hawaii. Three Waverider buoys are deployed in outer shelf waters at Barking Sands (91 m depth), Makapuu Point (119 m depth), and Barbers Point (183 m depth). In addition, an array of three submerged pressure gages, yielding directional data, is installed in 9 m water depth at Barbers Point.

Two wave gages have been operated off the island of Hawaii by Edward K. Noda and Associates (EKNA) of Honolulu. The first was a Waverider buoy in 40 m water depth on the north shore of Keahole Point, where measurements were logged at 12-hour intervals [8]. The second was a submerged pressure gage in 170 m water depth off Upolu Point, where measurements were logged at 8-hour intervals [9].

Since 1979, the National Oceanic and Atmospheric Administration (NOAA) has operated more than forty meteorological data buoys in the North Atlantic, North Pacific, Gulf of Mexico, and Great Lakes. Most are equipped with accelerometers for measuring wave conditions based on buoy heave response. Wave spectra are computed from 20-minute time-series measurements which are made once an hour. Statistical summaries from these buoys have been published by the National Climatic Data Center [10], while the original data are archived at the National Oceanographic Data Center in Silver Spring, Maryland.

NOAA has operated five data buoys in the vicinity of Hawaii. The three buoys closest to the islands are charted in Figure 2-1. Stations 51001 and 51003 are in very deep water (3285 m and 4848 m, respectively) and have a much wider exposure than the CDIP buoys at Barking Sands and Makapuu Point, which better represent wave conditions near the island coasts. Station 51005, in the Alenuihaha Channel, is considerably more sheltered from north Pacific swell than the EKNA gage at Upolu Point, which better represents wave conditions along the northwest coast of the Big Island.

WAVE CHARACTERISTICS IN HAWAII

The three primary sources of wave energy in Hawaii are seas built up by local trade winds, swell generated by extratropical storms in the north Pacific Ocean, and swell from similar but farther distant storms in the southern hemisphere. High waves are also generated by tropical storms and Kona winds, but these are relatively rare wave events in Hawaiian waters, occurring no more than a few times a year. Such waves represent a significant hazard that must be considered in the design of a wave power plant, but their contribution to the islands' wave energy resource is negligible.

Trade winds blow throughout the year in Hawaii, with monthly average wind speeds ranging from 10 to 15 knots (5 to 8 m/sec). At NOAA Station 51001, they are strongest in July, with secondary peaks in March-April and November [10]. Trade wind waves most commonly arrive out of the northeast, with dominant periods of 6 to 8 seconds and significant heights of 1 to 2 m.

Extratropical storms are born in the northwestern Pacific Ocean as prevailing westerly winds off the Asian continent pick up heat and moisture from the Kuroshio Current. These low-pressure systems typically develop sustained wind speeds up to 50 knots (25 m/sec), blowing over a 1000 km stretch of water for two to three days, as they follow northeasterly tracks into the Gulf of Alaska. Such storms are most frequent and intense from November through March, although they occur throughout the year.

Swell from north Pacific storms most commonly arrives out of the north to northwest, with dominant periods of 10 to 14 seconds and significant heights of 1.5 to 2 m, although periods as long as 18 seconds and deep-water heights up to 3 m are not uncommon. These long-period waves create spectacular curling breakers in shoaling water and are responsible for the popularity of surfing spots along the north shore of Oahu, such as Waimea Bay, Pipeline, and Sunset Beach [4].

Extratropical storms also occur in the Southern Ocean that encircles Antarctica, and are most frequent and intense during the southern hemisphere winter (May through September). Swell from these storms typically arrives from the south to southwest, and is longer and lower than north Pacific swell, with dominant periods of 14 to 18 seconds and significant heights less than 1.5 m.

The day-to-day and seasonal variability of wave energy in Hawaii depends largely on the orientation of a given island coast and the extent to which it is sheltered from the primary wave systems described above. This is well-illustrated by wave records from the four CDIP measurement sites in Hawaii during the months of May, August, October (1987), and January (1988), when all four gages were operating simultaneously. These records are described below and illustrated on the following pages.

Two high-wave events occurred at Makapuu Point during May 1987, one from the 7th through 11th, and one from the 23rd through 27th (Figure 2-2). The time series of wave spectra in Figure 2-3 shows the classic development of a wind-driven sea, with the spectral peak shifting to increasingly longer periods as more energy is transferred from wind to waves (see Appendix A). Neither of these high-wave events occurred at Barbers Point, and only the first event is evident at Barking Sands. Apparently, this first event was generated by winds blowing more out of the north than east, such that high wave energy levels occurred at both measurement sites. The second event, however, must have been due to more easterly winds, from which the Barking Sands buoy was sheltered by Kauai's Na Pali coast.

Also notable in Figure 2-2 are two moderate-wave events, on the 16th and 21st. The time series of spectra indicate that these are due to swell arriving from a distant storm, with the classic signature of a sudden increase in long-period wave energy, followed by a gradual shift of the spectral peak to shorter periods (exactly the opposite of a wind-driven sea; again, see Appendix A for an explanation).

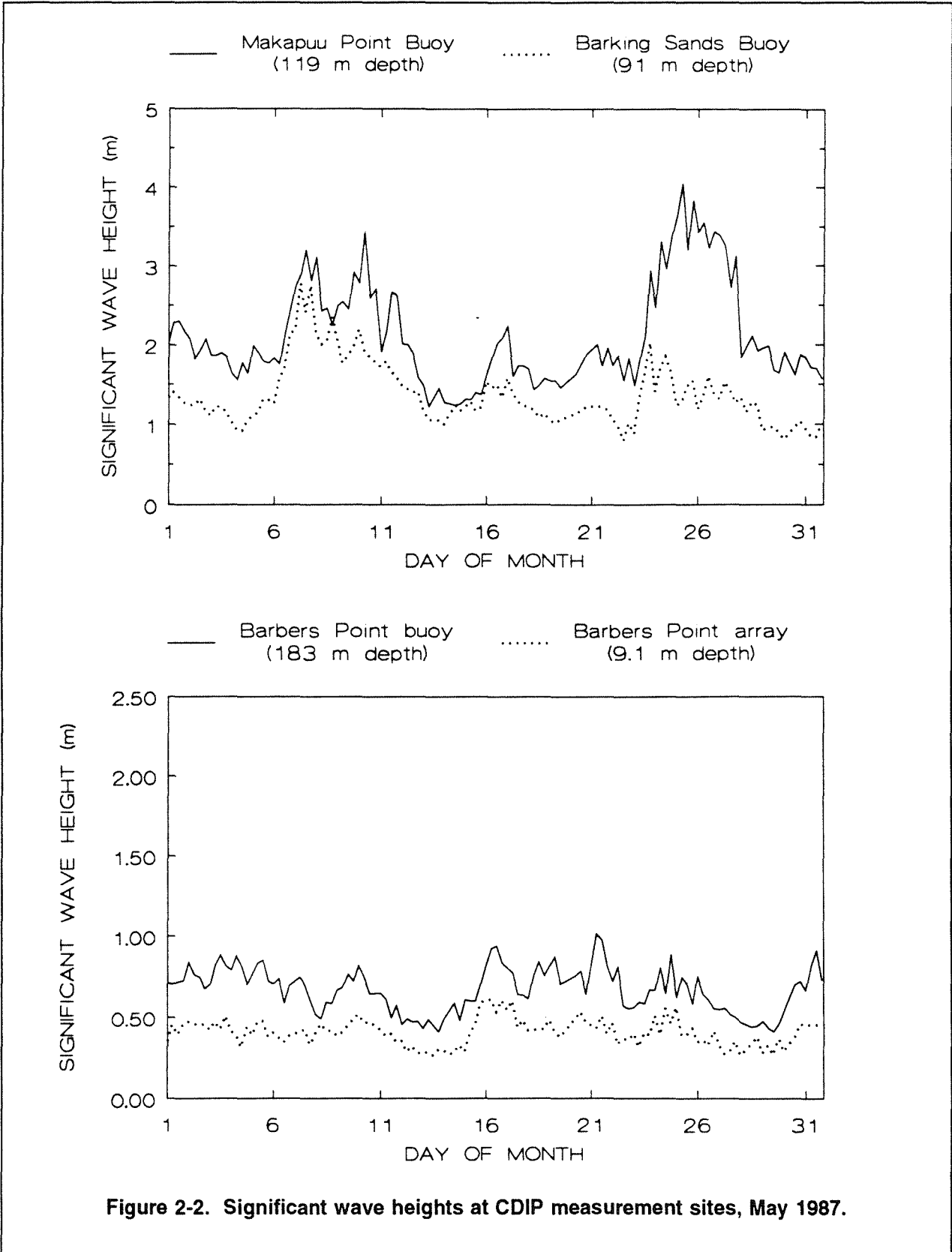


Figure 2-2. Significant wave heights at CDIP measurement sites, May 1987.

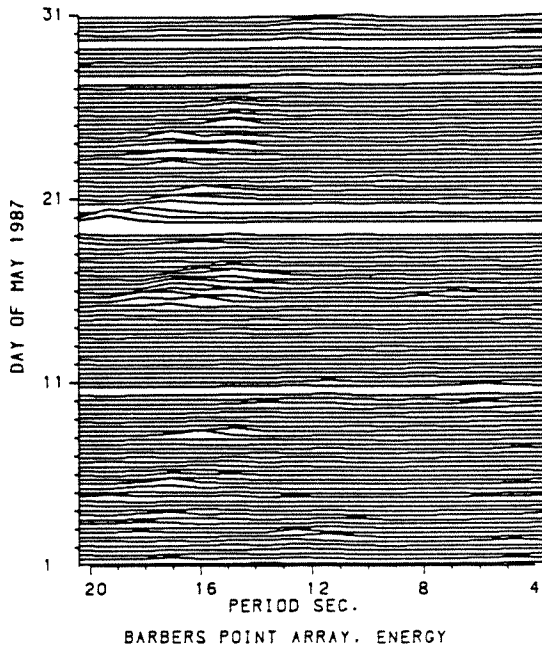
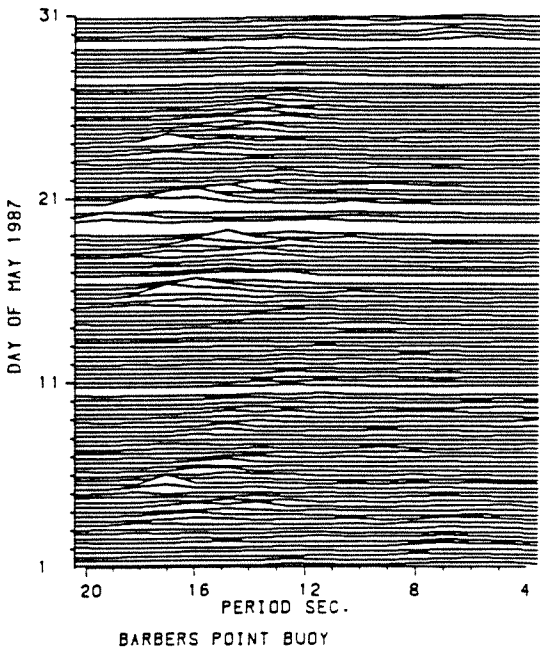
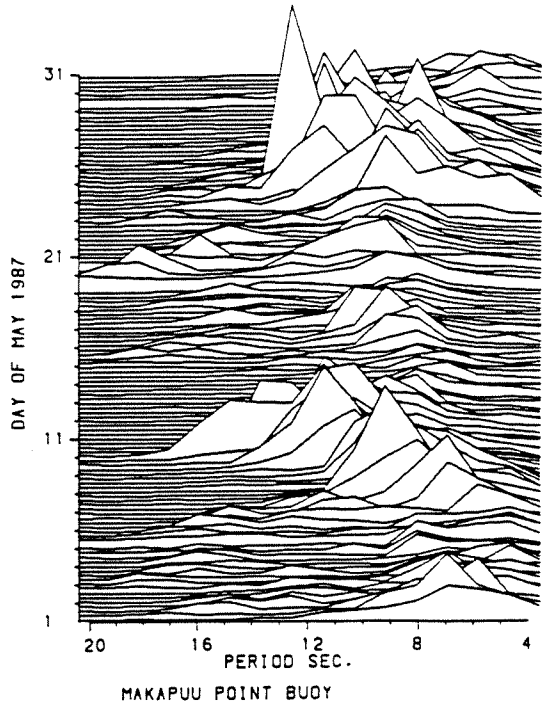
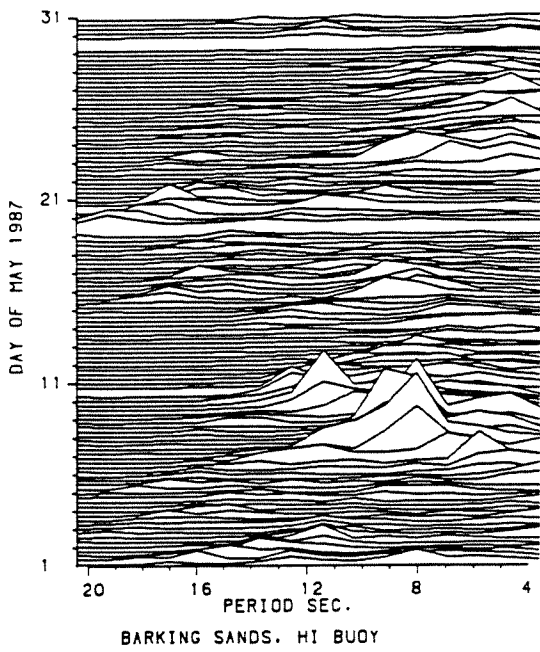


Figure 2-3. Wave spectra at CDIP measurement sites, May 1987.

Examination of time series from other CDIP gages, along the California coast, indicates that these swell were from southern hemisphere storms (north Pacific swell arrives off California about a day after it arrives in Hawaii, whereas Southern Ocean swell arrives two to three days later).

Turning next to August 1987, conditions were considerably calmer at Makapuu Point and Barking Sands than in May, whereas wave energy levels at Barbers Point actually increased, due to the arrival of swell from the southern hemisphere (Figure 2-4). Four distinct southern swell events can be identified on the 6th, 18th, 25th, and 28th. Note the persistent presence of trade wind wave energy at Makapuu Point, with spectral peaks of 5 to 8 seconds (Figure 2-5). As at the end of May, the Barking Sands buoy was largely sheltered from this trade wind wave energy by the Na Pali coast.

In October 1987, two high-wave events stand out, one on the 3rd and one on the 23rd (Figure 2-6). Examination of data from CDIP gages off the California coast indicates that high waves on 3 October were swell from the southern hemisphere, whereas those on 23 October were due to north Pacific swell. Also evident is the much higher level of background wave energy at Makapuu Point, particularly during the last half of the month. Again, this is due to trade wind wave energy peaking at 5 to 8 seconds, which is not present at Barking Sands (Figure 2-7).

Finally, in January 1988, four high-wave events occurred, all dominated by north Pacific swell (Figure 2-8). During the first two events, swell must have come more from the north than west, since wave energy levels at Makapuu Point were comparable to those at Barking Sands, with relatively little swell reaching Barbers Point. During the last two events, however, waves must have come more from the west, since a considerable amount of swell energy made landfall at Barbers Point (Figure 2-9), probably arriving from south of Niihau or the Kauai Channel. Furthermore, much of this swell did not reach Makapuu Point, which is sheltered from the west through northwest by the island mass of Oahu. Also note the high wind-driven seas at Makapuu Point on the 26th through 30th, which were largely absent from Barking Sands.

The above examples illustrate the differences in wave climate between northwest and northeast island coasts in Hawaii. Northwest coasts are dominated by north Pacific swell, which has a strong seasonal variability. Northeast coasts are partially sheltered from such swell, which means that they don't fully experience the extreme waves generated by north Pacific winter storms. During the summer, however, northeast coasts are fully exposed to trade wind waves, while northwest coasts are largely sheltered from wind-driven seas. While north Pacific swell occurs as discreet events associated with individual storms, trade wind waves tend to be more continuous, particularly during the summer months, when high wind speeds are more persistent. Therefore, wave energy levels along northeast coasts are more consistent seasonally and from day to day than they are along northwest coasts.

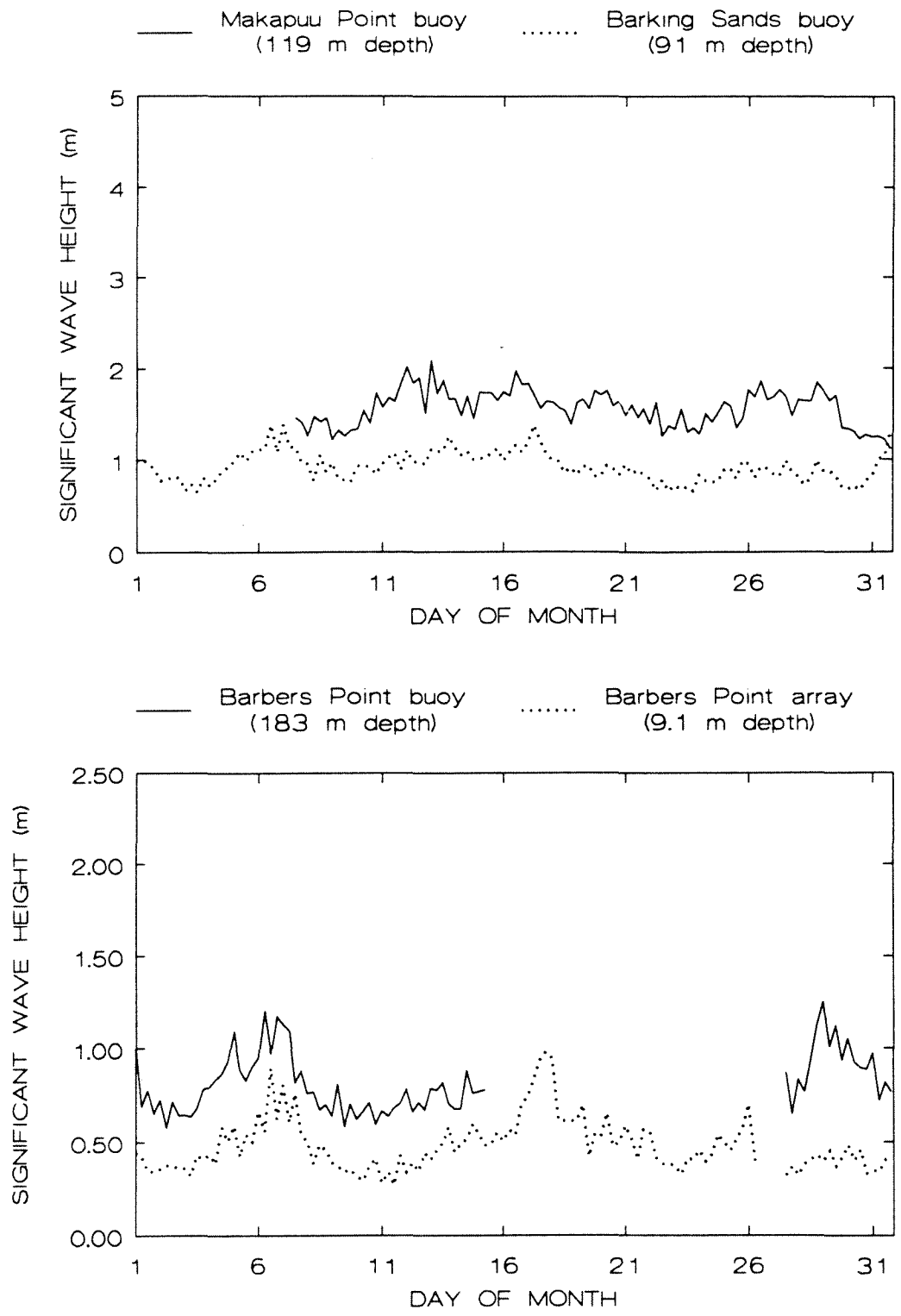


Figure 2-4. Significant wave heights at CDIP measurement sites, August 1987.

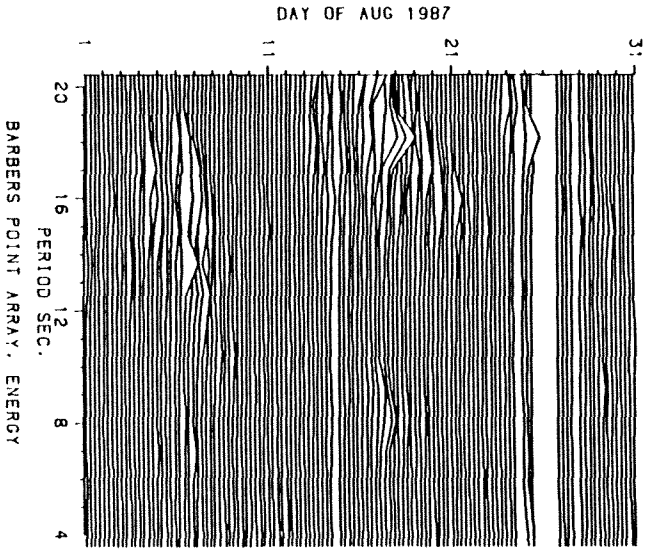
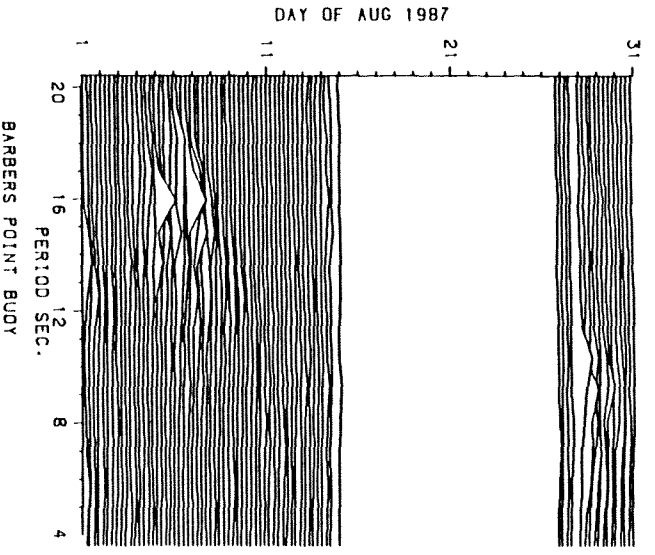
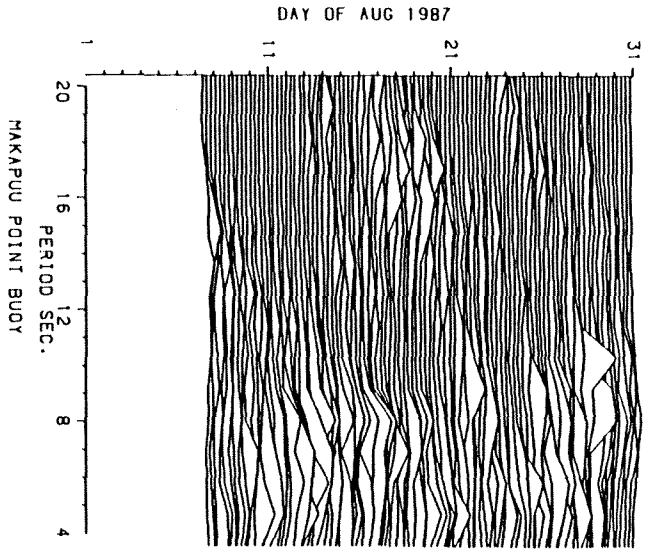
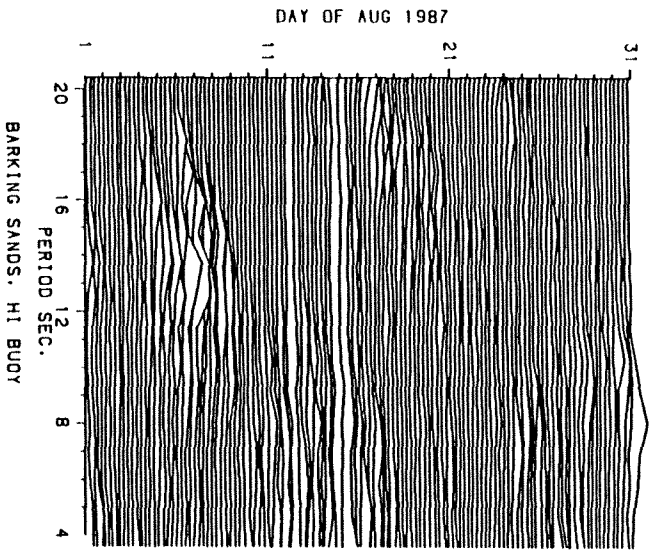


Figure 2-5. Wave spectra at CDIP measurement sites, August 1987.

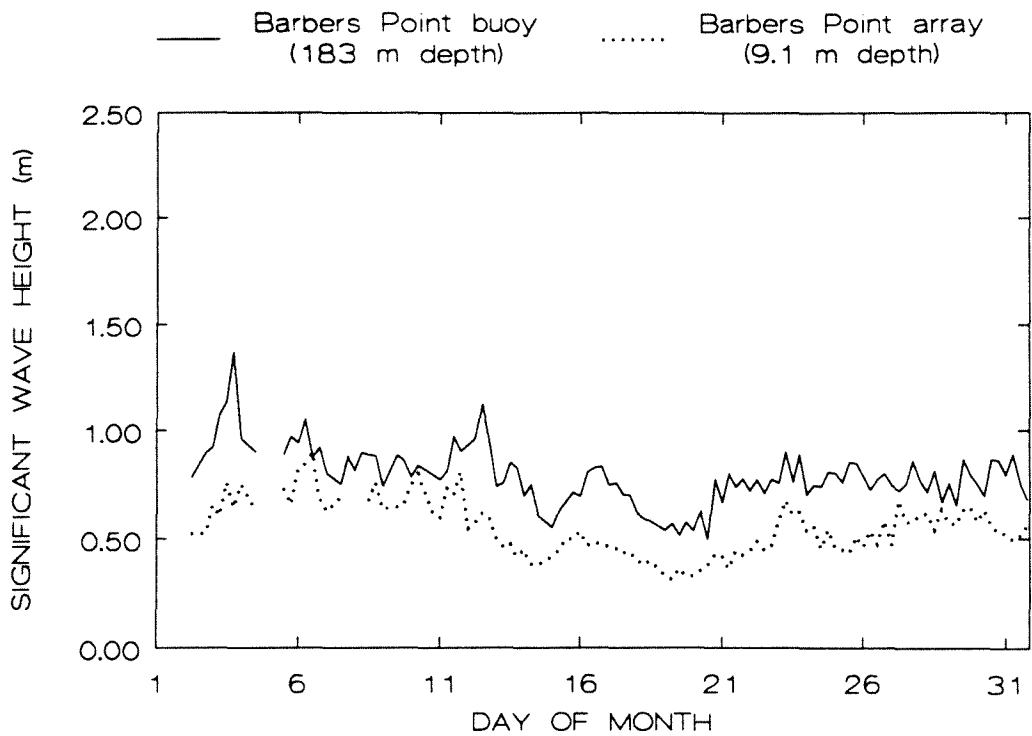
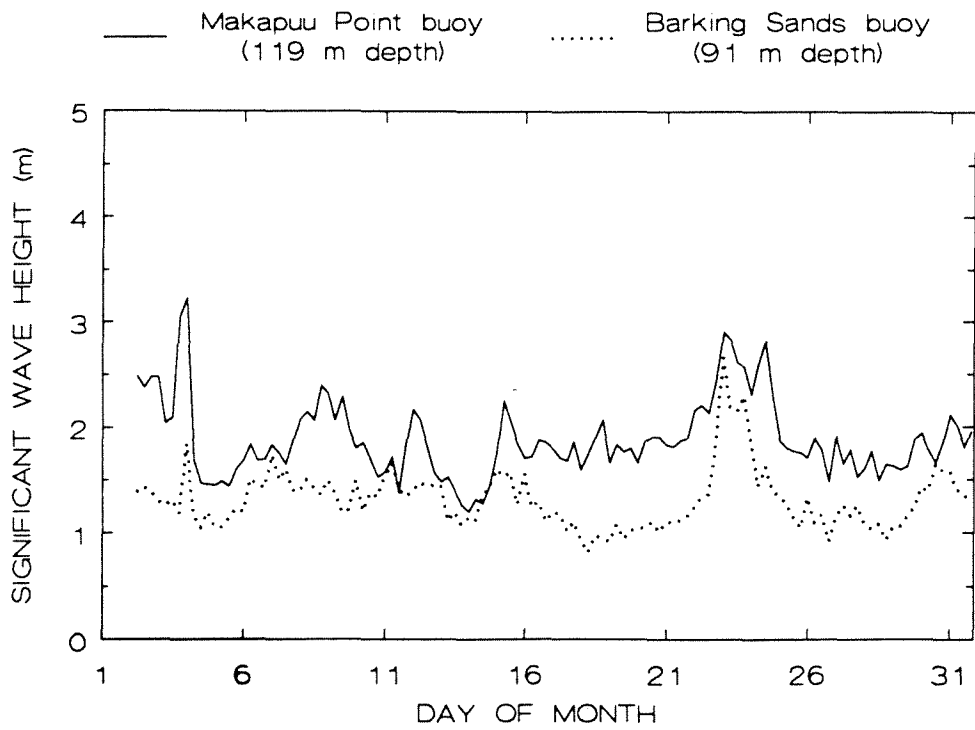


Figure 2-6. Significant wave heights at CDIP measurement sites, October 1987.

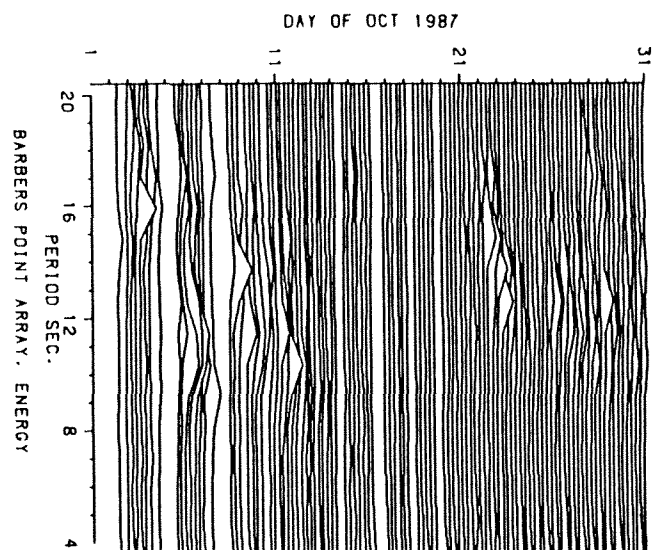
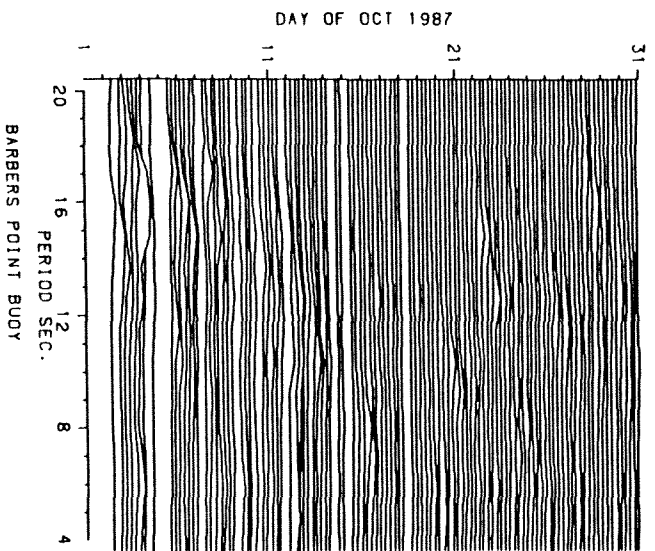
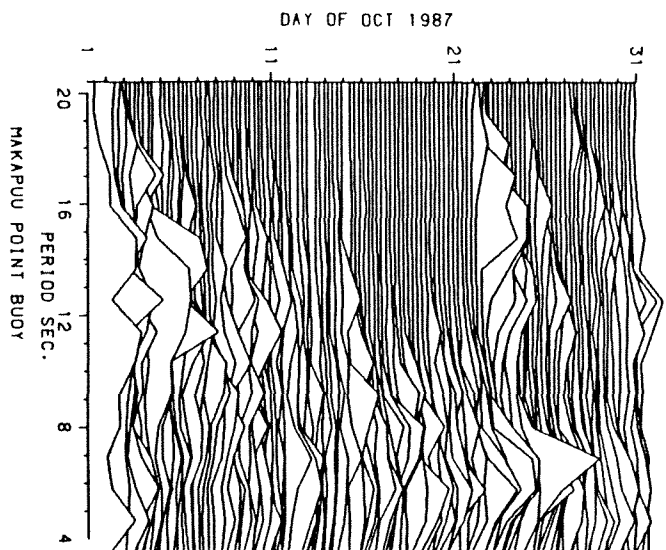
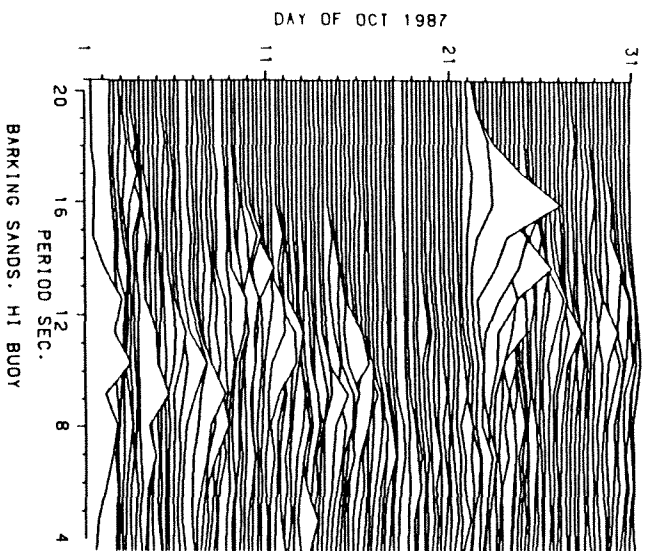


Figure 2-7. Wave spectra at CDIP measurement sites, October 1987.

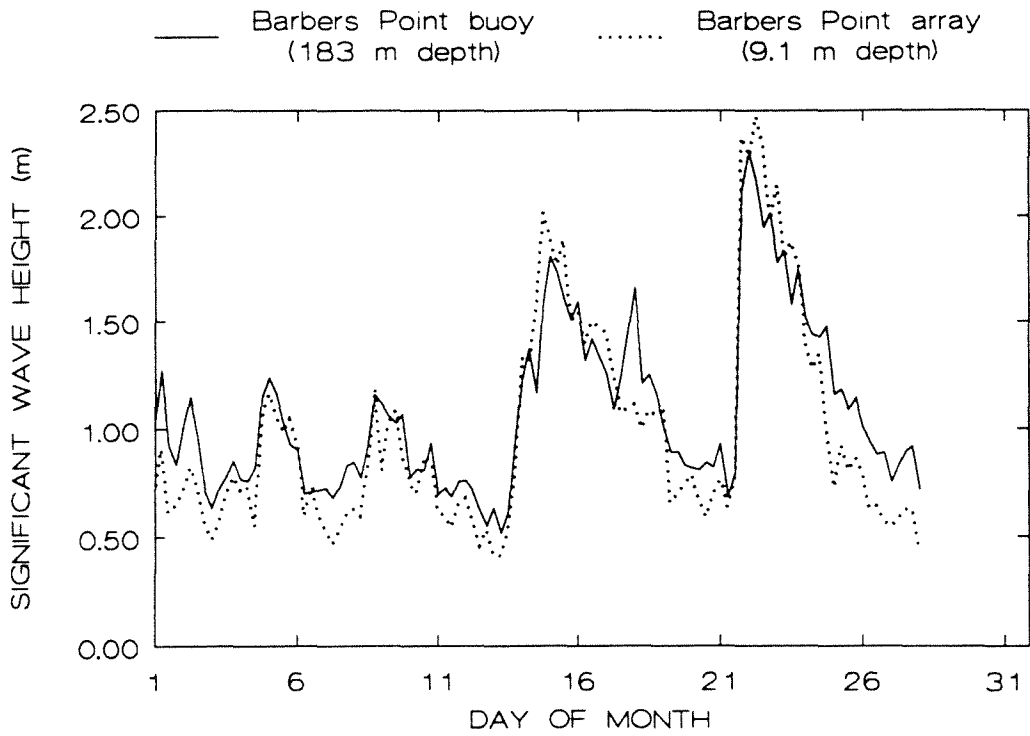
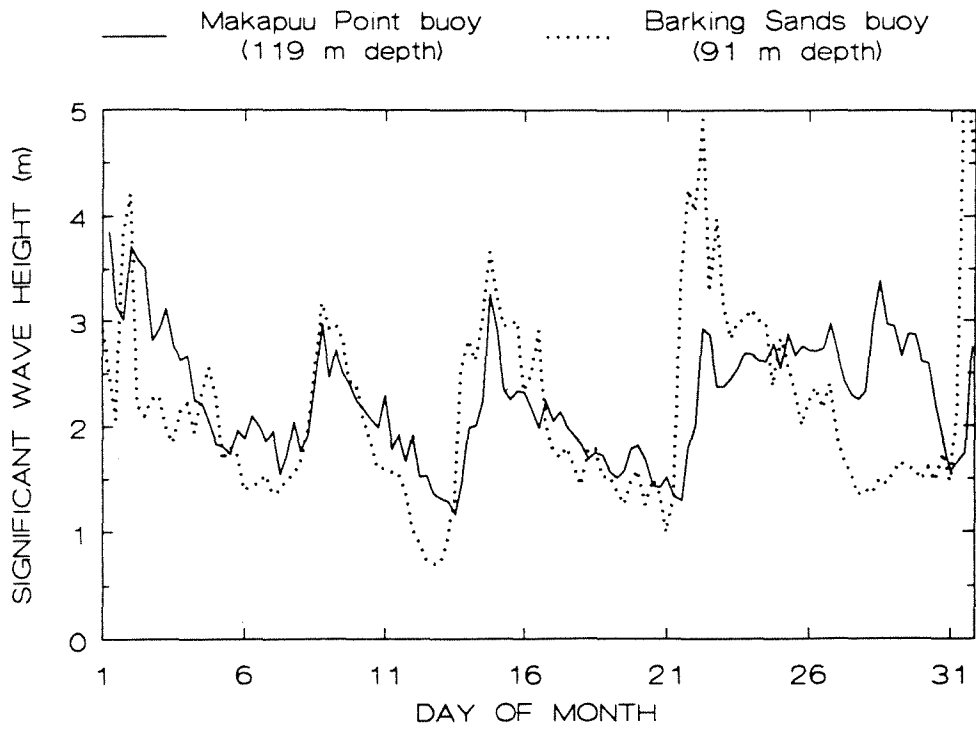


Figure 2-8. Significant wave heights at CDIP measurement sites, January 1988.

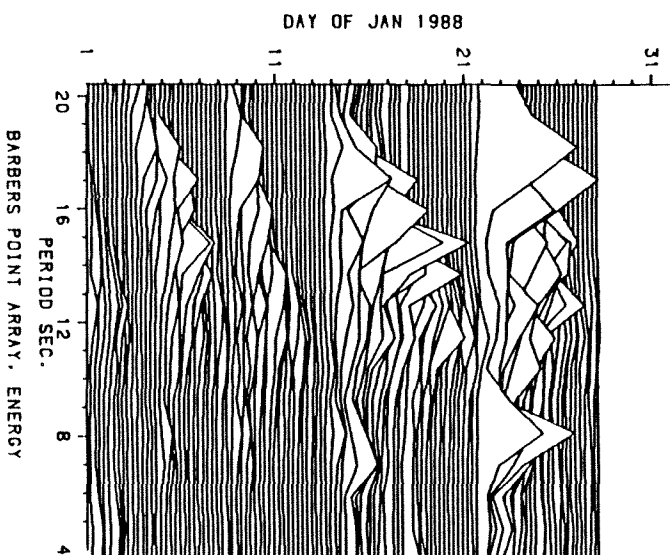
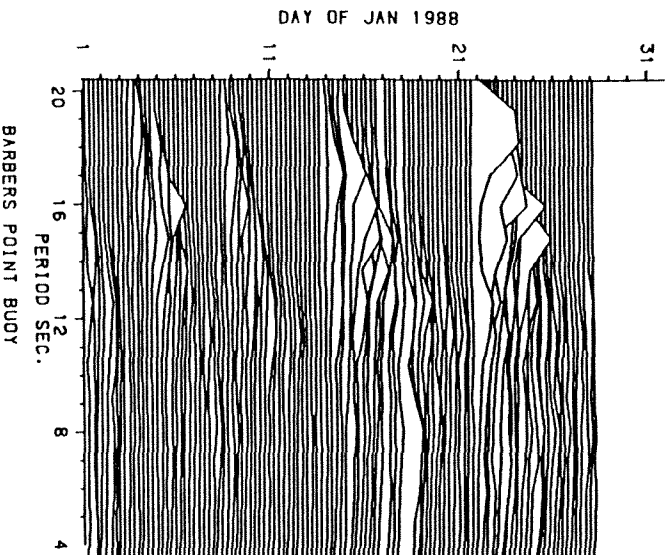
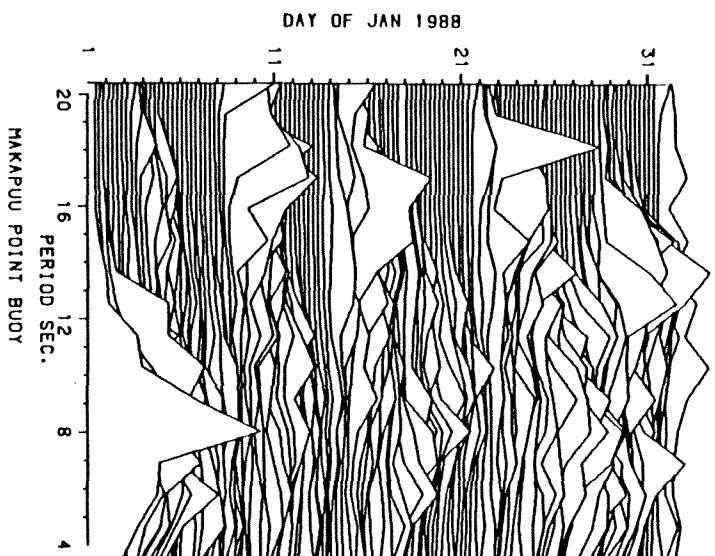
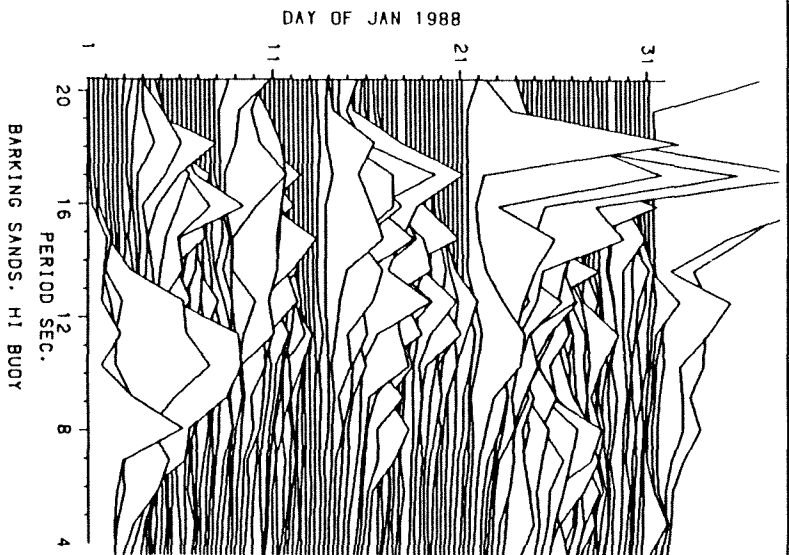


Figure 2-9. Wave spectra at CDIP measurement sites, January 1988.

At NOAA Station 51001, which is exposed to all three primary wave systems, winter waves are about 25% higher and summer waves about 25% lower than the annual average wave height (Figure 2-10). Winter waves are not as consistent as summer waves, however, as evidenced by the higher standard deviation of wave height relative to the monthly average during the winter. These seasonal patterns are explained by the predominance of north Pacific swell during the winter and trade wind waves during the summer. This is true even at Makapuu Point, which is partially sheltered from north Pacific swell. As expected, however, seasonal extremes are not as great at Makapuu Point as they are at Barking Sands, and wave heights are more consistent from day to day, particularly during the latter half of the year.

Annual wave statistics from the four measurement sites in outer shelf waters are compiled in Table 2-3. Incident wave power estimates are based on spectral formulas fitted to average wave spectra measured at Makapuu Point (procedure described below). Therefore, these formulas are not applicable to the other three measurement sites, which have significantly different degrees of exposure and sheltering.

As expected, dominant wave periods are shortest at Makapuu Point and Upolu Point, which are partially sheltered from long-period north Pacific swell. On the other hand, longer waves prevail at Barking Sands, due to the partial blockage of trade wind wave energy by Kauai's Na Pali coast. Prevailing waves are even longer at Barbers Point, which is completely sheltered from trade wind waves but exposed to north Pacific swell passing south of Niihau or between Kauai and Oahu. Furthermore, this site is fully exposed to Southern Ocean swell (unlike Barking Sands, where such swell is partially blocked by Niihau), giving Barbers Point the longest dominant wave periods listed in Table 2-2.

Due to the proximity of Maui, Upolu Point is more sheltered from northern north Pacific swell than Makapuu Point and thus has a lower average annual significant wave height. Like Barbers Point, Upolu Point is exposed to north Pacific swell passing south of Niihau. Coming more from the west, this swell originates with winter storms that are farther distant. Consequently, swell periods are somewhat longer at Upolu Point than at Makapuu Point. The average dominant wave period is shorter than at Barking Sands or Barbers Point, however, because of Upolu Point's better exposure to trade wind waves.

The Makapuu Point statistics in Table 2-2 illustrate the importance of accounting for incomplete data recovery when assessing year-to-year variability of the wave energy resource. Although these statistics suggest that 1983 was the least energetic year, this is an artifact caused by the absence of data in January through March, when unusually severe storms in the northwest Pacific Ocean actually generated *higher* waves than normal [11]. Although 1987 appears to have been the most energetic year, this again is an artifact, caused by the absence of data during 11 days in June, 26 days in July, and 6 days in August, biasing the record towards higher and longer-period winter waves.

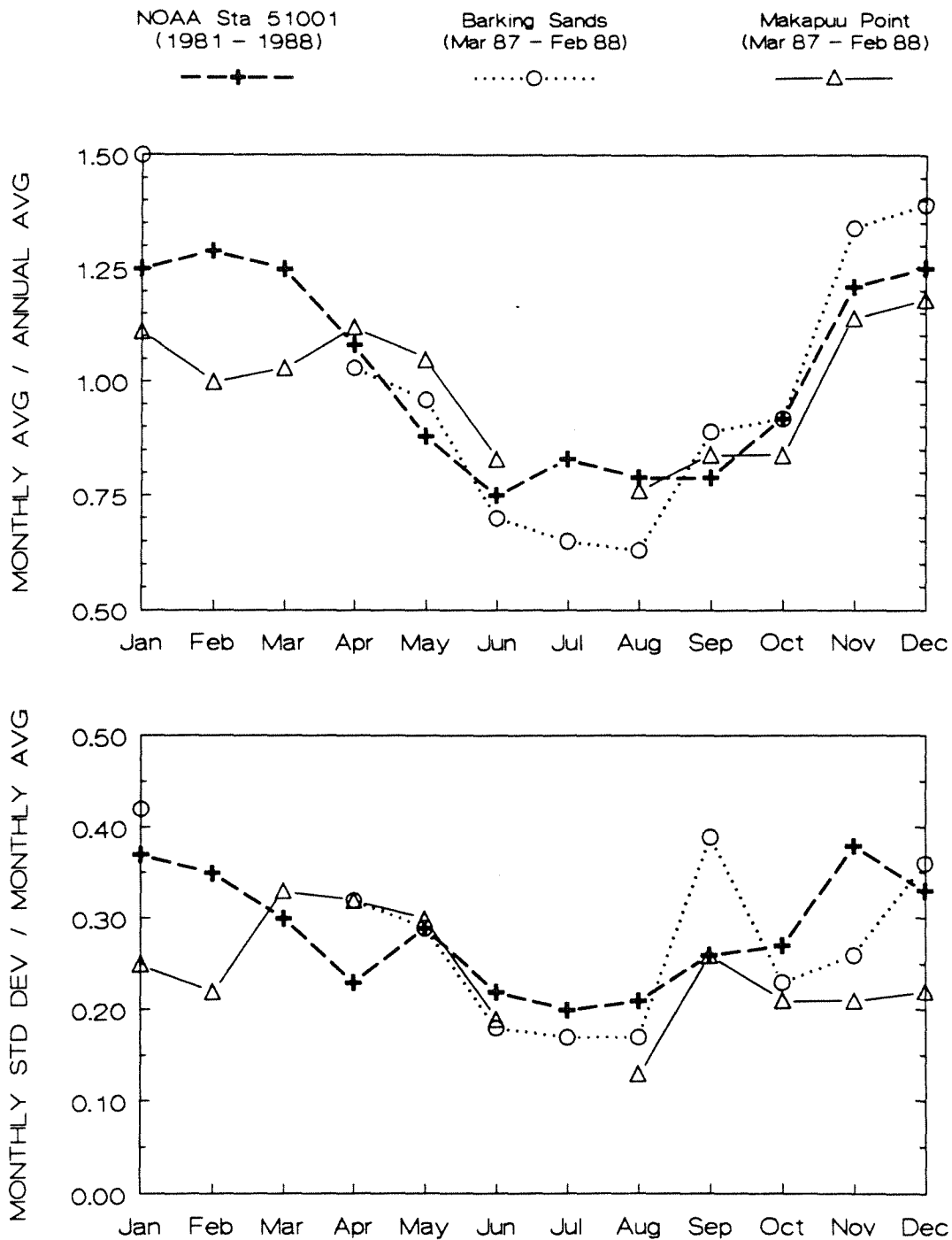


Figure 2-10. Seasonal variability of significant wave height.

Table 2-2
Annual Average Wave Statistics at Outer Shelf Measurement Sites

<u>12-Month Measurement Period</u>	<u>Missing Months</u>	<u>Data Recovery</u>	<u>Water Depth (m)</u>	<u>Significant Wave Height (m)</u>	<u>Dominant Wave Period (sec)</u>	<u>Incident Wave Power (kW/m)</u>
BARKING SANDS, KAUAI						
Dec 82 - Nov 83	Aug - Sep, Nov	63%	109	1.74	9.7	N/A
Feb 87 - Jan 88	Feb - Mar	80%	91	1.46	10.0	N/A
Jan 90 - Dec 90	Jun - Sep	61%	91	1.97	9.6	N/A
MAKAPUU POINT, OAHU						
Jan 82 - Dec 82	None	88%	187	1.96	8.3	15.9
Jan 83 - Dec 83	Jan - Mar	74%	187	1.81	7.9	13.3
Jan 84 - Dec 84	None	97%	187	1.80	7.9	13.7
Jan 86 - Dec 86	None	91%	119	1.86	8.5	14.9
Jan 87 - Dec 87	Jul	87%	119	2.05	8.8	18.4
Jan 88 - Dec 88	None	96%	119	1.85	8.0	14.5
Jan 89 - Dec 89	None	90%	119	1.83	8.3	14.3
BARBERS POINT, OAHU						
Jan 87 - Dec 87	None	85%	183	0.93	11.2	N/A
Jan 89 - Dec 89	None	86%	183	0.96	10.7	N/A
UPOLU POINT, HAWAII						
Jun 84 - May 85	Nov	86%	170	1.59	8.8	N/A
Jun 85 - May 86	None	97%	170	1.75	9.0	N/A

N/A Spectral formulas used in wave power computations are not applicable at these sites.

RESOURCE ASSESSMENT PROCEDURE

The first step in the resource assessment was to estimate the number of hours per year that various sea states occur in open, deep water off northern island coasts. To estimate the incident wave power associated with each sea state, a non-directional spectral formula was fitted to a set of measured spectra. Directional characteristics were then assigned to each component of the spectral formula. Finally, the directional spectra were subjected to a refraction and shoaling analysis, in order to map the wave energy resource at different depths along different island coasts.

Development of Deep-Water Sea State Probability Distribution

Wave conditions in open, deep water off northern island coasts were derived from the average annual joint probability distribution (JPD) table for the Waverider buoy at Makapuu Point, which has the widest northern exposure window and best data availability of any outer shelf measurement site in Hawaii. It should be noted that 1983 and 1987 are included in the average JPD table. Although these years are seasonally unbalanced, the lack of winter data in 1983 tends to offset the lack of summer data in 1987.

The annual average JPD table for Makapuu Point was modified as follows:

- Sea states having a dominant period greater than 10 seconds and a significant wave height less than 1.5 m were assumed to represent dominant southern swell.
- The balance between the other swell-dominated sea states and shorter-period sea states was adjusted to account for the fact that sea states dominated by north Pacific swell are under-represented at Makapuu Point, since waves coming out of the west through northwest are blocked by the island mass of Oahu.
- Outlying sea states having less than 0.1% probability of occurrence were removed, and the remaining probabilities were normalized to 100%.

The resulting JPD table is reproduced in Appendix B and has a total of 59 sea states with a non-zero probability of occurrence, six of which are dominated by southern swell.

Development of Spectral Formula

The equation for incident wave power in a random sea state is:

$$P = \frac{\rho g^2}{4\pi} \int \left(1 + \frac{2 k_f d}{\sinh 2 k_f d} \right) \tanh k_f d \frac{S(f)}{f} df$$

where ρ is water density, g is acceleration due to gravity, d is water depth, and k_f is the wave number ($k_f = 2\pi/L_f$, where L_f is wavelength). The subscript f indicates a particular harmonic component of the wave spectrum, where f is the component's frequency and $S(f)$ is the value of the spectrum at that frequency. The function $S(f)$ must be known so that the necessary integration can take place.

Table 2-3
Annual Average Joint Probability Distribution at Makapuu Point

Significant Wave Height Range (m)	Dominant Wave Period Range (sec)								
	<=6	6-8	8-10	10-12	12-14	14-16	16-18	18-22	>22
0.0
0.3
0.6
0.9	.03	.28	.27	.03	.02
1.2	1.38	1.78	2.27	.48	.30	.07	.	.	.
1.5	7.41	4.32	4.43	1.26	1.14	.42	.12	.	.
1.8	8.22	7.76	4.69	2.07	1.56	.52	.23	.	.
2.1	3.13	8.34	4.60	1.76	1.48	.38	.13	.01	.01
2.4	.65	6.34	3.06	1.51	1.20	.49	.18	.02	.01
2.7	.10	3.02	2.45	.84	.73	.42	.11	.	.02
3.0	.01	1.08	1.35	.56	.50	.28	.06	.	.01
3.3	.	.53	.65	.31	.30	.17	.03	.	.05
3.6	.	.18	.45	.15	.13	.08	.	.	.
3.9	.	.04	.26	.11	.05	.06	.01	.	.
4.2	.	.01	.14	.04	.05	.	.02	.	.01
4.5	.	.	.08	.02	.02
4.8	.	.	.04	.01	.01
5.101	.	.01	.01	.	.
5.401	.	.	.01	.	.
5.7
6.0

Sea states are characterized by significant wave height and dominant wave period. For example, the most common sea state at Makapuu Point has a significant wave height between 1.8 and 2.1 m, and a dominant wave period of 6 to 8 sec. This sea state has an 8.3% annual probability of occurrence, which corresponds to 727 hours (about 30 days) out of a year.

Therefore, the next step in the resource assessment procedure was to develop a wave spectrum for each sea state having a non-zero probability of occurrence in the modified JPD table. A three-component theoretical spectrum was fitted to 233 spectra measured at Makapuu Point during April and October 1987. Each component spectrum is represented by a three-parameter Ochi-Hubble formula [12], giving a total of nine parameters necessary to describe the spectrum. Two are fixed by the measured sea state parameters (overall significant wave height, H_s , and overall dominant wave period, T_p). The remaining seven parameters were adjusted by trial and error until the best fit to the average measured spectrum was obtained. Examples of the fit are shown in Figure 2-11. Spectral plots for each sea state having a non-zero probability of occurrence in the modified JPD are presented in Appendix B.

It should be noted that for a given H_s and T_p combination, the shape of the spectrum describes the frequency distribution of energy, which has considerable effect on the performance of any wave energy device whose efficiency is period-sensitive. The use of a single-peaked spectrum, such as the Bretschneider formula, to represent Hawaiian sea states could lead to errors not only in resource assessment, but also in model testing and performance projections by developers (Figure 2-12).

To check the accuracy of the formula, incident wave power was computed for each of the 233 original sea states by applying the spectral formula to the two measured sea state parameters. As shown in Figure 2-13, the computed wave power estimate was generally within $\pm 20\%$ of the measured value for a given individual sea state, and the aggregate fit for all 233 sea states is good. Overall, the formula underestimates measured wave power by about 5%, which is conservative.

Assignment of Directional Characteristics to Deep-Water Spectra

Finally, directional characteristics were assigned to the various component spectra. As previously mentioned, a deep-water directional wave hindcast has been published by the U.S. Army Corps of Engineers for seven grid points in Hawaii [6]. Directional statistics from the four grid points nearest the islands (Stations 30 through 33; see Figure 2-1) were averaged for sixteen H_s and T_p categories. The average directional distribution (Figure 2-14) was then applied to the dominant spectral component in each sea state of the modified JPD table. Mean directions were assigned to the lesser two component spectra according to the component's peak wave period: if 5 to 8 seconds, the lesser component was assumed to be background trade wind wave energy coming from the northeast; if 9 to 14 seconds, the lesser component was assumed to be background swell energy coming from the north-northwest.

The resulting directional distribution of wave power in open, deep water north of the islands is plotted in Figure 2-15. Note that lesser component spectra account for more than 60% of the annual wave energy flux, about evenly divided between background north Pacific swell and background trade wind waves.

LOW WAVE CONDITIONS ($H_s < 1.8$ m)

o Average measured spectrum

— Best fit theoretical spectrum

--- Theoretical component spectra

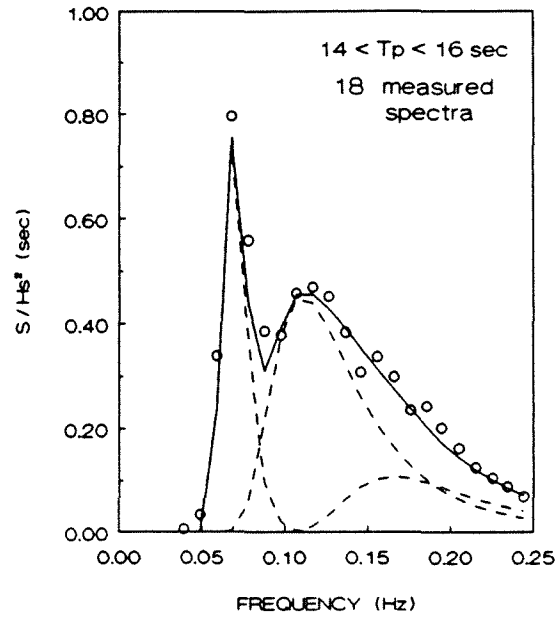
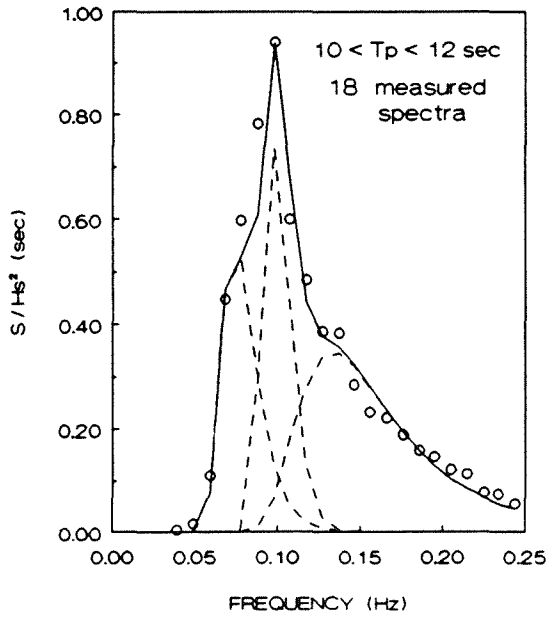
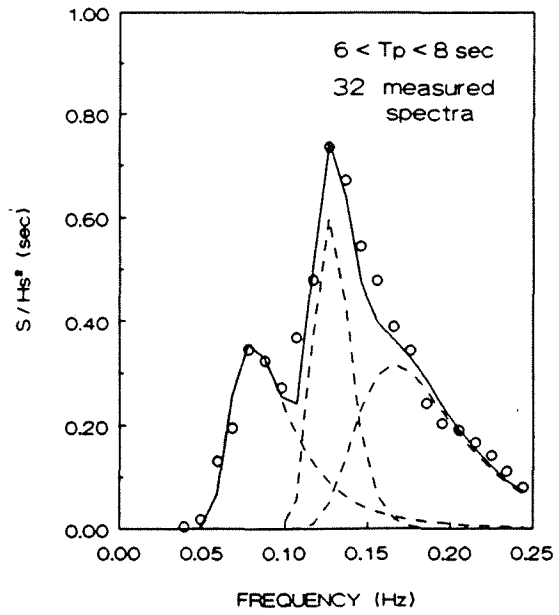
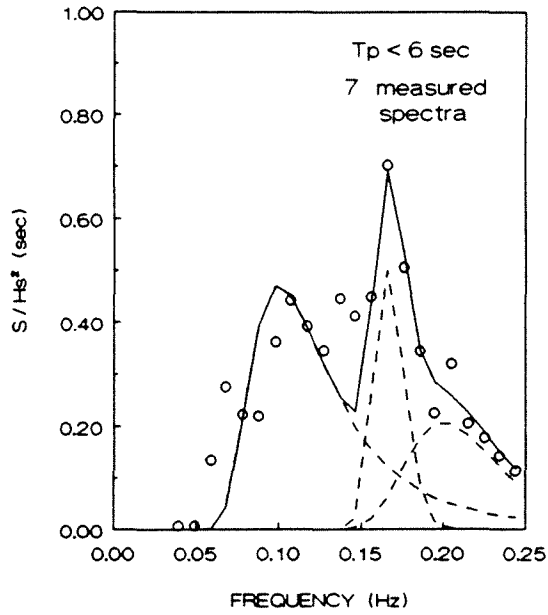


Figure 2-11. Fit of three-component spectra to measured spectra.

LOW WAVE CONDITIONS ($H_s = 1.65$ m)

— 3-component spectrum

..... Bretschneider spectrum

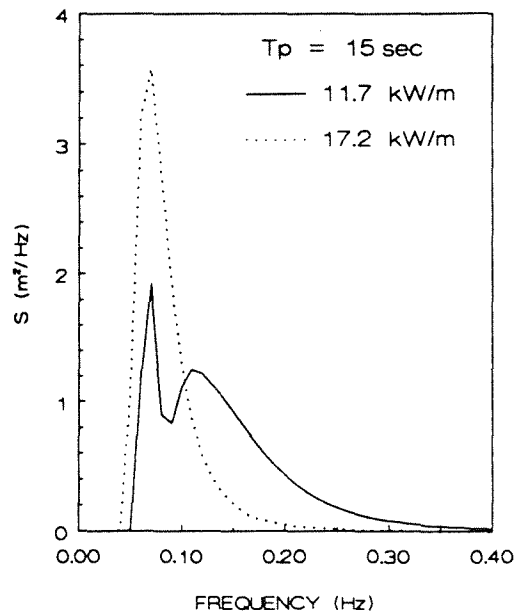
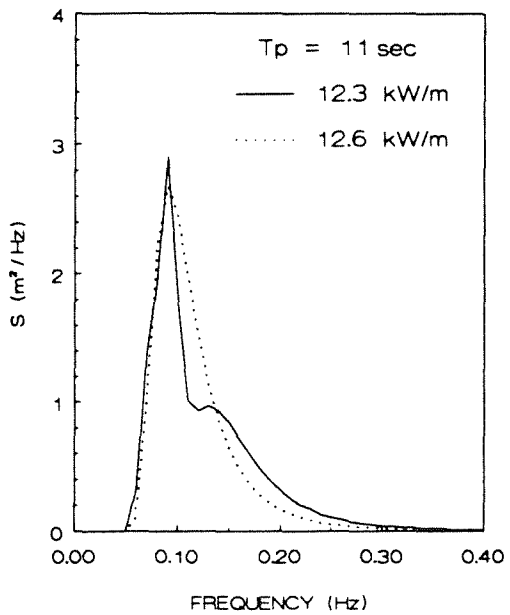
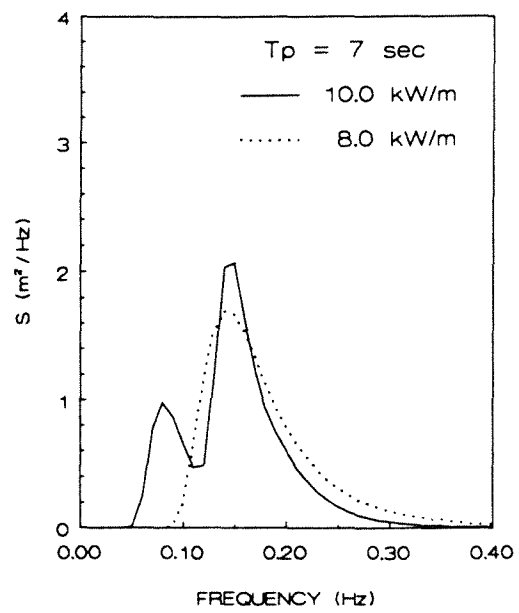
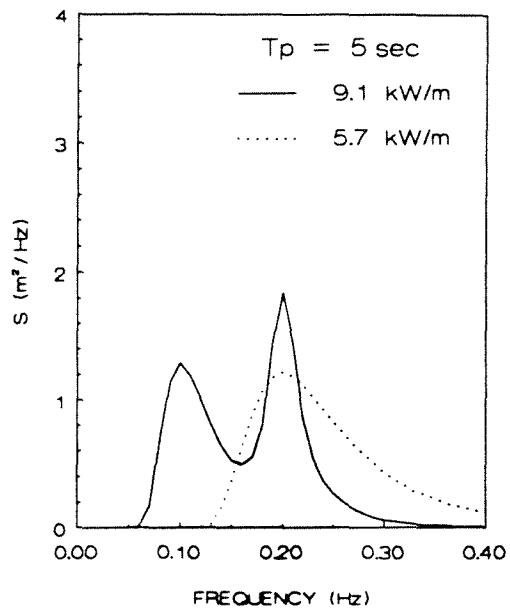


Figure 2-12. Comparison of Bretschneider and three-component spectra.

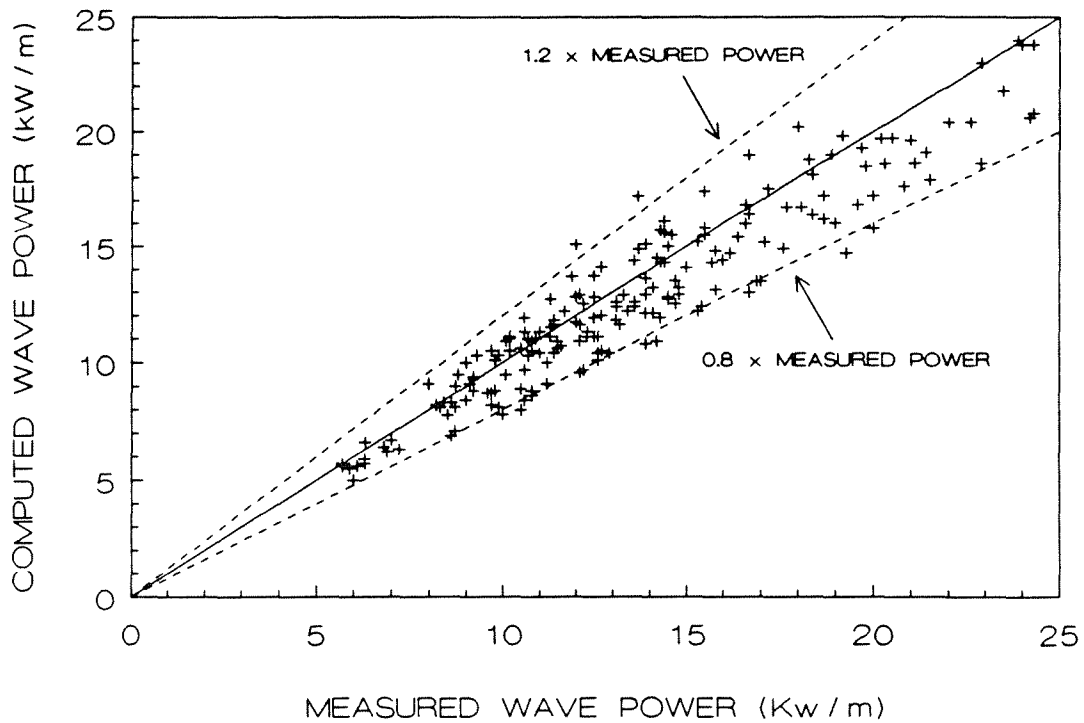
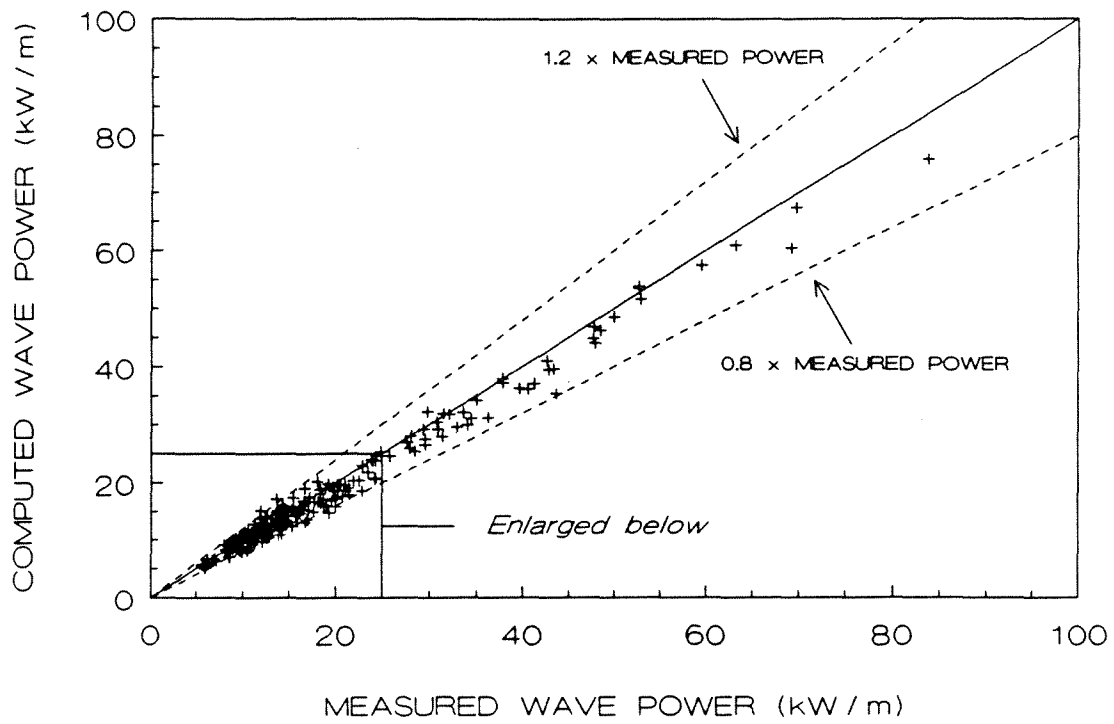


Figure 2-13. Accuracy of wave power estimates based on three-component spectra.

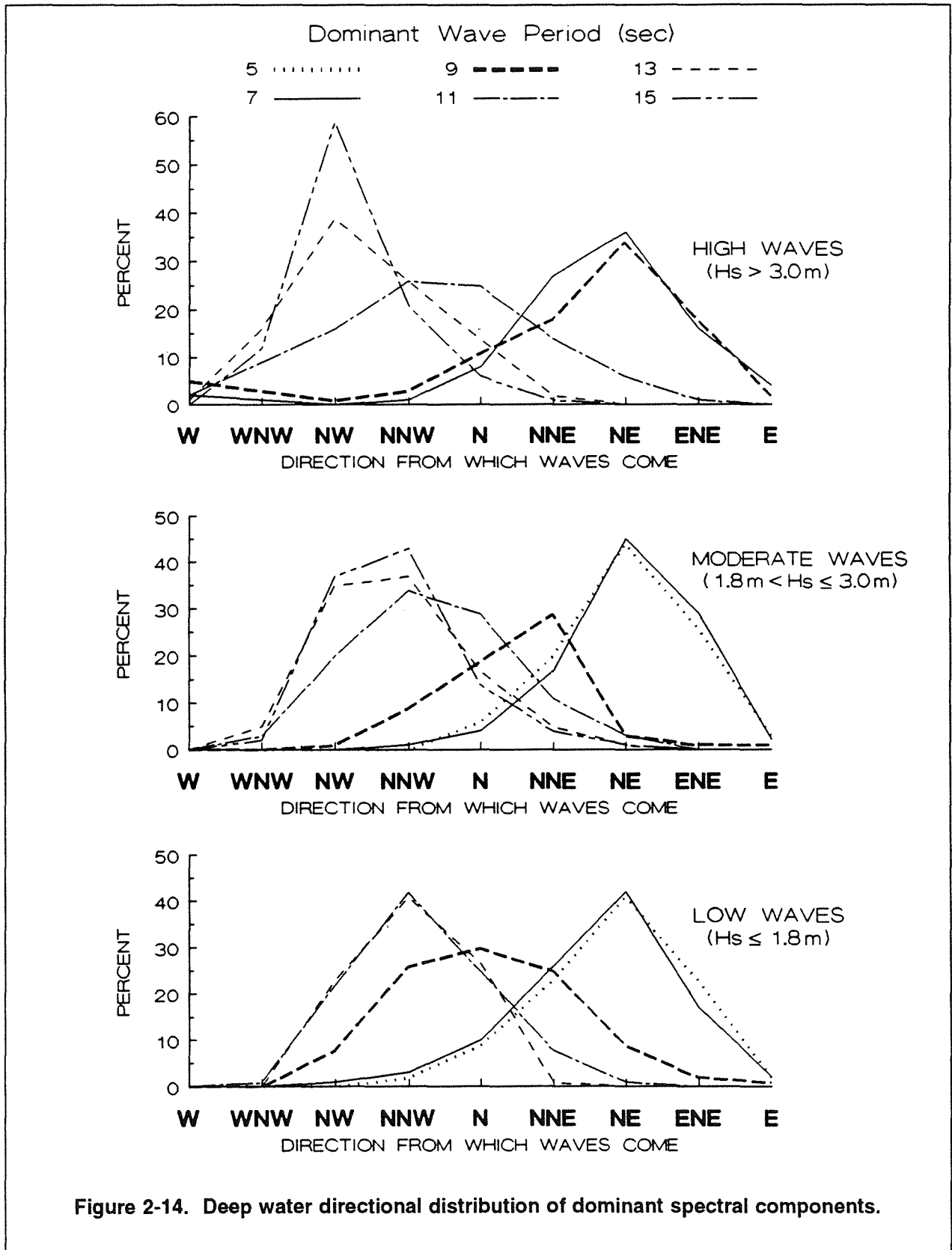


Figure 2-14. Deep water directional distribution of dominant spectral components.

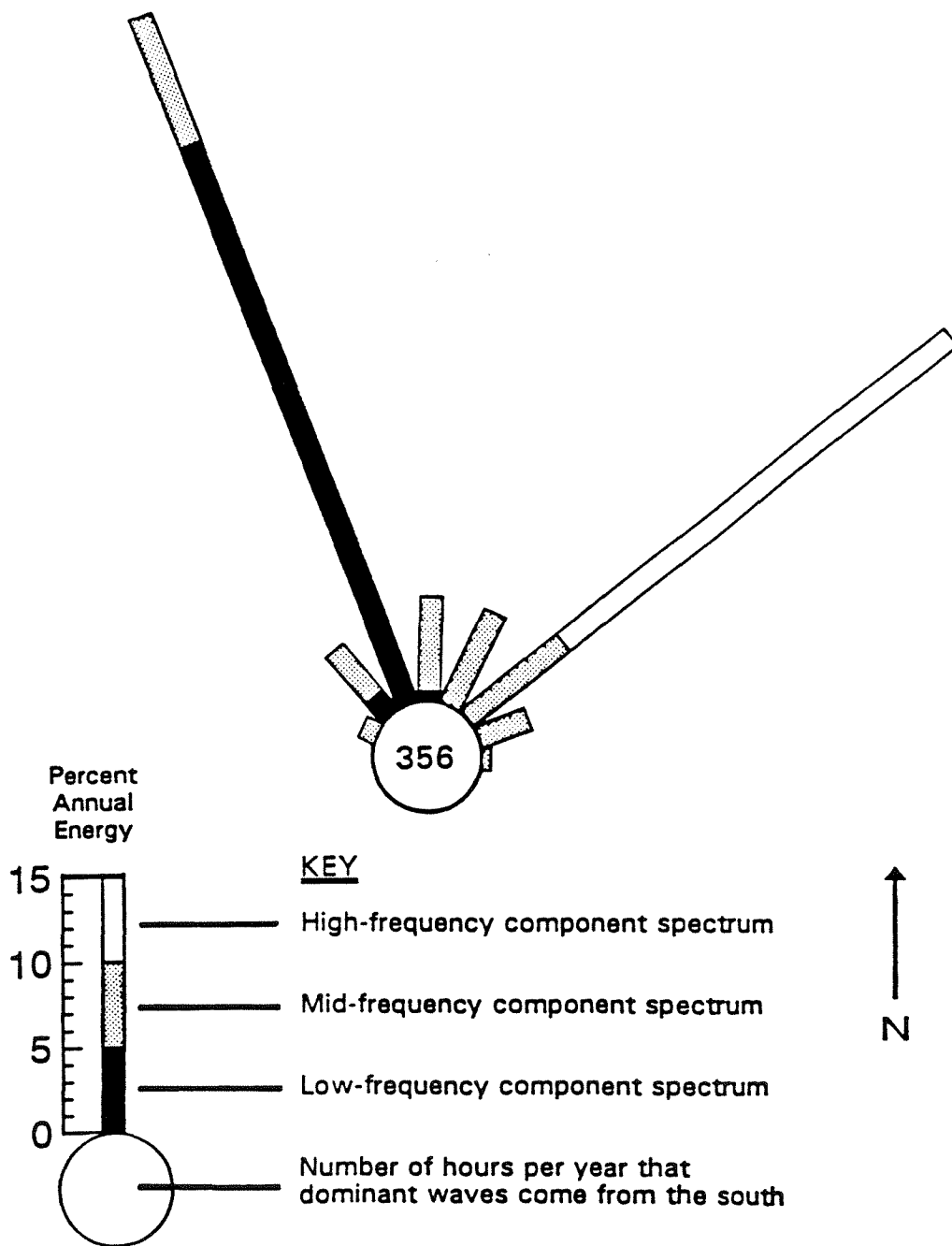


Figure 2-15. Deep water directional distribution of wave energy.

Refraction and Shoaling Analysis

Mitsuyasu's frequency-dependent directional spreading function [13] was used to describe the angular distribution of wave energy about the mean wave direction for each component spectrum. The maximum value of the spreading parameter (see Appendix A for definition) was assumed to be 50 for dominant swell, 10 for dominant sea, and 6 for lesser sea or swell.

The islands of Kauai, Oahu, Maui, Molokai, and Hawaii were divided into a total of twenty-four coastal segments, each having a different orientation and a different degree of sheltering by adjacent coastal features or neighboring islands (Table 2-4). Annual average wave power was then estimated at five water depths for each coastal segment, using a spectral refraction and shoaling program, which makes the following assumptions [14]:

- Depth contours are straight and parallel. This is a reasonable approximation for most coastal segments, and is necessary to keep the computation at a manageable level.
- The effects of bottom friction on wave energy dissipation are negligible. This is a reasonable assumption, given the narrowness of northern island shelves, with the possible exception of Kahului, Maui, where the shelf attains a width of 10 km.
- Non-linear shoaling and wave breaking are not accounted for. These phenomena are expected to be important in the shallowest water depths, and wave power estimates for the 5 m depth contour may be optimistic for this reason.

In addition to the above assumptions regarding wave transformation in shallow water, the computation procedure does not account for diffraction of waves into areas sheltered by a coastal peninsula or neighboring island. Likewise, dead calm conditions are assumed for sea states dominated by southern swell or wind-driven seas from the south. These are both conservative assumptions.

Finally, in applying the program to multi-peaked spectra, it was assumed that the shallow-water transformation of each component spectrum is independent of the other two component spectra; that is, to a first approximation, wave-wave interactions leading to the transfer of energy from one component spectrum to another can be ignored. Following numerical transformation, the component spectra were recombined in the depth of interest, to create the overall shallow-water spectrum.

It should be noted that the refraction and shoaling program was applied at the mid-point of each coastal segment. The results are adequate to reveal trends in the geographic distribution of the wave energy resource, but do not represent wave conditions at all potential project sites along a given segment. The degree of sheltering by adjacent coastal features and neighboring islands can vary substantially along even a single coastal segment, and site-specific wave modelling would be required for any sort of design study of a specific project. Bathymetric charts and data available to support such an effort are described in Appendix C.

Table 2-4

North-Facing Coastal Segments for Refraction and Shoaling Analysis

<u>Segment Designation</u>	<u>Description</u>	<u>Length</u>	<u>Facing Azimuth</u>	<u>Exposure Window *</u>
KAUAI-1	Nahili Point to Makaha Point	12 km	295°	-35° to +90°
KAUAI-2	Makaha Point to Haena	18 km	330°	-80° to +90°
KAUAI-3	Haena to Kepuhi Point	23 km	5°	-90° to +90°
KAUAI-4	Kepuhi Point to Kahala Point	12 km	50°	-90° to +60°
OAHU-1	Kaena Point to Kaiaka Point	18 km	355°	-55° to +55°
OAHU-2	Kaiaka Point to 4 km SW of Kahuku Point	17 km	310°	-15° to +90°
OAHU-3	Kahuku Point vicinity	8 km	0°	-70° to +90°
OAHU-4	4 km SE of Kahuku Point to Pyramid Rock	34 km	55°	-90° to +55°
OAHU-5	Pyramid Rock to Moku Manu Island	4 km	355°	-30° to +90°
OAHU-6	Moku Manu Island to Makapuu Point	20 km	65°	-75° to +35°
MOLOKAI-1	Ilio Point to 6 km SW of Kahi Point	26 km	10°	-65° to +75°
MOLOKAI-2	West coast of Kalaupapa Peninsula	6 km	315°	-15° to +90°
MOLOKAI-3	East coast of Kalaupapa Peninsula	6 km	55°	-90° to +40°
MOLOKAI-4	6 km SE of Kahi Point to Lamaloa Head	20 km	0°	-65° to +90°
MAUI-1	Nakalele Point to Kahului	18 km	50°	-90° to +45°
MAUI-2	Kahului to Opana Point	20 km	345°	-40° to +90°
MAUI-3	Opana Point to Pukaulua Point	34 km	35°	-90° to +90°
HAWAII-1	Upolu Point to Kukuihaele	33 km	30°	-55° to +80°
HAWAII-2	Kukuihaele to Laupahoehoe Point	36 km	25°	-65° to +90°
HAWAII-3	Laupahoehoe Point to Pepeekeo Point	23 km	40°	-80° to +90°
HAWAII-4	Pepeekeo Point to Hilo Bay	12 km	90°	-90° to +25°
HAWAII-5	Hilo Bay to Leleiwi Point	8 km	0°	-10° to +90°
HAWAII-6	Leleiwi Point to 3 km NW of Kaloli Point	12 km	80°	-90° to +55°
HAWAII-7	3 km NW of Kaloli Point to Cape Kumukahi	16 km	30°	-60° to +90°

* Exposure window of segment mid-point, relative to facing azimuth.

RESOURCE ASSESSMENT RESULTS

The average wave power density along the twenty-four coastal segments listed in Table 2-3 is plotted as a function of water depth in Figures 2-16 through 2-22. As can be seen from these charts, wave power density along the 80 m depth contour typically averages 10 to 15 kW/m. Because the island shelves are so narrow, even this outer shelf depth contour can be closely sheltered by adjacent headlands or peninsulas, which is the case at Kailua, Oahu, and in the vicinity of Hilo. At these locations, wave power density along the 80 m depth contour ranges from 7 to 9 kW/m.

Refraction and shoaling significantly reduce wave power densities in shallow water; along the 5 m depth contour, they are roughly 20% lower than along the 80 m contour. Due to the wide variety of coastal orientations and exposures, shallow water wave power has greater longshore variability than it does in deep water and can range anywhere from 5 to 12 kW/m. A description of the wave resource distribution on each island is given below.

Kauai

Kauai's coastal outline is more regular than that of the other islands, lacking any large-scale embayments or peninsulas. It is also not sheltered by any neighboring island; the blocking effect of Niihau is negligible because so little wave energy comes from south of west. Kauai thus illustrates the effect that coastline orientation alone has on the wave resource (Figure 2-16).

The coast north of Nahili (KAUAI-1) faces so much to the west that even north Pacific swell (black portion of bars in Figure 2-16) undergoes substantial refraction. This coastline is also so far west around the island that trade wind waves (white portion of bars in Figure 2-16) are blocked by the Na Pali coast and as shown previously, are conspicuously absent from wave spectra measured off Barking Sands.

KAUAI-2 faces directly into the north Pacific swell, which experiences almost no refraction as it travels into shallow water. Although KAUAI-2 is more exposed to trade wind waves, they still undergo considerable refraction, coming predominantly from the northeast, almost at right angles to the coast.

Moving eastward, KAUAI-3 faces almost due north. North Pacific swell begins to experience some refraction, while trade wind waves experience less refraction. This coastline is thus well exposed to both types of waves and has the greatest average wave power density on the island.

Finally, KAUAI-4 faces directly into the trade wind waves, which are thus little affected by refraction. On the other hand, north Pacific swell arrives almost parallel to the depth contours and undergoes considerable refraction as it travels into shallow water.

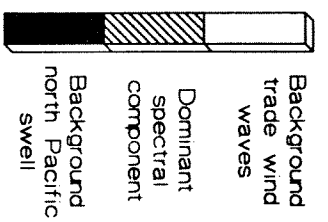
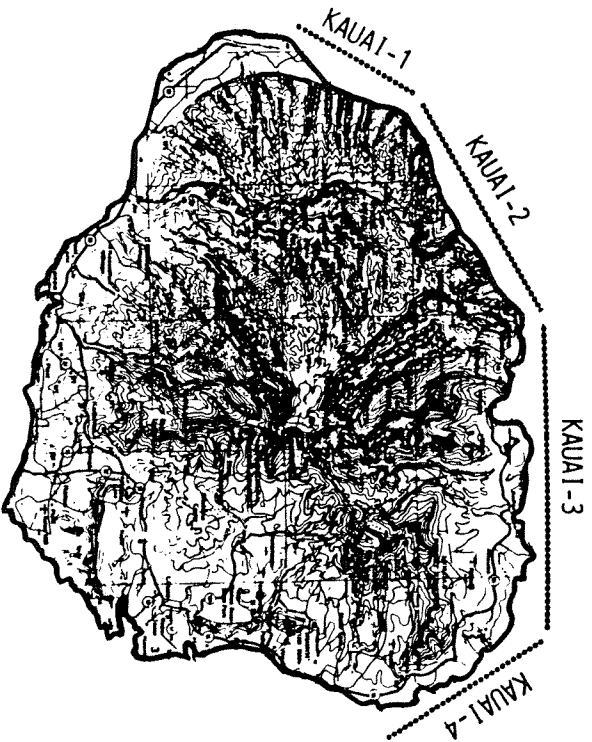
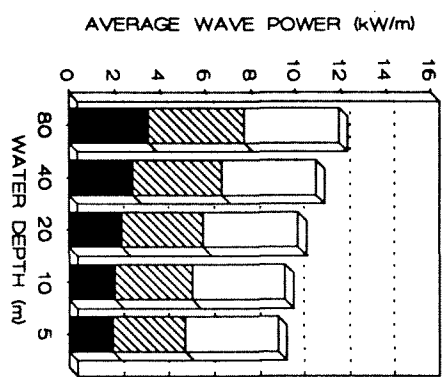
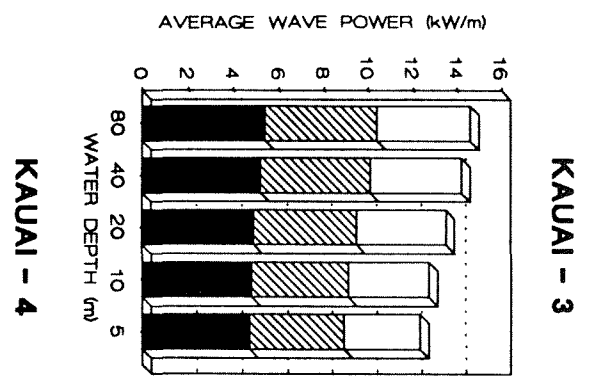
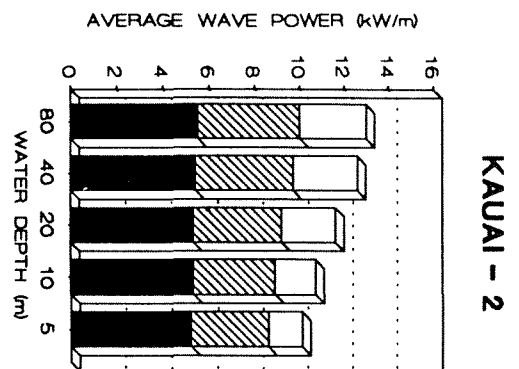
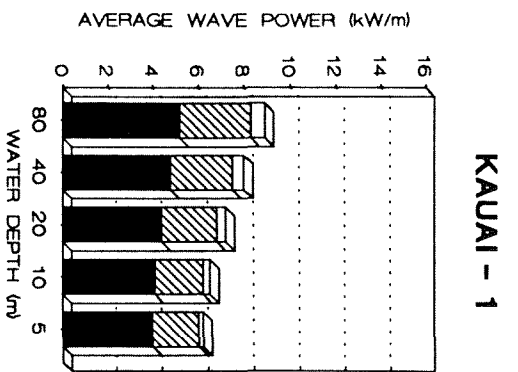


Figure 2-16. Wave power distribution along the north coast of Kauai.

Oahu

The effects of coastal orientation are similar to those described for Kauai. For example, OAHU-2 faces directly into the north Pacific swell, which is little affected by refraction (Figure 2-17). Consequently, these long-period waves build up into spectacular breakers, and are responsible for the popularity of such North Shore surfing spots as Waimea and Sunset Beach.

Wave power densities peak in the vicinity of Kahuku Point (OAHU-3) and then diminish as the coast becomes oriented farther away from the north Pacific swell (Figure 2-18). Kailua and Waimanalo Bay (OAHU-6) are closely sheltered by Mokapu Point, which blocks much of the swell that gets past Kahuku Point. This coastal segment is well exposed to trade wind wave energy, however, which shows up clearly in wave spectra measured by the CDIP buoy off Makapuu Point.

Molokai

Broad stretches of Molokai's coastline face almost due north, having good exposure to both north Pacific swell and trade wind waves (Figure 2-19). It is interesting to note that although both sides of the Kalaupapa Peninsula have similar wave power densities, the west coast (MOLOKAI-2) is dominated by north Pacific swell, while the east coast (MOLOKAI-3) is dominated by trade wind waves.

Maui

Even though MAUI-1 and MAUI-3 have roughly the same orientation, MAUI-1 is more closely sheltered by the island of Molokai, which partially blocks the north Pacific swell (Figure 2-20). As previously mentioned, these bar graphs represent wave conditions at midpoints along various coastal segments and should not be taken as indicative of the entire coastline. For example, Kahului Harbor is more sheltered from trade wind waves than the coastal midpoint of MAUI-1, and is more sheltered from north Pacific swell than the midpoint of MAUI-3. Furthermore, the shelf off Kahului is among the widest in the islands (10 km), and friction effects could be significant there.

Hawaii

The northwest coast of the Big Island (HAWAII-1) is closely sheltered by Maui. The wave energy resource improves considerably east of Waipio Bay (HAWAII-2), which has a wider exposure window and slightly more favorable orientation (Figure 2-21). North Pacific swell is blocked almost entirely from Hilo Bay and the coastline south of Lelewi Point (HAWAII-6), although these areas are well exposed to trade wind waves (Figure 2-22). HAWAII-7 is more exposed to north Pacific swell and wave power densities increase markedly in the direction of Cape Kumukahi.

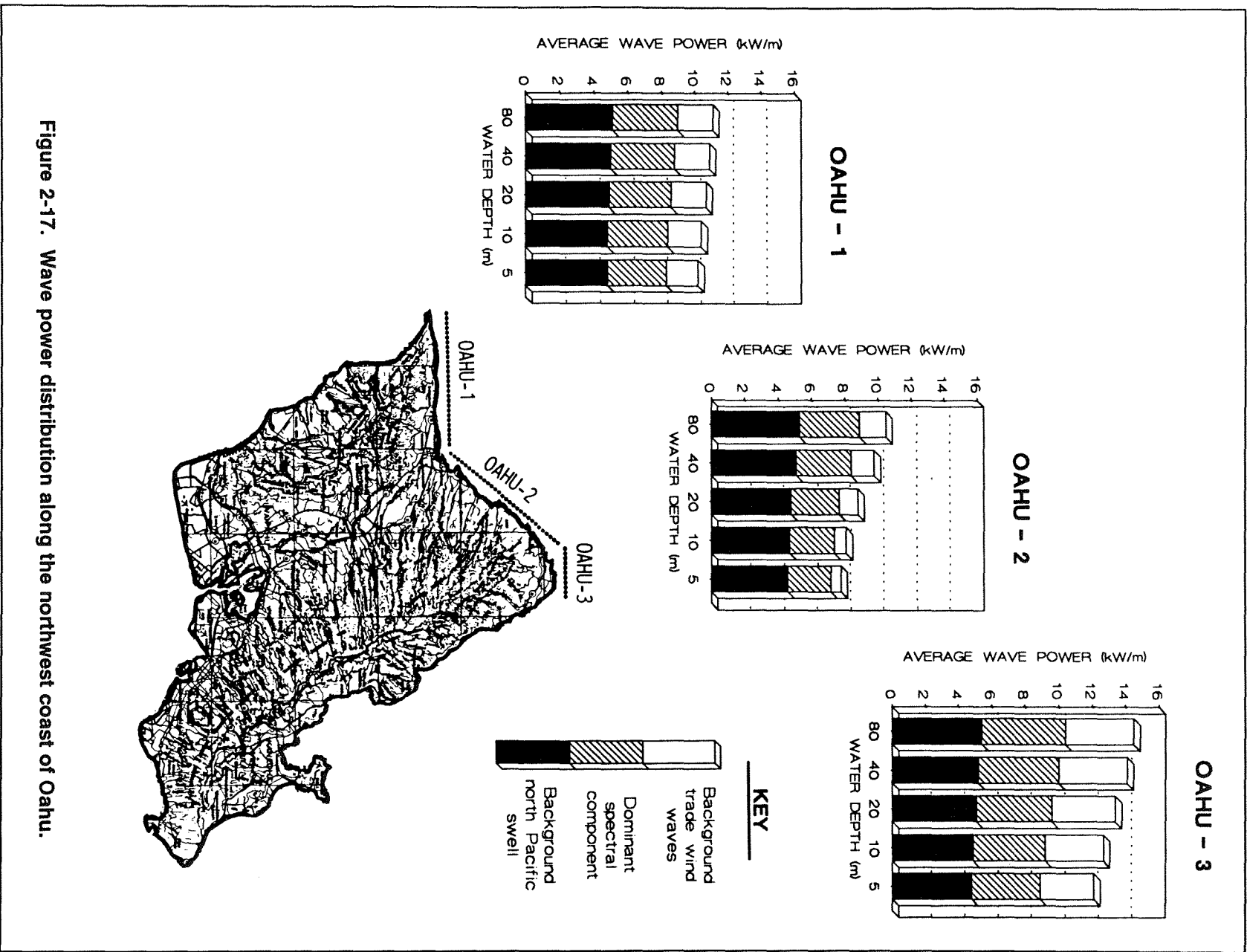


Figure 2-17. Wave power distribution along the northwest coast of Oahu.

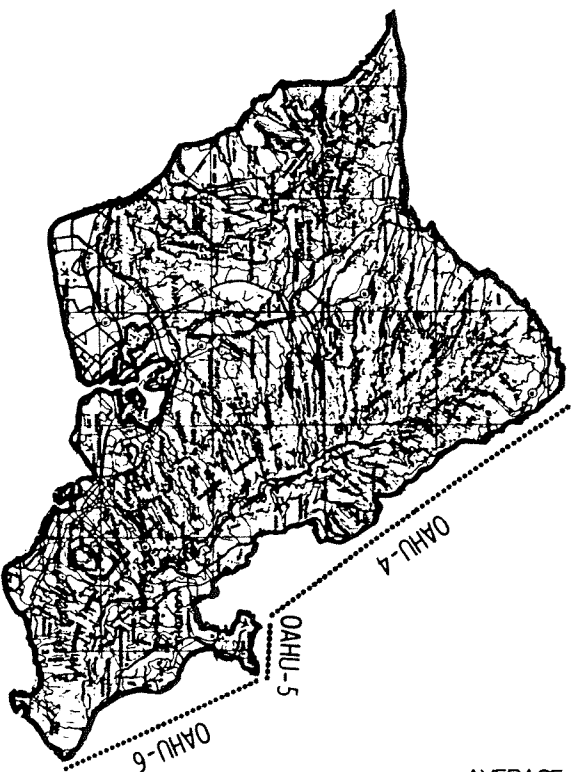
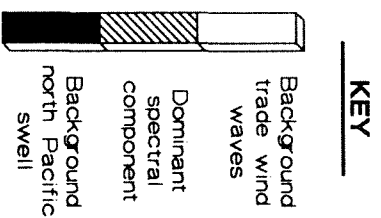
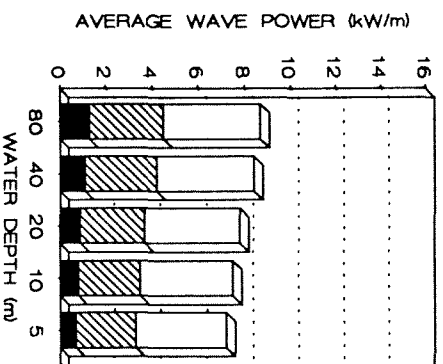
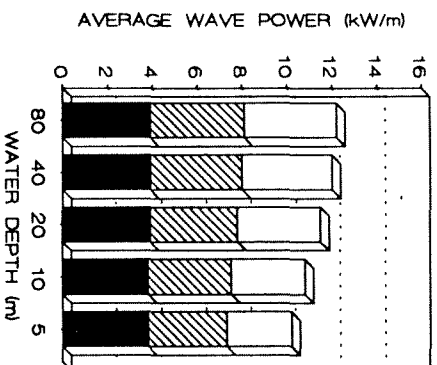
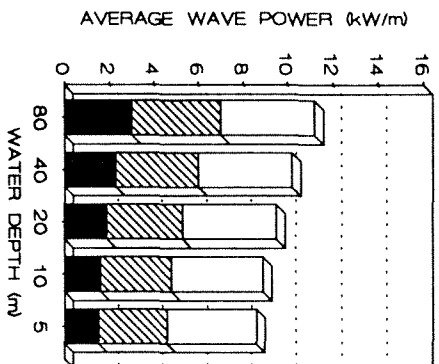
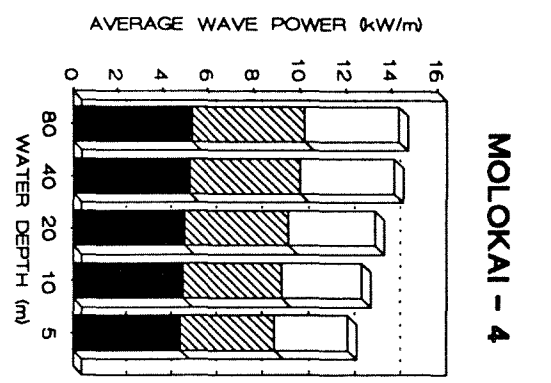
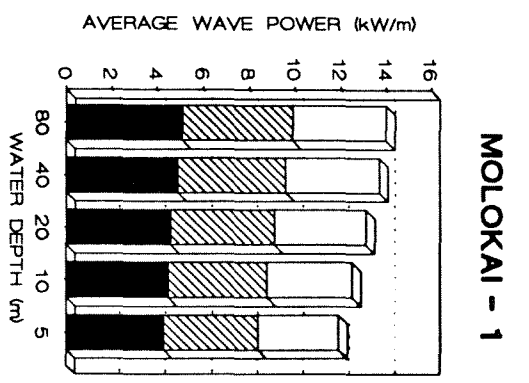
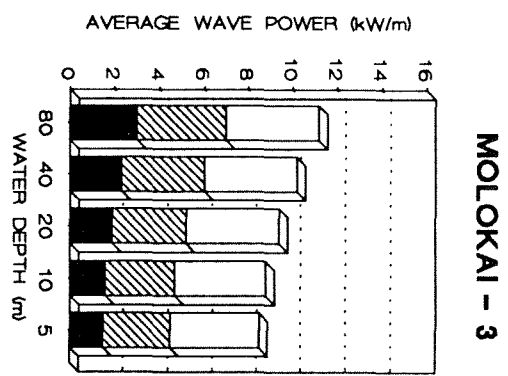
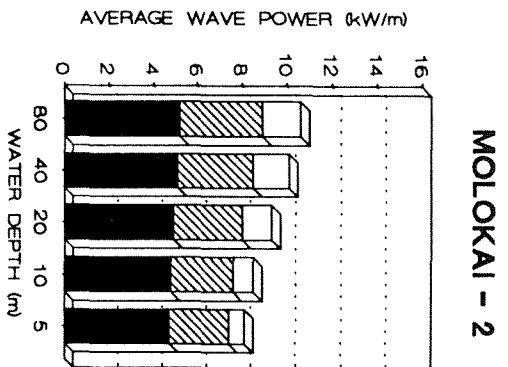


Figure 2-18. Wave power distribution along the northeast coast of Oahu.



KEY

- Background trade wind waves
- Dominant spectral component
- Background north Pacific swell

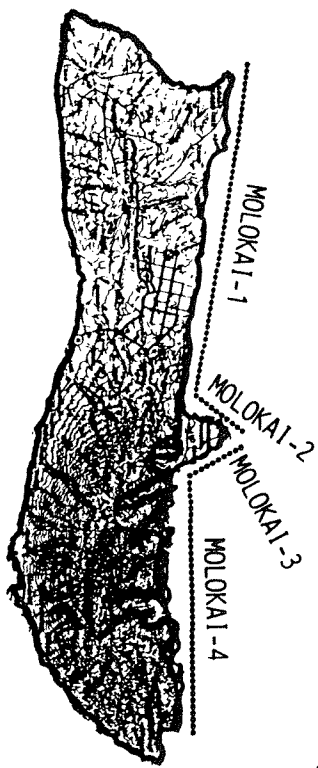
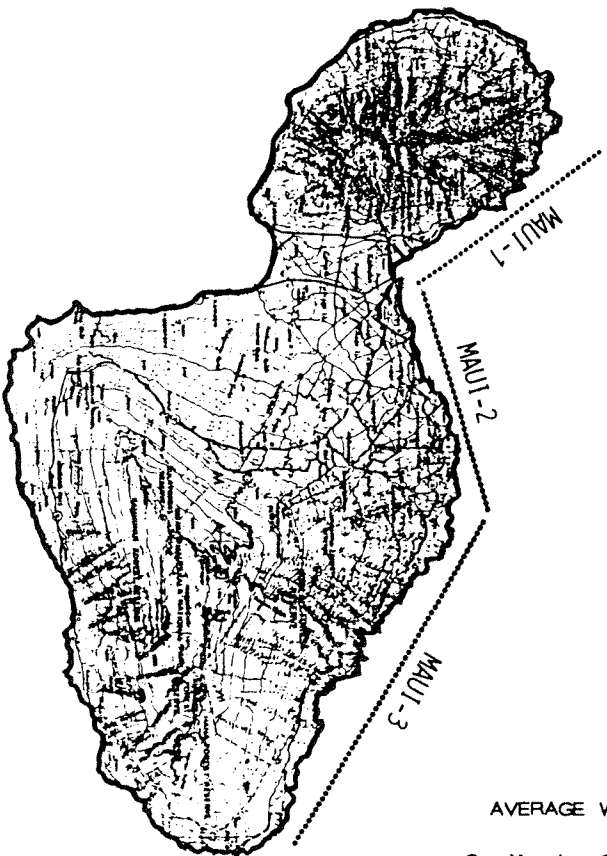
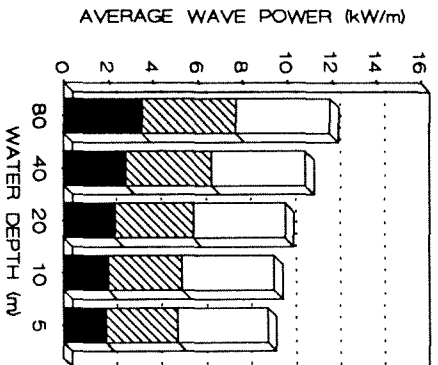


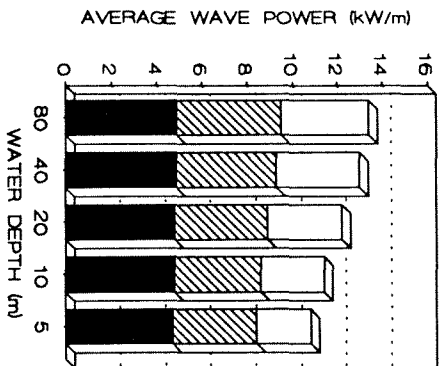
Figure 2-19. Wave power distribution along the north coast of Molokai.



MAUI - 1



MAUI - 2



MAUI - 3

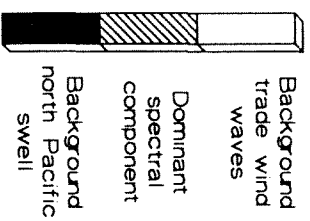
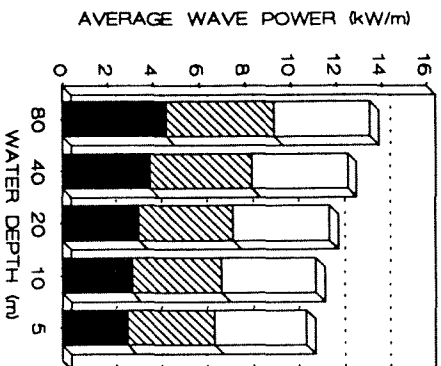


Figure 2-20. Wave power distribution along the north coast of Maui.

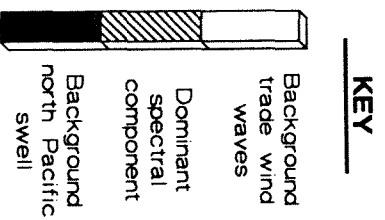
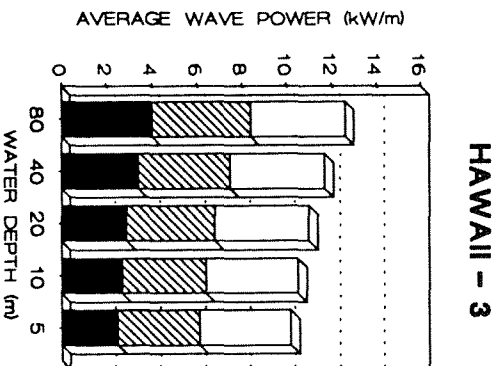
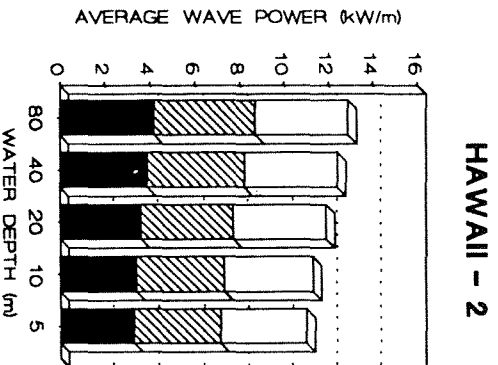
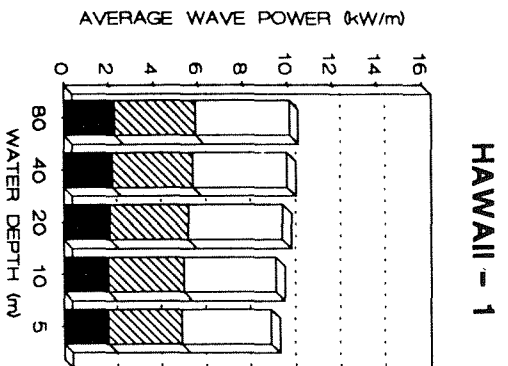
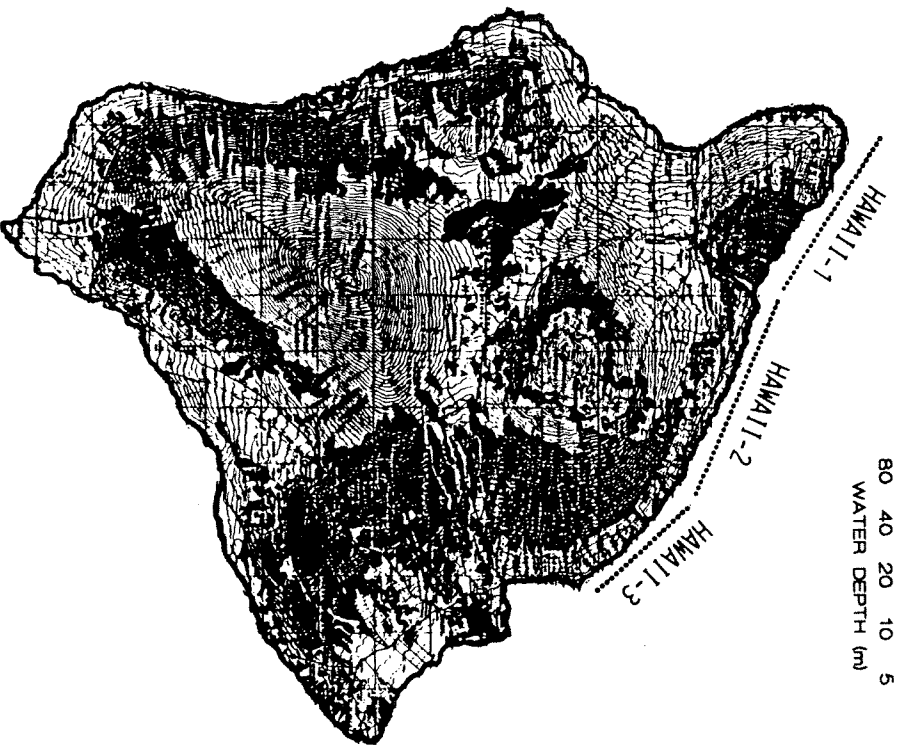


Figure 2-21. Wave power distribution along the north-northeast coast of Hawaii.

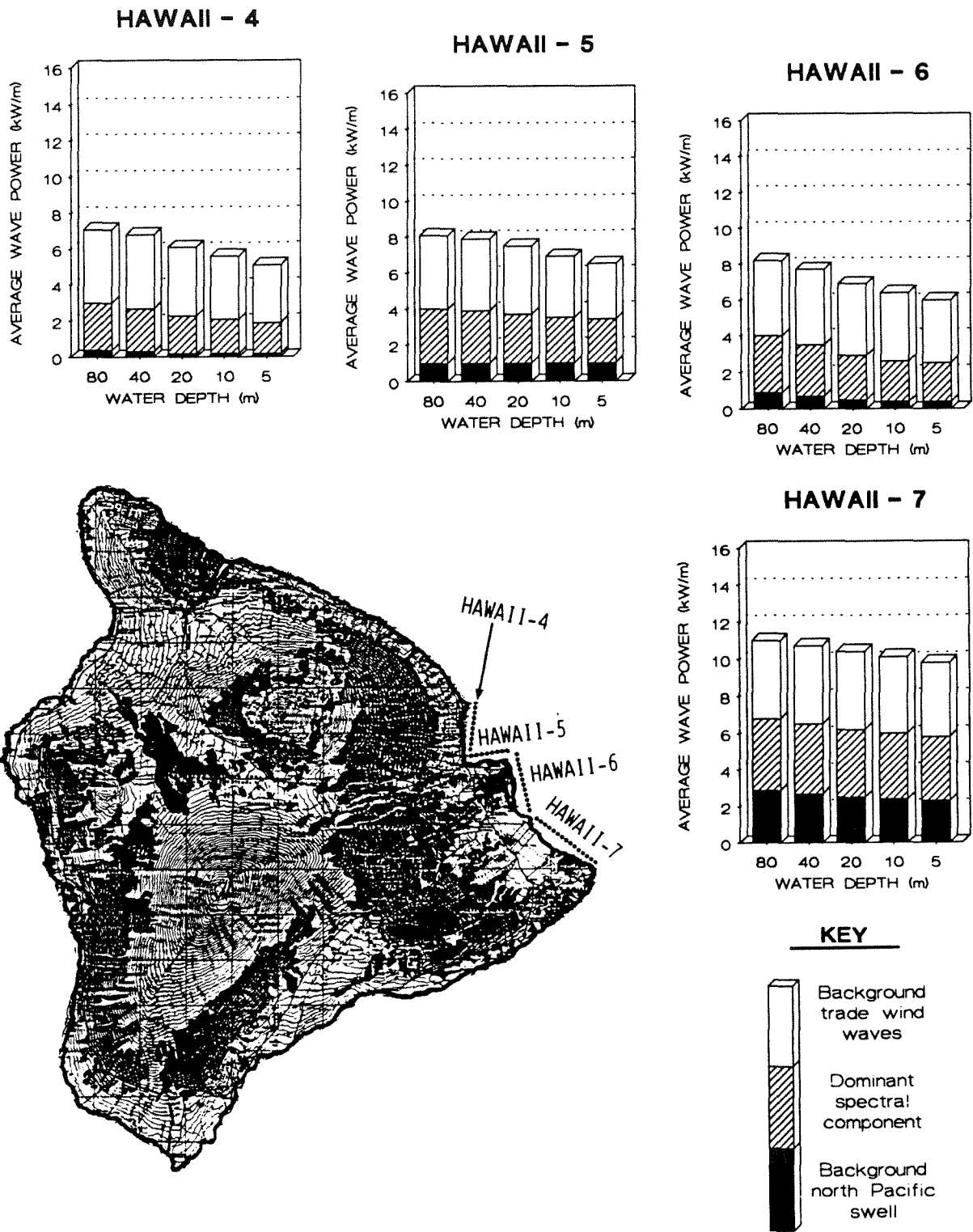


Figure 2-22. Wave power distribution along the east-northeast coast of Hawaii.

Total Resource Base

Multiplying the average wave power along a given depth contour by the length of each coastal segment and by the number of hours in a year, and summing the results for all segments, gives the annual wave energy resource for a particular island. This result is plotted for the 80 m and 5 m depth contours in Figure 2-23. Each island's annual electricity demand in 1990 is also plotted for comparison [15].

On Kauai, Maui, and Hawaii, recovering only 5% to 10% of the wave energy available along the 80 m depth contour could, in theory, meet the total electricity demand of these islands. Less than one half of one percent of Molokai's wave energy resource could meet the electricity needs of that island; recovering 5% of the wave energy off Kalaupapa Peninsula's west coast alone could do the same job. Except for Oahu, where electricity demand is comparable to two-thirds of the resource base, wave energy can be withdrawn at very low levels and still make a substantial contribution to island energy needs.

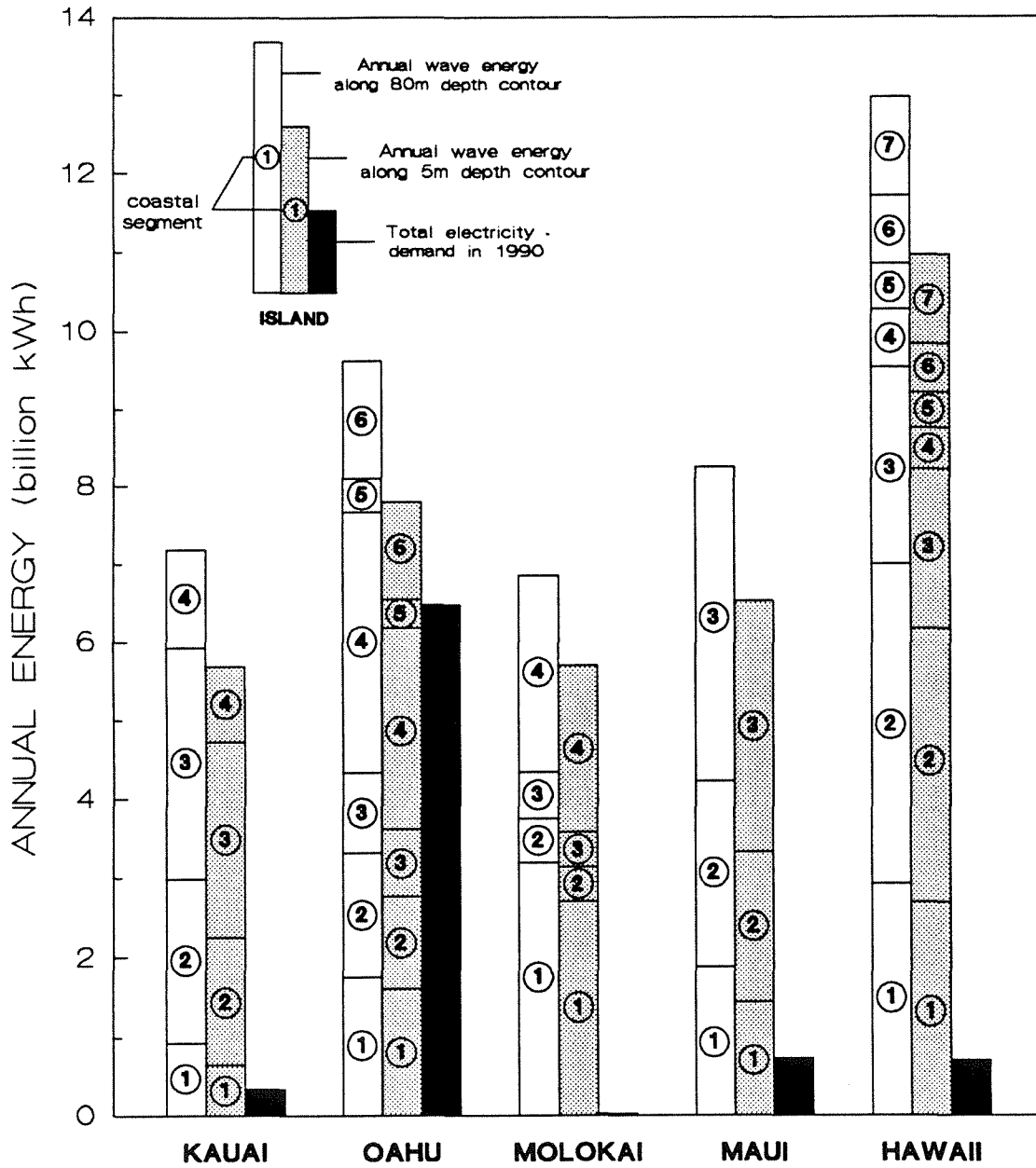


Figure 2-23. Annual wave energy resource compared with annual electricity demand.

Section 3
TECHNOLOGY SURVEY

The basic wave energy conversion process can be stated in very general terms: the force (or torque) of an incident wave causes relative motion between an absorber and a reaction point, which drives a working fluid through a generator prime mover. The periodic nature of ocean waves dictates that this relative motion will be oscillatory and have a frequency range of 3 to 30 cycles per minute, much less than the hundreds of revolutions per minute required for electric power generation. A variety of working fluids and prime movers are employed to convert these slow-acting, reversing wave forces into high-speed, unidirectional rotation of a generator shaft.

Twelve distinct process variations can be identified, as shown in Figure 3-1. The major distinguishing features among different conversion processes are as follows:

- Mode of energy absorption
 - Pitch (torque about an axis parallel to the prevailing wave crests)
 - Heave (vertical force on absorber)
 - Surge (horizontal force on absorber)
- Type of absorber
 - Free surface of the water
 - Fabricated structure (rigid or flexible)
- Type of reaction point
 - Fixed structure (concrete surfaces or land)
 - Seafloor anchor (deadweight or pile)
 - Inertial structure (suspended plate or buoyant spine)
- Type of working fluid
 - Air
 - Seawater
 - Hydraulic fluid

Wave power plants can be based on land, on caissons in relatively shallow water (5-15 m depth), or in deeper, offshore waters. Land-based systems include the Tapered Channel (Process 1) and a variety of fixed oscillating water column (OWC) devices (Process 2). Caisson-based systems include fixed OWC devices (Process 2), pivoting flaps (Process 4), and confined, heaving floats (Process 5). Offshore systems include floating OWC devices (Process 3), heaving buoys (Processes 6 and 7), contouring floats (Processes 8 and 9), the pitching Edinburgh Duck (Process 10), the SEA Clam (Process 11), and the submerged Bristol Cylinder (Process 12).

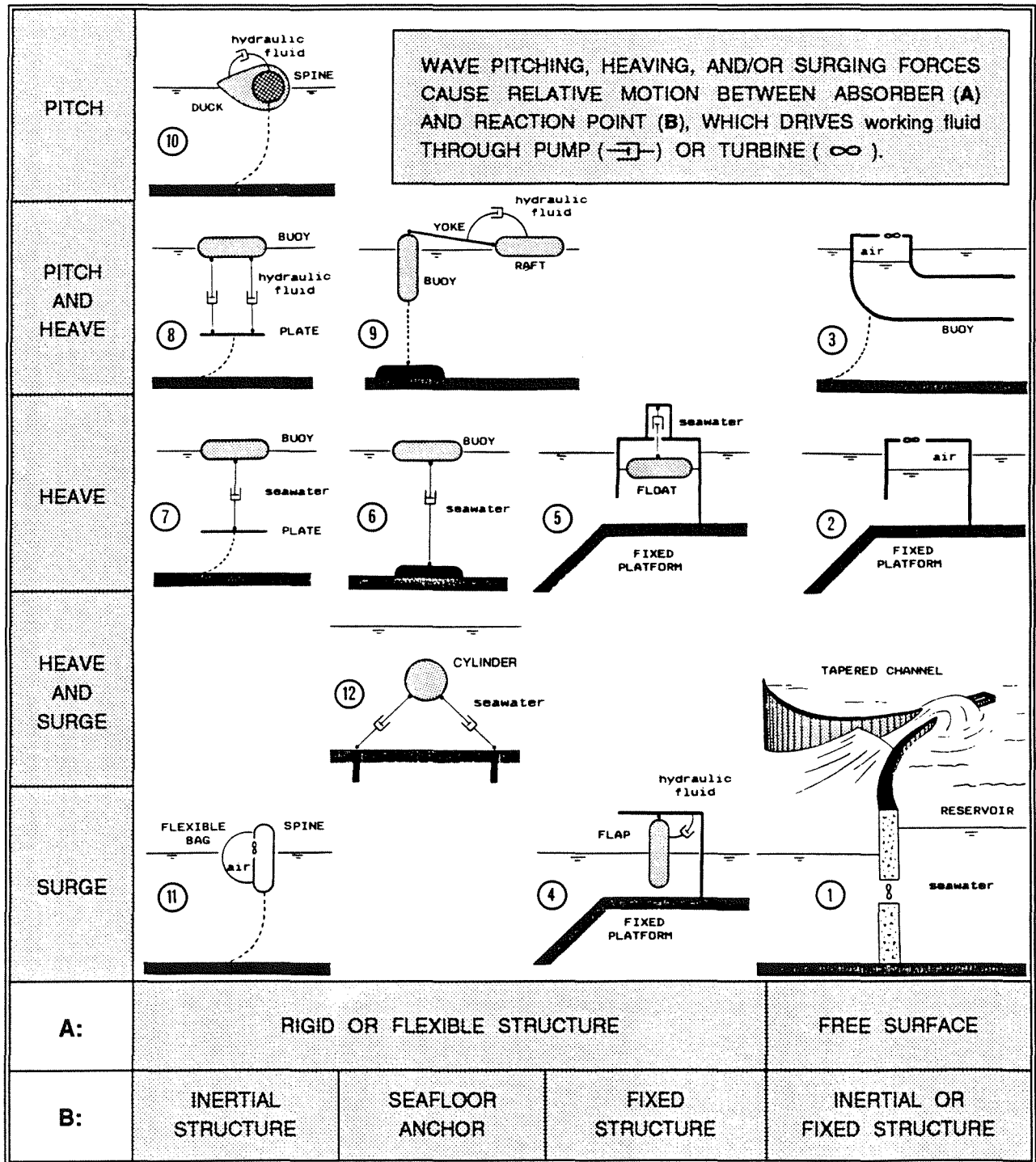


Figure 3-1. Wave energy conversion processes.

Land- and caisson-based systems have achieved the greatest development progress to date. A 350 kWe Tapered Channel plant has been operating continuously at Toftestallen, off the North Sea coast of Norway, since 1986. A 75 kWe onshore, gully-based OWC test plant has been operating since early 1991 on the Scottish island of Islay. A similar gully-based unit, rated at 40 kWe, operated as Sanzei, on the Sea of Japan, for six months during the winter of 1983-84. Three caisson-based wave power plants are now operating in Japan: a 30 kWe single-acting OWC system at Kujukuri, on the Pacific Ocean (since March 1988); a 60 kWe double-acting OWC system at Sakata Port, on the Sea of Japan (since November 1989); and a 20 kWe pivoting flap system at Mashike, on Hokkaido (since 1983).

Because of their advanced state of development, land- and caisson-based systems may be the first to find commercial application in Hawaii, and this section begins with an overview of those devices that have been demonstrated at full scale (all except Process 5, the caisson-based heaving float, which has not been tested outside the laboratory wave tank). Land-based systems, however, involve significant shoreline modification and attendant environmental impacts, which may severely limit their deployment. Likewise, wave energy breakwaters assembled from caisson-based devices are likely to be acceptable only at existing ports, or where construction of a new small-craft harbor has already been approved.

Offshore wave energy conversion processes are considerably less advanced. The specially built ship, *Kaimei*, was deployed twice in the Sea of Japan, to test various pneumatic turbines (used in oscillating water column processes and the SEA Clam). Electricity was landed ashore from only a single 125 kWe turbine/generator, however, and this only for four months during the winter of 1978-79.

Two heaving buoy systems have also been grid-connected for a period of months: a 30 kWe Swedish system in 1983-84, and a 45 kWe Danish system in the spring of 1990. Several much smaller devices have been tested in lakes or reservoirs at 1/10 to 1/15 physical model scale, and most of these have not involved electrical generating equipment.

Despite their less-advanced development status, offshore systems have much wider deployment potential in Hawaii, since they don't involve shoreline modification or breakwater construction. Heaving buoy systems that use high-pressure seawater as a working fluid are particularly attractive, since they can produce both electricity and fresh water. Also, the buoys' relatively small diameter and low freeboard minimize their visual impact on the offshore seascape. Two such heaving buoy systems are reviewed in this section, as is the SEA Clam, a leading British wave energy device that uses flexible bags, with air as the working fluid. This section concludes with a review of the Bristol Cylinder, which also uses high-pressure seawater but is totally submerged, thereby avoiding any offshore visual impact.

TAPERED CHANNEL

This is the simplest conversion process, similar in many ways to conventional low-head hydroelectric technology. Where site conditions permit construction of a large coastal reservoir without extensive blasting or dam-building, it is the most economical wave energy device developed to date.

Invented by Dr. Even Mehlum of Norway, the Tapered Channel consists of a collector, an energy converter, a reservoir, and a power house (Figure 3-2). The collector funnels waves into the entrance of the energy converter, which is a vertical-walled channel, having a depth of 6 to 7 m and built up to a height 2 to 3 m above mean sea level. The channel's width decreases in a shoreward direction, and its end is sealed off. As waves travel along the ever-narrowing channel, they increase in height, spilling water over its sides and into the reservoir. Water then drains back to the sea through a conventional low-head (e.g. Kaplan) turbine/generator.

In the spring of 1984, the Norwegian national government decided to cost share with private industry (on a 50% basis) the construction of two full-scale wave power plants at Toftestallen, on Norway's North Sea coast. One of these was a 350 kWe Tapered Channel, and the other was a 500 kWe fixed oscillating water column system, described later in this section. Although both plants were completed in 1985, the collector of the Tapered Channel plant had to be cleared of mined rock. This was done in June 1986 and the plant began automatic operation the third quarter of that year [16].

The reservoir of a Tapered Channel power plant does not provide long-term storage, but smooths the input from one high-energy wave group to the next. For example, the reservoir at Toftestallen is reported to have an area of 8,500 m², while the turbine is designed for a flow rate of 14 to 16 m³/sec and an operating head of 3 m. Should wave energy levels fall so low that waves no longer overtop the channel walls, the reservoir would drain to mean sea level in about 30 minutes. It should be noted, however, that the plant is designed to start automatically whenever sufficient head becomes available again.

Assuming a turbine/generator efficiency of 90%, the upper meter of the reservoir at Toftestallen is replaced once every six minutes, which represents a tremendous rate of seawater renewal. Thus, a Tapered Channel reservoir can also serve as a naturally flushed basin for closed-pond aquaculture.

All rights to the Tapered Channel are held by Norwave A.S., an Oslo-based company incorporated in 1987. Norwave now has firm commercial orders for two 1.5 MWe plants, one on the island of Java, in Indonesia, and the other on King Island, located just north of Tasmania, Australia. Financing for these projects is in hand for these projects, but construction has been delayed. The Indonesian plant will require 18 months to build, while the King Island plant can be built in one year [17].

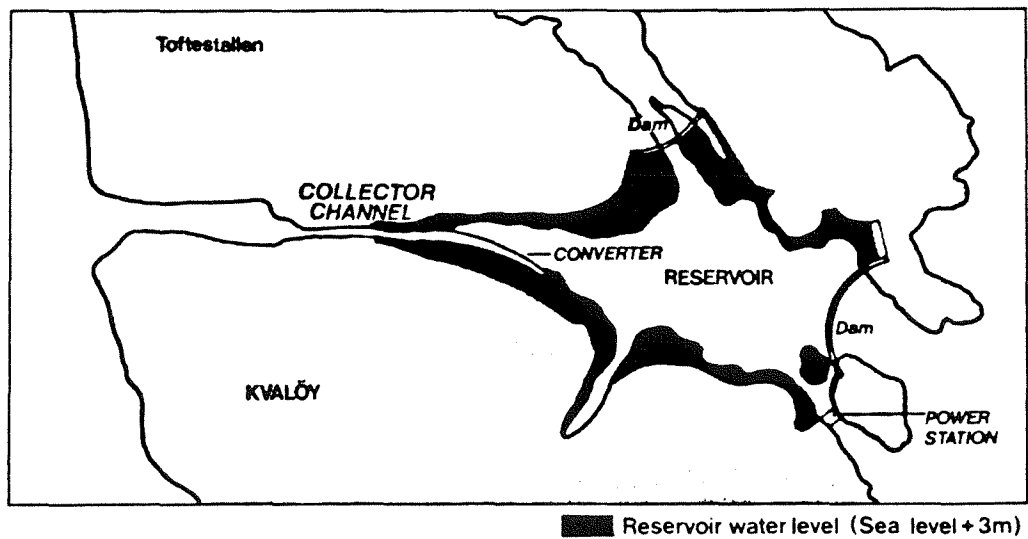
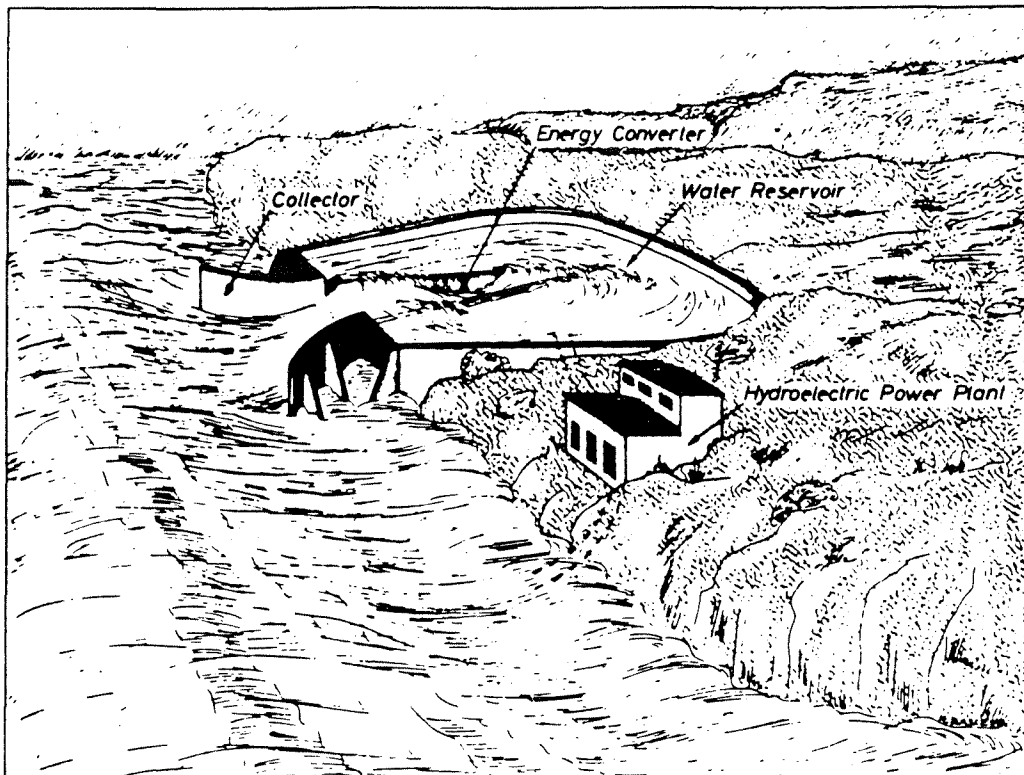


Figure 3-2. Tapered Channel concept and 350 kWe demonstration plant at Toftestallen.

FIXED OSCILLATING WATER COLUMN

The first application of wave power for electric power generation was based on this process. In 1910, one M. Bochaux-Praceque supplied the light and power to his house on the coast of France with a 1 kWe pneumatic turbine/generator driven by wave-induced water column motions in a vertical borehole near a seaside cliff [18]. The operating principle of the oscillating water column is explained below.

Consider a vertical circular cylinder, open at both ends, whose bottom end is submerged. As a wave crest passes, the column of water entrained in the submerged portion of the cylinder rises, pushing air out the top. Likewise, as a wave trough passes, the water column falls, drawing air in. If the natural period of the water column is near resonance with the incident wave period, then its amplitude of vertical motion can be significantly greater than that of the wave.

The motion of the oscillating water column (OWC) is greatest when the cylinder is completely open, since it is working only against atmospheric pressure. If the cylinder is capped with an orifice plate, the volume of air exchanged with the atmosphere has to flow through an opening that is much smaller in diameter than the cylinder itself. This creates an overpressure ahead of the rising water column and a partial vacuum behind the falling water column, damping the motion in both directions. The volume of air exchanged over a complete wave period is thus reduced in comparison with that of the open cylinder. Even so, since a somewhat reduced volume of air must flow through a greatly reduced opening, the air's flow velocity is increased to the point that it can be converted to electrical energy by a pneumatic turbine.

Pneumatic Turbine Designs

A conventional impulse turbine can be used if one-way valves are incorporated into the system to rectify the air flow so that it always travels in one direction through the turbine. During the "Kaimei" sea trials, such valves often became stuck in the open or closed position, seriously degrading turbine performance [19]. On the other hand, Takenaka Corporation has had good success with its valve arrangement, whereby the rectified air flow from several oscillating water columns is manifolded to an onshore air tank (Figure 3-3). This is a single-acting OWC, in that energy is absorbed only from the water column's rise. There is no sacrifice in efficiency, however, since the column's fall is relatively undamped, allowing a greater build-up of hydrostatic pressure to help drive the column's rise during passage of the next wave.

As an alternative to the use of one-way valves, several different self-rectifying turbine designs have been developed. The most widely used design was invented by Dr. Alan Wells of the Queen's University of Belfast in Northern Ireland. The Wells turbine absorbs energy from both the rise and fall of the oscillating water column, which is thus referred to as a double-acting OWC, and the water column's motion is damped in both directions.

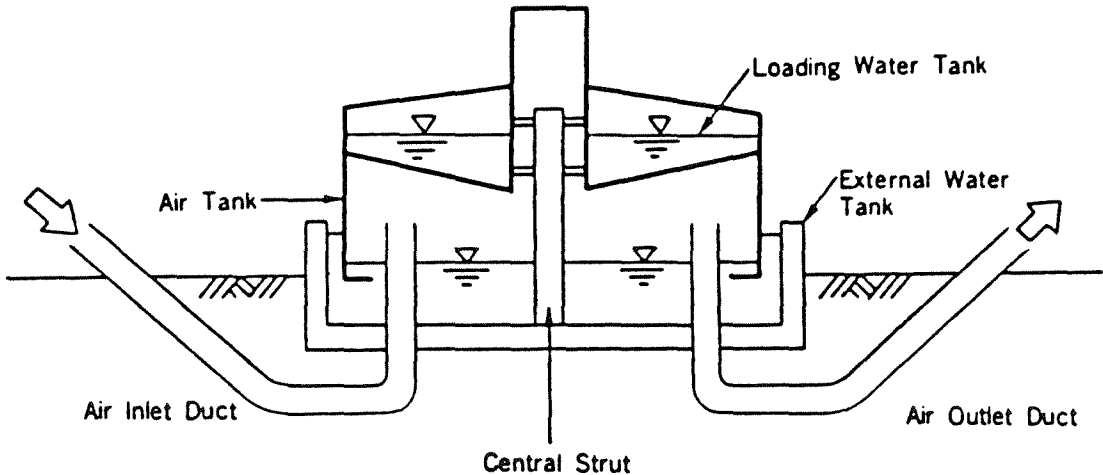
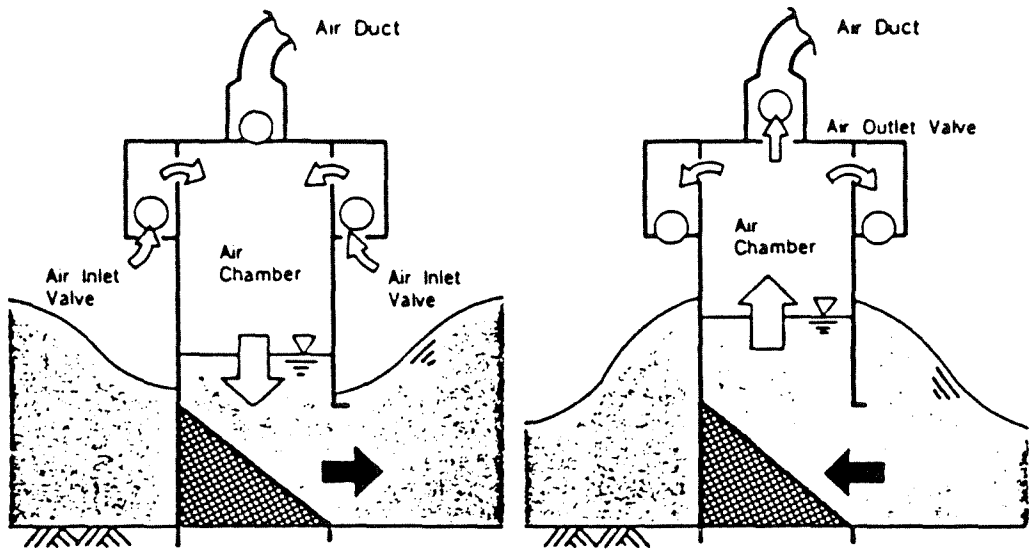


Figure 3-3. Use of non-return valves in a single-acting OWC system.

In the Wells turbine, the blades have a symmetric aerofoil section and are mounted on the generator shaft in such a way that they have no inclination to the plane of rotation (Figure 3-4). The rotation of the blades and the wave-driven axial air flow combine to produce an apparent air flow that generates a lift force, much like that on an airplane wing. Although the axial component periodically reverses direction, the forward component of the lift force always acts to drive the rotor in one direction, regardless of which way the axial air flow is directed.

Land-Based Systems

Shoreline gullies are naturally tapered channels, and an oscillating water column at the head of such a gully is exposed to higher wave power densities than found at the gully's mouth. Two such systems have been built, primarily for testing various pneumatic turbine designs. The first of these was located at Sanzei, on the west coast of Japan (Figure 3-5). This prototype was built in September 1983 by the Japan Marine Science and Technology Center, and a 40 kWe tandem Wells turbine was tested there until March 1984 [20]. A second gully-based system has been developed by the research team at the Queen's University of Belfast, led by Dr. Trevor Whittaker. A prototype system has been built on the Isle of Islay, near Portnahaven, Scotland. Civil works were completed in November 1988, and a 75 kWe biplane Wells turbine was installed at the end of 1990 [21].

The largest land-based OWC built to date was developed by Kvaerner-Brug A.S., a large Norwegian hydropower company. Kvaerner Brug's early work on the oscillating water column concentrated on developing means to adjust the natural frequency of the water column in order to tune the device as dominant wave period changes from sea state to sea state. In 1980, they shifted their approach to designing an absorbing structure that would resonate at several frequencies within the range of wave periods expected at a potential plant site. It was thought to be more cost-effective for a device to have several fixed resonant frequencies rather than a single, continuously variable one.

The structure designed by Kvaerner Brug to have such multiple resonances consists of a rectangular capture chamber, and a harbor formed by extending the side walls of the chamber in a seaward direction. A 500 kWe demonstration plant based on this concept was built at Toftestallen, alongside Norway's Tapered Channel plant [22]. The turbine/generator was a monoplane Wells design. A cleft in the island's cliff wall was enlarged to form the resonant harbor.

From November 1985 until December 1986, electric power was generated only when personnel were present to run tests and conduct measurements. The plant began fully automatic operation in January 1987, running for two years until it was destroyed by a severe storm in January 1989. According to reports, the steel tower was torn from its foundation and swept out to sea [23].

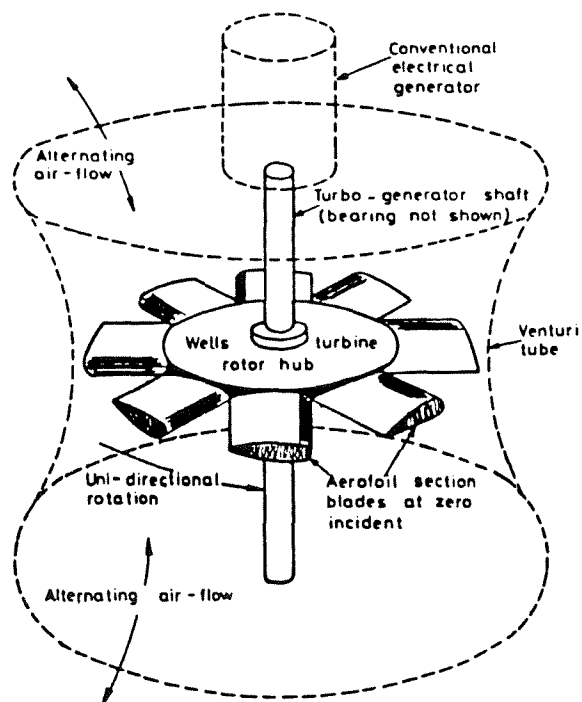
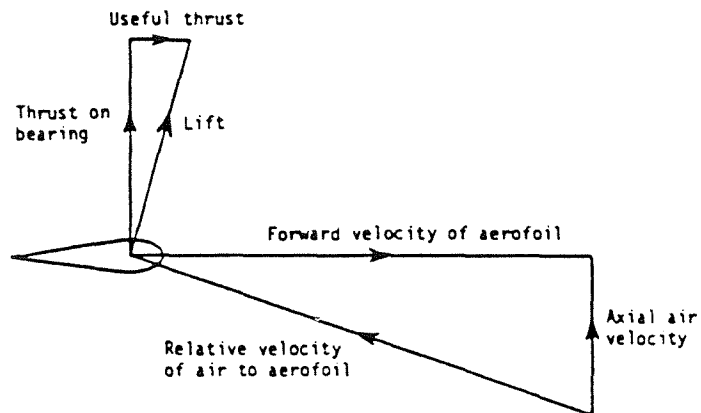


Figure 3-4. Wells turbine concept and monoplane rotor design.

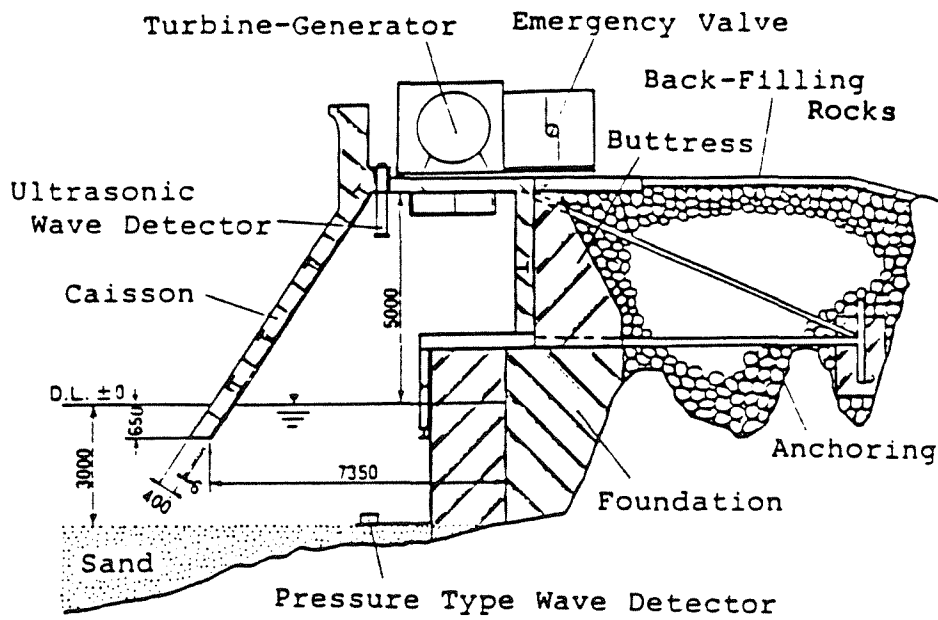
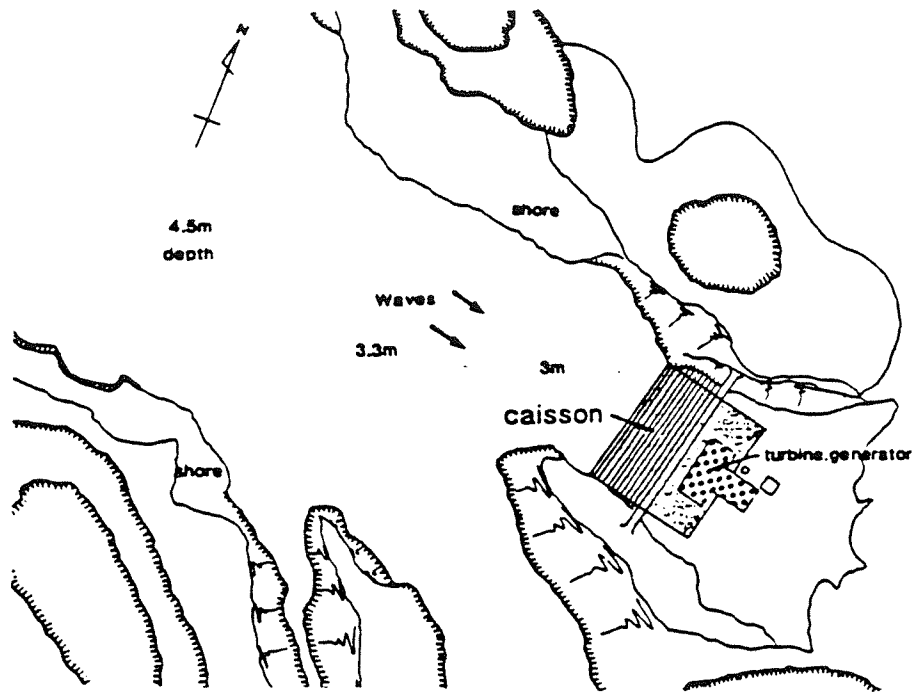


Figure 3-6. Land-based OWC - 40 kWe prototype at Sanzei.

Caisson-Based Systems

Kvaerner Brug also developed a commercial plant design for the south Pacific Kingdom of Tonga [24]. The resonant harbor would have been formed as part of a caisson, and four such caissons would have been deployed along the reef crest off Tongatapu (Figure 3-6).

An alternative to free-standing caissons is the use of caissons placed side by side, in the form of a breakwater. Such a basing scheme may have potential niche application in Hawaii at locations where harbor protection is needed. Three breakwater OWC systems have been developed in the past decade.

The first of these originated with the British government's wave energy program and was developed at the National Energy Laboratory (NEL). As with other devices developed in the United Kingdom at that time, the NEL breakwater design was directed towards establishing the feasibility of a 2,000 MWe central station in the Outer Hebrides Islands off Scotland's northwest coast [25]. The NEL 1982 Reference Design utilized non-return valves to rectify the air flow through a conventional impulse turbine.

A second breakwater-based OWC system has been developed by the Japanese Ministry of Transport, under the direction of Dr. Yoshimi Goda. In 1987, work began on a prototype unit installed as part of a new offshore breakwater built at Sakata Port, on the west coast of Japan [26]. The new breakwater consists of a row of caissons on a rubble mound foundation. One of the caissons was built with a "curtain wall", which forms the OWC capture chamber (Figure 3-7). A 60 kWe tandem Wells turbine/generator was installed in the machinery room behind the capture chamber. The test caisson was completed in the summer of 1989, and electric power generation began the following winter. A two-year test is planned.

A third and somewhat different OWC breakwater concept has been developed by Takenaka Corporation in Japan. It consists of relatively narrow caissons which act as capture chambers. Output from several caissons is manifolded and piped to a constant-pressure air tank, which drives a conventional impulse turbine (Figure 3-8). Air is drawn into the caissons through check valves as the water column falls. When the water column rises, the air is directed to the manifold through a different set of check valves.

A 30 kWe demonstration plant has been operating at Kujukuri, on Japan's Pacific Ocean coast, since March 1988 [27]. Ten steel caissons, 2.1 m in diameter and 11.8 m high, are connected by an 0.8 m diameter air duct to an onshore cylindrical tank. The air tank floats in a ground tank of water and can be weighted with ballast, such that the air tank sinks deeper into the ground tank, increasing the pressure against which the OWC units work (see Figure 3-3). Tank pressure can be adjusted from 3 to 13 kPa (0.4 to 1.8 psi). The compressed air drives a radial flow turbine/generator, which powers a seawater pump for a nearby flatfish aquaculture pond.

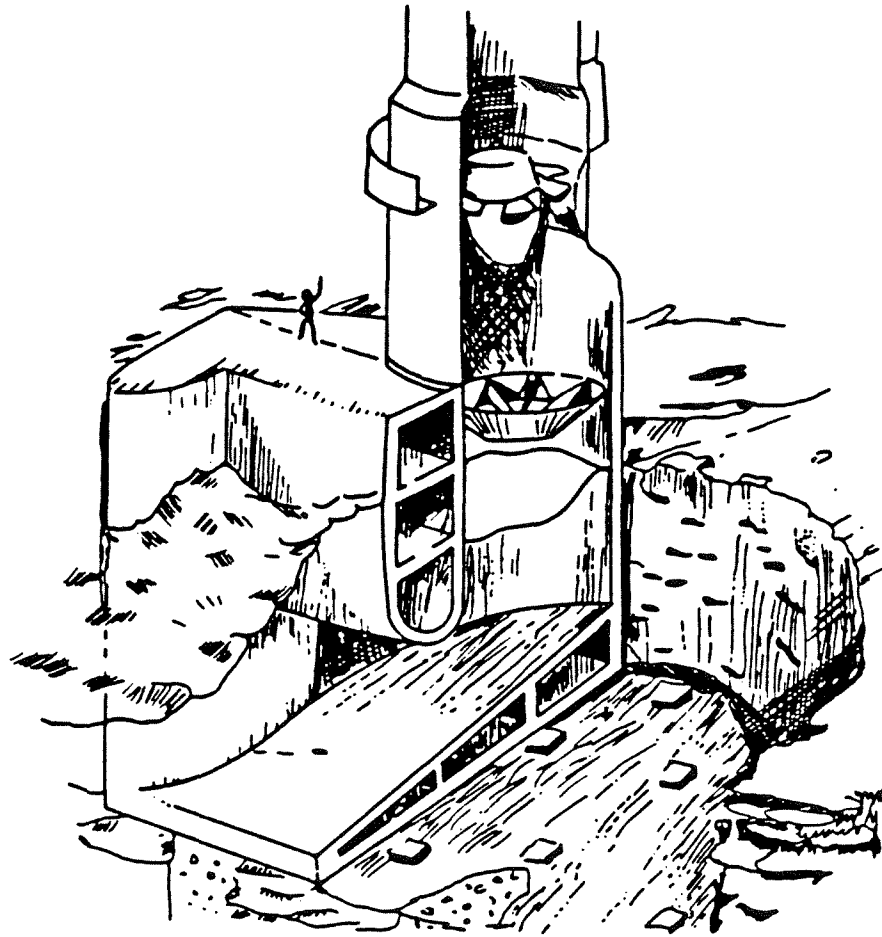


Figure 3-7. Caisson-based, multi-resonant OWC design developed for Tongatapu.

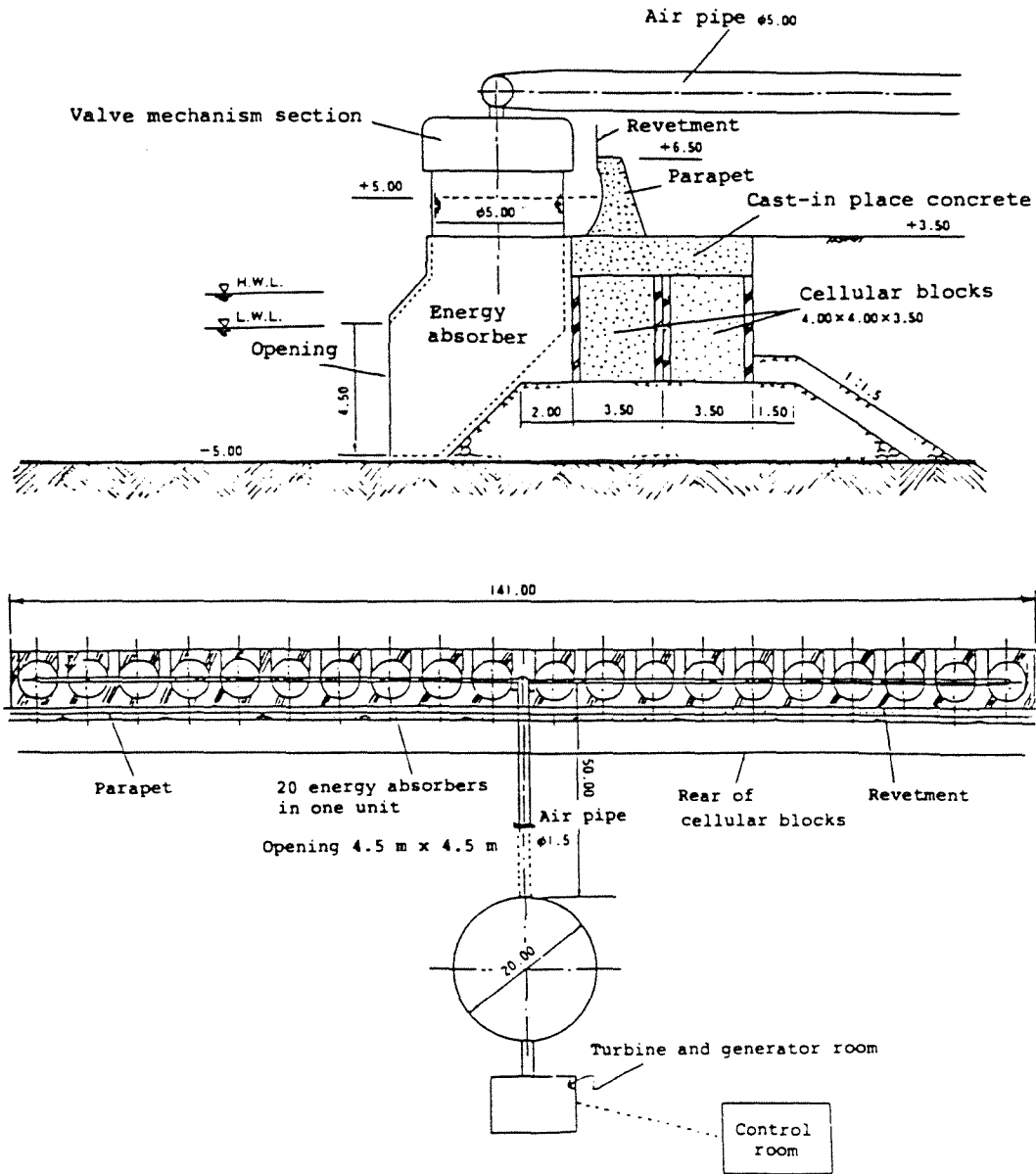


Figure 3-8. Single-acting OWC system - 1.5 MWe design developed for Kashima Port.

PIVOTING FLAP

For over a decade, the Muroran Institute of Technology has developed a caisson-based pivoting flap device, which it calls the "Pendulor" System [28]. The Pendulor itself is a stiffened steel plate that hangs down into a recessed capture chamber. Unlike fixed OWC systems, where the capture chamber extends below the sea surface, the Pendulor System caisson is entirely open to the sea (Figure 3-9). Incident waves interact with waves reflected off the back of the chamber to create a standing wave. The Pendulor is positioned at the node of this standing wave, where horizontal forces are at a maximum. As the Pendulor swings in response to these surge forces, it drives a double-acting hydraulic cylinder.

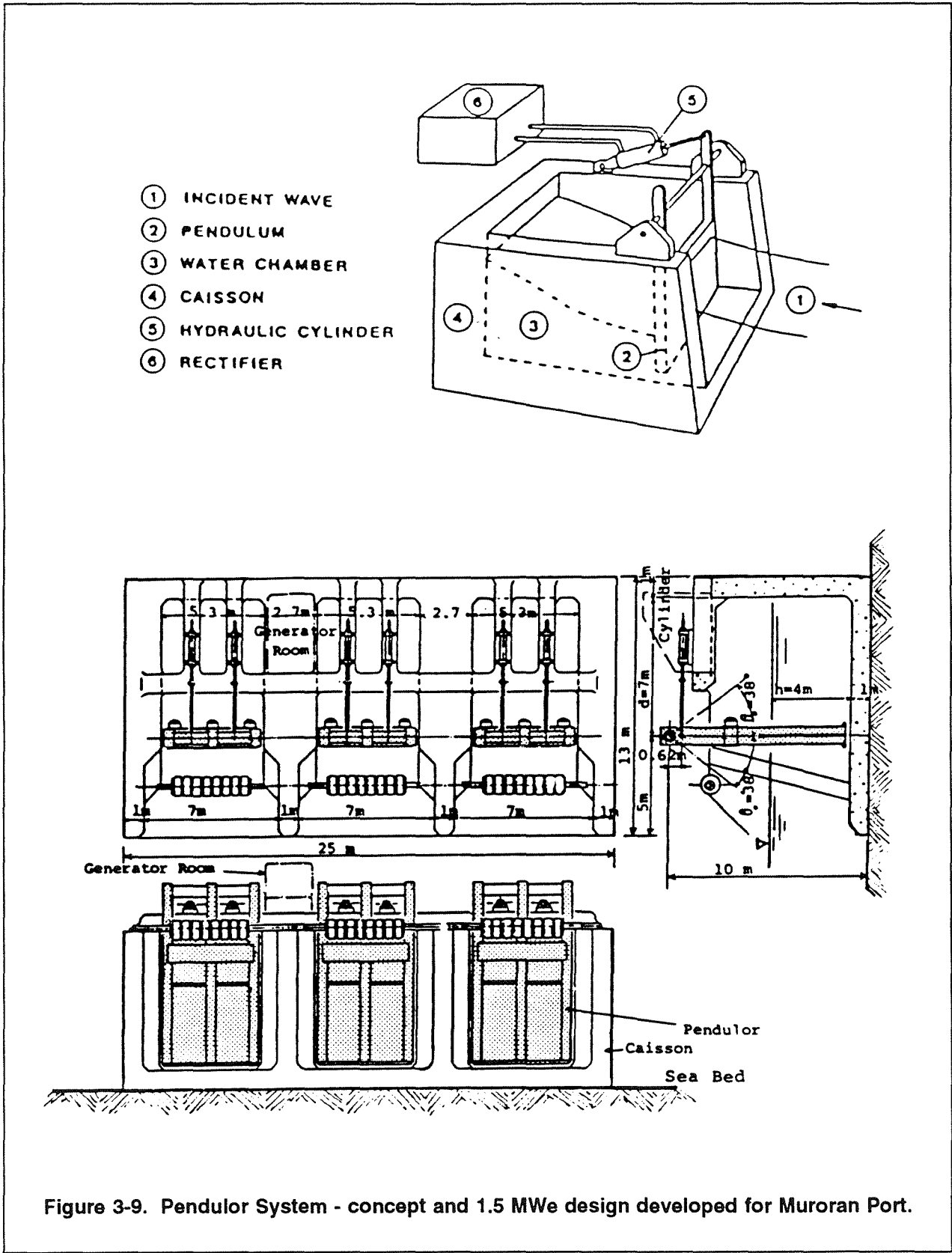
The fluid output of the cylinder is rectified such that one hydraulic motor is driven on the cylinder's compression stroke, and a second motor is driven on the cylinder's extension stroke. Thus, the torque and speed of the generator drive shaft remain relatively constant throughout the wave cycle (Figure 3-10).

In April 1983, a 5 kW (hydraulic motor rating) prototype was installed at Muroran Port, on the south coast of Hokkaido. The prototype caisson is sited in front of an existing seawall, in a water depth that ranges from 2.5 m at low tide to 4 m at high tide. Two capture chambers have been built into the caisson, but only one has been fitted with a Pendulor.

Twenty months after its installation, the Pendulor was bent during a severe storm, and the shock absorbers for the end-stops, which prevent over-stroking of the hydraulic cylinder, had to be redesigned. A new Pendulor was installed in November 1985, and the prototype has survived several severe storms since then, without damage.

A small Pendulor System that generates electric power was deployed in 1981. Rated at 20 kWe, this unit is used to heat the public bath of a fishing cooperative at Mashike Harbor, on Hokkaido's west coast [29]. Unfortunately, its Pendulor was also damaged by a storm, just three months after installation. It was replaced by a shorter Pendulor in 1983, which left a considerable gap at the bottom of the capture chamber. While this has prevented further damage, it also lowered the system's conversion efficiency. Nevertheless, the plant continues to operate.

An intriguing possibility, which has yet to be explored, would be to replace the closed-circuit hydraulic system with an open-circuit, high-pressure seawater system, making use of the elastomeric hose pump described later in this section. This would enable the production of both fresh water and electricity. At 5.5 MPa (800 psi), about 20% of the high-pressure seawater flow would pass through a reverse osmosis membrane as fresh water; the remainder would be discharged through a Pelton turbine/generator.



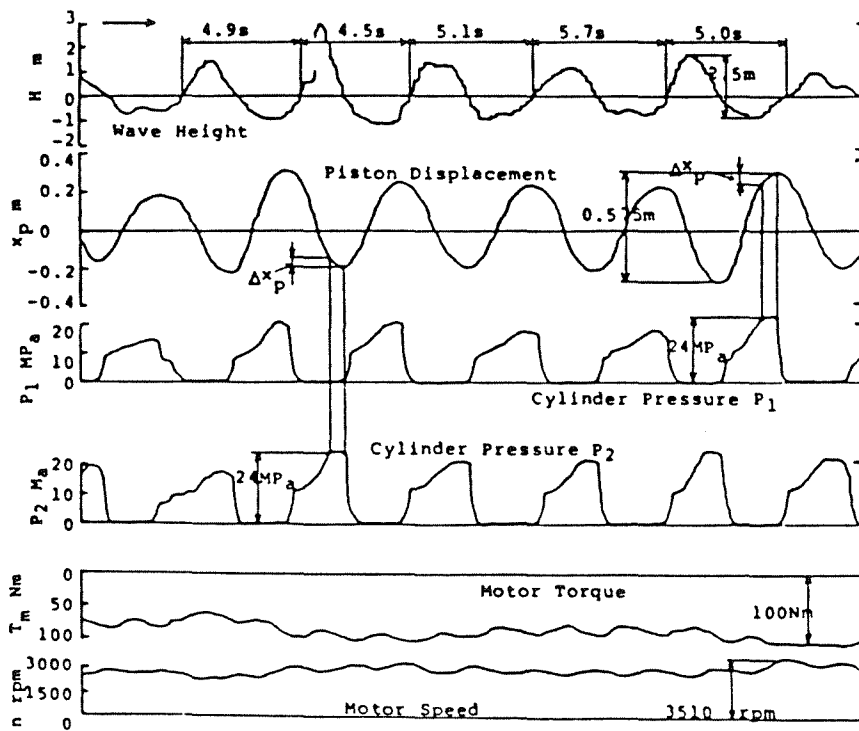
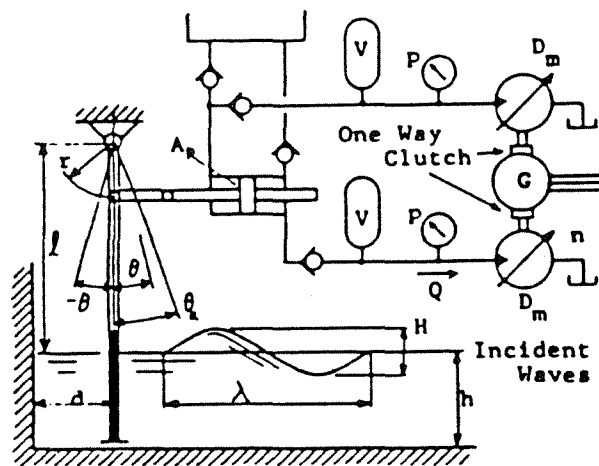


Figure 3-10. Pendulum System - hydraulic rectifier schematic and performance.

HEAVING BUOY

Wave forces are large, but act very slowly, and some sort of speed increase is necessary in order to drive an electrical generator. The OWC systems described above accomplish this by an area reduction between the capture chamber waterplane and the air turbine inlet.

Heaving buoys (and pivoting flaps) accomplish the necessary speed increase by virtue of the ratio of buoy waterplane area (or projected flap area) to pump cross-sectional area. Wave forces distributed over the entire absorber are transmitted to a much smaller diameter pump, thereby achieving a pressure increase and developing sufficient head to run a high-speed water turbine.

Dr. Kim Nielsen of Denmark has developed a heaving buoy system with a relatively small ratio of buoy diameter to pump diameter [30], which consequently operates at low pressures, less than 0.1 MPa (15 psi) . This section reviews two systems with much larger buoy/pump diameter ratios, creating pressures up to 5.5 MPa (800 psi), which is sufficient to enable the production of fresh water by direct reverse osmosis (RO), as well as the generation of electricity. Incorporation of an RO module into any wave energy device that uses high-pressure seawater as a working fluid would provide a valuable co-product that is in short supply at various locations in Hawaii and throughout the tropical Pacific Ocean. Therefore, despite the considerable progress that has been made on the Danish heaving buoy system, it does not have this co-product potential and is not reviewed in this section.

DELBUOY

This device was developed by Drs. Douglas Hicks and C. Michael Pleass at the University of Delaware. Since 1982, they have deployed an evolving series of full-scale prototypes off the southwest coast of Puerto Rico, where they have demonstrated fresh water production at a rate of 950 liters (250 gallons) per day from a single buoy [31]. The system is designed for the Caribbean Sea and along the arid coastal regions of Africa, where average incident wave power is on the order of 1-10 kW/m.

DELBUOY employs a 2.1 m diameter buoy tethered to a seafloor anchor by a single-acting hydraulic cylinder, which has a bore diameter of 4 cm (Figure 3-11). Six buoy/pump moorings supply one RO module that delivers 5680 liters (1500 gallons) of fresh water per day, in waves 1 m high, having a period of 3-6 seconds. As shown in the previous section, waves of this height and period occur commonly in Hawaii, even along sheltered coasts. It is outside the scope of this particular study to evaluate the cost and performance of wave-powered desalination. DELBUOY is significant, however, because it demonstrates that even with a relatively small absorber, wave energy can generate sufficient pressure to develop reverse osmotic flow in exploitable quantities.

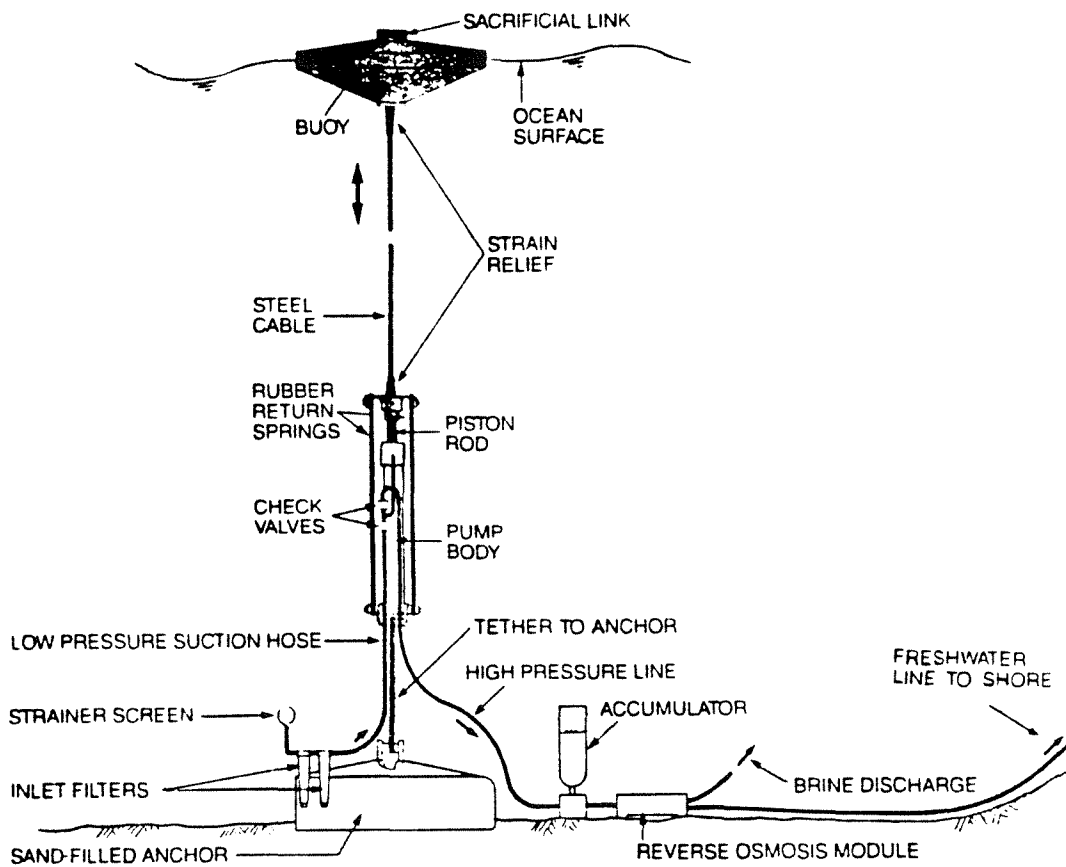


Figure 3-11. DELBUOY heaving buoy system for fresh water production.

Swedish Heaving Buoy System

Consider the series of buoys illustrated in Figure 3-12. Each buoy is attached to a collecting line by a length of specially designed elastomeric hose. During the passage of a wave crest, the buoy heaves up, stretching the hose. The helically wound, steel reinforcing wires in the hose wall cause the hose to constrict as it is stretched, thereby reducing its internal volume. This forces seawater out of the hose, through a check valve, and into the collecting line. After the wave crest has passed and the buoy drops down into the succeeding trough, the pump returns to its original length, restoring the hose diameter to its unstretched value. This increase in internal volume draws water into the hose through another check valve, which is open to the sea. The hose is thus primed to pump seawater into the collecting line during passage of the next wave crest.

In order to provide a reaction point for its pumping action, the bottom end of each hose is tethered to a horizontal damper plate. When the buoy heaves up, it attempts to move this plate vertically through the water. Due to its large surface area, the plate acts like a sea anchor and its motion lags behind that of the buoy. Thus, relative motion between each buoy and damper plate alternately constricts and dilates the elastomeric hose between them.

This arrangement makes the performance of the system insensitive to tidal changes in sea level. It also eliminates the need for seafloor anchors having extremely high uplift capacities.

A power plant would consist of several star-shaped clusters of buoys. Each arm of the star is a collecting line for the output of up to ten buoy/hose pump modules. These lines radiate symmetrically from a central underwater habitat that contains a vertical-axis Pelton turbine/generator (Figure 3-13). Pressures as high as 6 MPa can be developed in the collecting line, as seawater is pumped through the line-end nozzle. After striking the Pelton wheel, the water falls back into the sea through an air pocket in the habitat. Diverter valves prevent excess flow from reaching the turbine in extreme waves.

In 1983-84, a prototype system was installed near Vinga Island, off Sweden's west coast. Three buoys were deployed about 600 m from the island and supplied an onshore 30 kWe Pelton turbine/generator. Each buoy had a diameter of 5 m (about 1/3 that of a commercial plant buoy).

The prototype was deployed intermittently during the two-year period. Incident wave power at the test site averaged 1.5 kW/m, and generator output averaged 3 to 5 kWe. Very good agreement was obtained between measured energy production and that predicted by a numerical model of the system. The prototype also survived extreme storm waves (5 m high) without significant damage.

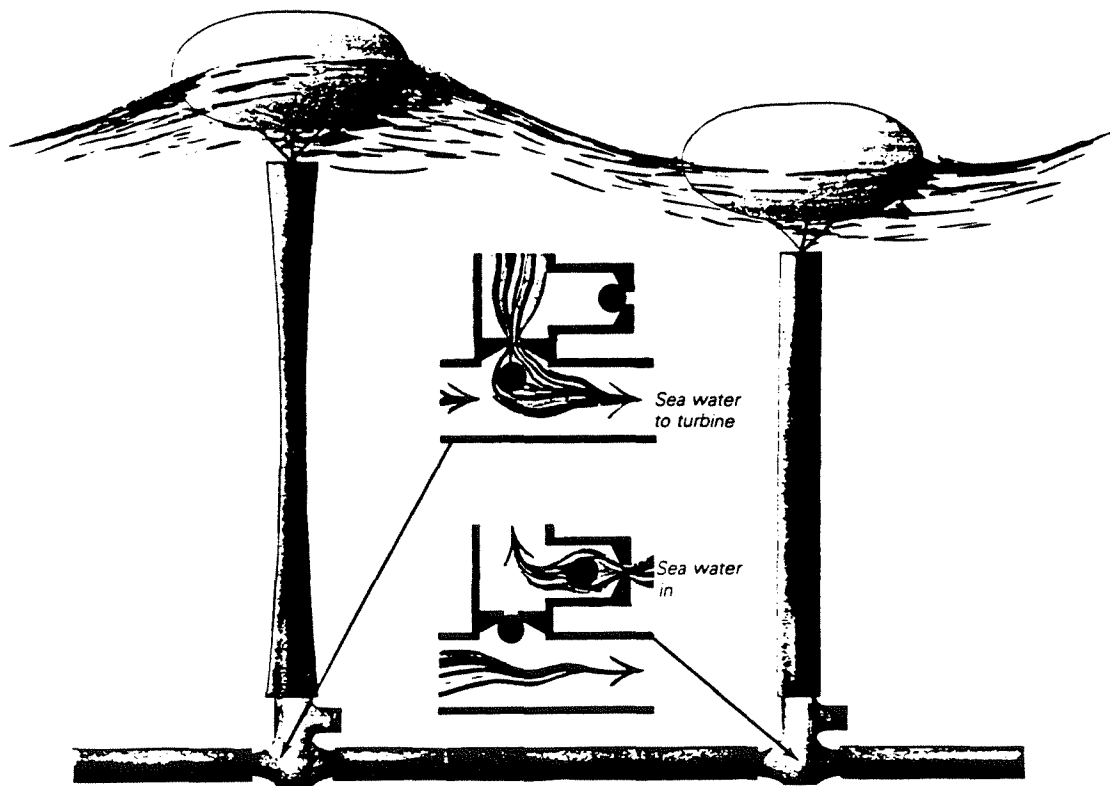
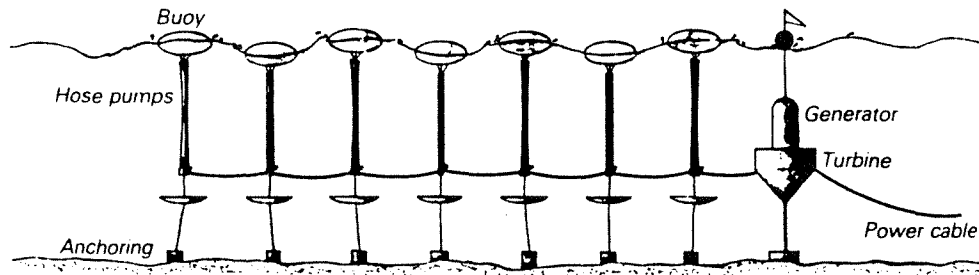


Figure 3-12. Swedish heaving buoy system - hose pump concept.

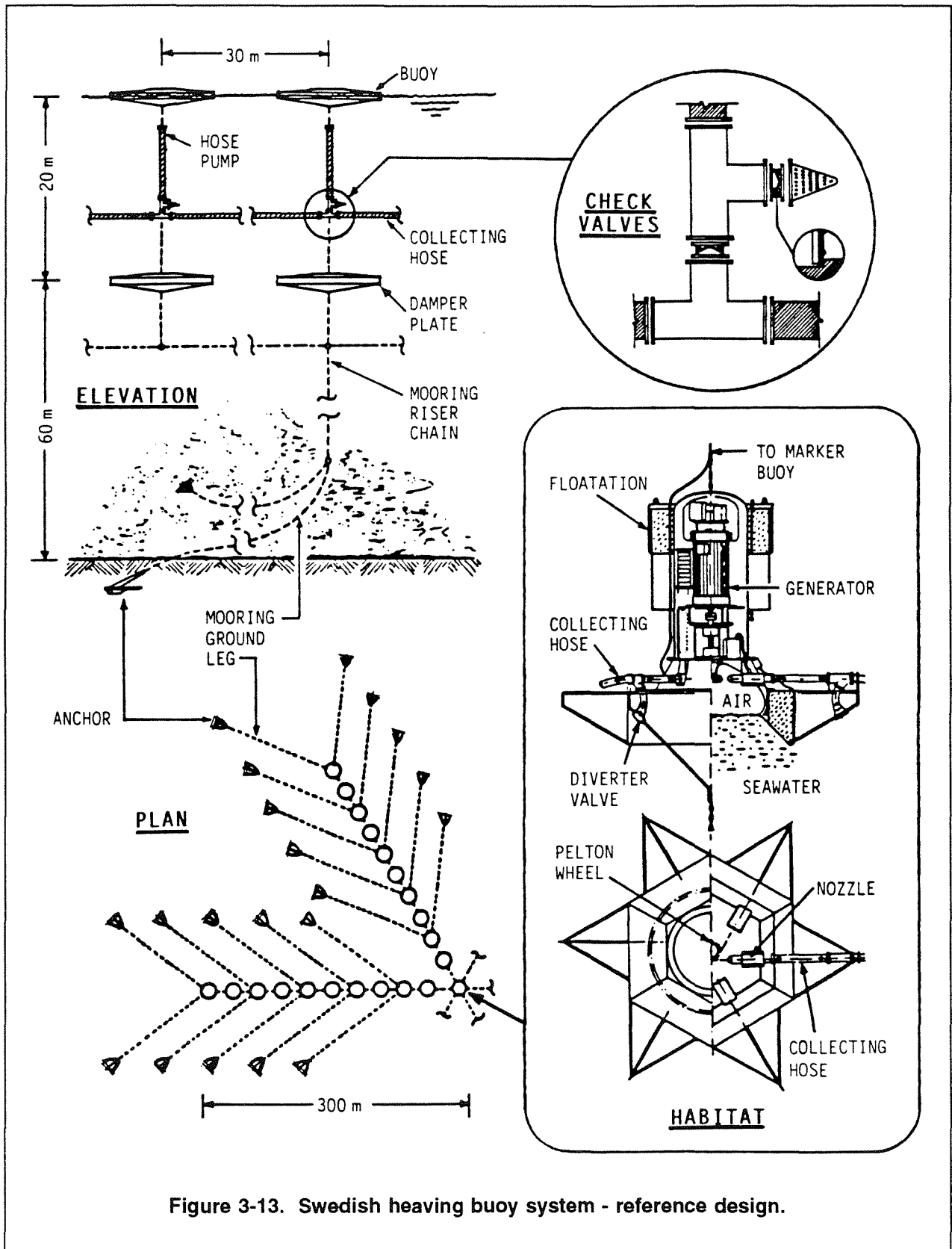


Figure 3-13. Swedish heaving buoy system - reference design.

The longest period of continuous immersion off Vinga was two months. At the end of this period, marine growth was observed on the steel buoy hulls and hose pump flanges, but the check valves and hose pump walls were clean. This suggests that even during periods of calm weather, there is enough hose flexing that fouling organisms are unable to settle on the hose wall.

In addition to its seemingly inherent resistance to biofouling, the hose pump has many advantages over DELBUOY's hydraulic cylinder. Apart from the check valves (which both pumps have in common), the hose pump has no distinct moving parts, eliminating the wear associated with sliding seals. Its simple design and material flexibility also make it less sensitive to rough handling during plant construction and deployment. Finally, from a manufacturing point of view, the hose pump can be built using conventional marine hose fabrication equipment. The only necessary modifications have to do with the laying of reinforcing cords at precise angles in order to achieve the pump's required stress-strain characteristics. The hose pump's size can be adjusted for different wave climates or buoy diameters simply by using a different size mandrel at the hose manufacturing plant. On the other hand, many of the plastic components in DELBUOY's hydraulic cylinder are fabricated via injection molding, and changing the pump size would require fabrication of new molds.

FLEXIBLE BAG

Having described several seawater and hydraulic fluid systems, it is evident that the use of air as a working fluid has much to recommend it in terms of equipment simplicity (no pumps or valves). Enclosing the air in a flexible bag prevents the turbine from being exposed to corrosive salt air, as is the case with oscillating water column systems. Use of a flexible rather than rigid structure also has the benefit of providing a large absorber with a relatively modest quantity of fabricated material.

SEA Clam

Sea Energy Associates, Ltd., (SEA) is a British industrial consortium that has collaborated with Coventry Polytechnic under the leadership of Dr. Norman Bellamy to develop the Clam system. This effort began in 1978 and grew out of the group's earlier work on another spine-based device, the Edinburgh Duck.

In its earliest form, the SEA Clam consisted of a straight, hollow spine, with a broad flap hinged along its bottom, seaward-facing edge. A flexible bag was sandwiched between the flap and the spine, much like a clam in its shell, hence the device's name. Wave surge against the flap caused the bag to act in the manner of a bellows, pumping air into and out of the hollow spine. It was soon found that more efficient transfer of wave power to air power could be obtained if the flap was removed, and the bag allowed to "breathe" freely, as shown in Figure 3-14. Air power is converted to electrical power by a Wells turbine placed in a duct between the bag and the spine.

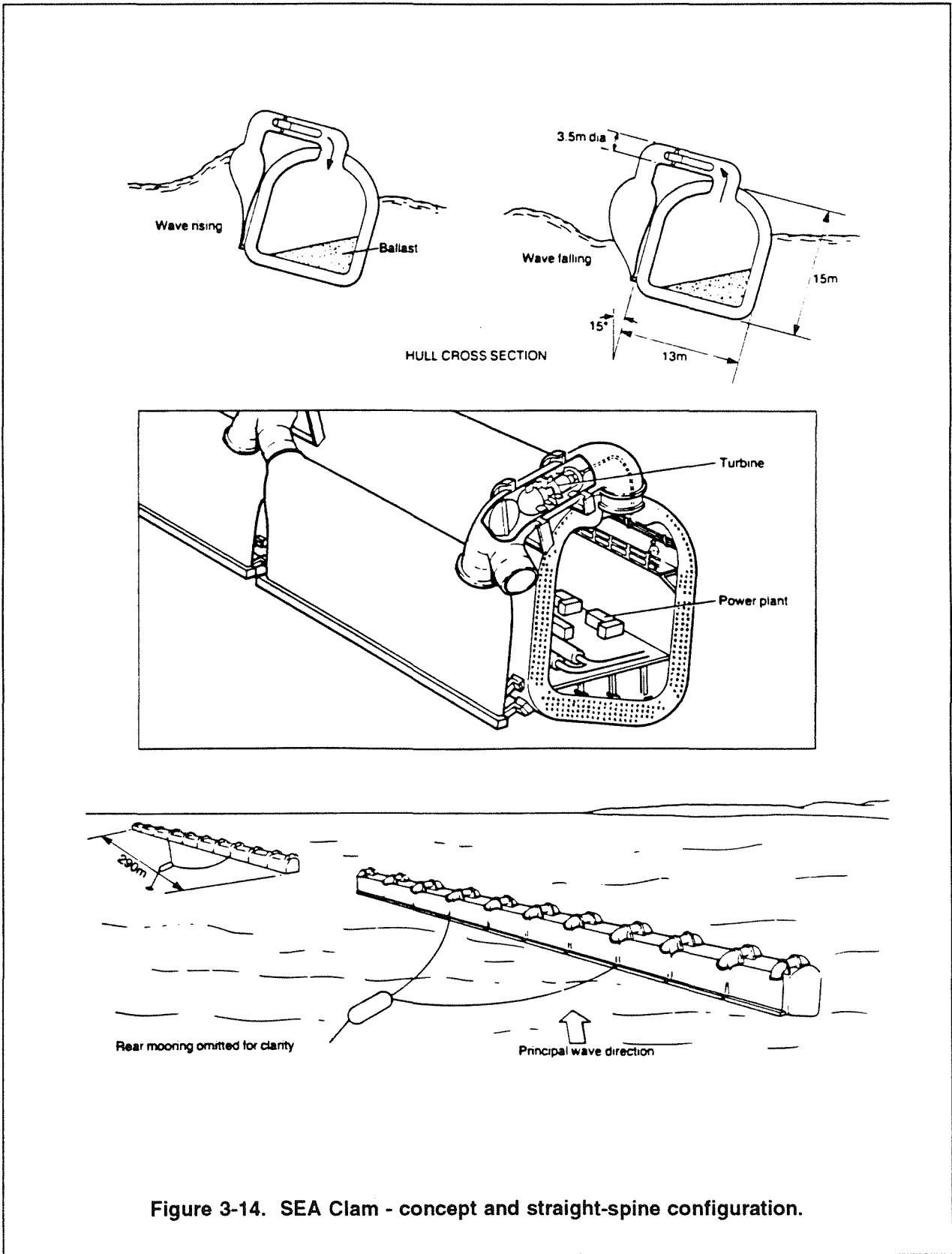


Figure 3-14. SEA Clam - concept and straight-spine configuration.

As part of the British national wave program, a 2 GWe reference design based on the straight spine configuration was prepared for the Outer Hebrides Islands [32]. Although this reference design was reported to be one of the most economical, there were several problems with the straight-spine configuration. Because the system was enclosed, the energy from any wave whose crest was parallel to the spine could not be absorbed, since the air had no place to go if all the bags were surged against at once. Therefore, the design called for an asymmetric mooring bridle to hold the spine at an angle to the prevailing wave crests. In a real sea, however, there will always be some wave energy coming from a direction other than the prevailing one, and any component whose crest was parallel to the spine would not be captured.

The most serious limitation of the straight spine arises from the balance of forces required for its hydrostatic stability. Experimental and theoretical work has shown that the maximum amount of power that can be absorbed by the SEA Clam is directly proportional to the total displacement of the air bags. A larger submerged bag volume allows the waves to develop larger flow rates through the turbines. Examination of Figure 3-14 indicates, however, that such an increase is limited by the pitch restoring moment that can be provided by ballast in the spine section.

Wrapping the straight spine back on itself in a circle overcomes these problems. Efficient bags, having a low spring rate, can be used, and the circle's radius of curvature is such that components of wave energy from all directions can be captured (Figure 3-15). Most importantly, the circular spine is pitch- and roll-stable, so that a higher ratio of bag capacity to total device displacement can be achieved.

Model tests and cost estimates have indicated the following improvements for the circular Clam over the straight Clam [33]:

- A 4-fold increase in device efficiency (based on the flux of incident wave power against the projected area of the device)
- A 3-fold increase in air power absorption per unit weight (based on total device displacement)
- A 2-fold decrease in the cost of electrical energy produced (based on devices of 1-2 MWe rating)

Cost and performance projections have been prepared for a 25 MWe plant, comprised of ten modules, each 60 m in diameter, with a freeboard of about 2 m, deployed in the Outer Hebrides Islands. Performance projections are based on a numerical model that was validated by 1/5-scale physical model tests in Loch Ness [34]. Although an earlier version of the circular spine structural design was based on welded tubular space-frame construction, box-shaped modules fabricated from welded steel plate were found to be 50-70% less costly [35]. Such modules can also be fabricated with concrete or ferrocement, further reducing capital costs.

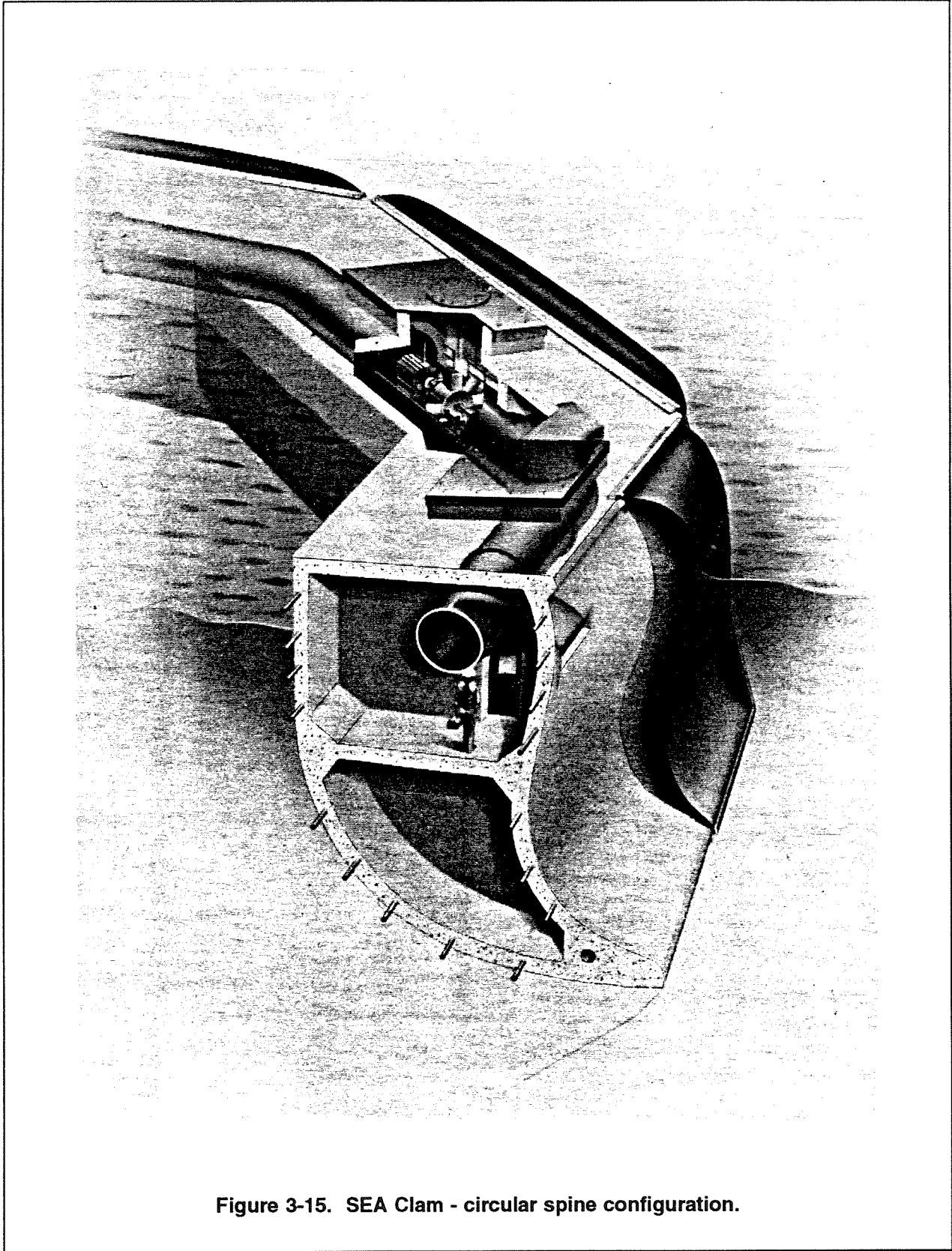


Figure 3-15. SEA Clam - circular spine configuration.

SUBMERGED BUOYANT CYLINDER

Although heave is the predominant energy absorption mode for buoys with a seafloor reaction point, they will also absorb energy in surge, particularly if sited in shallow water. By submerging the buoy and providing another mooring/pump to seaward, the resulting geometrical configuration will absorb a large amount of surge energy, comparable to or greater than that absorbed in heave.

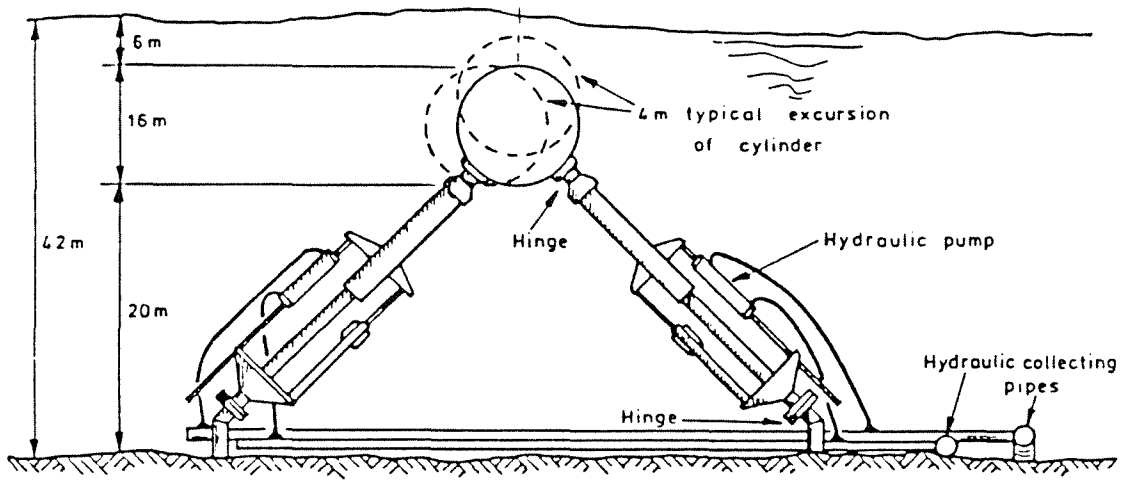
Bristol Cylinder

This device was invented by Dr. David Evans at the University of Bristol and developed in conjunction with Sir Robert McAlpine & Sons, Ltd., in the United Kingdom [36]. As with the NEL Breakwater, the Edinburgh Duck, and the SEA Clam, its development was pursued largely under the British national program aimed at establishing the feasibility of a 2 GWe central station in the Outer Hebrides Islands.

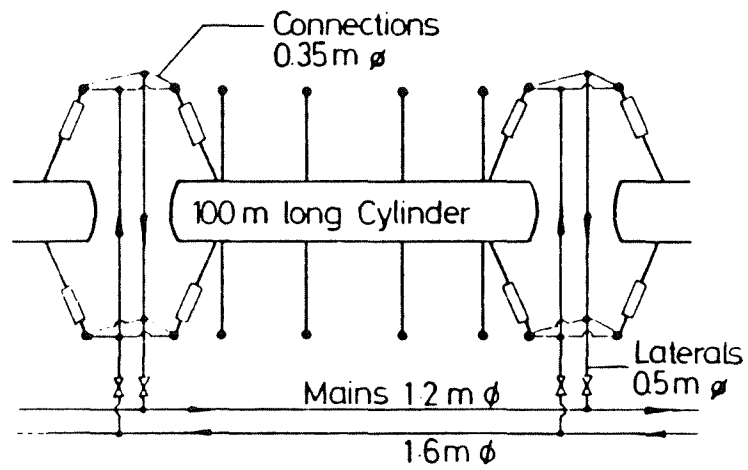
The absorber in the 1982 Reference Design is a hollow cylinder, fabricated from pre-cast reinforced concrete sections, 100 m long with a diameter of 16 m, and submerged 6 m beneath the sea surface in a water depth of 42 m. Each cylinder is anchored by eight mooring legs, with two double-acting pumps splayed off each end (Figure 3-16). The mooring legs are polymer tube springs, which are identical in form and function to the Swedish hose pump described earlier. The spring rate of the cylinder, and hence its tuning to incident wave frequencies, can be adjusted by changing the internal pressure of the tube springs. It is important to note that unlike the Swedish heaving buoy system, the seawater pumping function of the Bristol Cylinder is accomplished by stainless steel hydraulic rams.

The fluid power output from 46 cylinders is collected and transmitted via seafloor pipelines to a fixed platform containing three 120 MWe Pelton turbine/generators (Figure 3-17). For the 2 GWe central station, six such platform/cylinder groupings are arrayed along the 40 m depth contour off South Uist. Power is transmitted ashore via six 270 kV submarine cables, one from each platform.

The 40 m depth contour off most north-facing island coastlines in Hawaii is much closer to shore than it is in the Outer Hebrides Islands. This would enable the submerged cylinders to pump seawater directly to shore rather than to an offshore platform. Depending on the availability of land where seawater containment would be economically feasible and environmentally acceptable, the seawater could be stored in an elevated reservoir, or converted immediately into electric power by an onshore Pelton turbine/generator. This would eliminate any potential visual impact and increase plant availability, since all electrical equipment would be accessible by land for inspection and maintenance. As with the pivoting flap and heaving buoy, a sufficiently large ratio of cylinder width to pump diameter would enable the production of fresh water by reverse osmosis, in addition to electricity.



ELEVATION



PLAN

Figure 3-16. Bristol cylinder - absorber and mooring/pump arrangement.

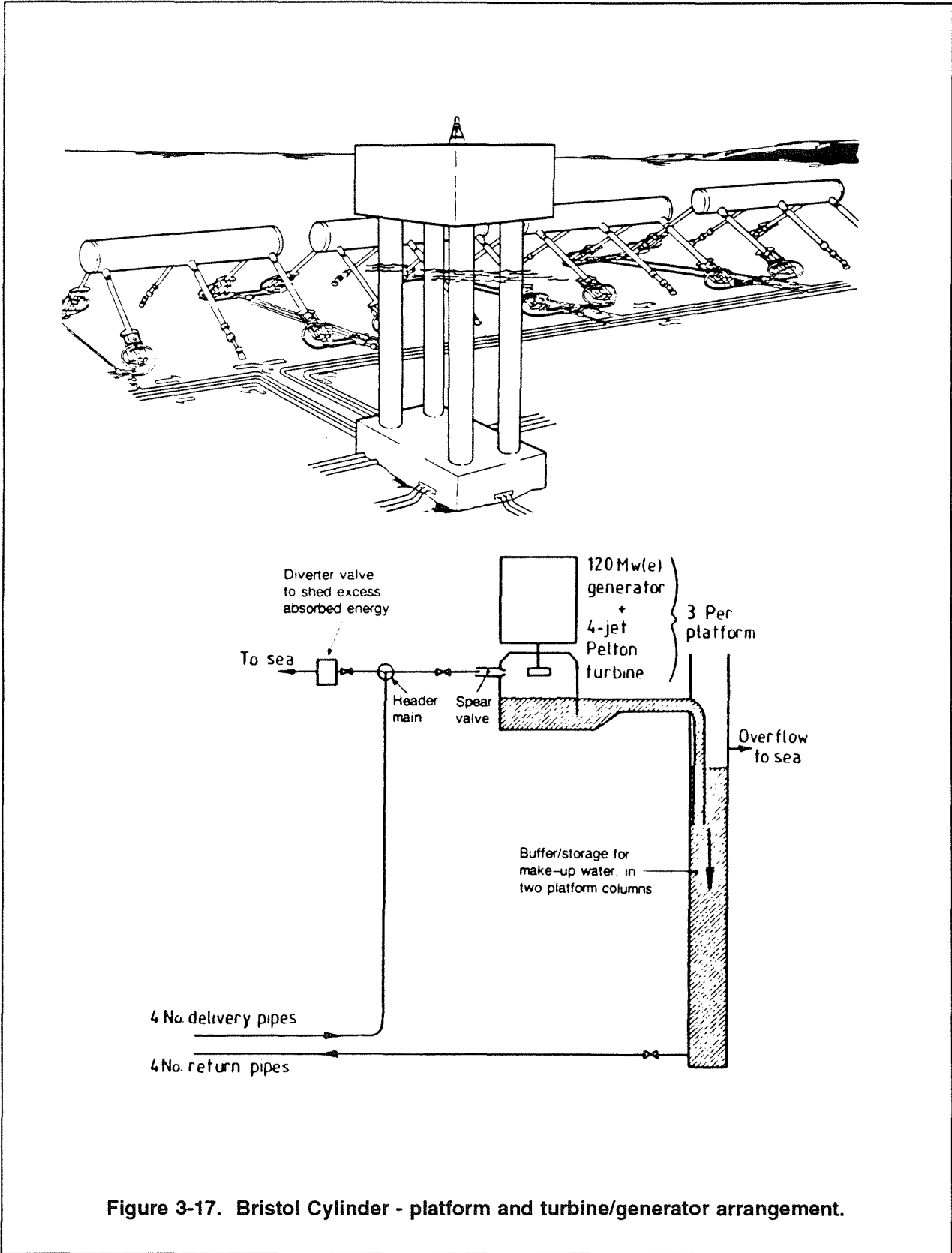


Figure 3-17. Bristol Cylinder - platform and turbine/generator arrangement.

Section 4

ECONOMIC ASSESSMENT

The economic feasibility of a wave power plant depends not only on the wave energy resource, but also on the conversion process. The cost and performance of land- and caisson-based systems are much more sensitive to site conditions than they are for offshore systems. It was beyond the scope of this study to perform a site-specific assessment of an onshore or breakwater-based wave power plant in Hawaii, but a general overview is given in the first part of this section. This is followed by cost and performance projections for an offshore heaving buoy system at Makapuu Point, Oahu.

LAND- AND CAISSON-BASED SYSTEMS

As mentioned in the previous section of this report, the development of land- and caisson-based wave energy devices is considerably more advanced than it is for offshore devices. Onshore wave power plants, however, involve significant shoreline modification, which may severely limit their deployment in Hawaii. Likewise, wave energy breakwaters are likely to be acceptable only at existing ports, or at locations where construction of a new small-craft harbor has been approved as part of a resort development plan.

The cost of a Tapered Channel power plant or a cliff-based oscillating water column depends greatly on the geology and topography of the local shoreline. Likewise, the cost of a breakwater-based system is influenced by the need for seafloor grading or blasting to prepare a level foundation, and the local availability of suitable rock for the rubble mound on which the wave-absorbing caissons would rest. The wave energy resource available to these systems depends on the degree to which refraction focuses waves towards or away from the potential plant site, which is a function of deep water wave period and direction, as well as the shape of nearshore bathymetric contours (see Appendix A).

Three steps are required to develop an economic assessment for an onshore or breakwater-based wave power plant. First, environmentally acceptable locations must be identified, based on the potential impacts of shoreline modification or breakwater construction. Second, nearshore bathymetric data must be obtained and gridded for the acceptable sites. Finally, the refraction of deep water wave spectra over nearshore bathymetric contours must be numerically simulated to obtain the shallow-water wave spectra, which can then be used to model the performance of the plant.

Such an effort was beyond the scope of this study. A general idea of what might be expected, however, is given in Tables 4-1 and 4-2, which present cost and performance projections for land- and caisson-based wave power plants at locations outside Hawaii. tables.

Table 4-1
Cost and Performance of Tapered Channel Power Plants.

Location:	Toftestallen (Norway)	Java (Indonesia)	King Island (Australia)
Average wave power:	25 kW/m	20-25 kW/m	30-32 kW/m
Collector opening width:	55 m	unknown	unknown
Reservoir surface area:	5,500 m ²	8,100 ²	unknown
Plant capacity:	0.35 MWe	1.5 MWe	1.5 MWe
Annual output:	1.7 GWh	10 GWh	9 GWh
Capacity factor:	25%	76%	68%
Initial investment:	\$3,560/kWe	\$2,000/kWe	\$3,290-3,840/kWe
Annual O&M cost:	\$18/kWe	\$33/kWe	\$33/kWe
Cost of energy:	8.0 ¢/kWh	3.6 ¢/kWh	6.2-7.2 ¢/kWh

A plant service life of 40 years and a construction time of one year was used for all projects. Costs are in 1990 constant dollars. See Appendix D for energy costing method, financial parameters, and currency exchange rates. (Data from [17], [18].)

Table 4-2
Cost and Performance of Caisson-Based Wave Power Plants.

Device:	Double-Acting MOWC	Double-Acting MOWC	Single-Acting OWC	Pivoting Flap
Developer:	Kvaerner Brug A/S	Kvaerner Brug A/S	Takenaka Corporation	Muroran Institute of Technology
Location:	Toftestallen (Norway)	Tongatapu (Tonga)	Kashima Port (Japan)	Muroran Port (Japan)
Water depth:	seaside cliff	reef crest	4.5 m	5 m
Average H_s :	unknown	unknown	1.4 m	2.0 m
Average T_s :	unknown	unknown	8 sec	6 sec
Average wave power:	15 kW/m	21 kW/m	unknown	11 kW/m
Caisson width:	10 m	18 m	7 m	25 m
Number of caissons:	one	four	20	10
Plant capacity:	0.5 MWe	2 MWe	1.5 MWe	1.5 MWe
Annual output:	0.64 GWh	5.8 GWh	4.1 GWh	6.9 GWh
Capacity factor:	15%	33%	31%	53%
Initial investment:	\$1,610/kWe	\$4,490/kWe	\$7,320/kWe	\$7,030/kWe
Re-investment:	none	none	none	\$2,560/kWe every 15 yr
Annual O&M cost:	\$16-32/kWe	\$45-90/kWe	\$57/kWe	\$70/kWe
Plant service life:	25 yr	25 yr	25 yr	45 yr
Cost of energy:	16-17 ¢/kWh	19-21 ¢/kWh	33 ¢/kWh	20 ¢/kWh

A construction time of one year was used for all projects. Costs are in 1990 constant dollars. See Appendix D for energy costing method, financial parameters, and currency exchange rates. (Data from [22], [24], [25], [26].)

Tapered Channel Power Plants

Regarding the demonstration plant at Toftestallen, the annual output given in Table 4-1 is based on a projected wave energy resource of 25 kW/m, whereas the incident wave power measured there during the past five years has averaged only 7 kW/m. It should also be noted that the projected capital cost is based on an identical plant built at the same site, incorporating "lessons learned" during the construction of the demonstration plant and not requiring extensive monitoring instrumentation [17].

The purpose of the Toftestallen project was to verify wave/channel hydrodynamic performance rather than optimize electric power generation. In order to keep costs down, a 350 kWe generator was used, even though it is much smaller than optimal for this size reservoir in the projected wave climate.

The Java plant best represents the relationship between generator capacity, plant output, and reservoir size. Its capital cost is less than two-thirds that of the King Island project, even though both plants have the same generation capacity. This is largely due to the remoteness of the King Island site, which requires the construction of a 5 km access road and overland transmission line.

Given the more energetic wave climate at King Island, Norwave expects a higher capacity factor there, but the plant's output is limited by the small size of the island's utility grid, which is now served by 2 MWe of diesel plant, generating approximately 10 GWh annually. As demand grows, output of the Tapered Channel plant can increase, resulting in a higher capacity factor and lower energy cost.

It is interesting to note that the Tapered Channel reservoir makes much more energy-efficient use of coastal land area than would a wind farm. For example, the projected annual output at Java is 10 million kWh. By comparison, a wind farm operating at 25% capacity factor would require twenty 225 kWe turbines to generate the same amount of energy. Assuming that the turbines have a rotor diameter of 27 m, and that they are arranged in two rows, with three rotor diameters between rows and eight rotor diameters between individual turbines in a row, the wind farm would occupy a land area of 157,500 m², about nineteen times greater than the Tapered Channel reservoir. Moreover, just as wind farm land can be used for livestock grazing, Tapered Channel reservoirs can be used for closed-pond aquaculture. The Crown Agents of London have estimated that the value of fish farmed in a Tapered Channel reservoir "may cover all capital costs of wave collectors, converters and basin" [37].

Caisson-Based Wave Power Plants

Table 4-2 presents cost and performance data for three oscillating water column (OWC) designs, and one pivoting flap system. Although Kvaerner-Brug's Toftestallen plant was a land-based unit, it is included in this table for ready comparison with the other Kvaerner-Brug project on Tongatapu.

As with Norwave, Kvaerner Brug's Toftestallen cost estimate is based on an identical plant built at the same site rather than the actual cost of the demonstration plant itself [22]. It is also important to note that the resource of 15 kW/m for Kvaerner Brug's performance estimate is based on the average incident wave power *when plant output was measured*, and so does not represent an annual average. While Norwave's turbine/generator was undersized for the reservoir at Toftestallen, Kvaerner Brug's 500 kWe unit was too large for a 10 m caisson, which accounts for its projected low capacity factor [38].

Kvaerner Brug also developed a commercial plant design for the south Pacific Kingdom of Tonga (see Figure 3-6). This project, now abandoned, better represents the relationship between turbine/generator capacity and capture chamber size [24]. The plant's capacity factor more than doubles, but the larger capture chamber involves a considerably higher concrete fabrication cost.

Takenaka Corporation has developed a conceptual design for a 1.5 MWe breakwater-based wave power plant at Kashima Port, using single-acting OWC caissons with an onshore air tank (see Figure 3-8). It should be noted that their capital cost estimate does not include fabrication of the wave-absorbing caissons, which is assumed to have been financed by some other source for shore protection [25].

The Muroran Institute of Technology has developed a conceptual design for a 1.5 MWe wave energy breakwater at Muroran Port (see Figure 3-9). Unlike Takenaka Corporation, their projected initial capital investment does include the caissons, and these account for 75% of the total plant cost [26].

The designers project a 50-year service life for the caissons at Muroran Port, but only a 15-year life for the other components. A 45-year plant life was used in Table 4-2, since it would not be cost-effective to replace balance-of-plant components at the end of the 45th year, for only five more years of caisson life.

Although incident wave power estimates were not published for either of these breakwater design studies, some inferences can be made by comparing wave statistics between Muroran Port and Kashima Port. Incident wave power is directly proportional to the square of significant wave height (H_s), multiplied by significant wave period (T_s). Thus, incident wave power at Kashima Port is about 35% less than that at Muroran Port, while Takenaka Corporation's proposed breakwater length is 45% shorter. If both plants were equally efficient, then the annual electricity output of Takenaka Corporation's design should be only about 2.5 GWh (65% x 55% x 6.9 GWh), but at 4.1 GWh, it is considerably higher.

This suggests that Takenaka Corporation's OWC is more efficient than Muroran Institute's pivoting flap. At \$7,030/kWe, it is also much more expensive. Apart from the breakwater caissons, the Pendulor System's balance-of-plant cost is only \$2,560/kWe. If caisson fabrication can be financed by some other

source (as has been assumed by Takenaka Corporation), and all other parameters in Table 4-2 remain the same, then the levelized energy cost at Muroran Port would be only 9.2 ¢/kWh over the 15-year service life of the balance-of-plant components.

Although environmental concerns will probably limit the coastal deployment of caisson-based wave energy devices to a few specific locations, they have much greater potential for blue-water ocean space utilization by very large floating structures (VLFS) in Hawaii's Exclusive Economic Zone. Barge-like VLFS modules are less costly than semisubmersibles, but require protection from wave action [39]. Fabricating the perimeter of a VLFS to accommodate wave energy absorbers such as oscillating water columns or pivoting flaps should not add significantly to its total construction cost. The capital investment for a wave power plant on such a VLFS would then be only for absorbers and power conversion equipment. As shown above, this would lead to a substantial reduction in the cost-of-energy.

The large inertia of the VLFS provides the necessary reaction point for these absorbers, which in turn act to remove energy from the wave before it passes under the platform. It is important to note that much of this energy is ultimately absorbed by the VLFS via structural foundations for power conversion equipment, but these may be less costly than designing the platform to withstand large sagging and hogging loads associated with undampened waves. As on shore, the wave-absorbing caissons would provide both a protective breakwater function, as well as a source of renewable energy to support the platform's primary function (airport, processing facility for deep-ocean mining, etc.).

OFFSHORE HEAVING BUOY SYSTEM

In addition to the Swedish heaving buoy device, the SEA Clam and Bristol Cylinder are two British offshore devices that have good potential for application in Hawaii. All three devices use either air or seawater as a working fluid, eliminating the risk of chemical pollution. They also have small waterplane areas and low freeboard (or are submerged), so their potential visual impact is low (or non-existent).

It was beyond the resources available for this study to prepare cost and performance estimates for all three offshore technologies. The Swedish heaving buoy system was selected, because a feasibility-level design had been recently prepared for Pacific Gas and Electric Company (PG&E) at a measurement site offshore Half Moon Bay, California, just south of San Francisco [40]. The PG&E design was based on up-to-date vendor quotes and cost estimates for fabrication and deployment in the San Francisco Bay area. Much less modification was required to adapt this design to Hawaii than would have been required to adapt either of the British designs, which had been developed for deployment in the Outer Hebrides Islands, off the northwest coast of Scotland. In addition, a more complete set of performance data was available for the Swedish heaving buoy system than for the other two offshore devices.

Reference Design Cost and Performance

The reference design consists of one or more star-shaped clusters of buoys, moored in 80 m water depth. Each star contains 60 buoys and six collecting lines arranged symmetrically around an underwater habitat, which houses a 10 MWe, vertical-axis Pelton turbine/generator (see Figure 3-13). There are ten buoys per collecting line, spaced on 30 m centers, giving the star a total diameter of 600 m.

It is important to note that this arrangement was originally intended for large mainland utility grids with broad continental shelves. The generator size (10 MWe) is not well-matched to the needs of small island utility grids, and the use of an underwater habitat is probably unnecessary; Hawaii's island shelves are sufficiently narrow that the turbine/generator could be installed on shore, which would reduce costs and increase plant availability. Reworking the plant arrangement to this extent, however, was beyond the resources available for this study.

In adapting the PG&E design to Hawaii, the following modifications were made. Because the island shelves are much narrower than the continental shelf off Half Moon Bay, a shorter submarine power cable is required to reach the 80 m depth contour. Smaller diameter buoys are optimal in the shorter period waves in Hawaii, which represents an even bigger cost saving. On the other hand, offshore deployment equipment is expected to be more costly, which results in a higher re-investment for periodic replacement of hose pumps, collecting lines, and mooring hardware.

Two plant sizes were evaluated, 10 MWe (the smallest possible with the given turbine/generator arrangement) and 30 MWe. Resource data for estimating plant performance were based on the annual average JPD table for the CDIP buoy off Makapuu Point (see Table 2-3). Although the depth at this measurement site is greater than 80 m, very little reduction in wave power is expected between the measurement depth and the reference depth, due to the narrowness of the island shelves. Cost and performance projections for these two plant sizes are given in Table 4-3.

Although the economic feasibility of offshore wave power plants is less sensitive to site conditions than it is for land- or caisson- based systems, the performance of some offshore devices is period-dependent. The Swedish heaving buoy/hose pump module is one such device, as shown in Figure 4-1, which plots wave energy absorption efficiency as a function of ka , the ratio of buoy circumference to wavelength. In 8-second waves, which are typical of Makapuu Point, a 16 m diameter buoy has a ka value of 0.5, giving it a "best fit" absorption efficiency of about 55% (Figure 4-1). In 10-second waves, which prevail at Barking Sands, ka is only 0.3, and the absorption efficiency drops to about 20%. Thus, the Swedish heaving buoy system is more likely to be economically feasible off northeast island coasts dominated by short-period trade wind waves, than off northwest coasts dominated by long-period north Pacific swell.

Table 4-3
Cost and Performance of Offshore Heaving Buoy Reference Design
at Makapuu Point

Distance offshore:	10 km	
Water depth:	80 m	
Average H_s :	1.88 m	
Average T_p :	8.2 sec	
Average wave power:	15.0 kW/m	
Buoy diameter:	16 m	
Plant capacity:	10 MWe	30 MWe
Number of buoys:	60	180
Annual output:	37 GWh	111 GWh
Capacity factor:	42%	42%
Initial investment:	\$2,300/kWe	\$1,970/kWe
Re-investment every 6 yr:	\$182/kWe	\$173/kWe
Annual O&M cost:	\$92/kWe	\$79/kWe
Cost of energy:	8.6 ¢/kWh	9.9 ¢/kWh

A service life of 30 years and a construction time of one year was used for both plants. Costs are in 1990 constant dollars. See Appendix D for energy costing method, financial parameters, and currency exchange rates.

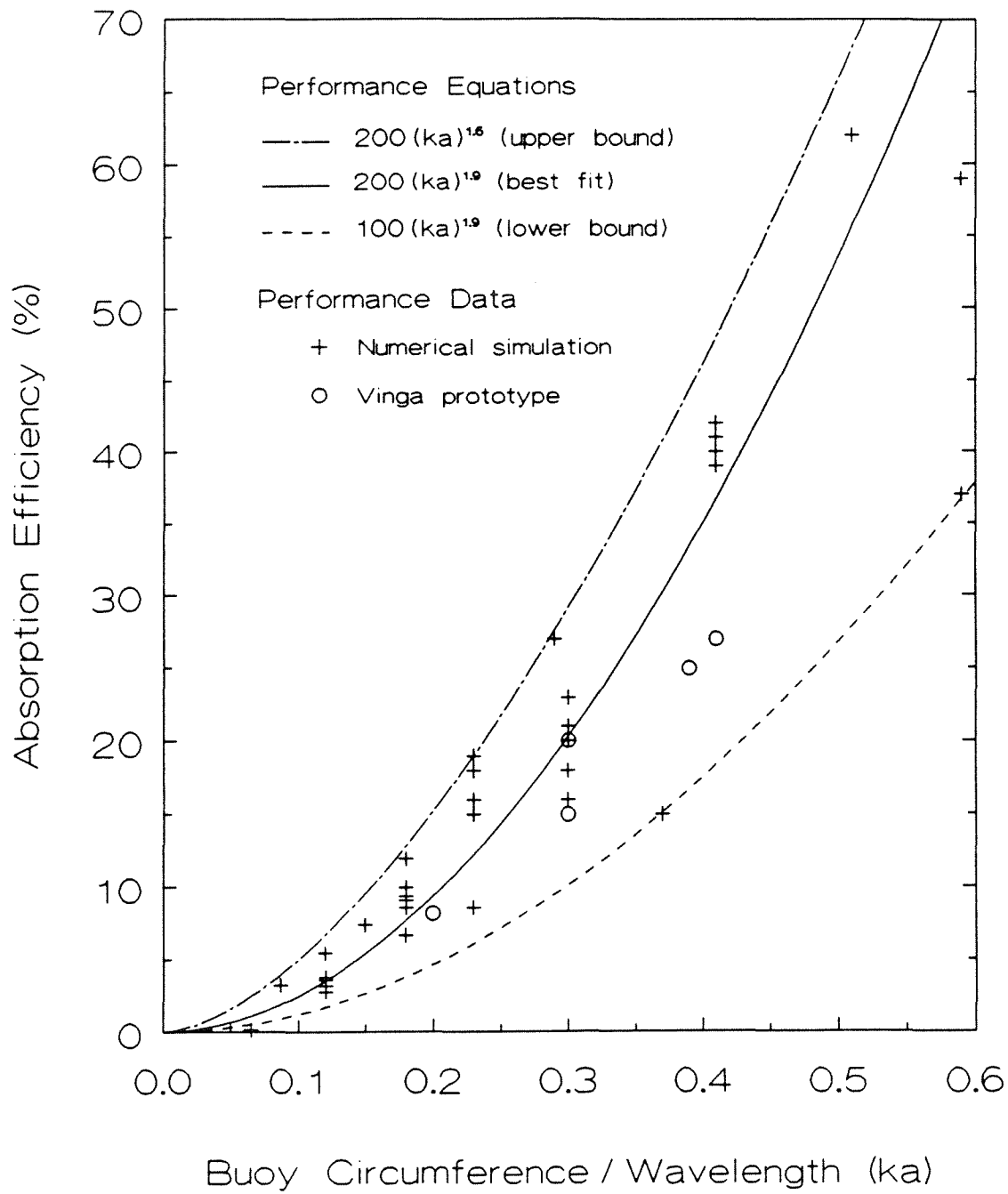


Figure 4-1. Absorption efficiency of heaving buoy/hose pump modules in random waves.

Project Development Risks

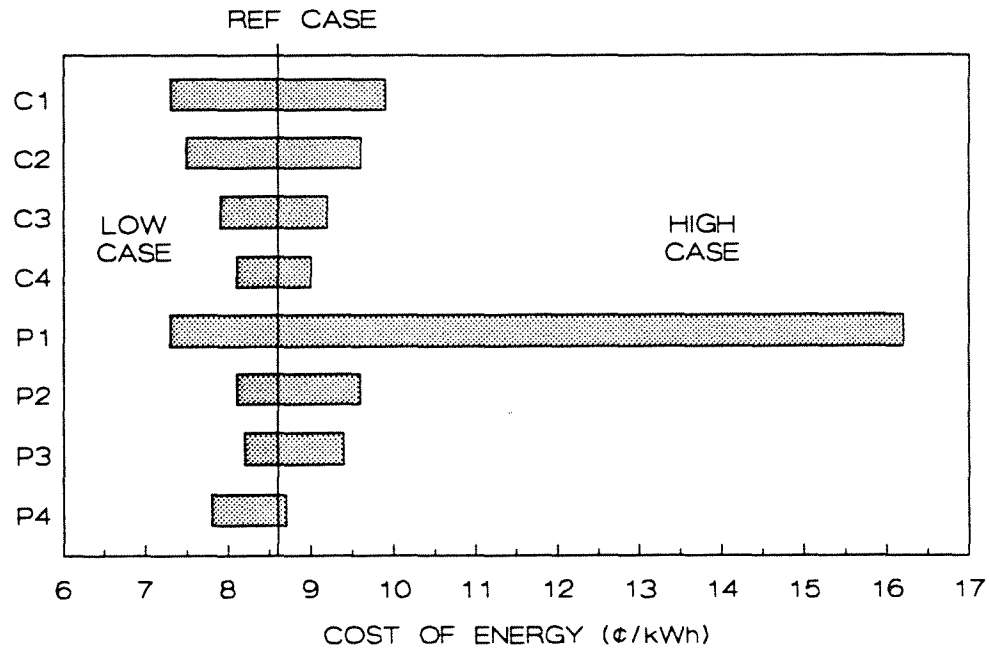
Although the Swedish heaving buoy system has been ocean tested at 1/3-scale, its development status is much less advanced than land- or caisson-based systems that have long-term operational experience with full-scale demonstration plants. Development of a wave power project based on this or other offshore technologies has several risks associated with uncertainties in capital and operating costs, as well as device performance projections.

To quantify project development risks for the Swedish heaving buoy system, a cost-of-energy sensitivity analysis was performed on the 30 MWe reference design at Makapuu Point. Uncertainty bands were estimated for eight cost and performance parameters. In order to determine which uncertainties are most significant, each parameter was varied from the reference case, one at a time. The results of this analysis are presented in Figure 4-2. The basis for each uncertainty band is described below.

Buoy Fabrication Cost. The low case is based on a 1986 estimate for ferrocement construction, derived from the scantlings of a prototype tank landing craft (LCT) built and successfully tested by the U.S. Navy in 1945. The high case is based on a 1988 estimate for thin-wall reinforced concrete construction. The difference between the two estimates reflects very different construction methods: use of floating forms and shotcrete laminating in the low case; conventional land-based concrete work in the high case. The reference case was simply chosen as the midpoint between these two estimates (both escalated at an annual inflation rate of 6% to 1990). Of the four cost uncertainties evaluated in this study, buoy fabrication has the biggest impact on the cost of energy, ± 1.3 ¢/kWh.

Operating and Maintenance Cost. Marine tanker terminals are the offshore structures that are most similar to floating wave power plants, and for which there is any sort of long-term operational history. Like wave power plants, they are unmanned facilities and must maintain high availability. The reference case is based on the annual maintenance cost (expressed as percent of capital cost) for Exxon's Tembungo Field Single Anchor Leg Mooring, located 93 km offshore Sabba, East Malaysia, in 91 m water depth [41]. Projecting O&M cost in this manner is not nearly as accurate as a line item estimate, but the latter could not be developed within the resource constraints of this study. Therefore, this parameter has a large uncertainty band and a significant impact on the cost of energy, ranging from -1.1 to +1.0 ¢/kWh.

Indirect Costs. Land-based general facilities are expected to range from 3% to 15% of the direct cost, while field engineering and home office fees are expected to range from 7% to 15% [42]. The uncertainty band represents the combined additive range of these estimates, with the reference case as the mid-point. This has a relatively small impact on the cost of energy, ranging from -0.7 to +0.6 ¢/kWh.



COST UNCERTAINTIES	<u>LOW CASE</u>	<u>REF CASE</u>	<u>HIGH CASE</u>
C1 Buoy fabrication cost (\$/m ²)	200	300	400
C2 Annual O&M cost (% of initial investment)	2	4	6
C3 Indirect costs (% of direct cost)	10	20	30
C4 Deployment cost (% relative to San Francisco Bay area cost)	100	150	200
PERFORMANCE UNCERTAINTIES			
P1 Wave energy absorption efficiency	upper bound	best fit	lower bound
P2 Hose pump service life (yr)	10	6	3
P3 Annual availability (%)	95	90	80
P4 Average wave power (kW/m) (time period of data set)	15.9 (1982)	15.0 (1982-89)	13.7 (1984)

Figure 4-2. Energy cost sensitivity analysis of 30 MWe reference design at Makapuu Point.

Deployment Cost. Mobilization and demobilization charges, as well as lease rates for offshore equipment, are expected to be higher in Hawaii than in the San Francisco Bay area. Relative to the PG&E reference design, the deployment cost for Hawaii was assumed to be the same in the low case, 50% higher in the reference case, and double in the high case. This uncertainty has the least impact on the cost of energy, ranging from -0.5 to +0.4 ¢/kWh.

Wave Energy Absorption Efficiency. There is a large amount of scatter in the projected absorption efficiency of heaving buoy/hose pump modules in random waves. For a 16-meter diameter buoy in wavelengths typical of the dominant wave period off Makapuu Point, the scatter in absorption efficiency data ranges from 25% to 65% (Figure 4-1). Of all project development risks, this one has by far the greatest impact on the cost of energy, ranging from -1.3 to +7.6 ¢/kWh.

Hose Pump Service Life. The reference case is based on the developers' estimate of 6 years, which was derived from accelerated testing of laboratory-scale prototype hoses [43]. The low case is based on a different set of laboratory tests, conducted by the Harwell Laboratory of the Energy Technology Support Unit in the United Kingdom to evaluate the fatigue characteristics of a polymer tube spring for mooring the submerged Bristol Cylinder wave energy device. Although developed independently of the Swedish hose pump, and for different purposes, the British tube spring is identical to the hose pump in form and function. The Harwell tests indicated a service life in excess of 25 years [44]. Other plant components (connecting hoses subject to bending, upper mooring chain and fittings) are not expected to last this long, however, and would have to be replaced more frequently, incurring the same buoy retrieval and re-deployment costs. Therefore, the low case assumed that the hose pumps, together with these other components, would be replaced at 10-year intervals.

The high case is based on the experience of offshore tanker terminals, where underbuoy hoses have demonstrated a service life of 3-4 years. These hoses are never in tension, but are subject to continual bending. They also carry petroleum products rather than seawater. Nevertheless, they are the only large-diameter submerged hoses for which there is any operational history in the offshore marine environment.

Annual Maintenance Availability. The reported availability of turbo-generating machinery in tidal power plants is 96-98% ([45], [46]), and that for offshore tanker terminals is 93-96% ([41], [47]). Taken together, these give a total availability of 89% to 94% for the underwater habitat and turbine/generator. Results from the British wave energy program suggested that the annual availability of a wave power plant off the northwest coast of Scotland would be 80% to 90%, based on a variety of devices under consideration at that time. These estimates were derived with a fairly sophisticated computer model and probably represent the best theoretical research in this area [48].

The reference case approximates the worst reported availability from tidal power/offshore terminal experience, which is similar to the best wave power simulations. The low-cost case approximates the best reported tidal/offshore experience. The high-cost case is based on the worst wave power simulations.

Wave Energy Resource. The wave data record from offshore Makapuu Point is one of the longest and most complete in Hawaii. Even so, it covers only five complete years and may not represent the long-term wave climate over a 30-year project life. To assess the consequences of this uncertainty, the most and least energetic individual years were used for the low-cost and high-cost cases, respectively.

A similar analysis for the PG&E design indicated that during the 1981-86 time period, wave energy levels were lowest in 1985 and greatest in 1983, when winter storms devastated much of the California coast [11]. Unfortunately, there are only five scattered months of wave data from Makapuu Point during low-energy 1985, and no data during the highest-energy months of 1983 (see Table 2-1). Of the remaining five years, for which seasonally complete records exist, there is relatively little year-to-year variability. Consequently, the cost-of-energy impact of this parameter at Makapuu Point is low, ranging only from -0.8 to +0.1 ¢/kWh. Generally speaking, however, use of only a single year's wave data to forecast device performance entails greater risk than indicated by this particular case.

Risk Reduction

As already noted, the uncertainty in absorption efficiency alone causes projected energy costs to range from 7.3 to 16.2 ¢/kWh. Although other uncertainties individually have a much lower impact than the uncertainty in absorption efficiency, they have a similar effect when all seven are combined, with a projected energy cost range of 4.6 to 15.4 ¢/kWh.

Other offshore technologies have similar cost and performance uncertainties, and private financing is unlikely to be available for offshore wave power projects without considerably reducing these risks.

Several measures can be taken to reduce the uncertainty in cost-of-energy projections:

- More detailed design work would increase the accuracy of component capital costs. Where a cost uncertainty has an especially large impact on the cost of energy (e.g. buoy fabrication), it may be worthwhile to build a prototype component, which would give a firmer basis for estimating mass-production costs.
- Ocean testing of full-scale prototypes in a wide variety of seastates would reduce the uncertainty in projections of wave energy absorption efficiency, which is the single biggest project development risk.
- Longer-term ocean tests (on the order of years) would reduce uncertainties in operating and maintenance costs, the required frequency of periodic re-investment in replacement equipment, and annual maintenance availability.

Over-estimation of incident wave power also represents a significant project development risk, and there are several examples of wave energy prototypes that did not perform well due to poor understanding of the local resource. For most projects, only a few years of site-specific measured wave data will be available, and an assessment should be made as to how well those years represent the long-term wave climate. A rough estimate can be obtained by statistical analysis of shipboard observations, which have been archived for nearly thirty years in Hawaii. A more accurate assessment requires the development of a long-term, site-specific numerical wave hindcast, which has become increasingly affordable with the development of high-performance desk-top computers and efficient wave hindcasting models [49].

Section 5

CONCLUSIONS AND RECOMMENDATIONS

The results of this study suggest that ocean waves can be an important renewable energy resource for the state of Hawaii. This is the first comprehensive wave energy assessment that has been done, however, and several important questions remain to be answered.

OVERALL ASSESSMENT

Recovering only 5-10% of the wave energy available in outer shelf waters off the northern coastlines of Kauai, Maui, and Hawaii could meet the total annual electricity demand of those islands. Less than one half of one percent of Molokai's wave energy resource could meet the electricity needs of that island. Except for Oahu, where electricity demand is comparable to two-thirds of the available resource, wave energy can be withdrawn at very low levels and still make a large contribution to island energy supply.

Wave energy costs less than 10 ¢/kWh appear to be feasible for offshore heaving buoy systems sited along coasts dominated by trade wind waves. Where shoreline topography exists that minimizes excavation and concrete placement, Tapered Channel plants and land-based oscillating water column systems might be able to realize similarly low energy costs. Caisson-based devices, however, appear to be economical only if the cost of caisson fabrication can be assigned to some other function such as harbor improvement, shore protection, or perimeter construction for large floating platforms.

UNRESOLVED ISSUES

Several issues must be resolved before any significant development of Hawaii's wave energy resource can take place. These can be grouped into three categories: utility integration, environmental impact, and technology cost and performance.

Utility Integration

Island utilities may severely limit the amount of wave generation capacity that can be installed in their service territories. The two main areas of concern are the time-dependent variability of wave energy and the transmission capacity of island utility grids.

Wind energy is another variable resource, and Hawaiian Electric Company has placed severe limits on its development [50]. On Maui, for example, the maximum permitted wind energy contribution ranges from zero in March, when grid-wide demand is at a minimum, to 4.2 MWe in July, when the grid is at peak load (118 MWe). Likewise, grid penetration limits for wind energy on the Big Island are 1.3 MWe at times of minimum load and 4 MWe at times of peak load.

Wave energy is more consistent than wind energy, however, and this may permit a greater degree of utility grid penetration. For example, at NOAA Station 51001, significant wave height has never been less than 1 m in eight years, yet sustained wind speeds fall below 5 knots (2.8 m/sec) an average of 25 days per year and are zero for an average of 61 hours per year [10].

A second concern is the transmission capacity of island utility grids. An accurate assessment of wave energy's cost/contribution profile must consider any grid reinforcement that would be necessary for transmitting wave power to load centers that are far removed from the high-energy, north-facing island coastlines. Such an assessment was beyond the resources available for this study but is clearly critical to understanding the true cost of wave energy development in Hawaii.

Where high-energy coastlines are remote from island load centers, they also tend to be remote from existing power plants. An early avenue for commercial wave energy development in Hawaii would be the installation of small wave power plants to offset the need for utility grid extension to such remote areas. In addition to meeting coastal load growth, a few megawatts of distributed wave generation capacity could benefit the island transmission network by providing grid stability and voltage support, particularly in the most remote areas that are at the far end of a transmission circuit.

Environmental Impact

Thus far, it has been assumed that the deployment of onshore and breakwater-based wave power plants will be limited by the environmental impacts associated with shoreline modification and breakwater construction. Nevertheless, where acceptable, such systems may make an important contribution to island energy needs. Environmentally suitable sites and their development potential (in terms of energy cost and installed capacity) have yet to be catalogued.

Although offshore heaving buoy systems are thought to be more widely acceptable, they are not without potential environmental problems. A 10 MWe plant sized for a trade wind wave climate occupies a circle of sea space 600 m in diameter (about the same area as Manana Island, which is located off the western coast of Oahu, just north of Makapuu Point). No matter how well marked, such a plant would be a potential navigation hazard under adverse sea and weather conditions. Therefore its location should be chosen to avoid areas of high boating activity or shipping traffic.

The submerged Bristol Cylinder presents less of a potential navigation hazard for small craft, although it is sufficiently close to the surface to threaten ships with a draft of more than about 2 m (see Figure 3-16). It also has potential conflict with commercial fisheries, particularly trawlers, and siting the absorbers on productive fishing grounds should be avoided.

Visual impacts will be more difficult to avoid. The visual intrusion presented by a wave power plant depends on six factors:

- Offshore distance of the plant
- Elevation of the shoreline observer
- Coastal weather conditions
- Size and shape of the individual units that make up the plant
- Color contrast between the individual units and the sea
- The presence of other natural or artificial structures in the seascape

An observer 6 feet (180 cm) tall, standing at the surf's edge (i.e. at mean sea level) has an offshore horizon of 5.2 km, which can be seen even in light haze. Except for the area just north of Kahului, Maui, where the shelf is about 8 km wide, the island shelves are so narrow that a wave power plant anchored in outer shelf waters will be within the visual horizon of any onshore observer, even one at sea level.

To get an idea of the plant's appearance, hold a ruler at arm's length and imagine that at the same time you are looking over the ruler's edge at a 10 MWe heaving buoy plant, located 3 km offshore. A buoy having a diameter of 16 m would span 4 mm along the ruler's edge (about 3/16-inch). With a freeboard of only 1-2 m, however, individual buoys would tend to be obscured by wave action unless viewed from a high elevation. A 600 m diameter cluster of buoys would span a distance of 14 cm and would certainly be visible to someone who knew where to look. The plant would not immediately draw one's attention, however, since it would occupy only 4-5% of a 180° field of view from the shoreline.

Technology Cost and Performance

A heaving buoy plant design developed specifically for Hawaii would differ significantly from the reference designs described in this report. Plant capacity would be more realistically matched to island utility grids, probably 1 to 2 MWe. Such a small plant would consist of 10 to 15 buoys pumping high-pressure seawater to an onshore Pelton turbine/generator. The underwater habitat would be eliminated, and the submarine power cable would be replaced with a high-pressure seawater pipeline. Onshore electrical equipment would be better protected from storm damage and more accessible for inspection and maintenance, increasing plant availability and reducing operating costs. On the other hand, a smaller plant would lose some economies of scale. Changing the design to this extent adds even further uncertainty to the economic assessment of the Swedish heaving buoy device presented in Section 4.

Extensive modification of the PG&E reference design was beyond the resources available for this study, but this would be the next step in assessing the economic feasibility of offshore heaving buoy systems in Hawaii. Similar small-scale designs should be prepared for other promising technologies as well.

RECOMMENDATIONS

In order to resolve the above issues, a four-phase wave energy development program is recommended, lasting eight years and leading to the construction of one or two small demonstration plants. Each phase would depend on the success of the previous phase before being initiated and would involve increased private-sector funding by commercial developers.

- Phase I - Develop resource supply curves based on existing wave data, feasibility-level designs, and cost/performance projections for six different conversion technologies. Entirely state funded. Completed in 1994.
- Phase II - Prepare a 2- to 3-year wave hindcast for ten to twenty of the most promising sites identified in Phase I, and solicit conceptual designs from commercial developers representing three or four of the most promising technologies to emerge from Phase I. Refine resource supply curves based on the developers' cost and performance projections. State funding supports hindcast preparation and 60% of the developers' design work. Completed in 1996.
- Phase III - Begin a wave measurement program at the most promising site identified in Phase II, prepare a 20- or 30-year hindcast for that site, and solicit preliminary designs from commercial developers representing one or two of the most promising technologies to emerge from Phase II. State funding supports hindcast preparation and 30% of the developers' design work. Completed in 1998.
- Phase IV - Continue wave measurements and carry preliminary design(s) of Phase III through detailed design and construction. State funding supports wave measurements and some plant monitoring instrumentation. Developers arrange private financing for design and construction of the actual plant(s), based on revenue anticipated from the sale of electricity and/or fresh water. Project becomes fully operational in 2000.

Nearly fifty different wave energy conversion technologies have been developed worldwide in the last decade (see Appendix E). In order for the above program to be manageable, the number of candidate technologies to be evaluated in Phase I must be greatly reduced, and six is thought to be a reasonable number. The main criterion for carrying a technology forward into Phases II and III will be its energy cost/contribution profile, as characterized by the resource supply curves developed in Phase I and refined in Phase II. Thus, Phase I sets the direction for the entire program and is described in more detail below.

Phase I, Task A - Quantify Time Variability of the Wave Resource

As shown in Table 2-1, parallel tracking of monthly average incident wave power at Makapuu Point, Barking Sands, and NOAA Station 51001 would provide a nearly complete ten-year record (1981-1990) of seasonal and annual trends. Ship-observed wave statistics would also be compiled to cover the period from 1963 (when both sea and swell parameters were first reported by ships) through 1992, to determine how well the ten-year measured data set represents the 30-year projected service life of a wave power plant. Finally, an analysis of wave energy's hourly variability would determine whether there is any correlation with hourly electricity demand, and would help utilities estimate the degree of island grid penetration they might permit for wave power.

Phase I, Task B - Assess Environmental and Utility Constraints at Candidate Sites

On each of the five major islands having good northern coastal exposure (Kauai, Oahu, Molokai, Maui, and Hawaii), candidate sites would be identified where a wave power plant would have minimum environmental impact and a high probability of public acceptance. This determination would be made for each of the six conversion technologies surveyed in this report:

- Land-based Tapered Channel
- Land- or caisson-based oscillating water column
- Caisson-based pivoting flap
- Offshore heaving buoy
- Offshore SEA Clam
- Offshore Bristol Cylinder

The advantages of these devices for potential application in Hawaii have been described in Section 3. They represent a wide variety of conversion processes and form a starting group from which several economical and environmentally acceptable projects are likely to emerge.

In identifying candidate project sites, the use of Tapered Channel reservoirs for closed-pond aquaculture would be explored, as would the use of wave energy breakwaters for creating harbors of refuge at locations such as Kawela Bay on Oahu and Waipio Bay on the Big Island. Such harbors would provide shelter for commercial fishing vessels and recreational small craft in the event of sudden storms, medical emergencies, engine problems, or the exhaustion of fuel supplies.

At the same time, island utility grids would be surveyed, to answer the following questions:

- What is the present demand and its projected growth at load centers along northern island coastlines? What is the transmission capacity of lines serving these load centers?
- Where might wave energy be used to meet local demand that is projected to grow beyond the transmission capacity of existing lines from the main island grid?
- Where does surplus transmission capacity exist for carrying wave power inland from the coast, and how much grid reinforcement would be required to support potential projects that are otherwise environmentally acceptable?
- Based on the variability analyses of Task A, above, what degree of grid penetration are island utilities likely to permit for wave power? What data would utilities need from a demonstration plant in order to better establish these limits?

As part of the information gathering process, slide presentations would be given on each island, so that utility representatives, environmental groups, and others potentially affected by wave power development can learn about the different conversion technologies and express their local concerns. Potential project sites would then be catalogued by island and ranked according to the total wave generating capacity that could be installed there for each different technology, based on environmental and utility constraints.

Phase I, Task C - Develop Average Wave Spectra for Candidate Project Sites

Additional measured spectra from Makapuu Point and NOAA Station 51001 would be analyzed to develop more reliable estimates of the deep water spectra that are used as input to the refraction and shoaling program developed in this study. For each sea state, an average spectrum would be computed (most likely resource), as would an upper-bound spectrum (optimistic resource) and a lower-bound spectrum (pessimistic resource) based on the scatter envelope of measured wave spectra. The refraction and shoaling program would then be run for those candidate sites where land- or caisson-based wave power plants would have minimum environmental impact and a high probability of public acceptance, as identified in Task B. Wave statistics would be developed for offshore candidate sites as well, accounting for the sheltering effects of neighboring islands.

Phase I, Task D - Develop Feasibility-Level Designs and Cost/Performance Projections

For each of the six conversion technologies listed on the previous page, three reference designs would be prepared, based on optimistic, pessimistic, and most likely projections of wave energy conversion efficiency. Parametric costing relationships would be developed such that plant designs can be moved from one site to the next (e.g. caisson weight - and thus fabrication cost - as a function of the site-specific extreme design wave height; deployment cost as a function of caisson weight and the ocean towing distance from fabrication yard to candidate site). Parametric relationships would also enable different project sizes, as set by the environmental and utility constraints surveyed in Task B, to be evaluated.

In order to ensure a consistent approach for all technologies and to accurately reflect fabrication and deployment costs in Hawaii (as opposed to Japan or Europe, for example), it is recommended that parametric costing relationships be developed by a single independent contractor, rather than six different technology developers. This would also provide a common benchmark against which to track the developers' evolving designs in subsequent program phases.

For each candidate technology, capital and operating costs would be estimated at all candidate sites where that technology is appropriate, as would total annual electricity output. Cost and performance projections would be made for four combinations of resource and conversion efficiency: most likely resource (average wave spectra) with optimistic and pessimistic efficiencies; and most likely efficiency, with optimistic (upper-bound spectra) and pessimistic (lower-bound spectra) resource estimates.

Levelized revenue requirements would then be computed for each potential project, using a common levelization procedure and a common set of financial parameters, such as those published in the EPRI Technical Assessment Guide (see Appendix D). It is essential that the cost of energy from each project also account for any new transmission line required to connect the project to the existing island grid.

Phase I, Task E - Prepare Resource Supply Curves

A resource supply curve describes the relationship between the value of electricity and the level of resource development that is economical at that value. The "level of resource development" can be quantified either in terms of installed capacity (e.g. MWe) or annual electricity generated (e.g. GWh/yr). Given the time variability of the wave energy resource, annual electricity generated is probably the more meaningful way to quantify resource development, since wave power's role in island energy supply is more likely to be one of displacing fossil fuels, rather than meeting growth in peak demand.

Two pairs of resource supply curves would be prepared for each island/technology combination. The first pair would be based on the most likely conversion efficiency for a given technology, combined with optimistic and pessimistic resource estimates. All other things being equal, a potential project site whose energy cost is less sensitive to resource projections would be a more promising candidate for subsequent program phases. The second pair of resource supply curves would be based on the most likely resource, combined with optimistic and pessimistic efficiency projections. All other things being equal, a conversion technology whose energy cost/contribution is less sensitive to efficiency projections would be a more promising candidate for subsequent program phases.

Phase I, Task F - Assess Phase I Results

For each of the six conversion technologies, prepare a state-wide aggregate resource supply curve. Based on these six curves, select the three or four technologies that have the most promising energy cost/contribution profiles. Select ten to twenty candidate project sites throughout the state, which have the greatest near-term development potential (lowest energy costs for a given technology). The selected technologies and sites would then be carried forward into Phase II. The state's decision to actually fund Phase II would be based on whether the resource supply curves for the most promising wave energy technologies were comparable to or better than those for other indigenous renewable resources, such as solar, wind, and biomass.

Section 6

REFERENCES

1. Venezian, 1978. Wave energy as a resource for wave power in Hawaii. *Look Lab/Hawaii*, Vol. 8, No. 2 (July), pp. 28-39.
2. Bretschneider, C.L., and R. C. Ertekin, 1989. Estimation of Wave Power as and Energy Resource for Hawaii. In *Proceedings of the International Conference on Ocean Energy Recovery*, edited by Hans-Jurgen Krock, pp. 189-201. New York, New York: American Society of Civil Engineers.
3. U.S. Naval Weather Service Command, 1971. *Summary of Synoptic Meteorological Observations: Hawaiian and Selected North Pacific Island Coastal Marine Areas, Volume 1*. Springfield, Virginia: National Technical Information Service.
4. Edward K. Noda & Associates, 1986. *Wave Energy Resource Evaluation for the Neptune System on Oahu, Hawaii*. Honolulu, Hawaii: Hawaiian Electric Company, Inc., EKN-1099-R-1-1.
5. MEC Systems Corporation, 1985. *Statistical Comparison of Ship and Buoy Marine Observations*. Manassas, Virginia: MEC Systems Corporation, MEC-85-8.
6. U.S. Army Corps of Engineers, 1986. *Pacific Coast Hindcast Deep Water Wave Information*. Vicksburg, Mississippi: Coastal Engineering Research Center, U.S. Army Waterways Experiment Station, WIS Report 14.
7. Seymour, Richard J., Meredith H. Sessions, and David Castel, 1985. Automated remote recording and analysis of coastal data. *ASCE Journal of Waterway, Port, Coastal and Ocean Engineering*, Vol. 111, pp. 388-400.
8. Edward K. Noda & Associates, 1986. *Hawaii Ocean Science & Technology Park, First Increment Design: Oceanographic Criteria for Design and Deployment of the Cold Water Pipe System*. Honolulu, Hawaii: R.M. Towill Corporation, EKN-1071-R-1-2.
9. Edward K. Noda & Associates, 1986. *Hawaii Deep Water Cable Program: Wave and Near-Surface Current Measurement Program in the Alenuihaha Channel*. Honolulu, Hawaii: Hawaiian Dredging and Construction Company, EKN-1028-R-3-2.
10. National Climatic Data Center, 1990. *Climatic Summaries for NDBC Buoys and Stations, Update 1*. NSTL, Mississippi: National Oceanic and Atmospheric Administration, National Data Buoy Center.
11. Seymour, R.J., 1983. *Extreme Waves in California During Winter 1983*. Sacramento, California: State of California, Department of Boating and Waterways.
12. Ochi, M.K., and E.N. Hubble, 1976. Six-parameter wave spectra. In *Proceedings of the 15th Conference on Coastal Engineering*, pp. 301-328. New York, New York: American Society of Civil Engineers.
13. Goda, Y., 1985. *Random Seas and Design of Maritime Structures*. Tokyo, Japan: University of Tokyo Press.
14. Collins, J.I., W.-L. Chiang, and F. Wu, 1981. Refraction of directional spectra. In *Proceedings of the Conference on Directional Wave Spectra Applications*, pp. 251-267. New York, New York: American Society of Civil Engineers.

15. State of Hawaii, 1990. *The State of Hawaii Data Book, 1990 - A Statistical Abstract*. Honolulu, Hawaii: Department of Business, Economic Development, and Tourism, Research and Economic Analysis Division, Statistics Branch, HA4007.H356.1990.
16. Norwegian Royal Ministry of Petroleum and Energy. 1987. *Norwegian Wave Power Plants 1987*. Oslo, Norway: Royal Ministry of Petroleum and Energy.
17. Telephone conversation between Even Mehlum (Norwave, A.S., Lysaker, Norway) and George Hagerman (SEASUN Power Systems, Alexandria, Virginia), 9 November 1990.
18. Palme, A. 1920. Wave motion turbine. *Power*, Vol. 52 (18), pp. 700-701.
19. Masuda, Yoshio. 1987. Experiences in pneumatic wave energy conversion in Japan. In *Utilization of Ocean Waves - Wave to Energy Conversion*, edited by Michael E. McCormick and Young C. Kim, pp. 1-33. New York, New York: American Society of Civil Engineers.
20. Hotta, H., Y. Washio, S. Ishii, Y. Masuda, T. Miyazaki, and K. Kudo. 1986. The operational test on the shore fixed OWC type wave power generator. In *Proceedings of the Fifth International Offshore Mechanics and Arctic Engineering Symposium*, pp. 546-552 (Vol. 2). New York, New York: American Society of Mechanical Engineers.
21. Telephone conversation between Stephen McIlwaine, (Queen's University of Belfast, Belfast, Northern Ireland) and George Hagerman (SEASUN Power Systems, Alexandria, Virginia), 9 November 1990.
22. Bonke, Knut, and Nils Ambli. 1987. Prototype wave power stations in Norway. In *Utilization of Ocean Waves - Wave to Energy Conversion*, edited by Michael E. McCormick and Young C. Kim, pp. 34-44. New York, New York: American Society of Civil Engineers.
23. Reuter News Service. 1989. Norwegian wave energy plant blown out to sea in storm. *International Solar Energy Intelligence Report*, 27 January, p. 20.
24. Telephone conversation between Andreas Tommerbakke (Kvaerner Brug A/S, Oslo, Norway) and George Hagerman (SEASUN Power Systems, Alexandria, Virginia), 27 August 1988.
25. Moody, G.W., and G. Elliot. 1982. The development of the NEL breakwater wave energy converter. In *Proceedings of the Second International Symposium on Wave Energy Utilization*, edited by H. Berge, pp. 421-451. Trondheim, Norway: Tapir Publishers.
26. Goda, Yoshimi, Katsumi Kanda, Yoshiyuki Hoshiyama, Hideaki Ohneda, Shigeo Takahashi, Youichi Nagasawa, Hiroshi Suzuki, and Masanori Hirano. 1990. Field verification experiment of a wave power extracting caisson breakwater. In *Proceedings of the International Conference on Ocean Energy Recovery*, edited by Hans-Jurgen Krock, pp. 35-42. New York, New York: American Society of Civil Engineers.
27. Chino, Hidenori, Kiyoshi Nishihara, and Yasuhide Nakakuki. 1989. Verification test of a wave-power generating system with a constant air pressure tank. In *Air Conditioning With Heat Pump*, pp. 1-26. Honolulu, Hawaii: Department of Business and Economic Development, Energy Division (photocopy on file).
28. Watabe, Tomiji, Hideo Kondo. 1989. Hydraulic technology and utilization of ocean wave power. *JHPS International Symposium on Fluid Power - Tokyo, March 1989*, pp. 301-308.

29. Telephone conversation between Tomiji Watabe (Muroran Institute of Technology, Hokkaido, Japan) and George Hagerman (SEASUN Power Systems, Alexandria, Virginia), 8 November 1990.
30. Nielsen, K., and C. Scholten, 1990. Planning a full-scale wave power conversion test: 1988-1989. In *Proceedings of the International Conference on Ocean Energy Recovery*, edited by Hans-Jurgen Krock, pp. 111-120. New York, New York: American Society of Civil Engineers.
31. Hicks, Douglas C., Charles M. Pleass, and George R. Mitcheson. 1988. DELBOUY: Wave-powered desalination system. In *Oceans'88 Proceedings*, pp. 1049-1055 (Vol. 3). Washington, DC: Marine Technology Society.
32. Bellamy, Norman W. 1982. Development of the SEA Clam wave energy converter. In *Proceedings of the Second International Conference on Wave Energy Utilization*, edited by H. Berge, pp. 175-190. Trondheim, Norway: Tapir Publishers.
33. Bellamy, Norman W. 1986. The circular SEA Clam wave energy converter. In *Hydrodynamics of Ocean Wave-Energy Utilization - Proceedings of the IUTAM Symposium, Lisbon, Portugal*, edited by David V. Evans and Antonio F. de O. Falcao, pp. 69-79. Berlin, Federal Republic of Germany: Springer-Verlag.
34. Lockett, F.P., 1991. The CLAM wave energy converter. In *Proceedings of the Seminar on Wave Energy*, pp. 19-25. United Kingdom: Institution of Mechanical Engineers.
35. Peatfield, A.M., 1991. The economic viability of the circular CLAM for offshore wave energy utilization. In *Proceedings of the Seminar on Wave Energy*, pp. 37-39. United Kingdom: Institution of Mechanical Engineers.
36. Clare, R., D.V. Evans, and T.L. Shaw. 1982. Harnessing sea wave energy by a submerged cylinder device. *Proceedings of the Institution of Civil Engineers, Part 2*, Vol. 73, pp. 565-585.
37. Mehlum, E., P. Anderssen, T. Hysing, J.J. Stamnes, O. Eriksen and F. Serck-Hanssen, 1990. The status of wave energy projects and plants in Norway. Part 2: Norwave TAPCHAN - a commercial overview. In *Proceedings: Oceans'89 Special International Symposium - A Global Review of the Development of Wave Energy Technologies*, edited by D. W. Behrens and M. A. Champ, pp. 29-36. San Ramon, California: Pacific Gas and Electric Company, Department of Research and Development, 007.6-90.8.
38. Letter from Andreas Tommerbakke (Kvaerner Brug A/S) to George Hagerman (SEASUN Power Systems, Alexandria, Virginia), 3 October 1988.
39. Chow, P.Y., T.Y. Lin, H.R. Riggs, and P.K. Takahashi, 1991. Engineering concepts for design and construction of very large floating structures. In *Proceedings, First International Workshop on Very Large Floating Structures*, edited by R.C. Ertekin and H.R. Riggs, pp. 97-106. Honolulu, Hawaii: University of Hawaii at Manoa.
40. SEASUN Power Systems, 1991. *Ocean Energy Technology Information Module*. San Ramon, California: Pacific Gas and Electric Company, Department of Research and Development, 007.6-91.4.
41. Gruy, R.H., W.L. Kiely, K.I. Pederson, W.R. Wolfram, and R.D. Swann, 1980. Five years experience with the first deepwater SALM. In *Proceedings of the 12th Annual Offshore Technology Conference*, Paper No. 3804.

42. Electric Power Research Institute, 1986. *Technical Assessment Guide, Volume 1: Electricity Supply-1986*. Palo Alto, California: Electric Power Research Institute, P-4463-SR, Vol. 1.
43. Svensson G., 1985. Swedish idea for wave power. *Energy Ahead 85*, pp. 40-44. Stockholm, Sweden: Vattenfall, Annual Research and Development Report.
44. Davidson, R., 1983. *The Mechanical Characteristics of Spirally Reinforced Moorings and Tube Pumps*. Oxfordshire, United Kingdom: Energy Technology Support Unit, Harwell Laboratory, WV-1551-P55b.
45. Carmichael, A.D., E.E. Adams, and M.A. Glucksman, 1986. *Ocean Energy Technologies: The State of the Art*. Palo Alto, California: Electric Power Research Institute, EPRI AP-4921.
46. Rice, R.G., and G.C. Baker, 1987. The Annapolis experience. In *Oceans'87 Proceedings*, pp. 391-396 (Vol. 2). New York, New York: Institute of Electrical and Electronics Engineers.
47. Versluis, J., 1980. Exposed location single buoy mooring. In *Proceedings of the 12th Annual Offshore Technology Conference*, Paper No. 3805.
48. Taylor, R., 1982. The availability, reliability, and maintenance aspects of wave energy. In *Proceedings of the Second International Symposium on Wave Energy Utilization*, edited by H. Berge, pp. 117-136. Trondheim, Norway: Tapir Publishers.
49. Earle, M. D., 1989. Microcomputer numerical ocean surface wave model. *Journal of Atmospheric and Oceanic Technology*, Vol. 6, pp. 151-168.
50. Davidson, 1988. Limits put on Hawaii wind. *Windpower Monthly*, September, p. 9.

APPENDIX A

WAVE ENERGY RESOURCE PRIMER

WAVE ENERGY RESOURCE PRIMER

The key to effective utilization of wave energy lies in understanding its variability. Wave energy devices must be designed to absorb energy from a spectrum of individual wave heights and periods. These quantities vary randomly from one wave to the next, although this variability is usually not apparent to a casual observer on shore. Indeed, such an observer may be impressed by the regularity with which waves break, one after the other, in apparently monotonous succession. The regular features of breaking waves are caused by interactions with the bottom as waves enter shallow water, and the illusion of regularity is dispelled when waves are viewed on the open ocean. Unlike a line of breakers, waves in deep water generally appear as a confusion of hills and hollows moving in several directions at once.

Such a confused sea state is represented mathematically as the sum of several simple harmonic waves, each having a specific height, period, and direction of travel (Figure 1). This random superposition of regular waves is a fundamental concept in ocean engineering and has proven to be an accurate basis for predicting the effects of natural waves on offshore structures.

In order to understand random waves then, it is first necessary to understand the properties of simple harmonic or regular waves, and these are described in the first section of this primer. The superposition of such waves all moving in the same direction creates a random seaway whose wave crests are infinite in extent. Such long-crested waves are not a natural phenomenon, but represent an intermediate step towards synthesizing the short-crested or confused sea. Long-crested random waves are described in the second section of this primer, which introduces the concept of the frequency spectrum and its associated statistics for individual wave height and period. Angular spreading of the harmonic components turns long-crested waves into short-crested waves, whose properties are described in the third section.

The first three sections of this primer deal with energy variability from wave to wave, over a time scale of seconds. Over a longer time scale, on the order of minutes, it is frequently observed that wave energy arrives off the coast in successive groups of high and low waves, a phenomenon well known to any surfer. Such wave grouping is described more fully in the fourth section.

Finally, over a time scale of hours to days, incident wave power at a given location changes in response to local wind conditions and the arrival of swell from offshore storms. The factors that influence such changes in sea state are described in the last section of this primer and are an important consideration for wave power plant operators, who must continually "tune" the plant to changing sea states, and for utility dispatchers concerned about variability in plant output.

A complete description of regular and random wave theories is beyond the scope of this primer. Readers interested in pursuing the subject further should consult one of the following references. Smith's book [1] provides a good introduction that focuses on the physical phenomena associated with water waves, rather than their mathematical description. A comprehensive mathematical treatment is given in the classic work by Kinsman [2]. Random wave statistics are covered in a recent book by Goda [3], which also provides a valuable review of Japanese research on the subject, much of which has not been published previously in English. Books dedicated to various coastal and ocean engineering topics frequently include chapters on wave theory. Komar's book on beach processes and sedimentation [4], Earle and Bishop's book on wave measurement [5], Sarpkaya and Isaacson's book on wave forces and the design of offshore structures [6], and Bhattacharya's book on ship design and seakeeping [7] are among those that provided material for this primer.

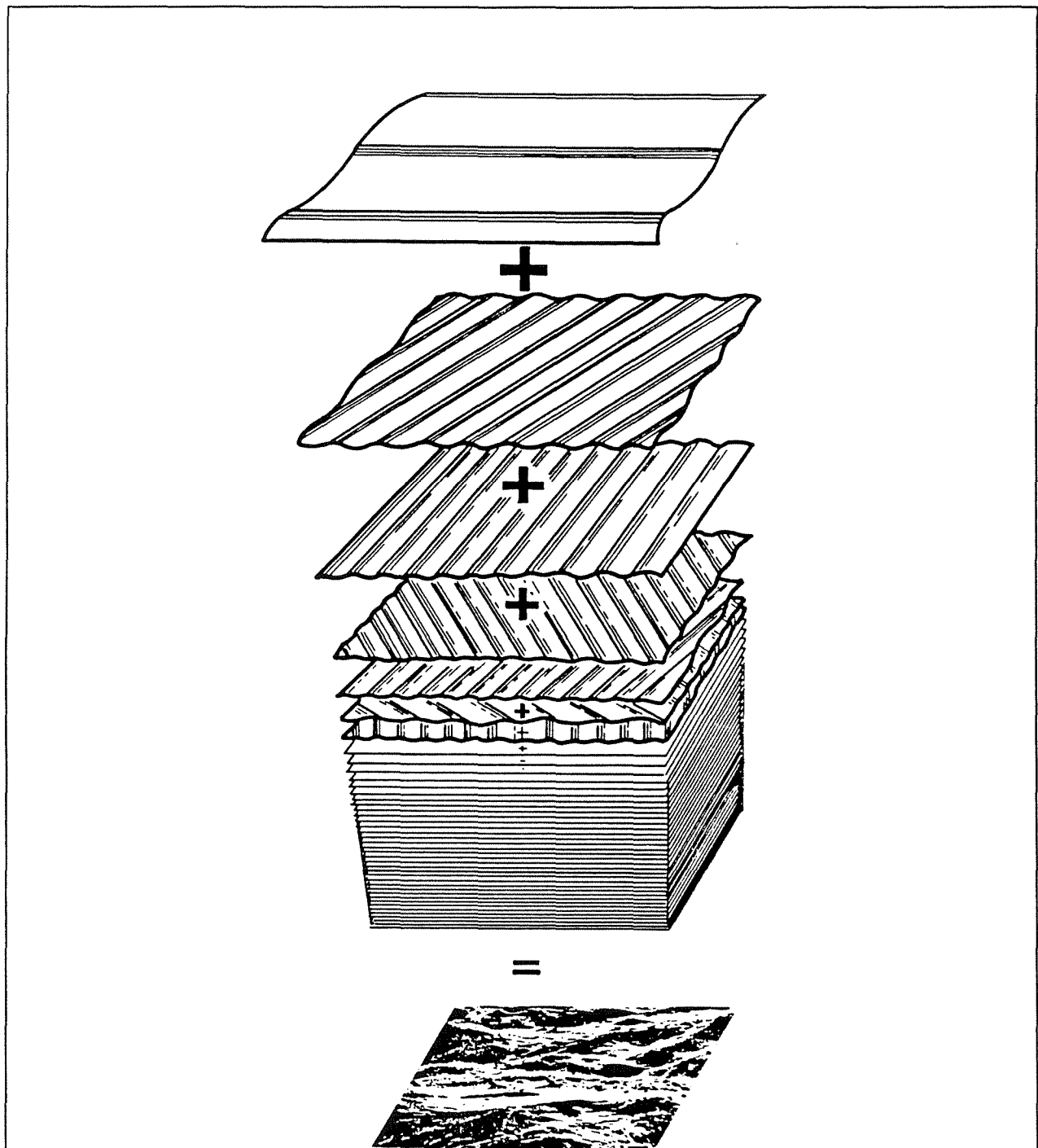


Figure 1. A random seaway realized as the superposition of several regular waves, each having a fixed height, period, and direction.

REGULAR WAVES

A simple harmonic water wave is described primarily by three parameters (Figure 2): its height (H), which is the vertical distance from crest to trough; its wavelength (L), which is the horizontal distance from one crest to the next; and its period (T), which is the length of time it takes for two successive crests (or any other phase of the wave) to pass a fixed point such as the vertical pile in Figure 2. Once a regular wave has been generated, its period remains constant, but its height and length are affected by the water depth in which it travels.

If one observes the motion of a floating object during the passage of regular waves in deep water, it will be seen that the object rises and falls, but makes no net progress in the direction of wave travel. This is because the changing sea surface slope of the passing wave induces hydrodynamic pressure gradients that accelerate the object and sub-surface water particles in circular orbits. Waves therefore transfer energy without transferring mass; to a first approximation, the water itself does not travel with the wave.

At the sea surface, the diameter of water particle orbits is equal to wave height. Orbital motion decays exponentially with depth, and half a wavelength down, its amplitude is only 4% of its surface value. In water depths less than half a wavelength, the vertical zone of wave-induced motion is compressed, and the circular orbits flatten into ellipses as the wave begins to "feel the bottom" (Figure 3).

In deep water, wavelength is directly proportional to wave period squared. Thus, as shown in Table 1, a 10-second wave is four times longer than a 5-second wave, and it will begin to feel the bottom in water that is four times as deep. Since the rate at which a wave travels (its phase velocity) is equal to wavelength divided by period, it travels twice as fast.

As waves begin to feel the bottom, they slow down. In the absence of any wave generation by local winds or dissipation by wave breaking, the number of waves travelling from deep to shallow water remains constant. Since they are travelling more slowly, the distance between them (i.e. wavelength) decreases. As explained by Walton-Smith [1], the situation is analogous to a reduced-speed zone on a highway. If traffic flow is to be maintained, the spacing between cars must decrease.

Consequently, a random group of short- and long-period waves becomes more uniform in length as it travels into shallower water, and the waves appear more regular to an observer on the beach. For example, by the time the 10-second wave in Table 1 enters a water depth of 3 m, it is only about twice the length of the 5-second wave, whereas it was four times longer in deep water.

Another consequence of the reduction in phase velocity with decreasing water depth is wave refraction. Consider a group of regular waves approaching the coast at an angle. Along a given wave crest, the end nearer shore will enter shallow water first and will be slowed accordingly. Meanwhile, the part of the wave crest in deeper water is moving at its original speed, causing the wave crest as a whole to become more nearly aligned with local depth contours.

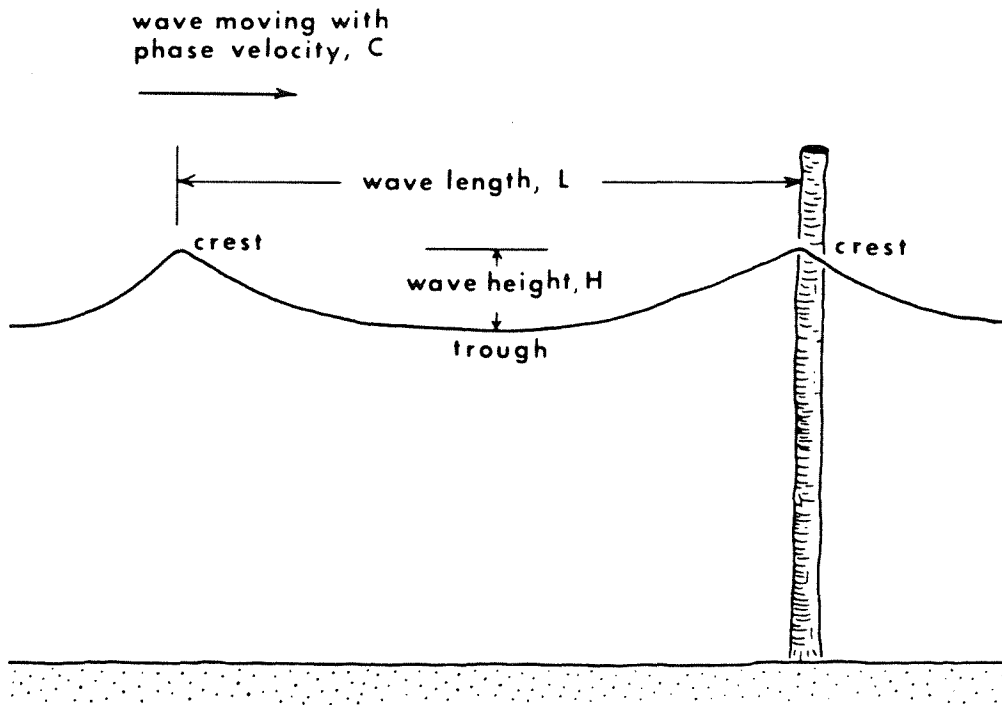


Figure 2. Definition sketch for regular wave parameters.

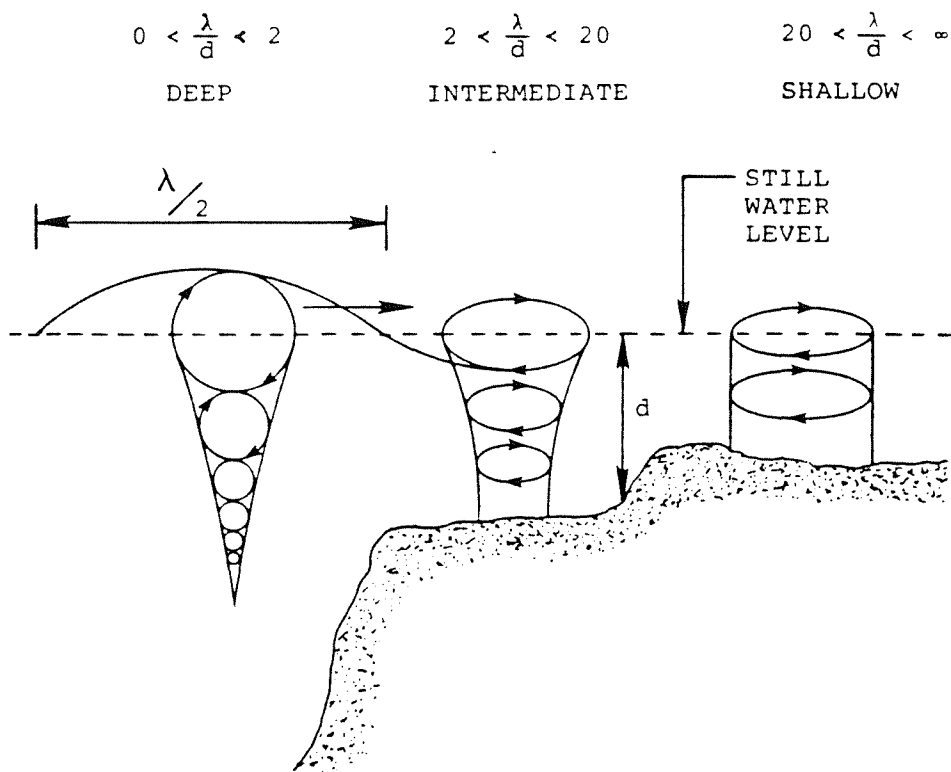


Figure 3. Orbital motion of water particles induced by passing waves. In water depths less than half a wavelength, the circular orbits become ellipses, which flatten with decreasing depth.

Table 1
Regular Wave Comparison for Three Different Periods

Wave period:	<u>5 sec</u>	<u>10 sec</u>	<u>15 sec</u>
Deep water wavelength:	39 m	156 m	351 m
Deep water phase speed:	7.8 m/sec	15.6 m/sec	23.4 m/sec
Depth at which wave begins to be affected by seafloor:	20 m	80 m	175 m
Wavelength in 10 m depth:	37 m	92 m	144 m
Wavelength in 5 m depth:	30 m	68 m	103 m
Wavelength in 3 m depth:	25 m	53 m	81 m
Phase speed in 3 m depth:	5.0 m/sec	5.3 m/sec	5.4 m/sec

On a straight coastline with parallel bathymetric contours, refraction of obliquely incident waves causes the wave rays to spread apart, as shown in Figure 4. Since the energy flux between rays must be conserved, this leads to a reduction in wave height and the amount of wave power per unit length of wave crest. Along with the effects of bottom friction, this causes the amount of wave energy incident on a wave energy conversion device of given width to be higher in deep water than in shallow water.

Irregular bathymetric contours, such as exist around a submarine canyon or off a headland or cape, may cause both convergence and divergence of wave rays (Figure 5). Understanding the effects of such bottom features on the local wave climate is an important step in siting a wave power plant. Locating the plant in a "hot spot" of wave ray convergence may significantly improve the project's economics.

Like refraction, shoaling is another wave transformation that results from shallow-water decrease in phase speed. In order for the energy flux between wave rays to remain constant as the waves slow down, the energy content between rays must increase, and this is evidenced by an increase in wave height. Thus, low ground swell may not be apparent to a shipboard observer in deep water, but is readily identifiable as it "peaks up" on its approach to the beach.

As a wave travels shoreward in shoaling water, its height continues to increase until it becomes unstable and breaks. On gently sloping bottoms, this generally occurs when the wave reaches a height equal to 0.78 times the local water depth [4]. The breaking process itself dissipates most of the wave's energy in the form of turbulence and sediment movement in the surf zone, and the balance is dissipated in the run-up of swash onto the beach at the surf's edge.

Refraction of water waves in shallow water is very similar to the refraction of light waves by glass. Diffraction is another light wave phenomenon that has a water wave counterpart. Wave diffraction into calm-water "shadows" behind offshore breakwaters and islands occurs as wave energy is transferred laterally along wave crests (Figure 6), and can be readily observed from the air.

Numerical models have been developed to simulate the diffraction of water waves, and one such model has been exercised to predict the potential impacts of offshore kelp farming on coastal sedimentary processes [8]. The effect of such a farm would be comparable to that of a wave power plant, since the kelp plants dampen but do not completely remove wave energy.

Simulation results for a fairly small kelp farm with close plant spacing (high damping of wave energy) are plotted in Figure 7. Immediately behind the farm, wave height is reduced to 20% of its original incident value. Within a distance of two to three farm widths, however, diffraction restores wave height to 60% of its original value.

The level of wave damping by such a kelp farm is much greater than that which would be expected for an offshore wave power plant. Even if a wave power plant removes 50% of the energy from the waves that pass through it, wave heights immediately behind the plant would still be 70% of their original value, since wave energy is proportional to wave height squared. This is considerably less reduction than described above. Although a noticeably calmer area might develop immediately to the lee of an offshore wave power plant, wave heights should be substantially re-established by diffraction within a few kilometers shoreward of the plant. On the other hand, caisson-based wave power plants must be sited in shallow water, close to shore, where there is less sea space in the lee of the plant. Furthermore, caissons reflect any wave energy that they don't absorb. Under these circumstances, diffraction may not be very effective in re-establishing the waves, and a distinct low-energy shadow may develop in the surf zone behind such a plant.

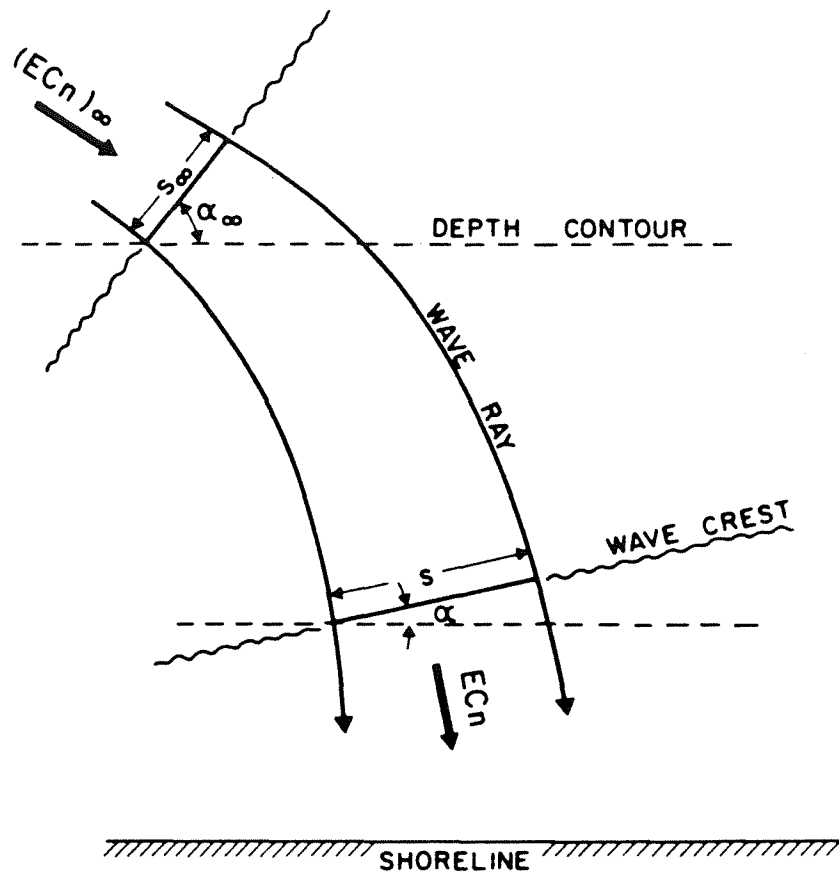


Figure 4. When waves slow down in shoaling water, the rate (C_n) at which their energy (E) is transferred decreases. The wave energy flux (EC_n) between wave rays is always conserved. Thus when refraction causes the wave rays to spread apart, the energy flux per unit crest width (or per unit width of a wave energy conversion device) decreases.

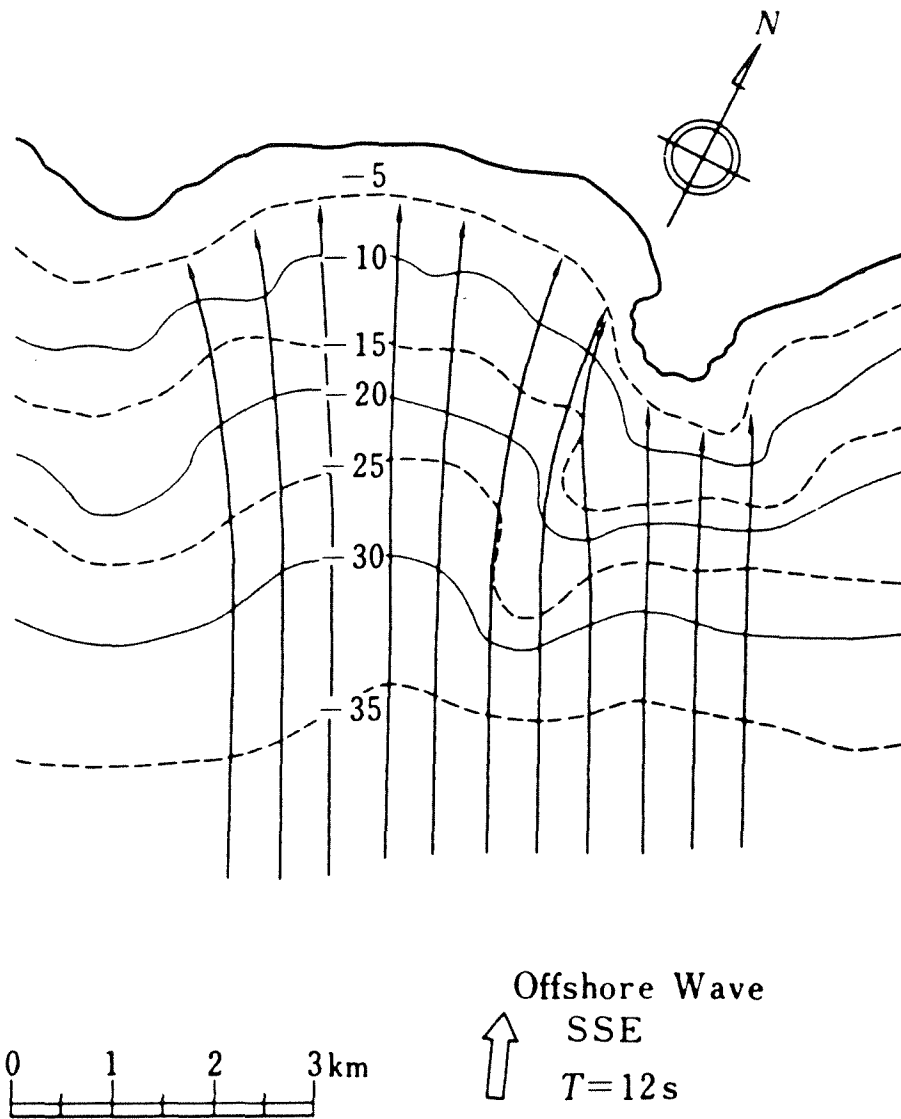


Figure 5. The refraction pattern over a given bathymetry depends on wave period and the deep-water angle at which waves approach the coast. In the above example, wave rays diverge along a shoreline embayment and converge just west of a rocky headland on the east side of the bay.

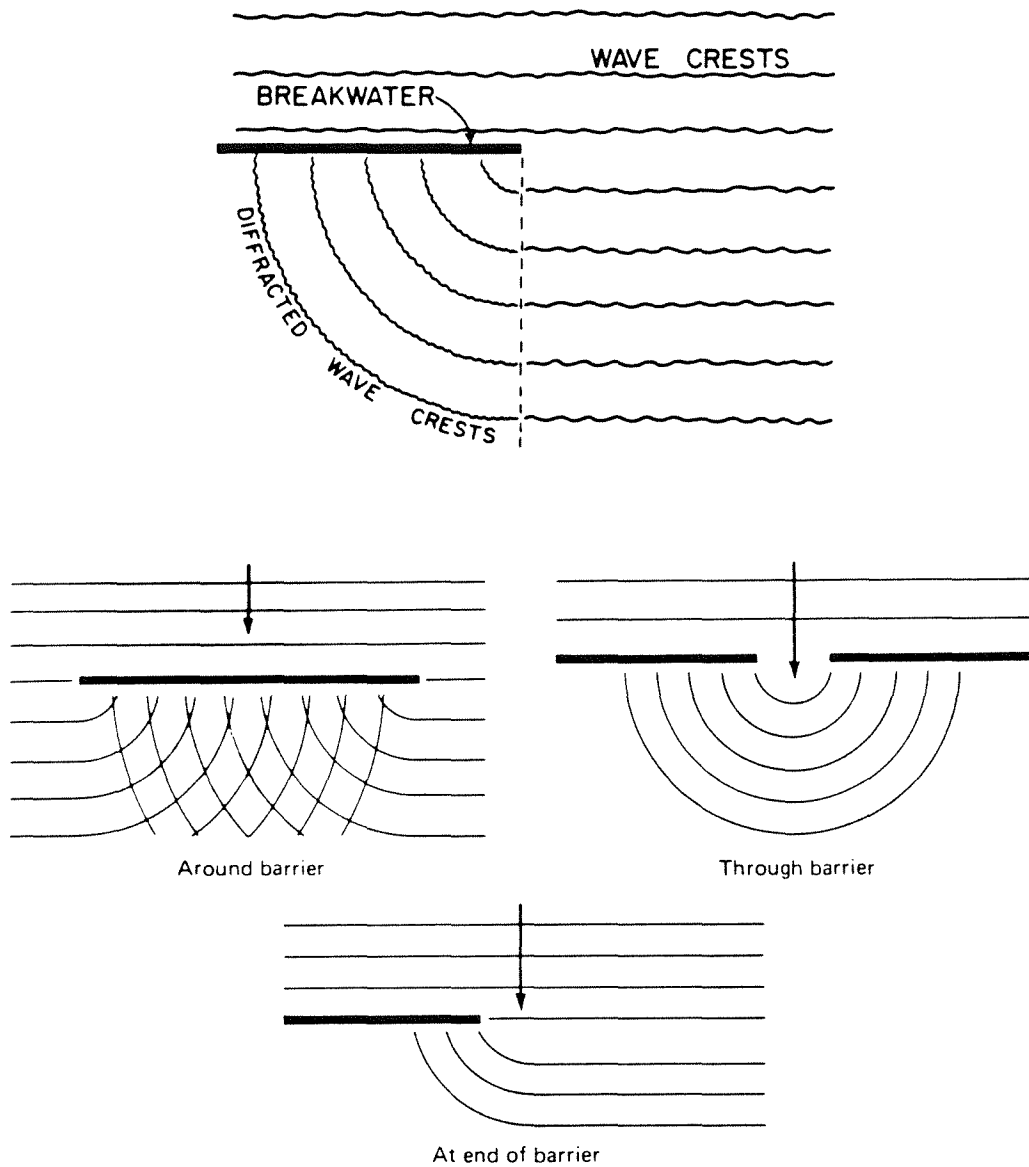


Figure 6. Lateral transfer of energy along wave crests behind an offshore breakwater. Also shown are various diffraction patterns for different barrier/opening configurations.

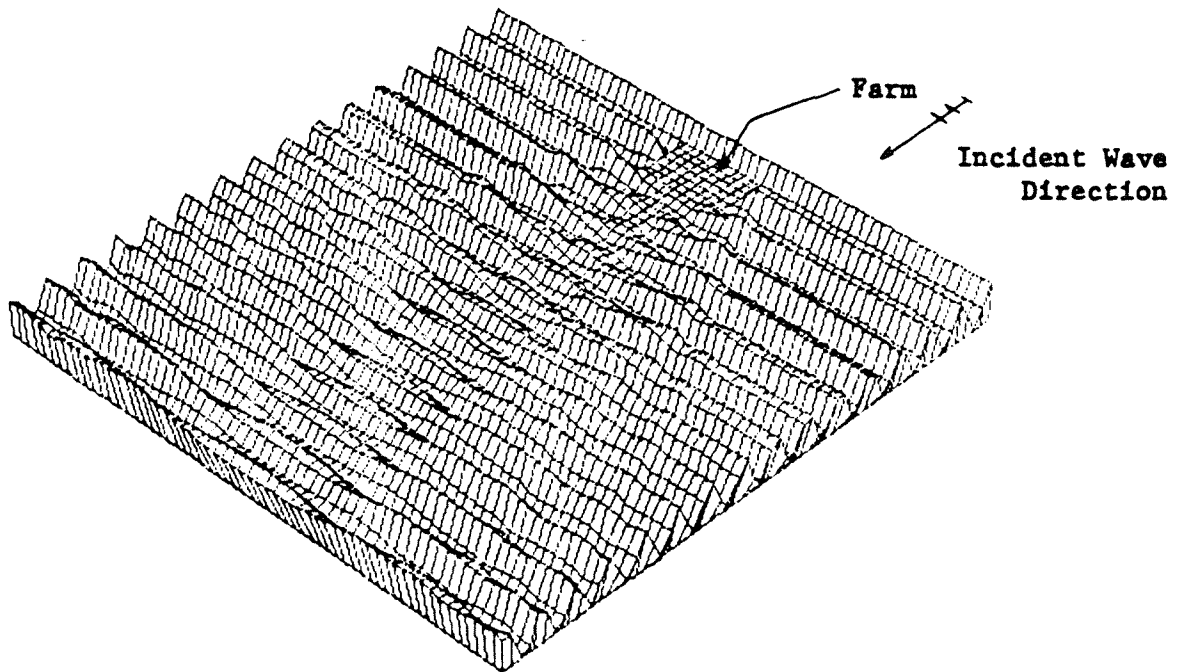


Figure 7. Numerical simulation of regular waves passing through an offshore kelp farm with high wave damping. Incident wave height = 6.1 m; wave period = 20 sec; water depth = 15 m. The farm's plan dimensions are 610 m longshore by 305 m wide; the simulated coastal area is 7.3 km longshore by 3.7 km wide.

In deep water, the energy contained in a group of waves travels at only half the speed of the individual waves. This can be demonstrated by throwing a stone into a pond or lake. In watching the circular wave fronts, it will be seen that an individual crest can be traced for only a short period of time before it disappears, even though the group as a whole continues to radiate outward. Careful observation will show that new waves continually appear at the rear of the group, grow to full height as they travel through the group, and die away at the group's leading edge.

This is a consequence of the way in which energy is partitioned in a wave and how it is transmitted. Half of the wave's energy is always stored in potential form, associated with the vertical displacement of the sea surface from its still-water condition. The other half is expressed as kinetic energy, associated with the orbital motion of water beneath the wave. Because the orbits are circular, kinetic energy does not travel with the wave, and only the wave's potential energy travels at phase velocity. Nevertheless, through conversion of potential energy to kinetic energy and vice versa, the total energy in a wave group does indeed travel across the sea surface, as described below.

Consider a group of regular waves travelling into previously undisturbed water (Figure 8). Only the potential energy of the leading wave travels at phase velocity, and there is a reduction in wave height as half of this is converted to kinetic energy when the sub-surface water particles, which were at rest, are set into motion. The remaining half is available to travel the next wavelength, where it again is used to supply kinetic energy to the undisturbed water. This conversion of potential to kinetic energy continues until the first wave is too small to identify.

Since the leading wave has left all of its original kinetic energy behind, the second wave to follow does not lose any of its potential energy when it occupies the leading wave's first position. At the next position, where the leading wave lost half of its potential energy, the second wave loses only a quarter in order to maintain the balance of potential and kinetic energy. Successive waves lose potential energy at an even lower rate as they progress through the group, building on the kinetic energy left behind by the previous waves. They begin to lose height quickly, however, when they reach the group's leading edge and move into undisturbed water.

At the rear of the group, all of the last wave's potential energy travels ahead at phase velocity. Half of the remaining kinetic energy is converted to potential energy as a crest and trough are formed by the relict orbital flow pattern. This new wave then travels ahead at phase velocity, gaining potential energy as it travels towards the group's center and losing it as it travels towards the group's leading edge. This process redistributes kinetic energy from the rear of the group to its front. Thus, the combined potential and kinetic energy of the waves travels at the velocity of the wave group, which in deep water is equal to half the phase velocity.

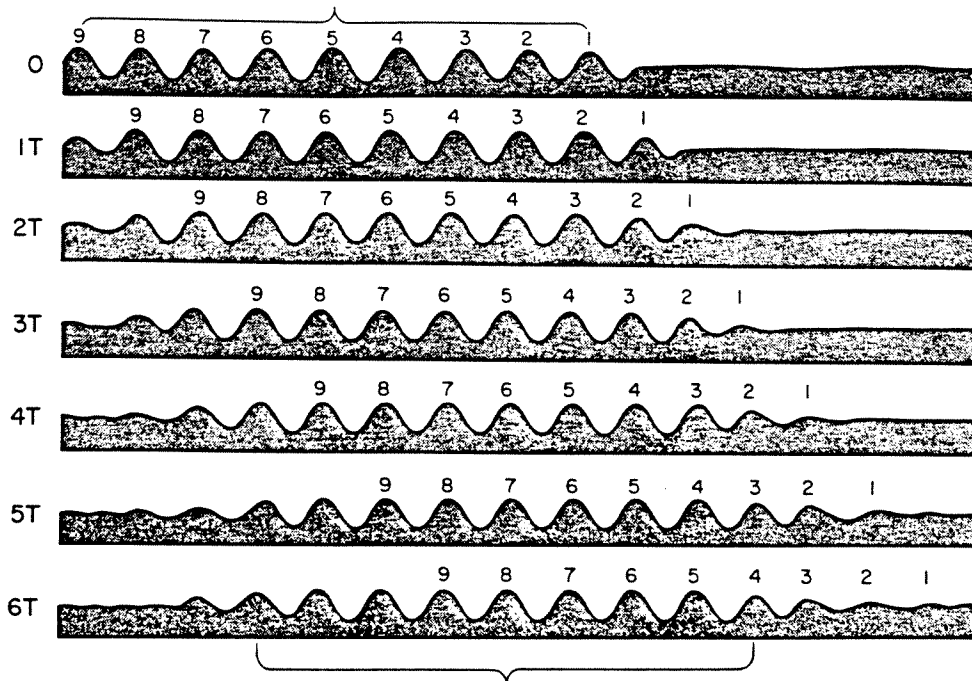


Figure 8. The advance of nine regular waves into still water. Each successive position corresponds to a time increment of one wave period. Note that at time $6T$, each individual wave has traveled six wavelengths, while the wave group has advanced only three wavelengths. Thus in deep water, group velocity is one-half of phase velocity. Also note that at time $6T$, the leading wave retains only $1/64$ of its original energy and has virtually disappeared.

LONG-CRESTED RANDOM WAVES

If several sinusoidal waves travelling in the same direction are superimposed on one another, an irregular wave profile is generated (Figure 9). Conversely, an apparently random signal can be broken down into its harmonic components by Fourier analysis. Each component contributes a certain amount to the total variance of the signal. This contribution is proportional to the square of the component's wave height, which in turn is proportional to its energy content. In this manner, a variance spectrum can be constructed for a random seaway.

More commonly, the variance contributed by a given component is divided by the frequency of that component. When plotted as a function of wave frequency, the resulting curve is referred to as the variance density spectrum, or more simply, the wave spectrum. Note that the area under the spectrum is equal to the total signal variance, and the square root of this area equals its standard deviation.

When multiplied by the density of seawater and the acceleration due to gravity, the area under the wave spectrum also represents the total energy per unit area of sea surface. Wave energy conversion devices are oriented so as to intercept this energy as it travels at the group velocity of its harmonic components. The amount of wave energy to cross a vertical plane per unit time is referred to as wave energy flux or incident wave power. Wave power is generally expressed in units of kilowatts per meter of wave crest. If the waves are travelling directly towards shore, this is equivalent to kilowatts per meter of coastline.

Consider again the irregular sea surface profile measured in a random seaway. Individual waves can be identified from one position where the sea surface crosses the still-water level to the next, and individual wave heights and periods can be measured as shown in Figure 10. An example of such a zero-crossing analysis is given in Figure 11. This example will be used to illustrate height and period statistics that are relevant to the design and performance of a wave energy conversion device.

In the example sequence of 21 waves, there are six occasions where wave height varies by at least a factor of two from one wave to the next. The absorption efficiency of a wave energy conversion device is maximum when the resistance (or applied damping) of the power take-off mechanism is matched to the exciting force of the wave. Since this exciting force is proportional to wave height, it follows that in a random wave train, a device having a fixed resistance (for example, a closed-circuit hydraulic system working against a constant-pressure accumulator) will be significantly overdamped in some waves and underdamped in others. Energy will not be absorbed with equal efficiency from all waves, although an average absorption efficiency exists for the sea state as a whole.

On the other hand, a device whose applied damping varies with wave height (for example, an oscillating water column with a Wells turbine, which spins faster in higher waves than lower waves, thus providing more resistance to air flow) will absorb energy with more uniform efficiency from in a random seaway (In practice, the example given only approximates this situation; the rotational inertia of the Wells turbine is such that its speed does not respond to changes in individual wave height. It does respond, however, to changes in average wave height over periods of minutes, such as occur when the waves in a random seaway are grouped. See the fourth section of this primer).

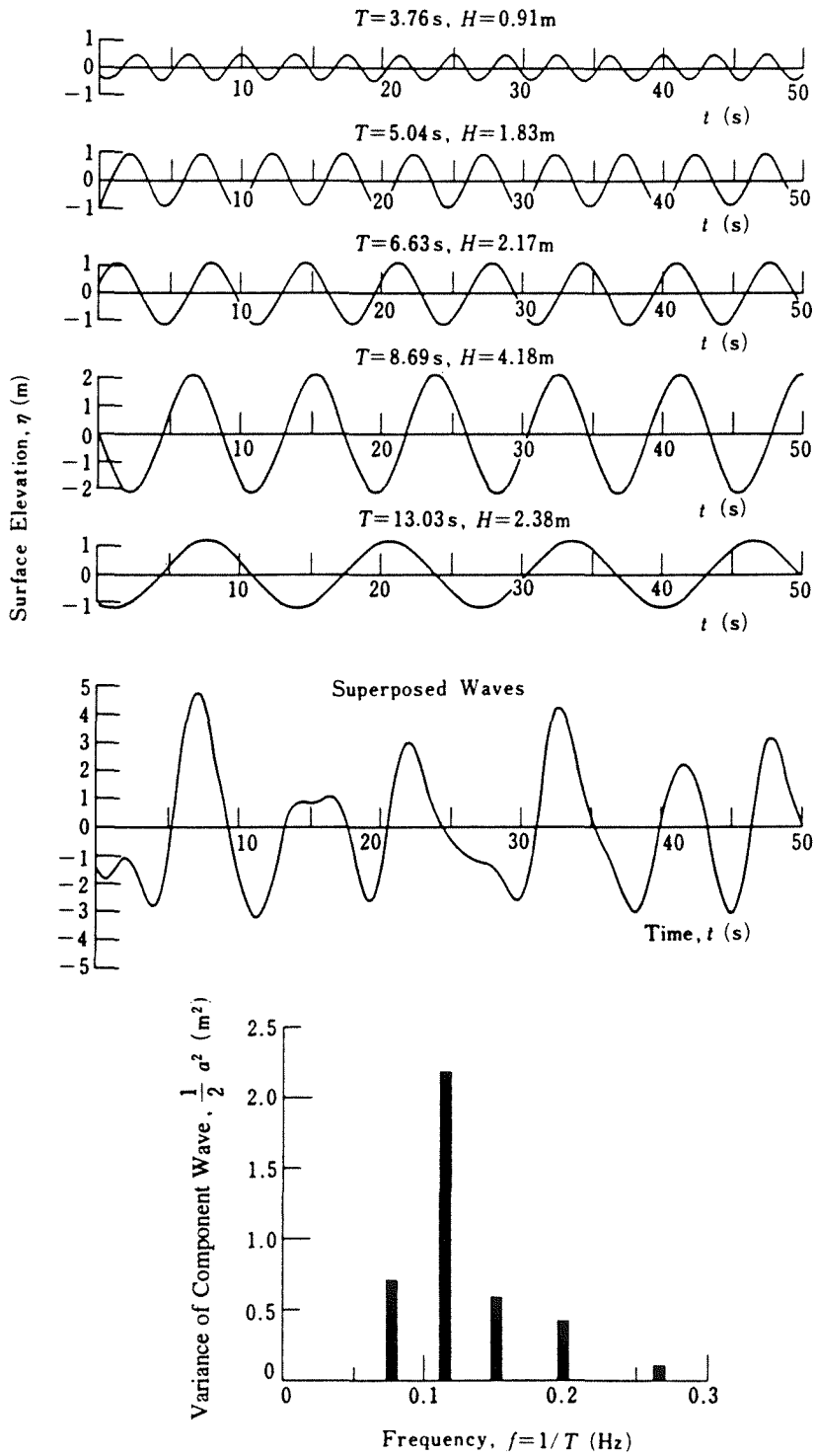


Figure 9. Superposition of five regular waves, and resulting variance spectrum.

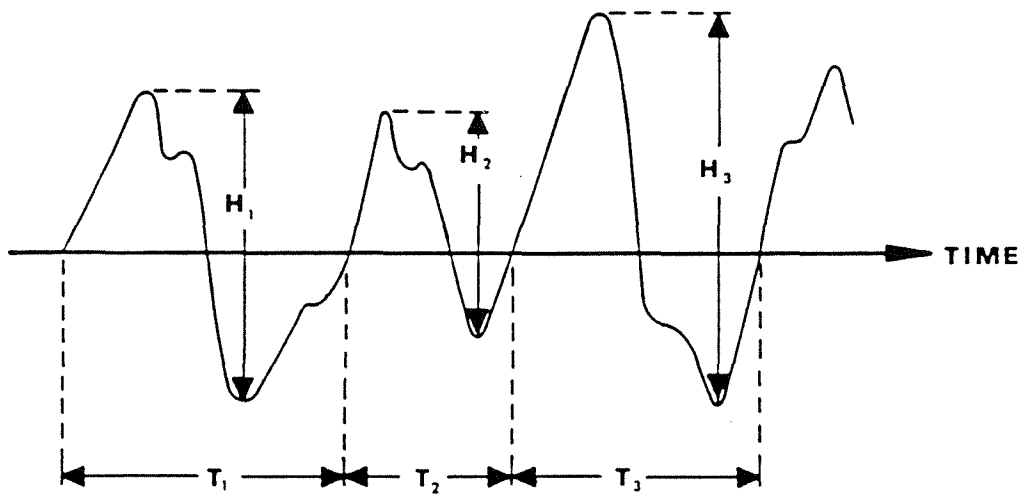
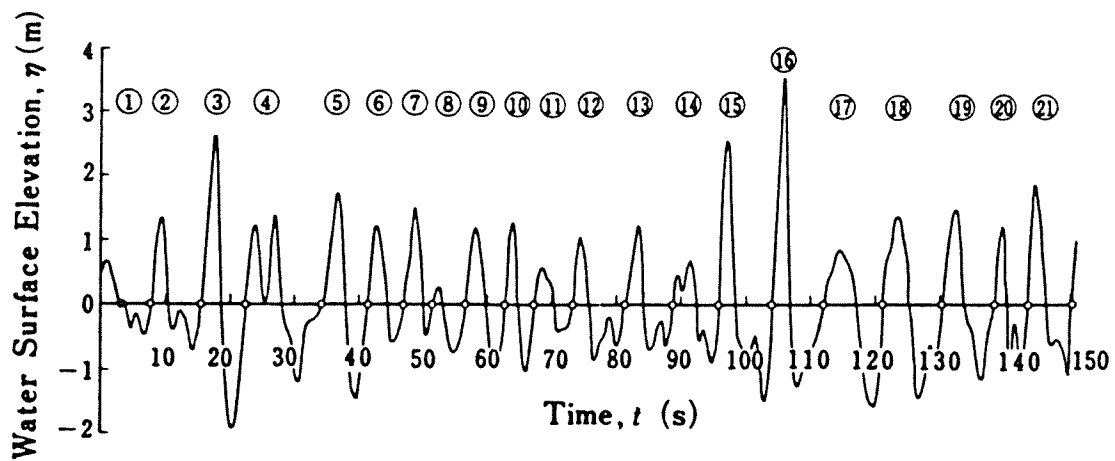


Figure 10. Determination of individual wave heights and periods from zero-crossing analysis.



Wave number	Wave height $H(m)$	Wave period $T(s)$	Order number m
①	0.54	4.2	21
②	2.05	8.0	12
③	4.52	6.9	2
④	2.58	11.9	8
⑤	3.20	7.3	4
⑥	1.87	5.4	17
⑦	1.90	4.4	16
⑧	1.00	5.2	20
⑨	2.05	6.3	13
⑩	2.37	4.3	10
⑪	1.03	6.1	19
⑫	1.95	8.0	15
⑬	1.97	7.6	14
⑭	1.62	7.0	18
⑮	4.08	8.2	3
⑯	4.89	8.0	1
⑰	2.43	9.0	9
⑱	2.83	9.2	7
⑲	2.94	7.9	6
⑳	2.23	5.3	11
㉑	2.98	6.9	5

Figure 11. Example random wave profile. The table gives each wave's individual height, period, and order number (1 = highest wave; 21 = lowest wave), based on zero-crossing analysis of the random wave profile.

The concept of significant wave height (H_s) is one of considerable importance. It is formally defined as the average height of the highest one-third waves in a given sea state. In the example of Figure A-11, the highest third consists of the 3rd, 5th, 15th, 16th, 18th, 19th, and 21st waves. Their average height is 3.6 m, which is thus the significant wave height for this record.

Significant wave height has been found to generally correspond to the wave height estimated by visual inspection of a random seaway. This is because an observer tends to overlook the small waves and notice only the larger ones when visually estimating wave heights. The practice of describing a sea state by its significant wave height is widespread, and the height of other waves in the sea state can be inferred from this parameter, as explained below.

Except in shallow water where wave heights are limited by breaking, the probability of occurrence of a particular wave height in a given sea state generally follows a Rayleigh distribution. Based on this distribution, other short-term wave statistics, such as the mean and most probable height, can be estimated as a simple multiple of significant wave height (Figure 12). Thus, 80% of the individual waves in a given sea state have a height between 0.23 and 1.07 times the significant wave height, and waves of half the significant wave height are the most common.

Platforms and moorings are high-cost items, and the economics of a wave power plant will be greatly influenced by the extreme waves that these components must be designed to survive without catastrophic failure. The maximum wave height associated with the most severe sea state expected during the service life of the plant represents this design condition. This is often taken to be 1.86 times the significant wave height, but as illustrated in Figure 13, this is not necessarily a conservative estimate. More appropriate design criteria have been developed by Ochi [9].

Turning now to wave period, examination of Figure 11 shows that individual wave periods do not vary as widely as heights. Nevertheless, the wave-to-wave variation is sufficiently great that the resonant amplification so often reported for wave energy conversion devices in regular wave tank tests will be greatly reduced in natural, random waves. As noted above, the absorption efficiency of many devices depends on uniformity of wave height; it also depends on uniformity of wave period, particularly for highly tuned devices. Therefore, advertised efficiencies for wave energy conversion devices should be viewed with great caution. Only those based on tests in random waves have any meaning as far as economic projections at a particular coastal location are concerned.

Just as a given sea state is characterized by its significant wave height, it is also characterized by some sort of statistically meaningful wave period. This may be the average wave period determined from zero-crossing analysis. More relevant to wave energy conversion is the dominant wave period (T_p). This is the inverse of the frequency at which the spectrum has its highest peak. Its physical meaning is that it represents the harmonic component having the greatest amount of wave energy in a random seaway. This is the target frequency to which a wave energy conversion device would be tuned for maximum absorption efficiency. It is typically 1.2 to 1.4 times the mean zero-crossing period.

As a final comment, it should be noted that significant wave height can be rather closely estimated as four times the square root of the area under the wave spectrum. Since the total energy content of the sea surface is proportional to the area under the spectrum, then it is proportional to significant wave height squared. Furthermore, the group velocity of the most energetic harmonic component is directly proportional to dominant wave period. Therefore, to a first approximation, the energy flux in random waves is proportional to the product of $(H_s)^2$ and T_p .

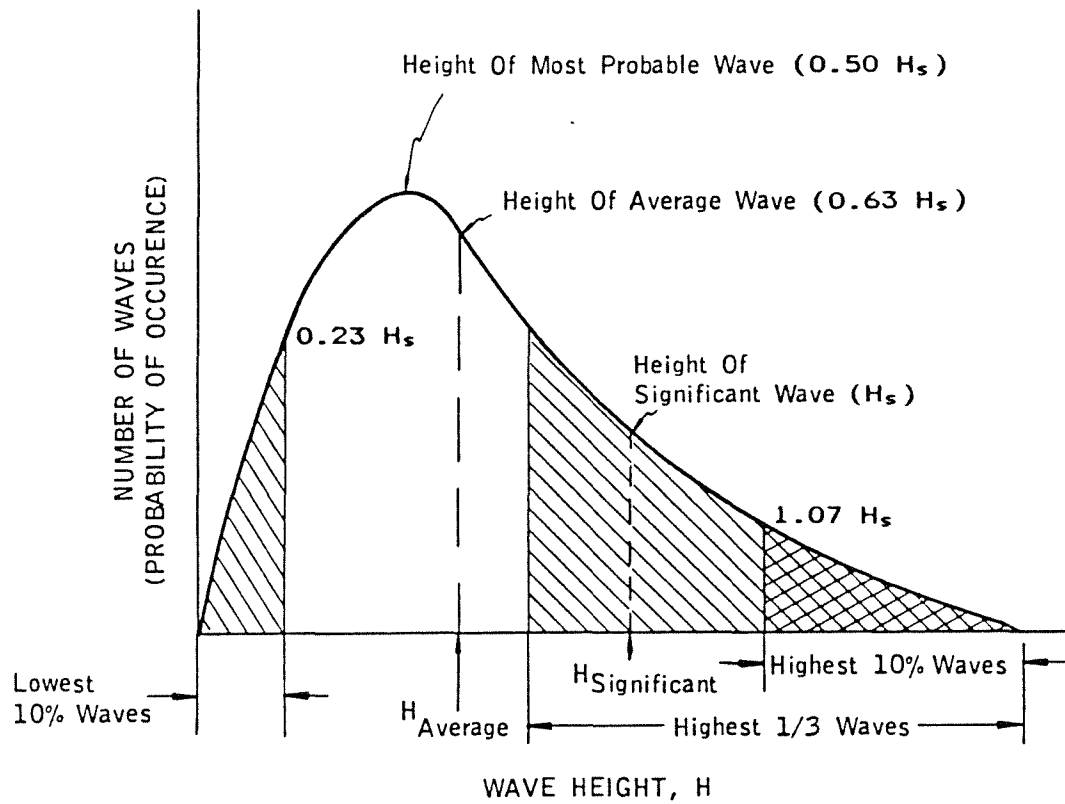


Figure 12. Rayleigh probability distribution of individual wave heights in a random seaway.

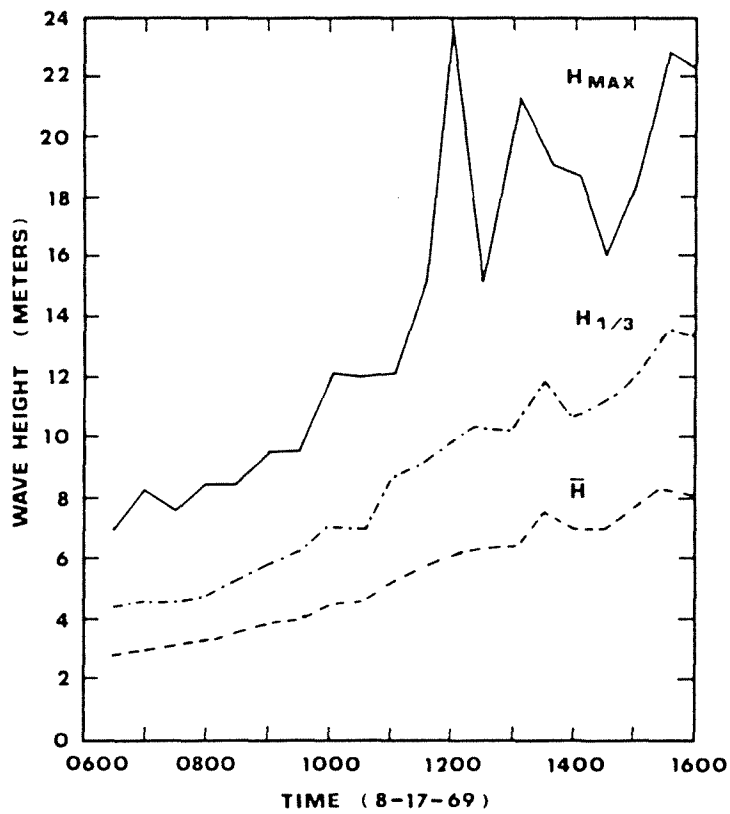


Figure 13. Wave height statistics derived from zero-crossing analysis of wave records measured during Hurricane Camille in the Gulf of Mexico. Note that the maximum height measured at 1200 was 2.4 times the significant wave height measured at the same time.

SHORT-CRESTED RANDOM WAVES

Up to this point, the discussion of random waves has assumed that all harmonic components are travelling in the same direction, such that the waves have infinitely long crests traceable from horizon to horizon. Due to the veering and gusty nature of the wind, however, components are generated that actually travel in several directions at once. Real wave crests are thus finite in width and continually appear and disappear as the various directional components move into and out of phase with one another. The variance density of such a short-crested random seaway is a function of both the frequency and direction of its harmonic components. This function is known as the directional wave spectrum, which is three-dimensional, as shown in Figure 14.

The directional spectrum can be broken down mathematically as the product of the non-directional wave spectrum, described in the previous section, and a directional spreading function. The directional spreading function at any given frequency is a bell-shaped curve generated by a cosine raised to the $2S$ power, where S is referred to as the spreading parameter. The higher the value of S , the more concentrated the spectrum is about the mean direction (Figure 15). The spreading parameter attains its maximum value (S_{max}) at the peak frequency of the spectrum; at higher and lower frequencies the energy is more directionally dispersed, and S has lower values.

Goda [3] has proposed that S_{max} has a value of 10 for waves in regions of active wind generation. A typical contour map of the sea surface in such a region, at any instant in time, is shown in the upper part of Figure 16. The confused and short-crested nature of the waves is readily apparent.

As waves leave the generating area, the high-frequency (short period) components are left behind because they travel more slowly. Since these are more highly dispersed in direction, the energy remaining in the ongoing waves (referred to as swell once they've left the region of active wind generation) is more directionally coherent. Goda suggests that S_{max} increases from 10 to 25 once swell has travelled a short distance from the generating area and may be as high as 75 for long-travelled swell [3]. A sea surface contour map of such swell is shown in the lower part of Figure 16. Linear wave crests are much more distinct and may extend for several wavelengths.

The angular coherence that develops as swell travels increasing distances from an offshore storm is due to shorter-period components being left behind, but in shallow water, the difference in group velocity between short- and long-period components is much less. As waves travel shoreward in such shallow water, refraction tends to align the crests of all frequency components in a direction parallel to the coast, thus reducing the degree of directional spreading.

Considering the short-crested nature of real ocean waves, the definition of wave power developed earlier now requires modification. It is more correctly defined as the amount of wave energy to cross a circle one meter in diameter in one second. Although still expressed in units of kilowatts per meter, this definition does not imply that the energy is travelling in only one direction (as it does with long-crested waves), and a vertical plane bisecting the circle may experience wave power from both sides at once.

This is particularly true where winds have recently experienced a major shift in direction such that newly developing waves are crossing the older waves at a wide angle. This may also occur when swell from a distant storm is arriving from a direction that is different from that of the local wind. In such cases, two or more distinct wave trains may exist, each with its own spreading function, and the total directional spectrum may wrap more than 180° around the circle (Figure 17).

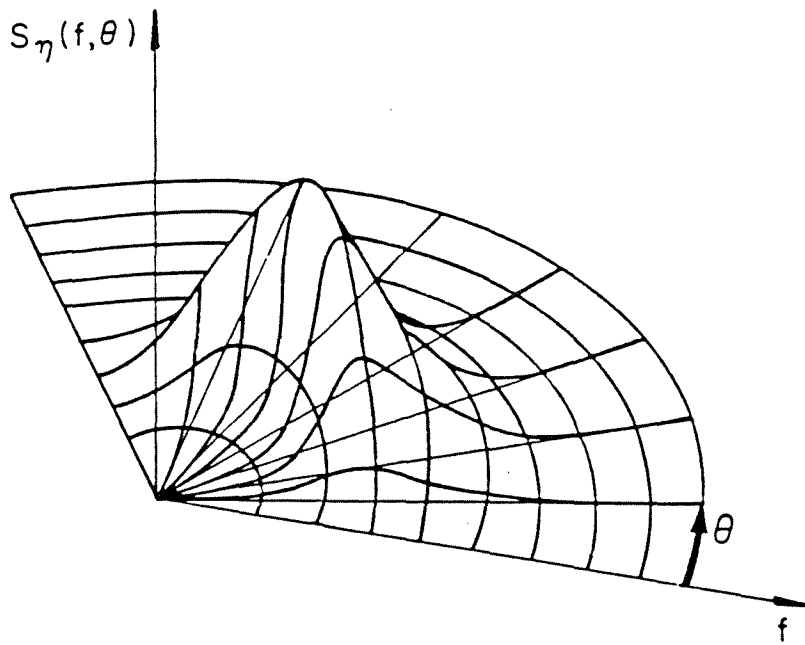


Figure 14. Directional wave spectrum.

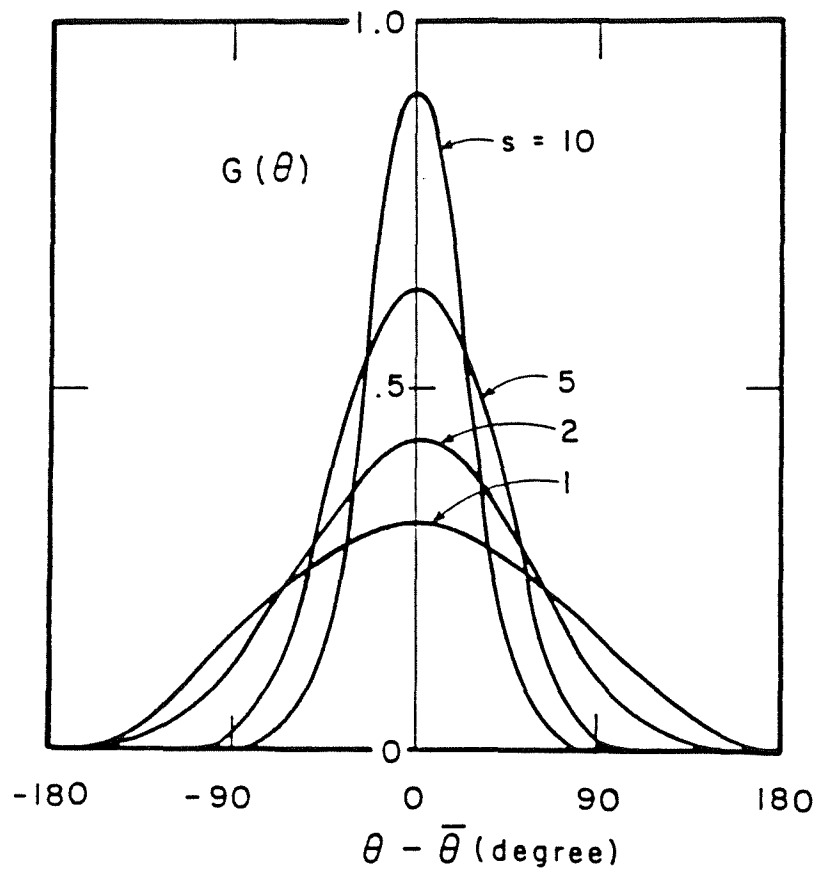


Figure 15. Directional spreading function, based on a cosine-power formula. Note that the angular distribution of wave energy is more concentrated with increasing values of the spreading parameter, S .

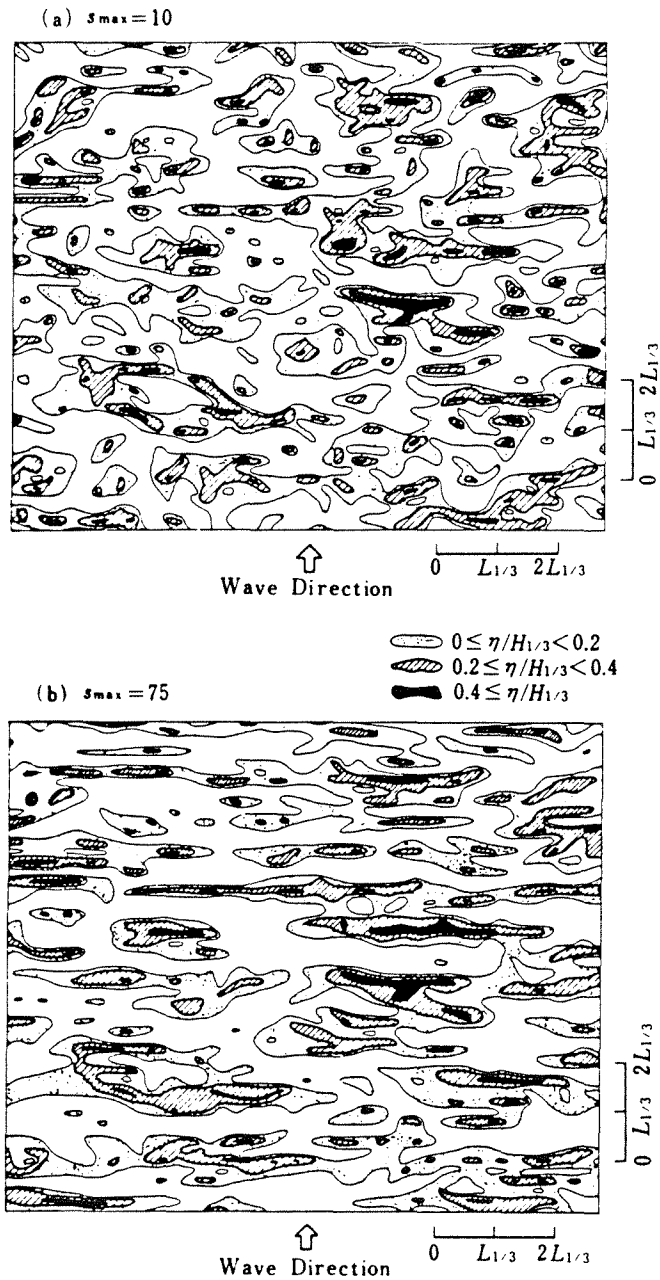


Figure 16. Computer simulation of sea surface elevation (η) at an instant in time, for a given directional wave spectrum. The upper contour map is typical of a wind-generated sea; the lower map is typical of long-traveled swell. $H_{1/3}$ and $T_{1/3}$ refer to the average height and period, respectively, of the highest one-third (or significant) waves.

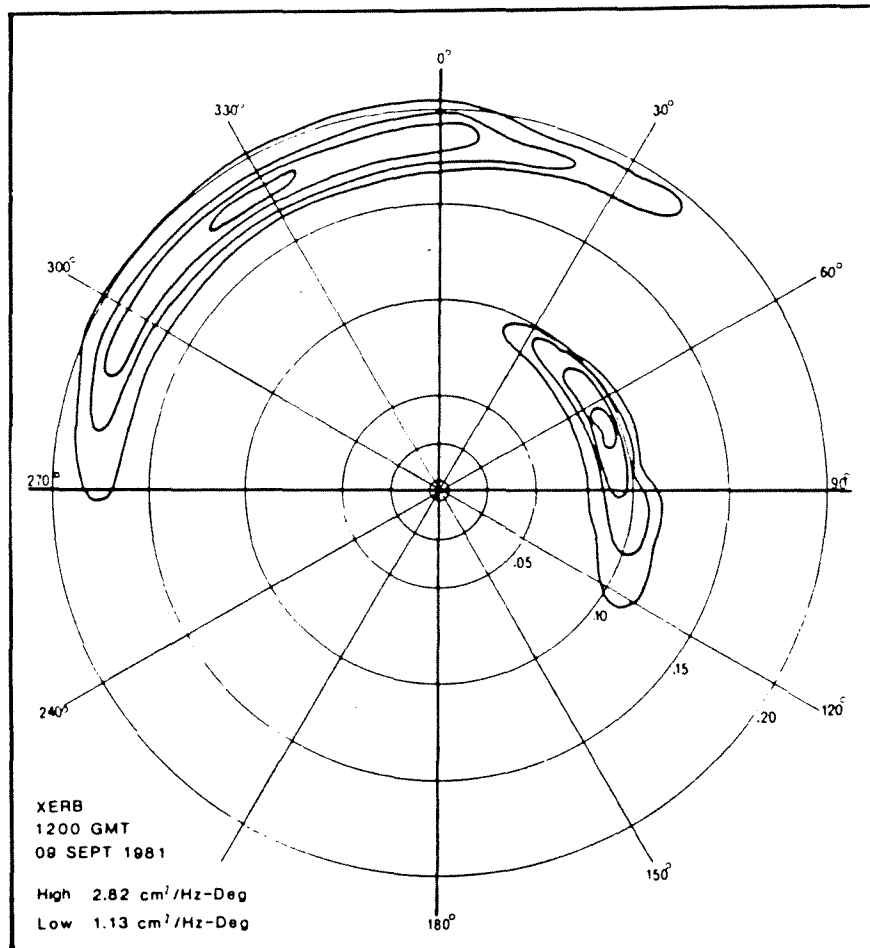


Figure 17. Directional wave spectrum measured at NOAA Station 44006 off Duck, North Carolina at 0700 EST on 9 September 1981. The highly spread wave train coming from the northwest was generated by local winds during passage of a cold front and has its peak energy at .18 Hz ($T_p = 5.6$ sec). The more directionally coherent swell arriving from the east-northeast is from two distant hurricanes and has its peak energy at .09 Hz ($T_p = 11.1$ sec).

WAVE GROUPING

Although individual wave height and period vary randomly from one wave to the next, waves often occur in successive groups of alternately high and low waves. Examples of such wave grouping are given in Figure 18. In the upper profile, a moving "window" has been used to compute the running level of wave energy. As can be seen, short bursts of high energy are separated by minutes-long periods of relative calm, even though the record as a whole can be described by a single wave spectrum and has an average wave power. In the lower profile, the bursts of high wave energy are longer and the periods of relative calm are shorter than those in the first example.

The output of wave energy conversion devices will tend to follow the envelope or profile of such wave groups (Figure 19). Means of smoothing this output, such as flywheels or hydraulic accumulators, may be a necessary first step in power conditioning for the utility grid.

It should be noted that little can be learned about wave grouping from examination of a wave spectrum [10]. Time history records such as those in Figures 18 can be subjected to a grouping analysis, however, and the results can be used to reproduce the same grouping characteristics in a laboratory wave tank or computer simulation [11].

As part of the design process for a wave energy conversion device, a physical or numerical model of the device should be exercised in a series of random wave tests that covers a range of wave grouping. This will ensure that all power conversion equipment has been properly sized to handle the bursts of high wave energy and intervening low-energy periods. It should also satisfy the utility that its power quality requirements will be met throughout the entire wave sequence.

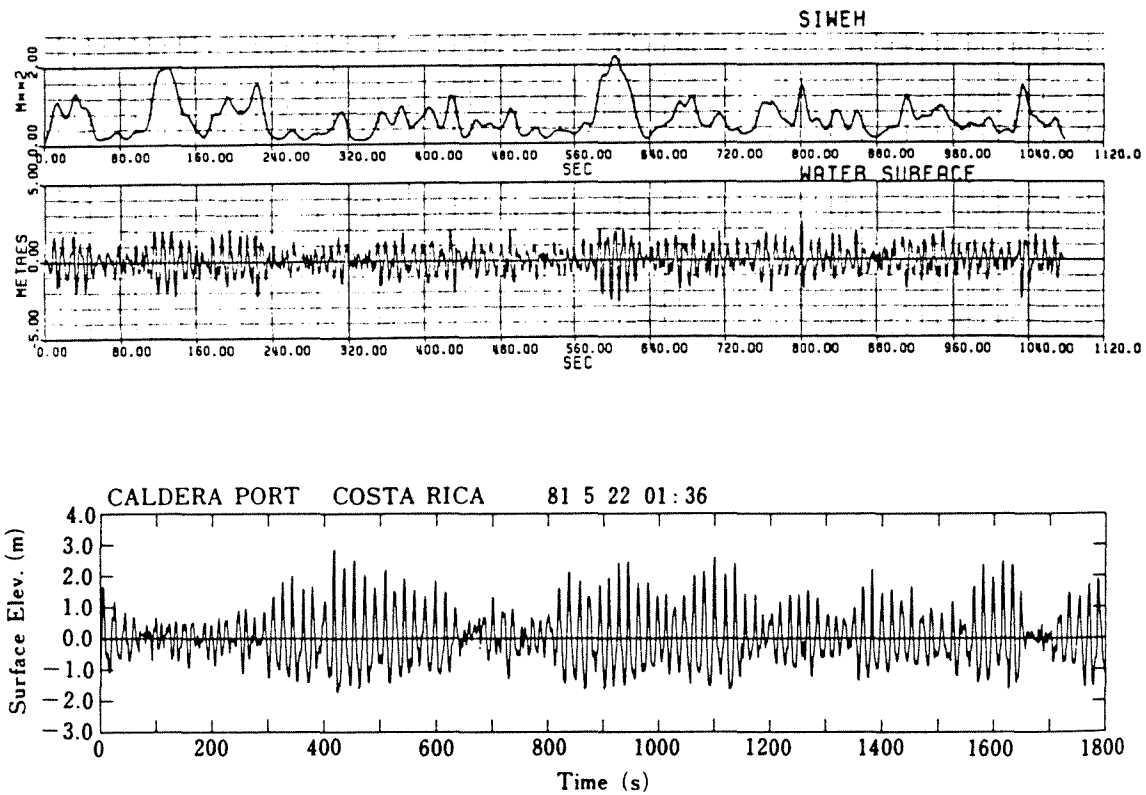


Figure 18. The upper two plots are the smoothed instantaneous wave energy history (SIWEH) and sea surface profile measured during the first deployment of the wave energy test ship "Kaimei" in the Sea of Japan, December 1979. The lower wave profile is from the Pacific Coast of Costa Rica in May 1981. This swell was generated by storms south of Australia and New Zealand and has travelled a distance of some 9,000 km. Although its spectrum is much narrower than that of the upper example, conspicuous wave grouping is still present.

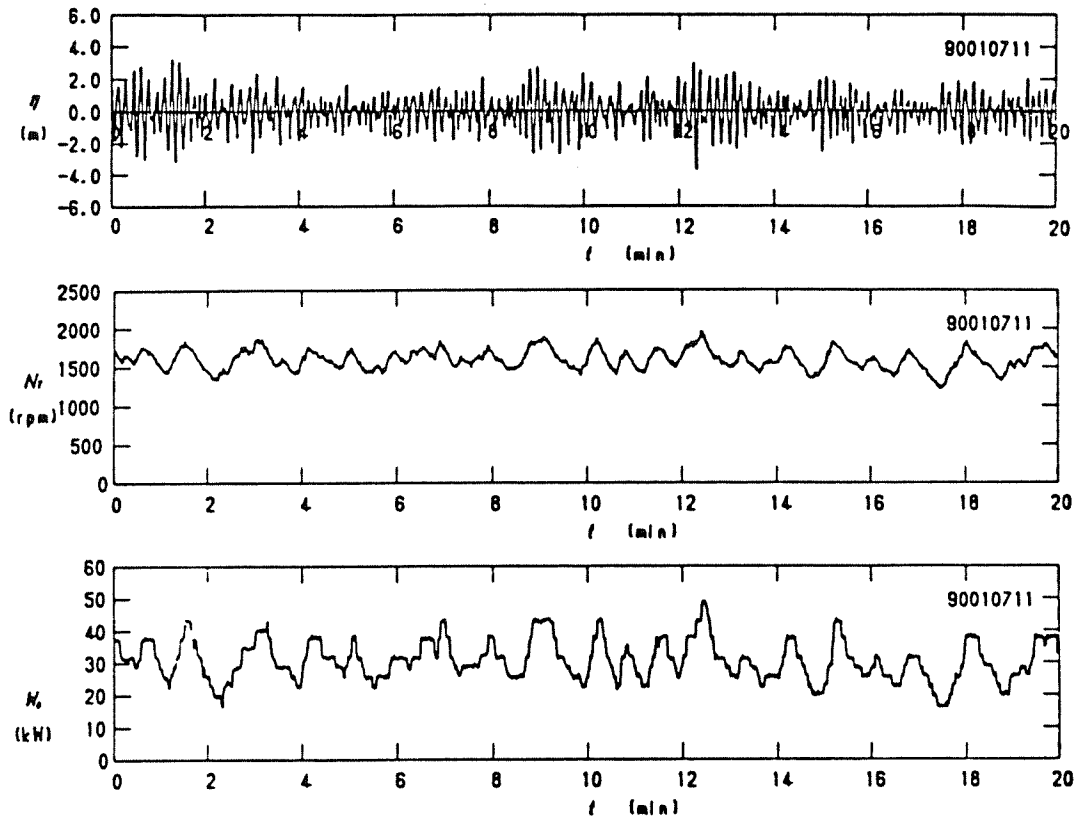


Figure 19. Measurements made during the demonstration of a 60 kWe breakwater-based oscillating water column plant at Sakata Port, on the Sea of Japan. This 20-minute record was made at 11:00 on 7 January 1990, when significant wave height and period were 3.2 m and 7.5 sec, respectively. Incident wave power was 40 kW/m. Top to bottom: incident wave profile, Wells turbine speed, and electrical generator output.

CHANGES IN SEA STATE

Wave conditions, as characterized by significant wave height and dominant wave period, typically change over a time scale of hours to days. Generally speaking, the lower the significant wave height, the longer it is likely to last. For example, Figure 20 shows the duration of various sea states at NOAA Station 51001, located in the northwest Hawaiian islands. A significant wave height greater than 1 m has a 30-35% probability of lasting at least 72 hours, whereas a significant wave height greater than 2 m has only a 10-15% probability of lasting this long. Wave heights greater than 4 m have less than 1% probability of lasting 72 hours.

In order to appreciate the factors that influence changes in wave energy levels over hours to days, it is helpful to understand the mechanisms by which waves are generated. Consider an area of the sea surface whose initial condition is one of flat calm or low ground swell from some far-distant storm. Even if low swell is present, the sea surface itself is glassy smooth, and there is no wind.

As a breeze develops, ephemeral and quickly moving patches of ruffled water, known as "cat's paws" appear wherever a gust brushes the water surface. These are small capillary waves, and when the local gust dies away, the glassy smoothness of the sea state is restored almost immediately. If the average wind speed increases to approximately 1.1 m/sec (2 knots) ripples develop, covering the entire area [4]. These are the first true gravity waves, and the height to which they grow depends on the speed of the wind, the duration for which it blows, and the downwind extent (or fetch) of the area over which it is blowing.

The growth of any harmonic component in a developing random sea follows the pattern illustrated in Figure 21. Note that either fetch or duration may limit wave growth before equilibrium is reached. If the wind stops blowing, wave growth will stop. Likewise, in a limited fetch, waves will be exposed to the wind for only a short time before leaving the area, no matter how long the wind blows. Assuming that wave generation is neither fetch- nor duration-limited, however, the growth pattern is as described below.

A component begins to grow rapidly (transition to exponential stage) when the curvature of the air flow over the wave reaches some critical value: the steeper the wave, the more curved the wind streamlines, the greater the rate of wave growth. Since shorter-period waves attain this critical steepness at a lower height than longer-period waves, these are the first to grow exponentially. Later, given sufficient wind duration and a great enough fetch so that the longer-period waves don't leave the area before they reach critical steepness, they too will begin to grow exponentially.

Meanwhile, the shorter-period waves will have reached equilibrium height, such that any more energy supplied by the wind is dissipated or transferred to lower-frequency waves. Once a component has attained equilibrium, it cannot grow much higher without becoming unstable and breaking. Whitecaps may form as shorter-period waves break on the crests of longer-period waves, imparting their momentum to them and accelerating the transfer of high-frequency energy to lower frequencies.

The delayed exponential growth of lower-frequency waves and the transfer of energy from higher-frequency waves once they've attained equilibrium causes the sea state to gain energy only at frequencies below the spectral peak, as shown in Figure 22. Thus a wave energy conversion device situated in an actively developing sea will experience a gradual increase in dominant wave period.

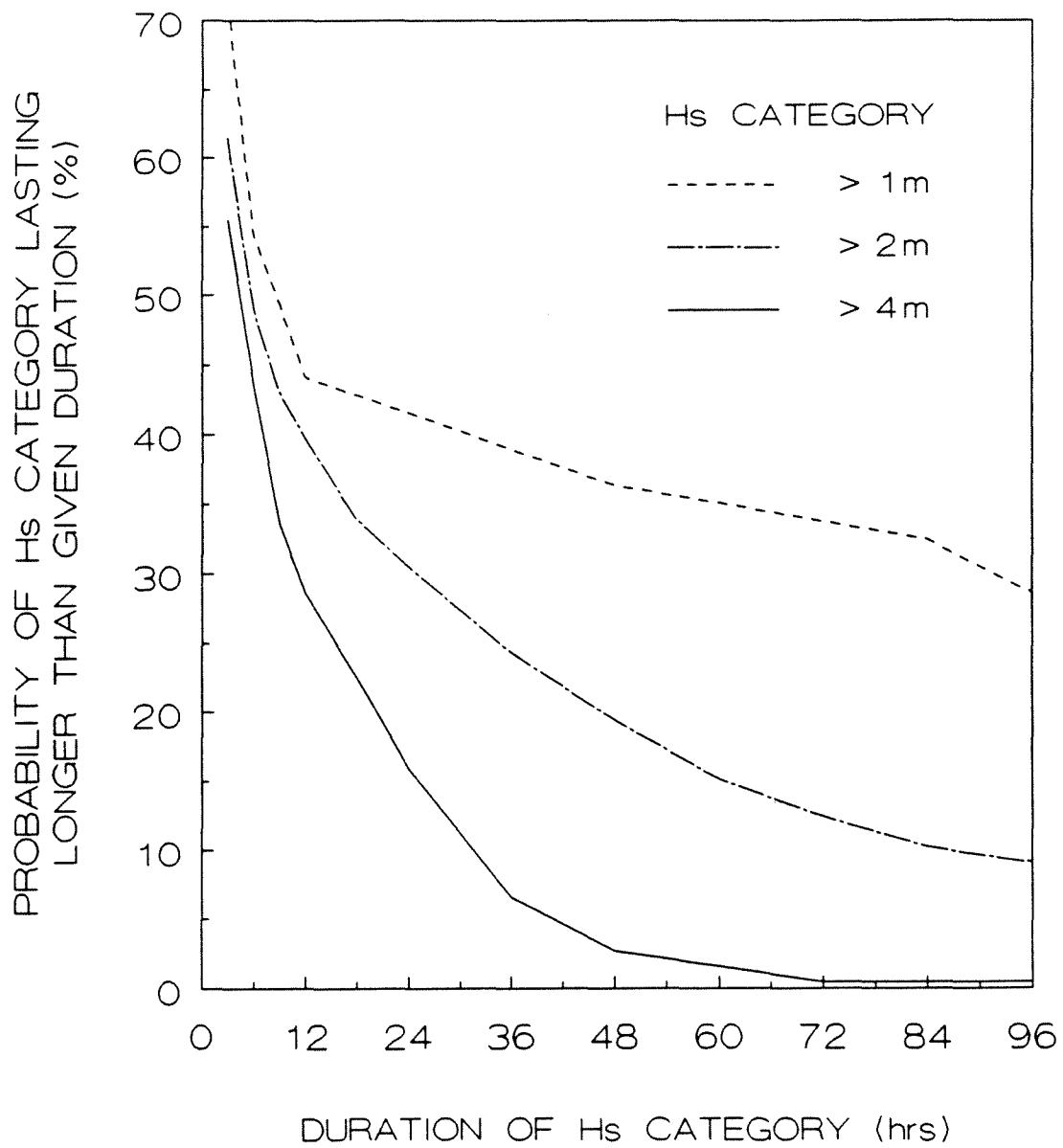


Figure 20. Duration probability for four different significant wave height categories at NOAA Station 51001, in the northwest Hawaiian Islands, near Nihoa.

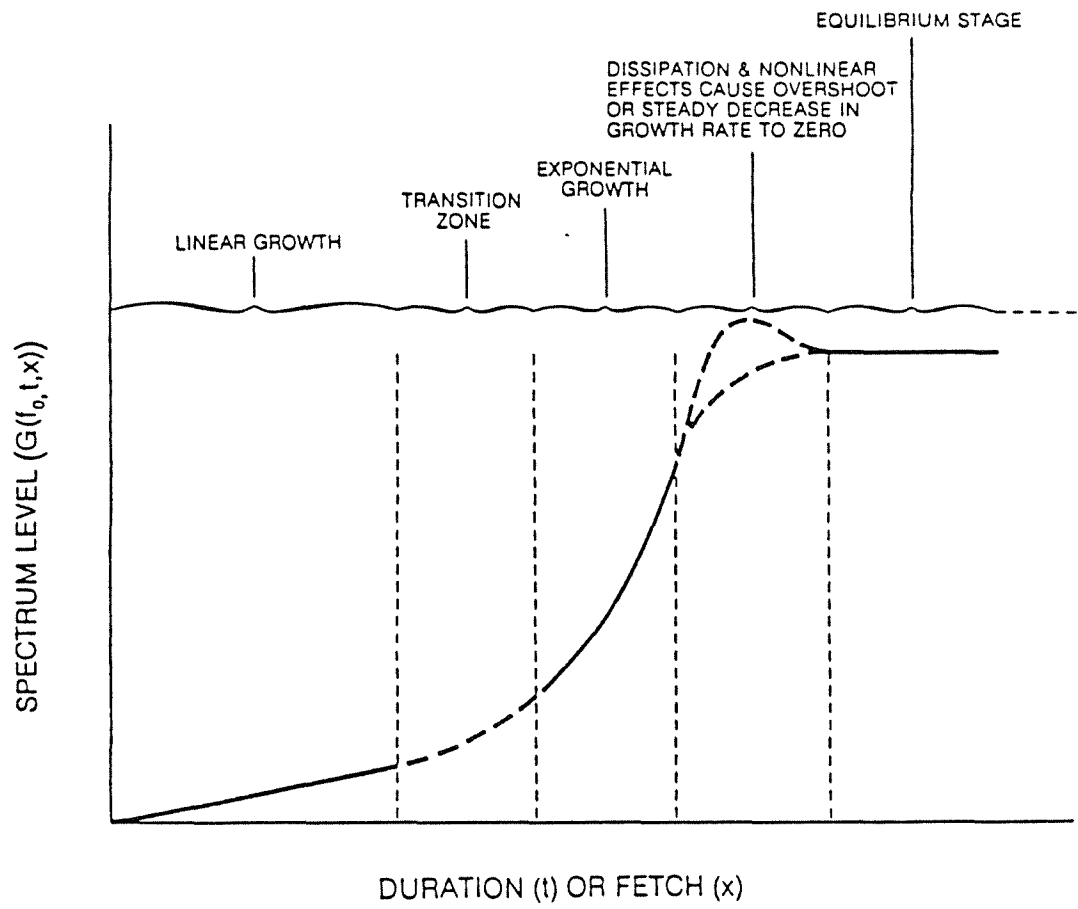


Figure 21. Growth of an individual harmonic wave component in a developing random sea.

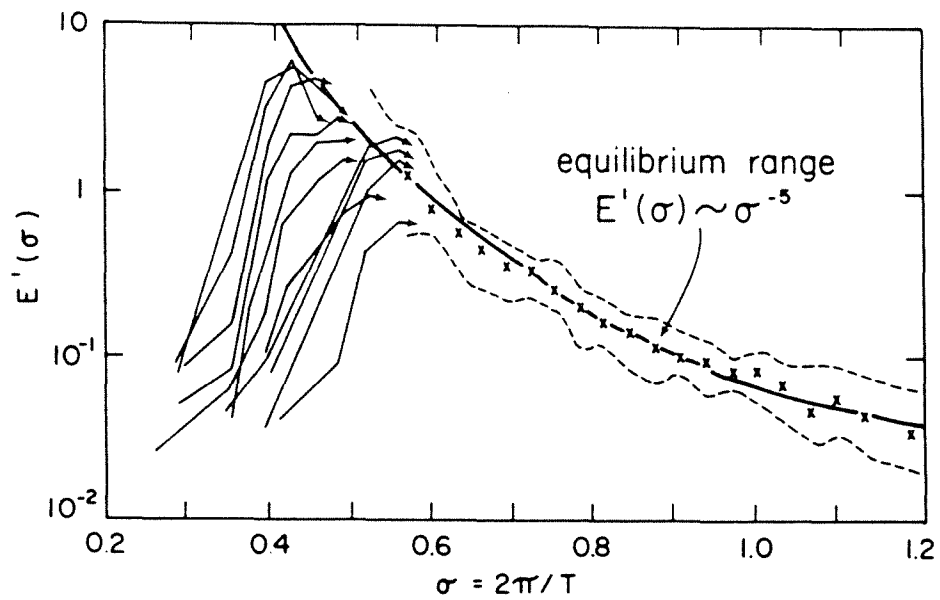


Figure 22. Growth of the wave spectrum in a developing sea. Harmonic components to the right of the spectral peak have reached equilibrium and can absorb no more wind energy. Longer-period components to the left of the spectral peak will continue to grow, however, until they also reach equilibrium.

Because group velocity is inversely proportional to wave frequency, there exists a low-frequency cut-off below which the energy in the waves is travelling faster than the wind. Thus at some point in the development of the spectrum, the waves stop growing, even if the wind continues to blow and the fetch is unlimited. The sea is then said to be fully developed for that particular wind speed.

Fully developed wave spectra for various wind speeds are illustrated in Figure 23. The higher the wind speed, the lower the cut-off frequency (since faster wind can keep up with faster travelling waves), and the greater the amount of energy that can be contained in the fully developed sea.

Conditions associated with fully developed wave spectra for wind speeds of 5 to 20 m/sec are listed in Table 2. The power levels in the wind and fully developed waves are also listed. Note that wind power is proportional to wind speed cubed, while wave power is proportional to wind speed raised to the fifth power. It is evident that wave growth dramatically concentrates the power of the wind.

Although waves are generated by the wind, high levels of wave energy can be present at a particular location even in the absence of strong winds. This occurs when swell from a distant storm arrives in the area. Swell waves tend to be more uniform in period than those in a wind-driven sea, and as previously mentioned, their energy is less directionally spread. They are thus "well-conditioned" for wave energy conversion. This conditioning results from the dispersive nature of wave energy once it leaves the area of wind generation, as described below.

Wave components of every frequency are present in a wind-driven sea. To a first approximation, the energy contained in each component travels independently, at its own group velocity. Although the different components start out together upon leaving the generation area, the longer-period waves travel faster and soon outdistance their shorter-period counterparts.

The energy of the fully developed sea is thus dispersed along a corridor emanating from the generation area. The effect is similar to that of a prism which spreads white light into several different bands of color, each one of a different constituent wavelength.

A wave gage moving at the group velocity of the peak spectral frequency would show a decrease in total energy and a narrowing of the spectrum as the shorter-period waves are left behind (Figure 25). A fixed gage (or wave power plant) located in the path of these waves experiences a rather abrupt increase in dominant wave period as the first, longest-period swell arrives. The dominant wave period then shifts gradually downward as the slower, shorter-period waves arrive.

Once the components of a wind-driven sea have dispersed and are well away from the generating area (500-1000 km distant), they travel thousands of kilometers with little loss of energy and can retain their identity over the span of an entire ocean basin. Even the longest waves do not begin to "feel the bottom" until they enter water depths of 300 m or less. Consequently, wave energy generated anywhere within an ocean basin ultimately arrives at some island or continental margin of that basin, virtually undiminished.

Thus, while sunlight and winds are distributed over the planet's entire surface, ocean waves are gathered along its coastlines. Therefore, waves have a much higher energy density than either of the natural processes that generate them. For example, annual average wave power densities along the northeastern coasts of the Hawaiian Islands range from 10 to 15 kW/m. By comparison, solar and wind energy fluxes are typically less than 1 kW/m².

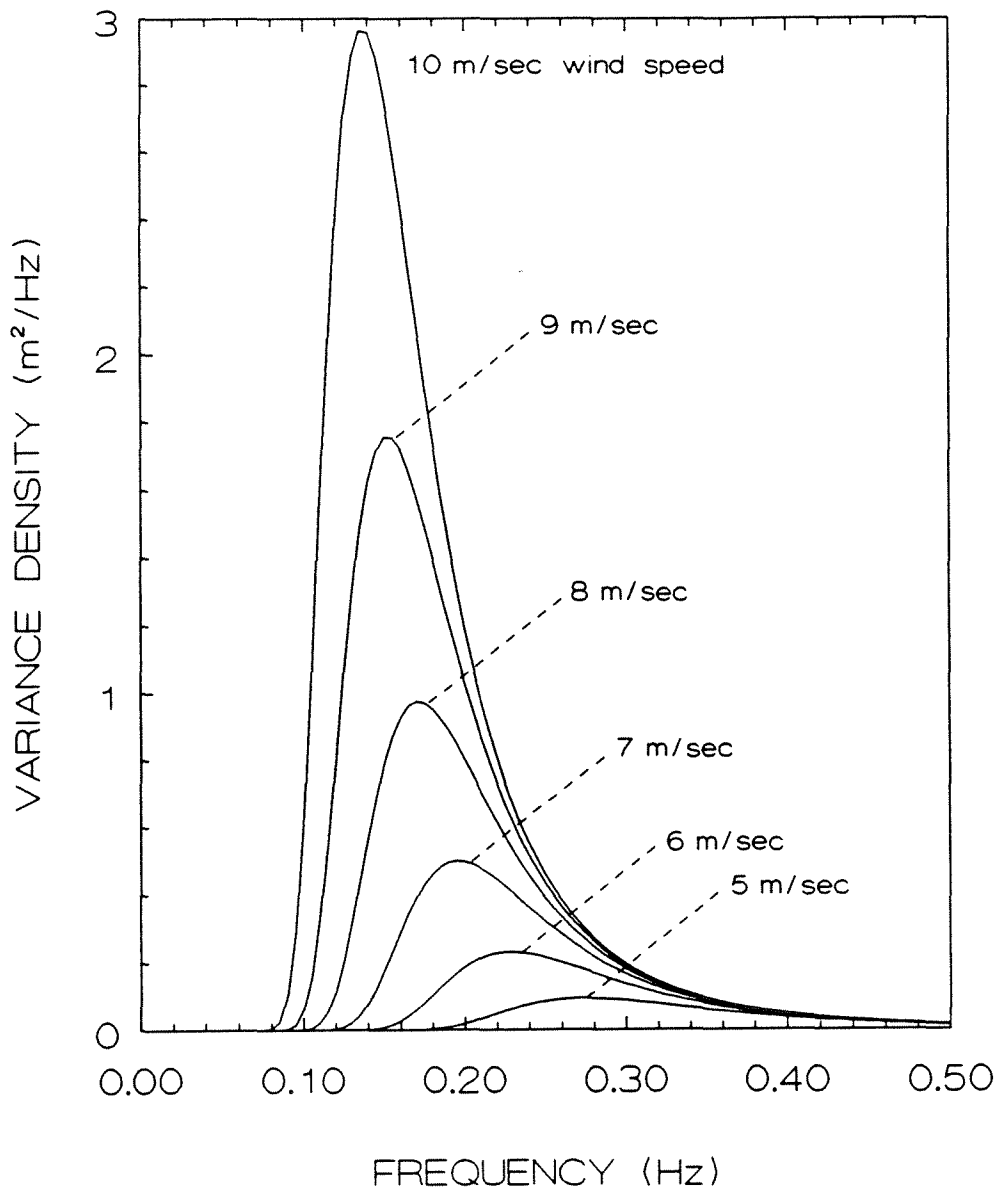


Figure 23. Fully developed wave spectra (Pierson-Moskowitz) for typical trade wind speeds.

Table 2

Wind and Wave Conditions Associated With Fully Developed Seas

Sustained wind speed:	<u>5 m/sec</u>	<u>10 m/sec</u>	<u>15 m/sec</u>	<u>20 m/sec</u>
Minimum duration:	2.3 hr	9.5 hr	22 hr	40 hr
Minimum fetch:	20 km	130 km	480 km	1,200 km
Significant wave height:	0.5 m	2.1 m	4.8 m	8.5 m
Dominant wave period:	3.7 sec	7.3 sec	11 sec	15 sec
Wave energy flux:	0.4 kW/m	14 kW/m	110 kW/m	450 kW/m
Wind energy flux:	.075 kW/m ²	.60 kW/m ²	2.0 kW/m ²	4.8 kW/m ²

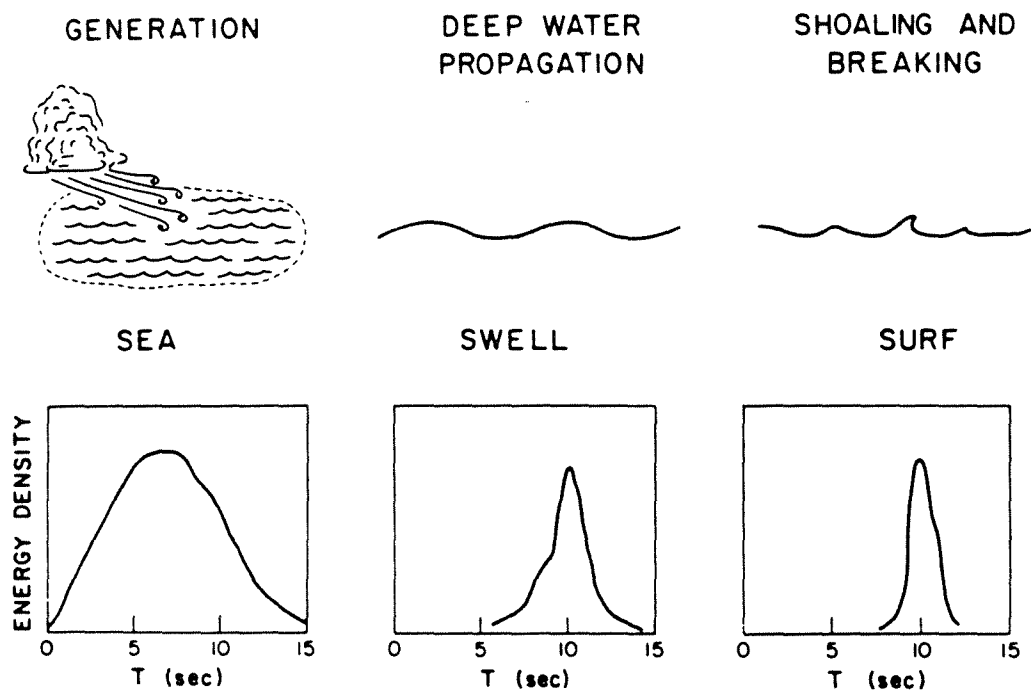


Figure 24. Wave spectrum transformation as waves leave a storm area.

REFERENCES

1. Smith, F.G.W., 1973. *The Seas in Motion*. New York, New York: Thomas Y. Crowell Company.
2. Kinsman, B., 1965. *Wind Waves*. Englewood Cliffs, New Jersey: Prentice-Hall, Inc.
3. Goda, Y., 1985. *Random Seas and Design of Maritime Structures*. Tokyo, Japan: University of Tokyo Press.
4. Komar, P.D., 1976. *Beach Processes and Sedimentation*. Englewood Cliffs, New Jersey: Prentice-Hall, Inc.
5. Earle, M.D., and J.M. Bishop, 1984. *A Practical Guide to Ocean Wave Measurement and Analysis*. Marion, Massachusetts: ENDECO, Inc.
6. Sarpkaya, T., and M. Isaacson, 1981. *Mechanics of Wave Forces on Offshore Structures*. New York, New York: Van Nostrand Reinhold Company.
7. Bhattacharya, R., 1978. *Dynamics of Marine Vehicles*. New York, New York: John Wiley & Sons.
8. Argonne National Laboratory, 1982. *Physical Engineering and Environmental Aspects of Ocean Kelp Farming*. Chicago, Illinois: Gas Research Institute, GRI-81/0111.
9. Ochi, M.K., 1973. On prediction of extreme values. *Journal of Ship Research*, Vol. 17, No. 1, pp. 29-37.
10. Mogridge, G.R., E.R. Funke, W.F. Baird, and E.P.D. Mansard, 1982. Analysis and description of wave energy resources. In *Proceedings of the Second International Symposium on Wave Energy Utilization*, edited by H. Berge, pp. 59-79. Trondheim, Norway: Tapir Publishers.
11. Funke, E.R., and E.P. D. Mansard, 1979. *On the Synthesis of Realistic Sea States in a Laboratory Flume*. Ottawa, Canada: National Research Council of Canada, Hydraulics Laboratory, LTR-HY-66.

APPENDIX B

DEEP WATER DIRECTIONAL WAVE STATISTICS AND SPECTRA

JOINT PROBABILITY DISTRIBUTION TABLE

As described in Section 2, the annual average joint probability distribution (JPD) of sea states measured off Makapuu Point, Oahu, was modified to represent wave conditions in open, deep water, away from the sheltering effects of coastal features and islands. The resulting JPD is presented in Table B-1. Note that six sea states in this table, accounting for a total of 329.2 hours, are assumed to be dominated by southern swell. For the resource assessment of this report, it was assumed that when southern swell predominates, wave conditions north of the islands are flat calm. Therefore, these six sea states were excluded from further analysis.

NON-DIRECTIONAL WAVE SPECTRA

For the remaining 53 sea states having a non-zero probability occurrence in Table B-1, theoretical spectra were developed based on the empirical fit of a three-component formula to measured spectra off Makapuu Point. These spectra are plotted on pages B-5 through B-10, and are digitized in ASCII computer files available from the Energy Division, Department of Business, Economic Development, and Tourism (DBED), 335 Merchant Street, Room 110, Honolulu, HI 96813.

There are 53 files, one for each sea state, named "SSxxODW.DAT", where xx is the sea state number (01 through 53; see Table B-1). Each file contains fifty-one lines. The first line contains four entries, separated by commas, in the following order:

- (1) Overall significant wave height (m)
- (2) Overall dominant wave period (sec)
- (3) Incident wave power (kW/m)
- (4) Average occurrence (hours per year)

Lines 2 through 51 list the best-fit spectral values for that sea state over the frequency range 0.01 through 0.50 Hz. Each line contains five entries, separated by commas, in the following order:

- (1) Frequency (Hz)
- (2) Low-frequency component spectrum (m^2/Hz)
- (3) Mid-frequency component spectrum (m^2/Hz)
- (4) High-frequency component spectrum (m^2/Hz)
- (5) Overall spectrum (m^2/Hz)

DIRECTIONAL DISTRIBUTION OF COMPONENT SPECTRA

The deep water mean directional distribution of dominant component spectra is plotted in Figure 2-14 of this report. This distribution has been digitized for each of the 53 sea states numbered in Table B-1, in an ASCII computer file, also available from DBED at the above address.

This file, named "DIRDISTR.ODW", contains fifty-three lines, one for each sea state. Each line contains thirteen entries, separated by commas, in the following order:

- (1) Sea state number (01 through 53)
- (2) Significant wave height (m)
- (3) Dominant wave period (sec)
- (4) Average annual occurrence (hours per year)
- (5) Fraction of time mean direction is out of W (270°)
- (6) Fraction of time mean direction is out of WNW (292.5°)
- (7) Fraction of time mean direction is out of NW (315°)
- (8) Fraction of time mean direction is out of NNW (337.5°)
- (9) Fraction of time mean direction is out of N (360° or 0°)
- (10) Fraction of time mean direction is out of NNE (22.5°)
- (11) Fraction of time mean direction is out of NE (45°)
- (12) Fraction of time mean direction is out of ENE (67.5°)
- (13) Fraction of time mean direction is out of E (90°)

It should be noted that for some sea states, the fractions do not sum to unity over the entire directional range from W through E. This is due to the occasional dominance of waves driven from the south by Kona winds. These are rare occurrences, accounting for a total of only 26.5 hours annually.

Excluding sea states dominated by southern swell (329.2 hours) and Kona storms (26.5 hours), wave energy comes from the W-N-E sector 8404.3 hours per year. The average power in these sea states is 15.5 kW/m. Assuming calm conditions for the remaining 355.7 hours, when waves out of the south predominate, the annual average wave power in open deep water north of the islands is 14.9 kW/m.

Table B-2 indicates the mean direction and directional spreading parameter (S_{max} ; see Appendix A for definition) assigned to each of the three component spectra in the refraction and shoaling analysis performed for this report. Pending the development of more refined directional data, it is recommended that these values be used for site-specific studies as well.

Table B-1
Annual Average Joint Probability Distribution in Open Deep Water

Significant Wave Height Range (m)	Dominant Wave Period Range (sec)						
	<=6	6-8	8-10	10-12	12-14	14-16	16-18
0.0
0.3
0.6
0.9	.	No.01 (22.6)	No.02 (22.4)
1.2	No.03 (113.9)	No.04 (146.5)	No.05 (187.1)	(42.5)	(26.9)	.	.
1.5	No.06 (609.7)	No.07 (355.8)	No.08 (364.8)	(111.3)	(100.9)	(37.1)	(10.5)
1.8	No.09 (676.2)	No.10 (638.0)	No.11 (386.1)	No.12 (246.5)	No.13 (185.7)	No.14 (61.4)	No.15 (27.7)
2.1	No.16 (257.3)	No.17 (686.5)	No.18 (378.3)	No.19 (209.2)	No.20 (175.8)	No.21 (44.8)	No.22 (16.0)
2.4	No.23 (53.1)	No.24 (521.2)	No.25 (251.9)	No.26 (179.1)	No.27 (142.7)	No.28 (58.7)	No.29 (21.5)
2.7	.	No.30 (248.7)	No.31 (201.5)	No.32 (99.8)	No.33 (86.6)	No.34 (50.0)	No.35 (12.8)
3.0	.	No.36 (89.0)	No.37 (111.0)	No.38 (66.5)	No.39 (59.4)	No.40 (33.8)	.
3.3	.	No.41 (43.3)	No.42 (53.3)	No.43 (37.3)	No.44 (35.9)	No.45 (20.4)	.
3.6	.	No.46 (14.9)	No.47 (36.6)	No.48 (17.9)	No.49 (15.8)	No.50 (9.5)	.
3.9	.	.	No.51 (21.4)	No.52 (13.3)	.	.	.
4.2	.	.	No.53 (11.7)

Sea states bordered by dashed line are assumed to be dominated by southern swell; remaining 53 sea states are numbered consecutively as shown. Average number of hours that each sea state occurs annually is indicated in parentheses.

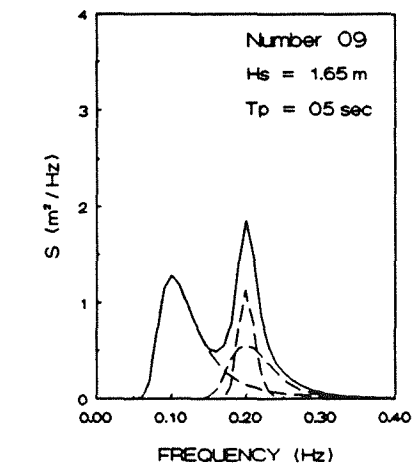
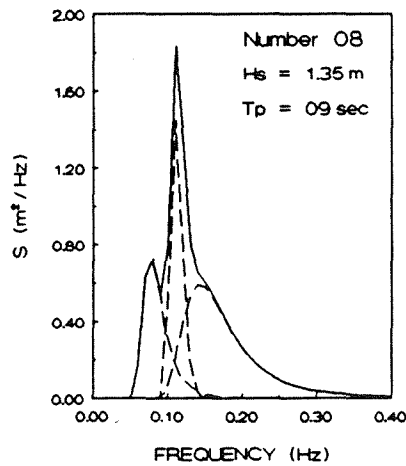
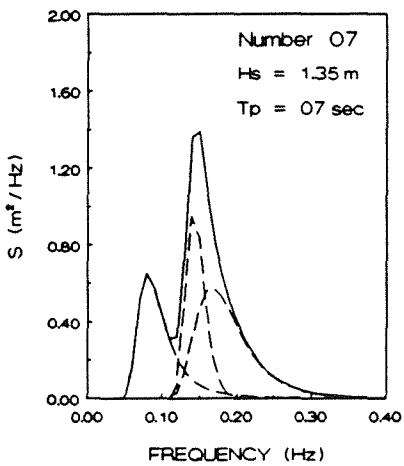
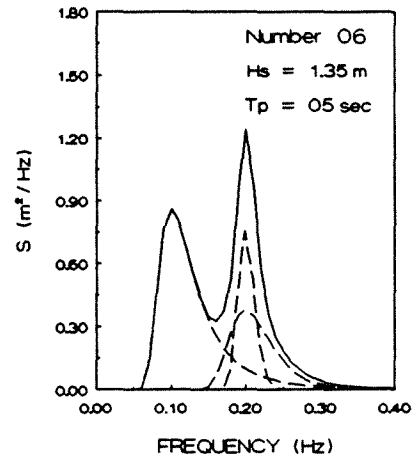
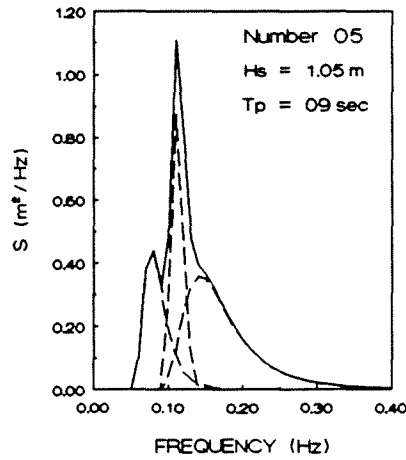
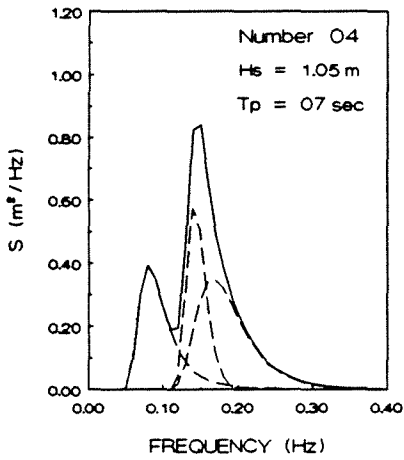
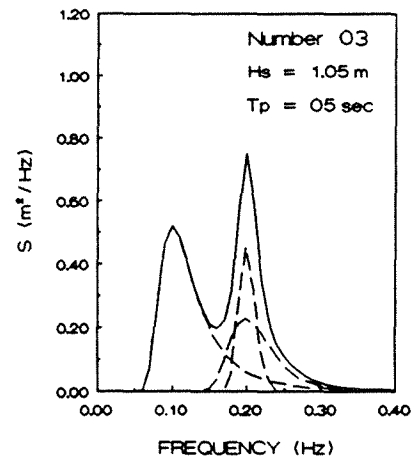
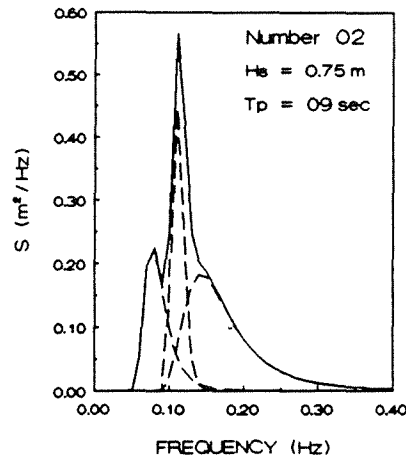
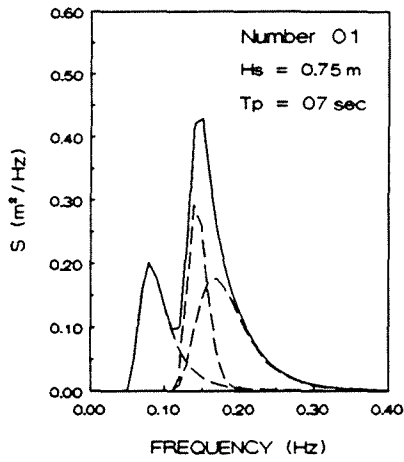
Table B-2

Mean Directions and Directional Spreading Parameters Assigned to Component Spectra

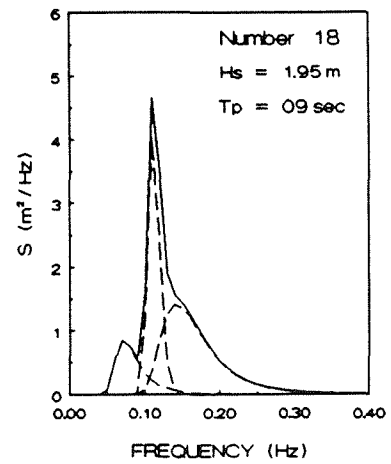
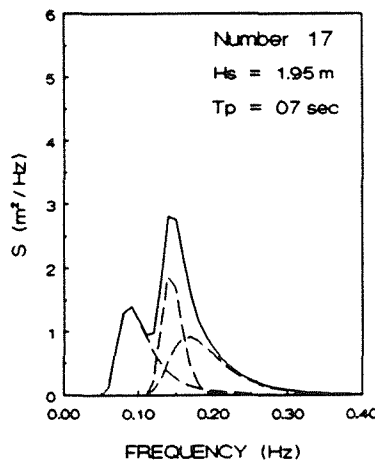
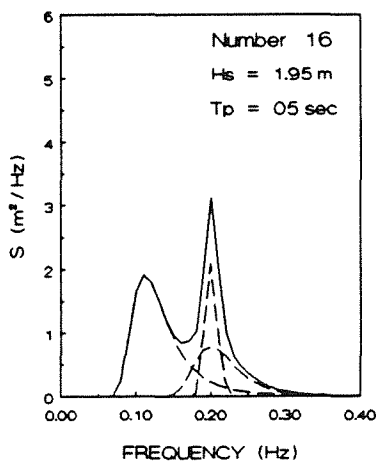
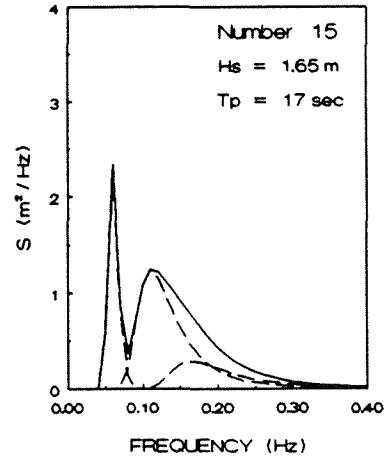
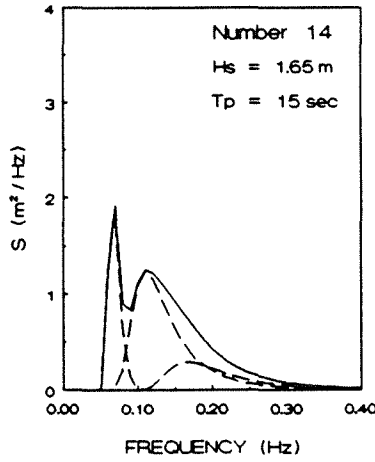
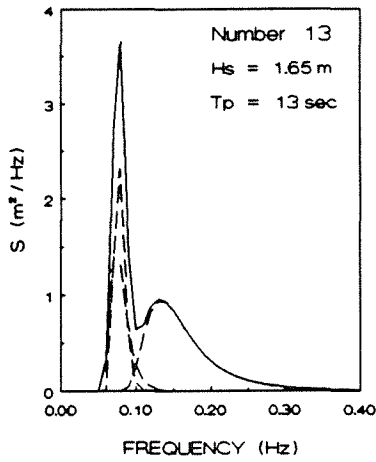
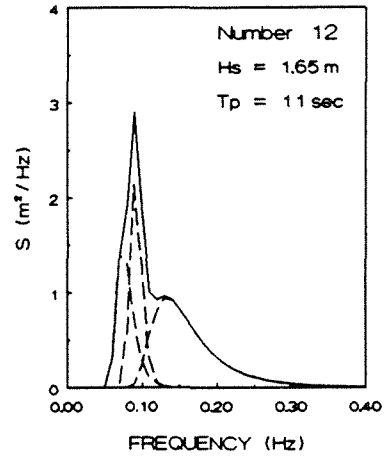
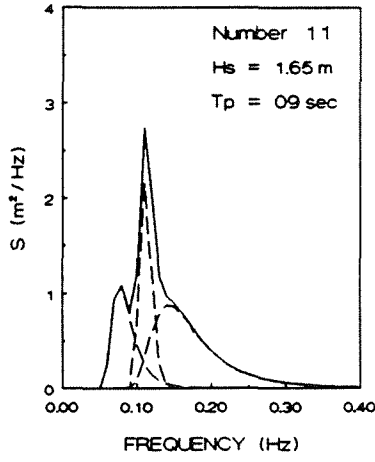
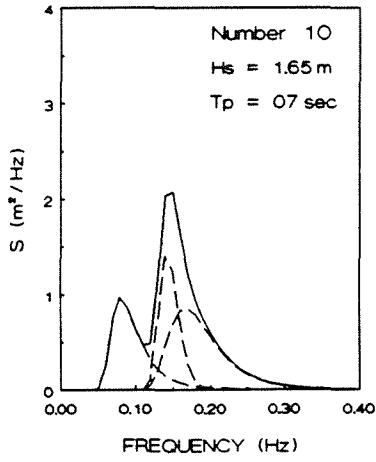
Overall Dominant Wave Period	Low-Frequency Component Spectrum		Mid-Frequency Component Spectrum		High-Frequency Component Spectrum	
	Mean Direction	Smax	Mean Direction	Smax	Mean Direction	Smax
5 sec	337.5°	6	Fig. 2-14	10	45°	6
7 sec	"	"	"	"	"	"
9 sec	"	"	"	"	"	"
11 sec	"	"	"	50	"	"
13 sec	"	"	"	"	"	"
15 sec	Fig. 2-14	50	337.5°	6	"	"
17 sec	"	"	"	"	"	"

The value of the directional spreading parameter, Smax, was assigned as follows. Dominant component spectra having peak periods of 9 sec or less were assumed to be seas associated with existing wind conditions, and were assigned an Smax value of 10. Lesser component spectra having peak periods of 8 sec or less were assumed to be decaying seas developed by winds no longer existing, and were assigned an Smax value of 6. Dominant component spectra having peak periods of 11 sec or more were assumed to be swell from a single active storm system in the northwest Pacific Ocean, and were assigned an Smax value of 50. Lesser component spectra having peak periods of 9 sec or more were assumed to be background swell, coming from more distant or less intense storms. Unlike predominant swell from a single storm, crossing wave trains from several different storms were assumed to make up this background swell, which was therefore assigned an Smax value of 6.

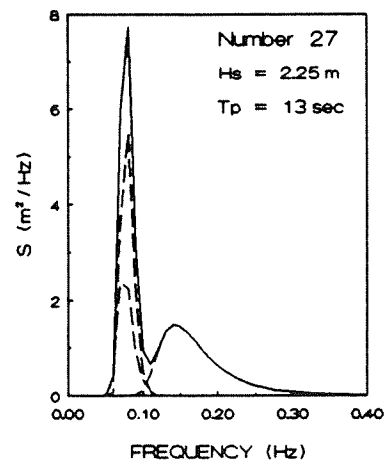
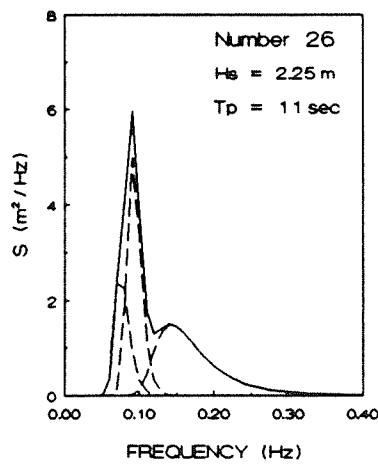
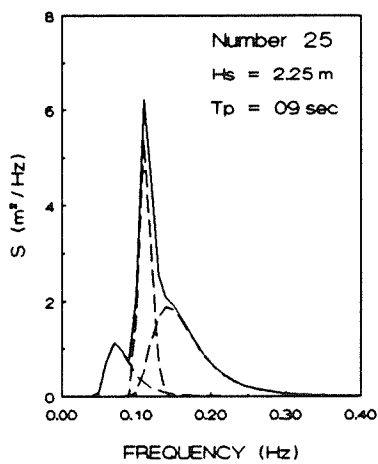
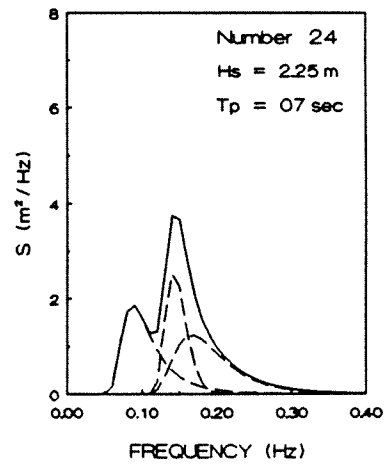
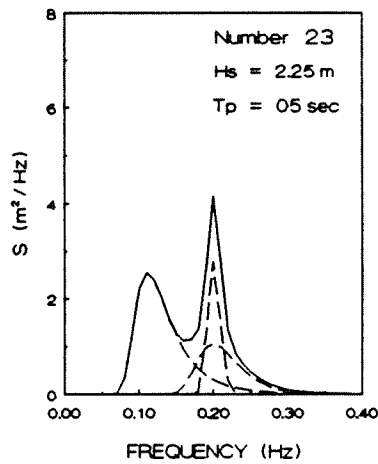
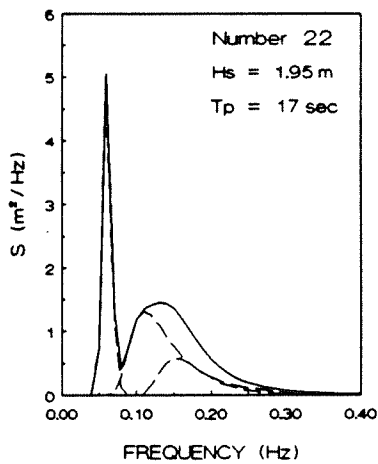
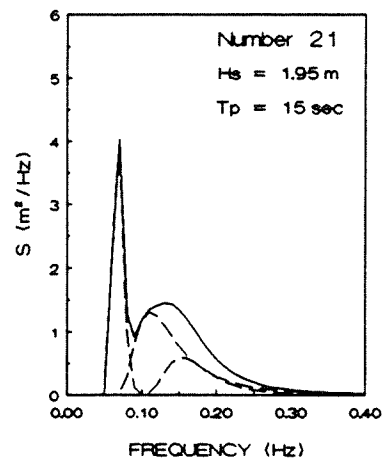
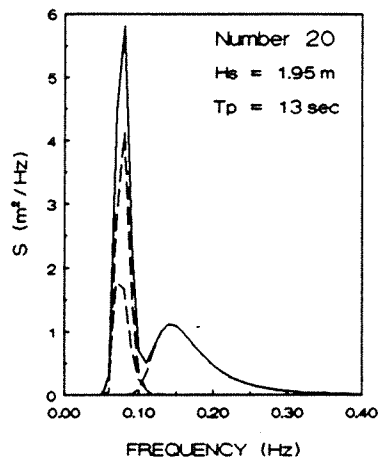
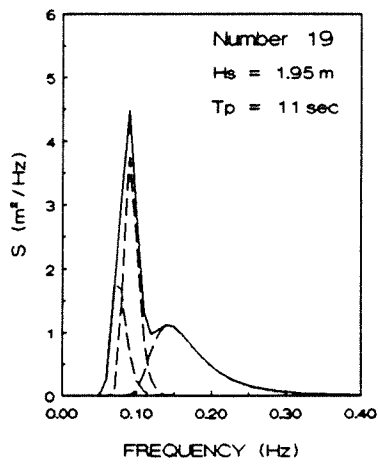
Sea states 01 through 09. Component spectra are plotted as dashed lines; overall spectrum as solid line.



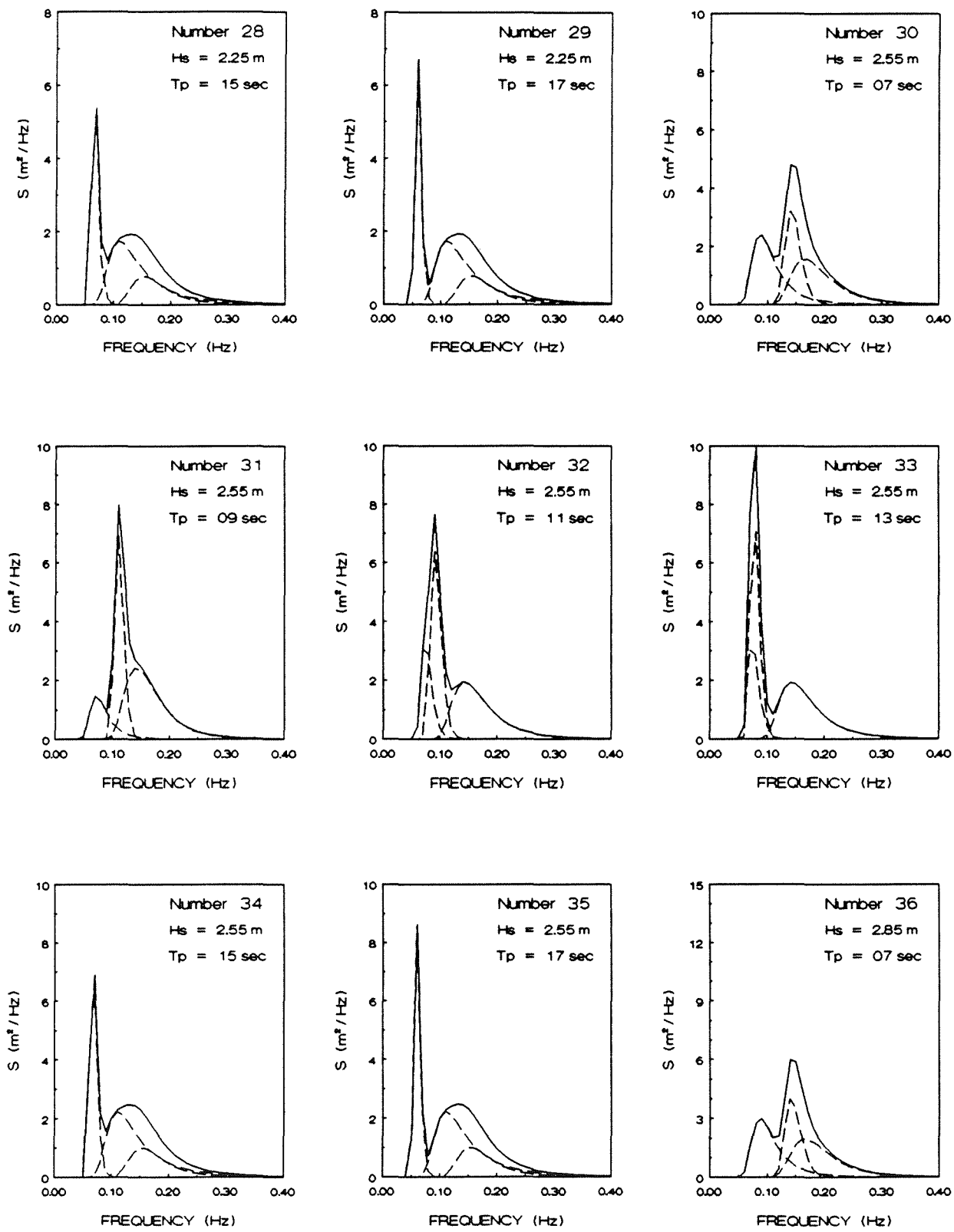
Sea states 10 through 18. Component spectra are plotted as dashed lines; overall spectrum as solid line.



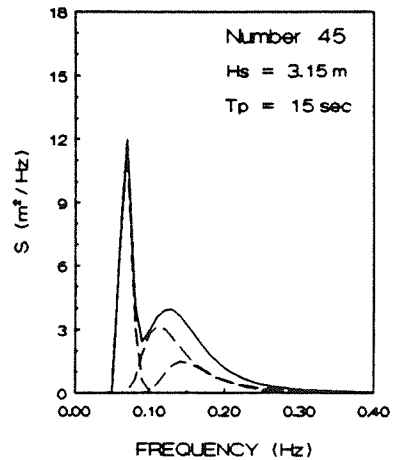
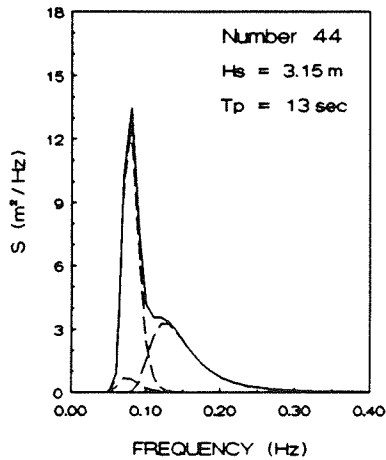
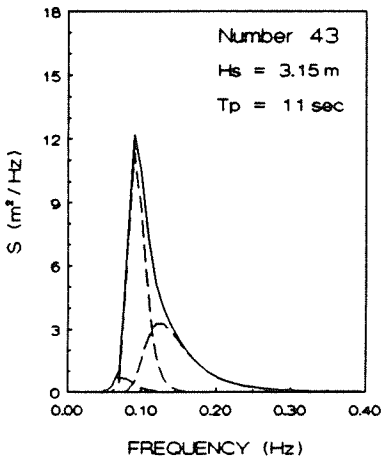
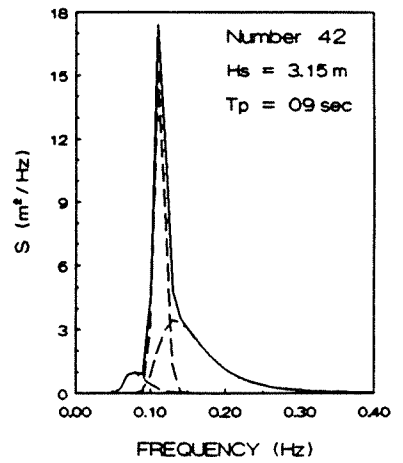
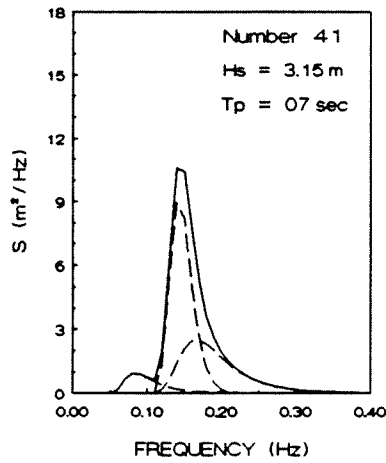
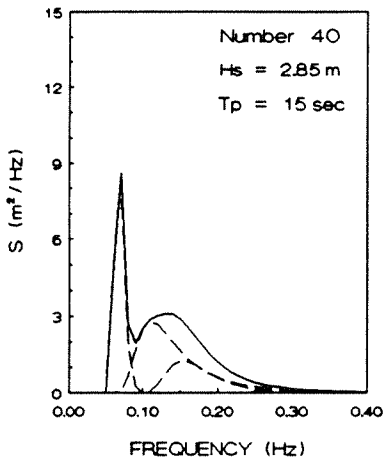
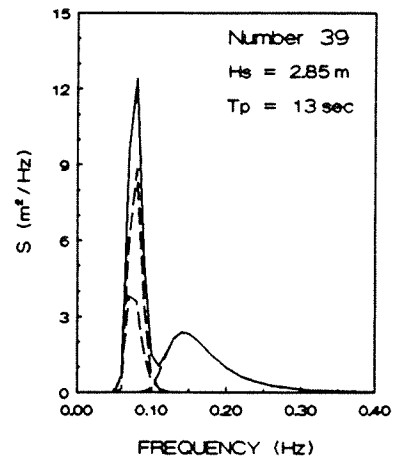
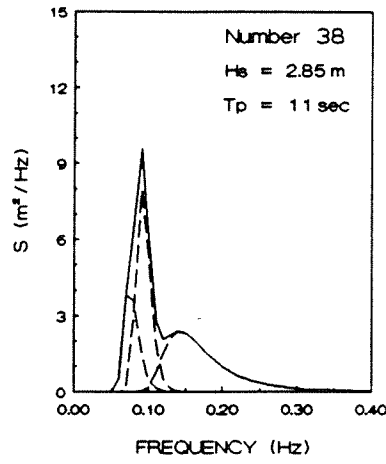
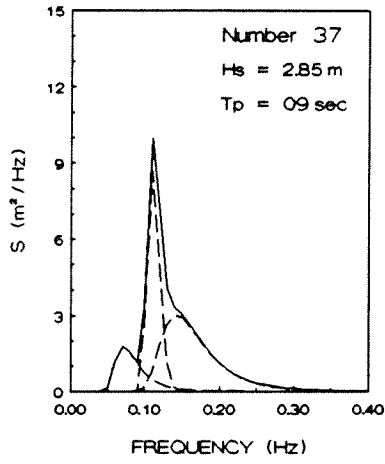
Sea states 19 through 27. Component spectra are plotted as dashed lines; overall spectrum as solid line.



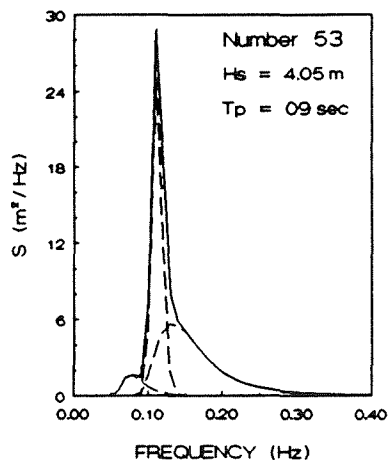
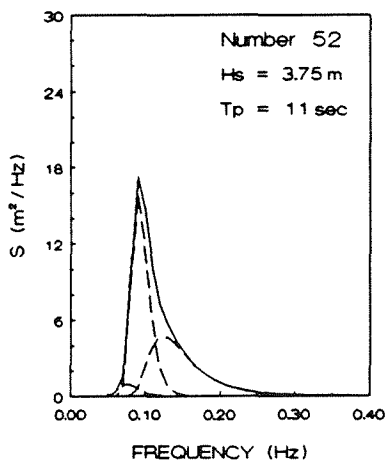
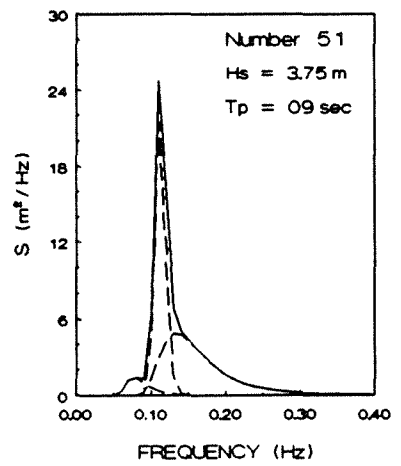
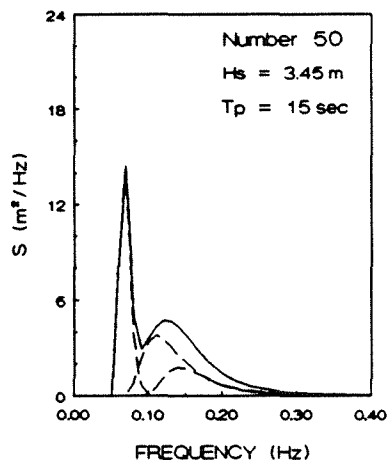
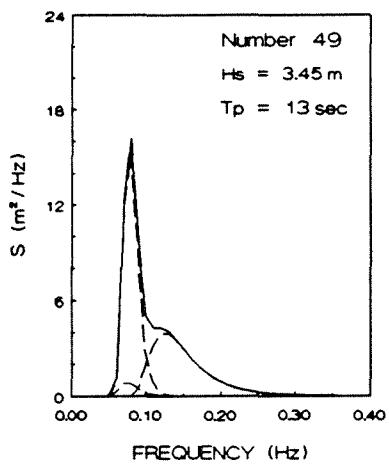
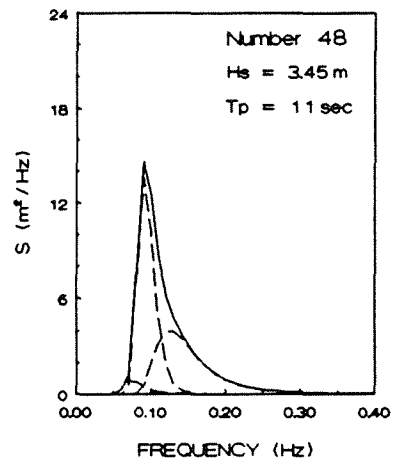
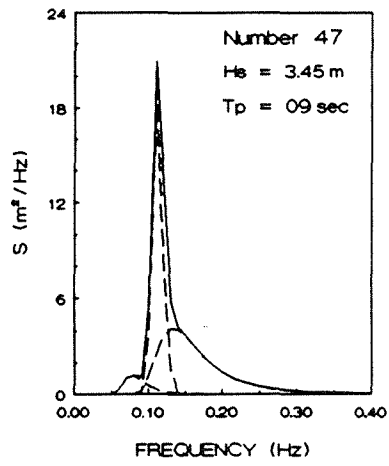
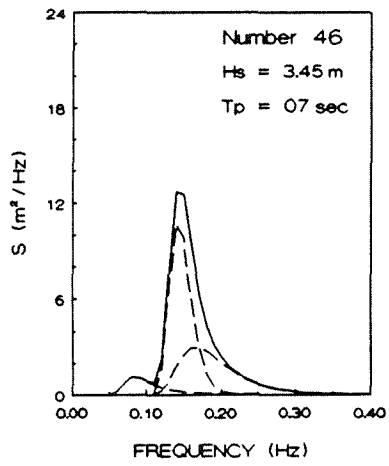
Sea states 28 through 36. Component spectra are plotted as dashed lines; overall spectrum as solid line.



Sea states 37 through 45. Component spectra are plotted as dashed lines; overall spectrum as solid line.



Sea states 46 through 53. Component spectra are plotted as dashed lines; overall spectrum as solid line.



APPENDIX C

BATHYMETRIC CHARTS AND DATA AVAILABILITY

BATHYMETRIC CHARTS

The most recently compiled bathymetric charts for Hawaii are published in:

Campbell, J. F., 1987. *Bathymetric Atlas of the Southeast Hawaiian Islands*. Honolulu, Hawaii: University of Hawaii, UNIHI SEAGRANT MR-87-01.

This publication is available at a cost of \$3.75 from:

University of Hawaii
Sea Grant College Program
1000 Pope Road
Marine Science Building, Room 200
Honolulu, HI 96822

The charts in the above atlas are printed at a scale of 1:200,000, with a depth contour interval of 25 m. They are of limited use for land- or caisson-based wave power plant studies, since the shallowest depth contour is 50 m. It should also be noted that the above atlas does not include Kauai, and covers only the northernmost part of the Big Island (in the vicinity of Upolu Point).

The charts used for the wave energy resource assessment of this report were published by the U.S. Geological Survey in Reston, Virginia (Figure C-1). Although adequate for the simple refraction and shoaling analysis of this report, these charts are not suitable for site-specific studies, which require digitized depth data, gridded or contoured at much higher resolution than available on these charts.

BATHYMETRIC DATA

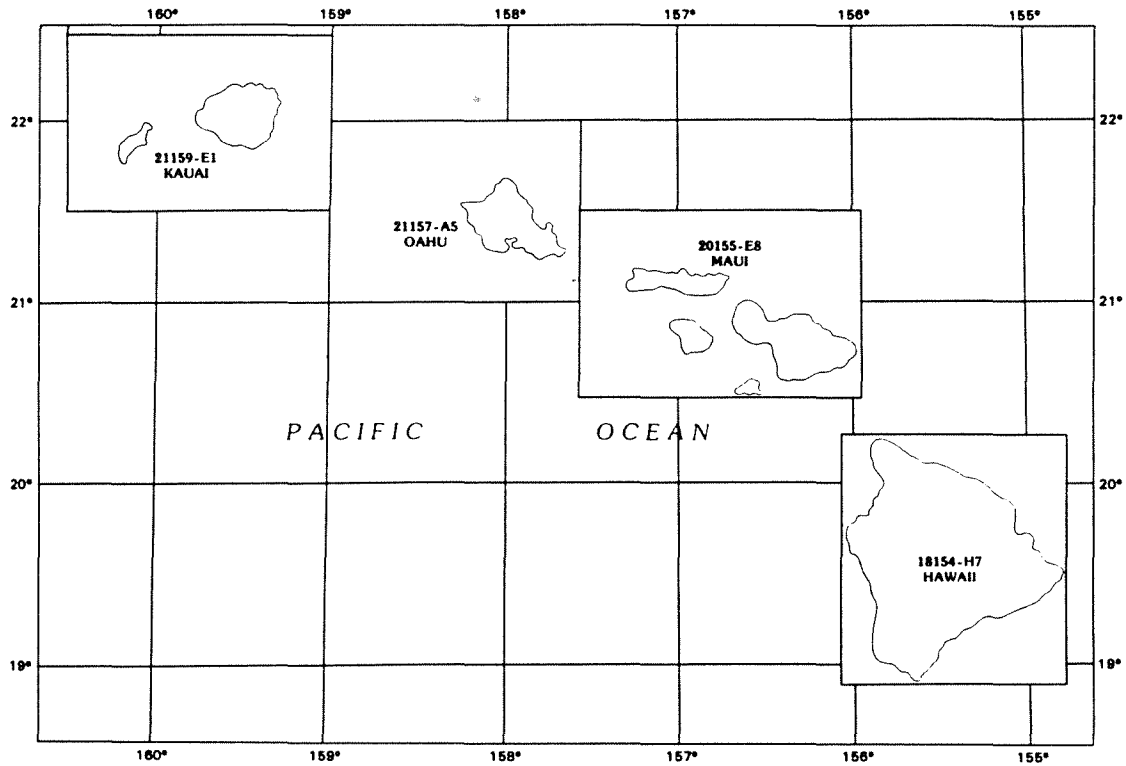
Digitized hydrographic survey data are archived at the National Geophysical Data Center (NGDC) in Boulder, Colorado, and can be ordered by contacting the NGDC Office of Marine Geology and Geophysics (telephone 303-497-6338). Data points are listed as 40-character records containing survey information, latitude and longitude to the nearest 0.01-second, and depth relative to mean lower low water. NGDC furnishes the data in user-specified, one-degree squares of latitude and longitude; the user must further sort the data if a smaller area is to be analyzed.

The Hawaii Institute of Geophysics maintains mapping software for gridding or contouring NGDC data and offers this service for a fee to non-University researchers. Inquiries should be directed to:

Marine Data Archives, SOEST
University of Hawaii
2525 Correa Road
Honolulu, HI 96822

In order to accurately assess wave refraction and shoaling effects, depth data should be gridded at a resolution of 200 m; finer if complex bathymetric features, such as coral reefs, lie offshore the site. The area covered should extend from the site ± 20 km along the coast, out to a depth of at least 100 m.

**1 X 2 DEGREE SERIES
1:250 000 SCALE**



<u>Chart</u>	<u>Number</u>	<u>Depth Contours</u>
Kauai	21159-E1	36, 60, 120, 300, 600 feet
Oahu	21157-A5	30, 60, 300, 600 feet
Maui	20155-E8	10, 20, 50, 100 fathoms
Hawaii	18154-H7	30, 60, 120, 300, 600 feet

Shoreline surveys to locate potential sites for land-based wave power plants may benefit from the 7.5-minute map series (printed at 1:24,000 scale) published by the U.S. Geological Survey. There is no charge for the *Hawaii Index to Topographic and Other Map Coverage*, which can be used to locate the 7.5-minute quadrangles mapped on Hawaii's principal islands.

Figure C-1. Charts used for resource assessment of this report.

APPENDIX D

ENERGY COSTING METHOD AND FINANCIAL PARAMETERS

ENERGY COSTING METHOD

The energy costing method used in this report computes the levelized annual revenue requirement over the book life of a wave power plant, and divides this by the plant's annual output. If all electricity generated by the plant were sold for this amount, the total collected revenue would have the same present value as the sum of all fixed charges and expenses paid out during the life of the plant. Levelization thus makes it possible to compare investment alternatives in terms of a single cost.

It should be noted that depreciation of the plant and periodic reinvestment in new equipment will cause the actual revenue requirement to change from year to year, whereas the levelized revenue requirement represents a constant annual payment and does not indicate the effect that a particular investment will have on actual cash flow.

Energy costs can be computed in both constant dollars and current dollars. Constant dollars were used, because they have a purchasing power more akin to the reader's recent experience. Current dollars represent what the energy would actually cost at the time payments are made.

Revenue requirements accounted for by this method are listed below. A more detailed description, including an explanation of levelization, can be found in:

Electric Power Research Institute, 1987. *Technical Assessment Guide, Volume 3: Fundamentals and Methods, Supply-1986*. Palo Alto, California: Electric Power Research Institute, P-4463-SR.

The annual revenue that must be collected to pay for the construction and operation of a power plant consists of fixed charges and expenses. Fixed charges are long-term financial obligations associated with building the plant and periodically replacing equipment that may wear out during the plant's life. They are "fixed" in the sense that they must be paid, regardless of how much electricity the plant generates. The following fixed charges were applied to the computation of energy costs presented in this report:

- Return on capital investment, in the form of debt return to creditors and equity return to shareholders
- Book depreciation
- Property taxes and insurance
- Income taxes; depreciation, property taxes, insurance, and interest on debt are assumed to be tax-deductible

Expenses are annual payments associated with operating and maintaining the plant. Although no economic assessment was made of wave-powered desalination or the use of Tapered Channel reservoirs for aquaculture, the sale of co-products would be credited towards expenses. If co-product sales exceed expenses, then the difference (which is profit) would be subject to income tax. For this report, it was assumed that annual expenses would not be subject to real price escalation over the life of the plant.

FINANCIAL PARAMETERS

The financial parameters used to compute the levelized energy costs in Section 4 of this report were taken from page A-1 of:

Electric Power Research Institute, 1986. *Technical Assessment Guide, Volume 1: Electricity Supply -1986*. Palo Alto, California: Electric Power Research Institute, EPRI P-4463-SR.

These parameters are as follows:

Constant-dollar cost of debt financing:	4.6%
Constant-dollar cost of equity financing:	7.65%
Debt-to-equity ratio:	50%
Annual inflation rate:	6%
(The above combination gives a current-dollar discount rate of 12.5%)	
Federal and state income tax rate:	38%
Annual property tax and insurance rate:	2%

In addition, straight-line depreciation was assumed over the entire project book life, with zero net end-of-life salvage value (salvage pays for decommissioning). It was also assumed that there would be no tax preferences or credits.

FABRICATION COST FOR CONCRETE CAISSONS

For the Pivoting Flap device, caisson weight was originally given as 70 tonnes per meter of breakwater length with a weight unit cost of 85,700 ¥/tonne. Weight was converted to reinforced concrete volume by assuming a density of 2.61 tonnes per cubic meter. At a foreign exchange rate of 138 ¥/\$, this corresponds to a volume unit cost of \$1,620/m³. This was reduced to US\$ 1,000/m³, which is thought to be more representative of small-yard fabrication costs in Hawaii.

FOREIGN EXCHANGE AND INFLATION

Cost estimates originating outside the United States were converted to U.S. dollars (US\$) using the exchange rate in effect at the time the original cost estimate was made. Exchange rates were obtained from the International Monetary Fund in Washington, DC, and are as follows:

<u>Table</u>	<u>Project</u>	<u>Original Currency</u>	<u>Exchange Rate</u>
4-1	Tapered Channel (Toftestallen)	Norwegian crown (NOK) 1985 annual average	8.60 NOK/US\$
4-1	Tapered Channel (King Island)	Norwegian crown (NOK) September 1990 average	6.07 NOK/US\$

FOREIGN EXCHANGE AND INFLATION (continued)

<u>Table</u>	<u>Project</u>	<u>Original Currency</u>	<u>Exchange Rate</u>
4-2	Double-Acting MOWC (Toftestallen)	Norwegian crown (NOK) 1985 annual average	8.60 NOK/US\$
4-2	Single-Acting OWC (Kashima Port)	Japanese yen (¥) 1989 annual average	138 ¥/US\$
4-2	Pivoting Flap (Muroran Port)	Japanese yen (¥) 1989 annual average	138 ¥/US\$

Original cost estimates made prior to 1990 were escalated at an annual inflation rate of 6%. Currency exchange, where necessary, was made before escalation. Note that cost data for the Tapered Channel plant on Java (Table 4-1) and the MOWC plant on Tongatapu (Table 4-2) were originally in U.S. dollars.

APPENDIX E

LISTING OF WAVE ENERGY TECHNOLOGY DEVELOPERS

<u>Technology</u>	<u>Developer (Contact)</u>	<u>Developer's Address</u>	<u>Status</u>
Process 1 - Reservoir Filled by Wave Surge			
Tapered Channel Toftestallen project	Norwave, A.S. (Dr. Even Mehlum)	P.O. Box 316 1324 Lysaker Norway	Demonstration plant (350 kWe) operating
Mauritius project	Crown Agents (Sir A.N. Walton-Bott)	United Kingdom	Advisors to Norwave, A.S.
Floating ramp and reservoir	SEA POWER AB (Goran Lagstrom)	Kjellmansgatan 14 S-414 63 Gothenburg Sweden	Ocean test of 100 kWe pontoon underway
Dam-Atoll	Lockheed Missiles & Space Company, Inc.	Sunnyvale, CA USA	Inactive
HRS Rectifier	Hydraulics Research Station, Wallingford	United Kingdom	Inactive
Process 2 - Fixed Oscillating Water Column			
LAND-BASED SYSTEMS			
Multi-resonant OWC (monoplane Wells turbine) Toftestallen project	Kvaerner Brug A/S (Nils Ambli)	Postboks 3610 Gb N-0135 Oslo 1 Norway	Demonstration plant (500 kWe) operated 4 yrs; developer now inactive
Islay project (biplane Wells turbine)	The Queen's University of Belfast (Dr. Trevor Whittaker)	Dept. Civil Engineering Stranmilis Road Belfast BT7 1NN Northern Ireland	Demonstration plant (75 kWe) operating
Sanzei project (tandem Wells turbine)	Japanese Marine Science and Technology Center (Takeaki Miyazaki)	2-15 Natsushima Cho Yokusuka 237 Japan	Ocean test of 40 kWe plant completed
Kujukuri project (single-acting OWC with onshore air tank)	Takenaka Corporation (Yoshio Kishima)	13-1, Kachidoki 1-Chome, Chuo-Ku Tokyo Japan	Demonstration plant (30 kWe) operating
Dawan Island project	Guangzhou Institute of Energy Conversion (Dr. Gao Xiang Fan)	81, Central Martyrs' Rd. Guangzhou 510070 People's Rep. of China	Demonstration plant (8 kWe) near completion
Azores project	Instituto Superior Tecnico (Dr. Antonio Falcao)	Mechanical Engr. Dept. 1096 Lisboa Codex Portugal	Demonstration plant under investigation

<u>Technology</u>	<u>Developer (Contact)</u>	<u>Developer's Address</u>	<u>Status</u>
Process 2 - Fixed Oscillating Water Column (continued)			
LAND-BASED SYSTEMS (continued)			
Bull Rock project	University College Cork (Dr. Anthony Lewis)	Maritime Research Lab. Cork Technology Park Model Farm Road, Cork Ireland	Demonstration plant under investigation
CAISSON-BASED SYSTEMS			
Sakata Port project (tandem Wells turbine)	Ministry of Transport (Shigeo Takahashi)	Port and Harbour Research Institute 3-1-1, Nagase Yokusuka 239 Japan	Demonstration plant (60 kWe) operating
Trivandrum project (monoplane Wells turbine)	Indian Institute of Technology (P.V. Inderesan)	Electrical Engr. Dept. New Delhi 110016 India	Demonstration plant (150 kWe) on hold
NEL Breakwater Madras project	National Engineering Laboratory (Dr. George Elliot)	East Kilbride Glasgow G75 0QU Scotland	Feasibility study (5 MWe) completed
Water valve, air flow rectifying system for single- acting OWC	Tohoku Electric Power Company, Inc. (Kuniya Watanabe)	3-7-1 Ichibancho Sendai Migamiyagi 980 Japan	Laboratory wave tank model tests completed
Stellenbosch Converter	University of Stellenbosch	South Africa	Inactive
Submerged Resonant Duct	Vickers, Ltd.	United Kingdom	Inactive
Process 3 - Floating Oscillating Water Column			
NAVIGATION BUOYS			
Japanese buoy	Ryokuseisha Corporation (Yoshio Masuda)	4-18-2 Shonan Takatori Yokusuka 237 Japan	Commercial production
PRC buoy	Guangzhou Institute of Energy Conversion (Dr. Gao Xiang Fan)	81 Central Martyrs' Rd. Guangzhou 510070 People's Rep. of China	Commercial production
UK buoy	Munster-Simms Engineering, Ltd. (J.J. Gault)	Old Belfast Road Bangor BT19 1LT Northern Ireland	Commercial production

<u>Technology</u>	<u>Developer (Contact)</u>	<u>Developer's Address</u>	<u>Status</u>
Process 3 - Floating Oscillating Water Column (continued)			
UTILITY-SCALE SYSTEMS			
Backward Bent Duct Buoy	Ryokuseisha Corporation (Yoshio Masuda)	4-18-2 Shonan Takatori Yokusuka 237 Japan	Small-scale ocean tests completed
Floating attenuator (test ship <i>Kaimei</i>)	Japanese Marine Science and Technology Center (Takeaki Miyazaki)	2-15, Natsushima Cho Yokusuka 237 Japan	Ocean tests of 40 to 125 kW air turbines completed
Floating terminator ("Mighty Whale")	Japanese Marine Science and Technology Center (Takeaki Miyazaki)	2-15 Natsushima Cho Yokusuka 237 Japan	Laboratory wave tank model tests completed
Tension-leg platform	Taisei Corporation (Yoshihiro Tanaka)	1-25-1 Nishi-shinjuku Shinjuku-ku Tokyo 163 Japan	Laboratory wave tank model tests completed
Process 4 - Pivoting Flap			
FIXED SYSTEMS			
Pendulor System	Muroran Institute of Technology (Tomiji Watabe)	Dept. Mechanical Engr. 27-1 Mizumoto-cho Muroran 050 Japan	Demonstration plant (20 kWe) operating; ocean test of 5 kW hydraulic unit underway
Bottom-hinged single flap	Kansai Electric Power Company, Inc. (Shohei Shimodaira)	11-20 Nakodi, 3-chome Amagasaki Hyogo-Ken 661 Japan	Ocean test of 100 W / 1 kWe unit underway
Tandem Flap	Q Corporation (Richard Wilke)	11211 McPherson Way Ventura, CA 93001 USA	Lake test of 20 kWe unit completed
FLOATING SYSTEMS			
Triplate Converter	Royal Military College of Science, Shrivenham	United Kingdom	Inactive
P.S. FROG	University of Lancaster (Dr. Michael French)	Dept. of Engineering Lancaster LA1 4YR United Kingdom completed	Laboratory wave tank model tests

<u>Technology</u>	<u>Developer (Contact)</u>	<u>Developer's Address</u>	<u>Status</u>
Process 5 - Heaving Float in Caisson			
Neptune System	E O Tech, Inc. (Dr. Frank Wu)	Suite 885 150 N. Santa Anita Ave. Arcadia, CA 91006 USA	Laboratory wave tank model tests completed
Wave Pump	Kajima Corporation (Akira Shiki)	5-16 Akasaka, 6-chome Minato-ku Tokyo 107 Japan	Laboratory wave tank model tests completed
Water turbine suspended from float ("Seamill")	Hydropower, Inc. (Robert Bueker)	7233 Columbus Dr. Anaheim Hills, CA 92807 USA	Bench test of 10 kWe turbine completed
Process 6 - Freely Heaving Float and Seafloor Reaction Point			
Danish system	Danish Wave Power, Aps (Dr. Kim Nielsen)	Norregade 7A 1165 Copenhagen K Denmark	Ocean test of 45 kWe plant (6 m dia buoy) completed
DELBUOY	CHPT, Inc. (Dr. Douglas Hicks)	100 Dock Road Henlopen West Lewes, DE 19958 USA	Demonstration of 2.1 m dia buoy, 300 gal/day fresh water, completed
US system	Wave Energy, Inc. (Tom Windle)	3500 SE Washington Blvd. Bartlesville, OK 74006 USA	Ocean test of 2.4 m dia buoy underway
Scrap-tire	E.I. duPont de Nemours & Co. (Walter Simmons)	Potomac River Works P.O. Drawer 863 Martinsburg, WV 25401 USA	Ocean test of 2.5 m dia buoy completed
Process 7 - Freely Heaving Float and Inertial Reaction Point			
NAVIGATION BUOYS			
UK buoy	AB Pharos Marine, Ltd. (Robin Hewett)	Beacon Works Brentford, Middx TW8 0AB United Kingdom	Commercial production
UTILITY-SCALE SYSTEMS			
Swedish system	Technocean AB (Bengt-Olov Sjöström)	Trondheimsgatan 12 S-417 22 Gothenburg Sweden	Ocean test of 30 kWe plant (three 5 m dia buoys) completed

<u>Technology</u>	<u>Developer (Contact)</u>	<u>Developer's Address</u>	<u>Status</u>
Process 7 - Freely Heaving Float and Inertial Reaction Point (continued)			
UTILITY-SCALE SYSTEMS (continued)			
Buoy <i>Elskling</i>	Interproject Service AB (Gunnar Fredriksson)	Gripensas S-640 33 Bettna Sweden	Ocean test of 3 m dia buoy completed
Three linked floats ("Waveberg")	27th Century Energy, Inc. (John Berg)	P.O. Box 189 Chester, Nova Scotia B0J 1J0 Canada	Bay test of 10 m prototype completed
Process 8 - Contouring Float and Inertial Reaction Point			
Wave Energy Module	U.S. Wave Energy, Inc. (Harry Hopfe)	65 Pioneer Drive Longmeadow, MA 01106 USA	Lake test of 1 kWe unit completed
Process 9 - Contouring Float and Seafloor Reaction Point			
Heaving and pitching raft	Sea Energy Corporation (Carroll Gordon)	1330 Whitney Bank Bldg. New Orleans, LA 70130 USA	Laboratory wave tank model tests completed
Jack-up platform <i>Kaiyo</i>	Japan Foundation for Shipbuilding Advancement (Dr. Atsuo Yazaki)	2-28-7 Nagasaki Toshima-ku Tokyo 171 Japan	Ocean test of 20 kWe plant completed
Process 10 - Pitching Float and Inertial Reaction Point			
Edinburgh Duck	University of Edinburgh (Dr. Stephen Salter)	Dept. of Mechanical Engr. The King's Buildings Edinburgh EH9 3JL Scotland	Lake test (1/10-scale) completed
Cockerell Raft	Wavepower Limited	United Kingdom	Inactive
Process 11 - Flexible Bag and Inertial Reaction Point			
SEA Clam	Coventry Polytechnic (Dr. Norman Bellamy)	Faculty of Engineering Priory Street Coventry CV1 5FB United Kingdom	Lake test (1/15-scale) completed
Lancaster Flexible Bag	University of Lancaster (Dr. Michael French)	Dept. of Engineering Lancaster LA1 4YR United Kingdom	Laboratory wave tank model tests completed

<u>Technology</u>	<u>Developer (Contact)</u>	<u>Developer's Address</u>	<u>Status</u>
Process 12 - Submerged Buoyant Absorber and Seafloor Reaction Point			
Bristol Cylinder	Shawater Ltd. (Dr. Tom Shaw)	The Old Vicarage Ston Easton Bath BA3 4DN United Kingdom	Laboratory wave tank model tests completed